

**Synthesis, NMR spectroscopic investigations and absolute
quantification of dietary triacylglycerols**

Tahira Musarrat

a Thesis submitted in partial fulfillment
of the requirements for the degree of

**Doctor of Philosophy
in Field**

Chemistry

Approved Dissertation Committee

Prof. Dr. Arvid Kappas (Chair of the Dissertation Committee) (Jacobs University
Bremen)

Prof. Dr. Nikolai Kuhnert (Supervisor) (Jacobs University Bremen)

Prof. Dr. Gerd-Volker Roeschenthaler (Reviewer) (Jacobs University Bremen)

Prof. Dr. Adam Le Gresley (Reviewer) (Kingston University UK)

Date of PhD defense: 06.10.2021

Life Sciences & Chemistry, Jacobs University Bremen

Statutory Declaration

Family Name, Given/First Name	MUSARRAT, TAHIRA
Matriculationnumber	2033 2025
What kind of thesis are you submitting: Bachelor-, Master- or PhD-Thesis	PhD -Thesis

English: Declaration of Authorship

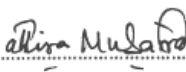
I hereby declare that the thesis submitted was created and written solely by myself without any external support. Any sources, direct or indirect, are marked as such. I am aware of the fact that the contents of the thesis in digital form may be revised with regard to usage of unauthorized aid as well as whether the whole or parts of it may be identified as plagiarism. I do agree my work to be entered into a database for it to be compared with existing sources, where it will remain in order to enable further comparisons with future theses. This does not grant any rights of reproduction and usage, however.

The Thesis has been written independently and has not been submitted at any other university for the conferral of a PhD degree; neither has the thesis been previously published in full.

German: Erklärung der Autorenschaft (Urheberschaft)

Ich erkläre hiermit, dass die vorliegende Arbeit ohne fremde Hilfe ausschließlich von mir erstellt und geschrieben worden ist. Jedwede verwendeten Quellen, direkter oder indirekter Art, sind als solche kenntlich gemacht worden. Mir ist die Tatsache bewusst, dass der Inhalt der Thesis in digitaler Form geprüft werden kann im Hinblick darauf, ob es sich ganz oder in Teilen um ein Plagiat handelt. Ich bin damit einverstanden, dass meine Arbeit in einer Datenbank eingegeben werden kann, um mit bereits bestehenden Quellen verglichen zu werden und dort auch verbleibt, um mit zukünftigen Arbeiten verglichen werden zu können. Dies berechtigt jedoch nicht zur Verwendung oder Vervielfältigung.

Diese Arbeit wurde in der vorliegenden Form weder einer anderen Prüfungsbehörde vorgelegt noch wurde das Gesamtdokument bisher veröffentlicht.

31.08.21 
.....
Date, Signature

Abstract

Fats and oils are important biological compounds. These are composed of fatty acids, phospholipids, cholesterol, sterols and triacylglycerols. Triacylglycerols (TAGs) are energy reservoirs for living organisms. TAGs are important components of lipid bilayer in the cells and cellular vesicles i.e., lipid droplets (LD). The most common fatty acids present in the plasma membrane are palmitic, stearic, linoleic, and linolenic acids. Proteins are attached to lipids in the plasma membrane and diffuse with a specific diffusion coefficient. The diffusion of the molecules across the membrane is described in terms of diffusion coefficients. The protein-lipid interactions play important role in the cell signaling and trafficking. The cell signaling and trafficking property of membrane lipids and proteins are important in the transport of drugs across the membrane. The fluidity of the membrane depends upon viscosity, chain length and degree of unsaturation of the unsaturated fatty acid chains.

Several symmetrical and unsymmetrical TAGs have been synthesized in purity as a synthetic standard for the analytical studies. The synthesis of symmetrical triacylglycerols (TAGs) is done using previously reported Hassner esterification method. Following this method tripalmitin [PPP], tristearin [SSS], triolein [OOO], trilinolein [LLL], trioctanein [OcOcOc] and trilaurein [LaLaLa] have been synthesized in purity. The basic scheme of the reaction is the same as reported. However, the change in the reaction time, temperature and catalyst showed different yield of the product. The detailed scheme of reaction and experimental procedures have been explained. The unsymmetrical TAGs have been synthesized in two-step reaction following a reported method. Firstly, four 1-monoacylglycerols have been synthesized enantiomerically. These include 1-palmitoyl glycerol, 1-stereoyl glycerol, 1-oleoyl glycerol and 1-linoleoyl glycerol. In the second step, asymmetrical TAGs are synthesized through esterification of 1-monoacylglycerol with fatty acyl chlorides. Total of 10 asymmetrical TAGs have been synthesized. These are 1-palmitoyl-2,3-dioleoyl glycerol [POO], 1-palmitoyl-2,3-distereoyl glycerol [PSS], 1-palmitoyl-2,3-dilinoleoyl glycerol [PLL], 1-stereoyl-2,3-dipalmitoyl glycerol [SPP], 1-stereoyl-2,3-dioleoyl glycerol [SOO], 1-stereoyl-2,3-dilinoleoyl glycerol [SLL], 1-oleoyl-2,3-dipalmitoyl glycerol [OPP], 1-oleoyl-2,3-dilinoleoyl glycerol [OLL], 1-linoleoyl-2,3-dipalmitoyl glycerol [LPP] and 1-linoleoyl-2,3-dioleoyl glycerol [LOO]. The chemical structures of all the synthesized TAGs have been confirmed by the ^1H - and ^{13}C - NMR spectroscopy. The purity of these synthesized TAGs has been checked by LC-MS analysis.

2D NOESY spectra of unsaturated TAGs showed cross peaks for in-space coupling of $-\text{CH}=\text{CH}-$ protons and methylene protons. This suggests a folded structure of fatty acyl chains in triacylglycerol molecules. The similar cross peaks are observed in 2D ROESY which shows that these protons are very close in space. ^1H -NMR, ^{13}C - NMR, 2D NOESY and 2D ROESY analysis of synthetic TAG is very useful to understand the metabolites in natural systems and in biochemical processes. The NMR

peaks of synthetic TAGs can serve as a reference for the identification of TAGs in complex mixtures through HPLC-NMR spectroscopy.

The diffusion NMR of the synthesized TAGs has been measured. The diffusion coefficients of the TAGs showed a difference regarding saturated and unsaturated fatty acid chains in the TAGs. The saturated TAGs have larger diffusion coefficients for the higher molecular weight than the lower molecular weight TAGs. The unsaturated TAGs have greater diffusion coefficients than the saturated TAGs. This showed that the TAGs with a double bond in their fatty acyl chains have a bent and folded structure. The diffusion coefficient of the POO is larger than the PLL. This suggests a rigidity is created by the presence of more double bonds in the fatty acyl chains of TAGs. The diacylglycerol shows the fastest diffusion rate. This explains the active role of diacylglycerols in the plasma membrane for the signaling and trafficking.

The absolute quantification of the TAGs was performed by 8-point calibration curves. The calibration curves were plotted from the chromatogram peak area and sample concentration. The linear trends have been observed with R^2 in the range of 0.99. The statistical regression analysis with ANOVA gave negative intercept. This shows that the TAGs have good sensitivity for the HPLC detection at small concentrations. The negative intercept shows mathematically that the subset x is not equal to zero. The calibration curves of the synthetic triacylglycerols have been used to quantify the TAGs in cocoa butter from Ghana, Ecuador, and Cameron. The discriminate analysis of the cocoa butter from the Ghana and Ecuador has been performed on Metaboanalyst software. The samples were analyzed by HPLC. The LC-MS data was processed to mzxml files by Mzmine software. The principal component analysis (PCA) and partial least square- discriminant analysis (PLSDA) of the samples showed variance up to 86.6 %. The discriminate analysis can be a good method for the detection of adulteration in cocoa butter.

Acknowledgements

I would like to acknowledge and thank my PhD supervisor and advisor Prof. Dr. Nikolai Kuhnert for his comprehensive support at all stages of my PhD studies and research work. I have been blessed with the opportunity to receive the skillful training and knowledge of analytical and organic chemistry from the kind and skillful supervision of Prof. Dr. Nikolai Kuhnert. He has been a source of knowledge and moral support to me throughout the whole time of my PhD research work and studies. His knowledge, motivations, inspiration, and considerations will always be soul light of guidance in my life. I thank to Prof. Dr. Nikolai Kuhnert for being my supervisor and for giving me this valuable knowledge and guidance.

I thank to the members of my defense committee Prof. Dr. Gerd Roeschenthaler and Prof. Dr. Adam Le Gresley for being a member pf my dissertation committee and for giving their valuable time to go through my dissertation and take part in my final exam.

I am grateful and thankful to my mother Ms. Musarat Begum and my father Mr. Zahoor Hussain for being a constant source of moral support and love for me. Without their love and support, I would have not been able to reach my goal. My parents are my spiritual guiders and source of love for my whole life. I am very thankful to my mother for taking so much care for me and bringing me up to high level of dignity and education. I am very thankful to my father for making my personality groomed and making me able to serve good for life. I thank to my brothers Mr. Tahir Zahoor Mirza and Mr. Anjum Zahoor and my loving younger sister Mrs. Rehana Musarrat for being there to help me in all my difficulties and to make up my life. Together this I cannot forget the love and care of families of my elder brother, younger brother, and my sister. A precious part of my life is being made by my nephews and nieces. I never had been alone in all my journey of PhD research here in Germany.

I am thankful to DAAD (Deutsche Akademischer Austausch Dienst) for the funding support and giving me an opportunity to carry out my research work. I am also thankful to Prof. Dr. Nikolai Kuhnert for providing me short funding support from his research group budget. It was very helpful to me. I thank to the academic and teaching resource services for providing me an opportunity of serving small student jobs. It fulfilled my wish and desire of serving at Jacobs community. I am thankful for the cooperative support of Mr. Stefan Liesche for the comprehensive support and guidance to run my computer software as it was necessary to complete my PhD thesis work. I express my thanks to Ms. Maureen Trinder for her generous support in all matters of academics. I, from a rural life background would have seeked extra help for the academics matters here. I thank to the whole

Jacobs community and administrative staff for the wonderful, loving, and cooperative environment that is a big support in the education of every student at Jacobs university.

I would like to thank Ms. Anja Müller for providing me technical support and Ms. Theresa Peters for providing me laboratory assistance to complete my research work. I thank to Dr. InamUllah Hakeem Said for support and help to complete LC-MS quantification of my PhD research work. I am thankful to the members of Jacobs university for providing me support and guidance in academic affairs.

I especially thank to Prof. Dr. Arvid Kappas for being the head of my dissertation committee and opening a door of education for me. I thank to Dr. Svenja Frischholz for the help and cooperation in the academic matters.

I thank heartily to Prof. Dr. Adam Le Gresley and his research group Dr. Cameron Robertson and Ms. Tomris Coban for their help for the measurement of diffusion NMR spectra and NOESY and REOSY spectroscopic analysis of the TAGs from the laboratory of Kingston University, UK.

I would like to thank Prof. Thomas Nugent and his lab fellows for their support to complete last part of my chemical synthesis work. I thank to Dr. Falguni Goswami and Ms. Samarpita Debnath for providing me friendly and happy environment to complete some part of my PhD research work in a creative environment.

These are my gratitude and thanks to those people whose help and support has made me to reach my goal and complete my thesis. Thank you.

Contents

Abstract.....	ii
Acknowledgements.....	iv
List of Figures.....	ix
List of Tables.....	xii
Abbreviations.....	xiii
Chapter 1: Introduction.....	1
1.1 Triacylglycerols.....	1
1.2 Biological significance of triacylglycerols.....	6
1.3 Biosynthesis of Triacylglycerol.....	11
1.4 Biomolecules in nature.....	17
1.4.1 Nucleotides and nucleic acids.....	17
1.4.2 Amino acids, peptides, and proteins.....	18
1.4.3 Glycolipids	19
1.4.4 Terpenes.....	20
1.4.5 Steroids.....	21
1.4.6 Polyketides.....	22
1.4.7 Glycerophospholipids.....	23
1.4.8 Sphingolipids.....	25
1.5 Dietary oil composition.....	26
1.6 Health effects of fats and oils.....	28
1.7 Qualitative and quantitative analysis.....	29
1.7.1 Ultraviolet spectroscopy (UV)	29
1.7.2 Infrared spectroscopy	29
1.7.3 Mass spectrometry	29
1.7.4 High performance liquid chromatography	30
1.7.5 Nuclear Magnetic spectroscopy	30
1.8 Synthesis.....	30
References	32
Chapter 2 Synthesis of symmetrical and unsymmetrical triacylglycerols.....	45
2.1 Introduction.....	45
2.2 Experimental.....	47
2.2.1 LC-MS analysis	47
2.2.2 HPLC	47
2.2.3 Thin layer chromatography	47

2.3 Synthesis of symmetrical triacylglycerols.....	48
2.3.1 Synthesis of 1,2,3-Tripalmitoyl glycerol [Tripalmitin (PPP)] (1)	48
2.3.2 Synthesis of 1,2,3-Tristearoyl glycerol [Tristearin (SSS)] (2)	51
2.3.3 Synthesis of 1,2,3-Trioleoyl glycerol [Triolein (OOO)] (3)	52
2.3.4 Synthesis of 1,2,3-Trilinoleoyl glycerol [Trilinolein (LLL)] (4)	54
2.3.5 Synthesis of 1,2,3-Trioctanoyl glycerol [Trioctanein (OcOcOc)] (5)	55
2.3.6 Synthesis of 1,2,3-Trilauroyl glycerol [Trilaurein (LaLaLa)] (6)	55
2.4 Synthesis of unsymmetrical triacylglycerols (TAGs).....	56
2.4.1 Synthesis of 1-Palmitoyl-2,3-isopropylidene glycerol (7)	56
2.4.2 Synthesis of 1-Palmitoyl glycerol (8)	57
2.4.3 Synthesis of 1-Palmitoyl-2,3-dioleoyl glycerol [POO] (9)	58
2.4.4 Synthesis of 1-Palmitoyl-2,3-distearoyl glycerol [PSS] (10)	60
2.4.5 Synthesis of 1-Palmitoyl-2,3-dilinoleoyl glycerol [PLL] (11)	61
2.4.6 Synthesis of 1-Stearoyl-2,3-isopropylidene glycerol (12)	61
2.4.7 Synthesis of 1-Stearoyl glycerol (13)	62
2.4.8 Synthesis of 1-Stearoyl-2,3-dipalmitoyl glycerol [SPP] (14 a and 14 b)	62
2.4.9 Synthesis of 1-Stearoyl-2,3-dioleoyl glycerol [SOO] (15)	63
2.4.10 Synthesis of 1-Stearoyl-2,3-dilinoleoyl glycerol [SLL] (16)	64
2.4.11 Synthesis of 1-Oleoyl glycerol (17)	64
2.4.12 Synthesis of 1-Oleoyl-2,3-dipalmitoyl glycerol [OPP] (18)	65
2.4.13 Synthesis of 1-Oleoyl-2,3-dilinoleoyl glycerol [OLL] (19)	65
2.4.14 Synthesis of 1-Linoleoyl-2,3-isopropylidene glycerol (20)	66
2.4.15 Synthesis of 1-Linoleoyl glycerol (21)	67
2.4.16 Synthesis of 1-Linoleoyl-2,3-dipalmitoyl glycerol [LPP] (22)	70
2.4.17 Synthesis of 1-Linoleoyl-2,3-dioleoyl glycerol [LOO] (23)	71
2.5 Results & Discussion	72
2.5.1 2D NOESY and 2D ROESY NMR measurements	74
2.6 Conclusion	76
References	77
Chapter 3 Absolute Quantification of Triacylglycerols (TAGs)	81
3.1 Introduction	81
3.2 Experimental	86
3.2.1 Chemicals and Reagents	86
3.2.2 LC-MS conditions	86

3.2.3 Sample preparation (calibrants) for the calibration curves	86
3.3 Results & Discussion	87
3.4 Conclusion	91
References	92
Chapter 4 Diffusion NMR of dietary triacylglycerols	97
4.1 Introduction	97
4.2 Experimental	100
4.3 Results & Discussion	101
4.4 Conclusion	107
References	109
Chapter 5 Cocoa butter adulteration	112
5.1 Introduction	112
5.2 Experimental	116
5.2.1 Chemical and reagents	116
5.2.2 Sample preparation	116
5.2.3 Sample analysis	116
5.2.4 Statistical analysis	116
5.3 Results & Discussion	117
5.4 Conclusion	126
References	127
Conclusion	131
Supplementary information	133

List of Figures

Figure 1.1 Triacylglycerol hydrolyze into its components (fat and glycerol)	1
Figure 1.2 Structures of TAGs molecular species, positional isomers and enantiomers	3
Figure 1.3 Sub cell structures and (b) chain length structures of triacylglycerol	4
Figure 1.4 Conformation of glycerol group in triacylglycerol (White circles= oxygen atoms, Black circles= glycerol carbon atoms, Zig-zag lines= hydrocarbon chains)	5
Figure 1.5 Structural representation of oleosins, caleosins and steroleosins at the surface of a TAG-filled lipid droplets (LD)	7
Figure 1.6 Structure and interconversion of steroid hormones in animals and plants (Mammals= 17 β estradiol; plants= brassinolide)	7
Figure 1.7 Diffusion of bilayer membrane (a) Cell signaling via complex formation (b) Receptor-mediated virus diffusion (c) Differences in the mobility or size of the membrane-associated objects (e.g., proteins, lysosomes)	10
Figure 1.8 Schematic representation of biosynthesis of TAGs	11
Figure 1.9 The tricarboxylate transport system to transfer acetyl-CoA from the mitochondrion to the cytosol	12
Figure 1.10 CO ₂ activation by Biotin-enzyme and formation of malonyl-CoA	13
Figure 1.11 The phosphopantetheine group in acyl-carrier protein (ACP) and in CoA	13
Figure 1.12 The reactions involved in the biosynthesis of fatty acids	14
Figure 1.13 Chemical reactions of the biosynthesis of TAGs	16
Figure 1.14 The chemical structures of ATP and ADP	18
Figure 1.15 ADP-glucose. The glucose (blue) is attached to adenosine by two phosphate groups (red)	18
Figure 1.16 Uncharged and Zwitterionic form of alanine	18
Figure 1.17 The scheme for the terpene metabolism. A presentation of different classes of terpenoid compounds and their classification on the basis of volatility and polarity	20
Figure 1.18 The chemical structures of R- and S- limonene	21
Figure 1.19 Cyclopentanoperhydrophenanthrene	21
Figure 1.20 The basic mechanism of biosynthesis of polyketides	23
Figure 1.21 Glycerophospholipid	23
Figure 1.22 Common classes of glycerophospholipids	24
Figure 1.23 Cellular functions of glycerophospholipids	25
Figure 1.24 Chemical structures of sphingomyelin, sphingosine and ceramide	26
Figure 2.1 A general scheme for the esterification reaction	45
Figure 2.2 The mechanism of the esterification reaction	46

Figure 2.3 Reaction scheme for the synthesis of 1,2,3-Tripalmitoyl glycerol [Tripalmitin (PPP)] (1)	48
Figure 2.4 ^1H -NMR (400 MHZ, CDCl_3) spectrum of 1,2,3-tripalmitoyl glycerol [Tripalmitin (PPP)] (1)	49
Figure 2.5 ^{13}C -NMR (100 MHZ, CDCl_3) spectrum of 1,2,3-tripalmitoyl glycerol [Tripalmitin PPP] (1)	49
Figure 2.6 2D NOESY of 1,2,3-tripalmitoyl glycerol [Tripalmitin PPP] (1)	50
Figure 2.7 2D ROESY of 1,2,3-tripalmitoyl glycerol [Tripalmitin PPP] (1)	50
Figure 2.8 ^1H -NMR (400 MHZ, CDCl_3) spectrum of 1,2,3-trioleoyl glycerol [Triolein OOO] (3)	52
Figure 2.9 ^{13}C -NMR (100 MHZ, CDCl_3) spectrum of 1,2,3-Trioeloyl glycerol [Triolein OOO] (3)	53
Figure 2.10 2D NOESY of 1,2,3-Trioeloyl glycerol [Triolein OOO] (3)	53
Figure 2.11 2D ROESY of 1,2,3-Trioeloyl glycerol [Triolein OOO] (3)	54
Figure 2.12 Structures of symmetrical triacylglycerols synthesized	56
Figure 2.13 ^1H -NMR (400 MHZ, CDCl_3) spectrum of 1-Palmitoyl isopropylidene glycerol (7)	57
Figure 2.14 ^1H -NMR (400 MHZ, CDCl_3) spectrum of 1-Palmitoyl glycerol (8)	58
Figure 2.15 ^1H -NMR (400 MHZ, CDCl_3) spectrum of 1-Palmitoyl-2,3-dioleoyl glycerol [POO] (9)	59
Figure 2.16 ^{13}C -NMR (100 MHZ, CDCl_3) spectrum of 1-Palmitoyl-2, 3-dioleoyl glycerol [POO] (9)	59
Figure 2.17 2D NOESY of 1-Palmitoyl-2,3-dioleoyl glycerol [POO] (9)	60
Figure 2.18 ^1H -NMR (400 MHZ, CDCl_3) spectrum of 1-Linoleoyl-2,3-Isopropylidene glycerol (20)	66
Figure 2.19 ^{13}C -NMR (100 MHZ, CDCl_3) spectrum of 1-Linoleoyl-2,3-Isopropylidene glycerol (20)	67
Figure 2.20 ^1H -NMR (400 MHZ, CDCl_3) spectrum of 1-Linoleoyl glycerol (21)	68
Figure 2.21 ^{13}C -NMR (100 MHZ, CDCl_3) spectrum of 1-Linoleoyl glycerol (21)	69
Figure 2.22 Synthesis of 1-acyl isopropylidene glycerols	69
Figure 2.23 Mechanism of formation of 1-acyl isopropylidene glycerol	70
Figure 2.24 Mechanism of hydrolysis of 1-acyl isopropylidene glycerol	70
Figure 2.25 Chemical structures of unsymmetrical triacylglycerols synthesized by a multistep synthesis (15-23)	71
Figure 2.26 Comparison of 1D ^1H NMR spectra of triacylglycerols and diacylglycerols referenced to TMS in CDCl_3 , NS = 16	73
Figure 2.27 Comparison of 1D ^1H NMR spectra of tripalmitin [PPP] and 1-stereoyl-2,3-dipalmitoyl glycerol [SPP]and their isomeric fraction separated from the esterification reaction mixtures referenced to TMS in CDCl_3 , NS = 16	74

Figure 2.28 Comparison of PLL (Purple), PPP (Blue) and POO (Red), 2D NOESY spectra referenced to TMS in CDCl ₃ , NS = 32	74
Figure 2.29 Comparison of 2D NOESY spectra triacylglycerols (TAGs), diacylglycerol (DAG) and a monoacylglycerol referenced to TMS in CDCl ₃ , NS = 32	75
Figure 3.1 Chromatogram of TAGs adducts [M+NH ₄] ⁺ for different concentrations showing a shift in the retention time with the change in the concentration	88
Figure 3.2 Chromatograms of the cocoa butters from Cameron, Ecuador and Ghana	90
Figure 4.1 Pulse sequence for the DOSY experiment	98
Figure 4.2 2D DOSY of 1,2,3-tripalmitoyl glycerol [Tripalmitin PPP] (1)	102
Figure 4.3 2D DOSY of 1,2,3-Trilinoleoyl glycerol [Trilinolein LLL] (4)	103
Figure 4.4 (A) 1D DOSY spectra referenced to TMS in CDCl ₃ , D20 = 0.2s, P30 = 600μs. (B) Comparison of PLL (Red), PPP (Blue) and POO (Purple) DOSY spectra referenced to TMS in CDCl ₃	104
Figure 4.5 Comparison of PLL (Red) and POO (Blue) DOSY spectra referenced to TMS in CDCl ₃	106
Figure 5.1 Stages in the processing of cocoa from tree to chocolate bar	113
Figure 5.2 Mass spectrums in MS mode of A. Almond oil B. Cocoa butter Ghana and C. Cocoa butter Ghana and 10% Almond oil showing the difference in TAGs profiles	119
Figure 5.3 Principal component analysis (PCA) showing explained variance for the cocoa butter adulterant samples	120
Figure 5.4 PCA plot obtained from the LC-MS data of the cocoa butter Ghana, cocoa butter Ecuador, soybean oil, palm oil, apricot oil, lard and their 10% adulterants mixtures	120
Figure 5.5 Scree plot showing the variance explained by PCs. The green line shows the accumulative variance explained and blue line shows the variance explained by individual PCs	121
Figure 5.6 Score plots of the LC-MS data (2D) and 3D score plots. The explained variances are shown in brackets	122
Figure 5.7 Loading plot of the LC-MS data for selected PC of the TAGs profiles of the samples	122
Figure 5.8 Score plots of PLS-DA based on the triacylglycerol profiles from the LC-MS data. The 2D score plots (left) and 3D score plot (right); the variance is shown in the brackets	123
Figure 5.9 VIP score of the important features identified by PLS-DA	124
Figure 5.10 Hierarchical cluster from the LC-MS data of cocoa butter, vegetable oils, lard, CHOCOMATE-3100 and adulterant mixtures shown as dendrogram	125

List of Tables

Table 1.1 Structure of common fatty acids	2
Table 1.2 Characteristics of triacylglycerol polymorphs	4
Table 3.1 The retention times and $[M+NH_4]^+$ masses of the synthetic triacylglycerols	87
Table 3.2 The statistical data for R^2 , residual standard deviation (RSD), S_{xo} , t-stat and P- value of the synthetic TAGs by ANOVA table	89
Table 3.3 Relative quantity of cocoa butter TAGs from different origins as calculated per 100 g	91
Table 4.1 Diffusion coefficients of TAGs with Gyromagnetic ratio 4257.7000 gamma HZ/ G	105
Table 4.2 Diffusion coefficients of TAGs with Gyromagnetic ratio 26770.7000 gamma HZ/ Gauss	107
Table 5.1 Chemical structures of biomarkers (TAGs) identified in vegetable oils and fats from the LC-MS data	118
Table 5.2 Chemical structures of biomarkers (TAGS) of the vegetable oils identified in VIP scores	124

Abbreviations

TAG	Triacylglycerol
O _L	Orthorhombic unit cell
T _{//}	Triclinic unit cell
DCL	Double chain length structure
TCL	Triple chain length structure
QCL	Quarto chain length structure
POP	1-palmitoy-2-oleoyl-3-palmitoyl glycerol
POS	1-palmitoy-2-oleoyl-3-stereoyl glycerol
SOS	1-stereoyl-2-oleoyl-3-stereoyl glycerol
Sat-U-Sat	Saturated-unsaturated-saturated (monounsaturated triacylglycerols)
SCS	Skew-cis-skew
LD	Lipid droplets
BR	Brassinosteroids
OOO	Triolein
LLL	Trilinolein
LnLnLn	Trilinolenin
NLSD	Neutral lipid storage disease
WD	Wolman's disease
NEFA	Non-esterified fatty acids
ACP	Acyl-carrier protein
A	Adenine
G	Guanine
C	Cytosine
U	Uracil
T	Thymine
FAD	Flavin adenine dinucleotide
NAD	Nicotine adenine dinucleotide
PKSs	Polyketides
CDP-DAG	Cytidine diphosphate- diacylglycerol
PA	Phosphatidic acid
PC	Phosphatidylcholine
PE	Phosphatidylethanolamine
CL	Cardiolipin
PS	Phosphatidylserine

PUFA	Polyunsaturated fatty acids
Sph	Sphingosine
SM	Sphingomyelin
HDL	High-density lipoproteins
HPLC	High performance liquid chromatography
4-DMAP	4- dimethyl amino pyridine
DCC	N, N'-dicyclohexylcarbodiimide
DOSY	Diffusion ordered spectroscopy
DCM	Dichloromethane
NARP-HPLC	Non-aqueous reverse phase high-performance liquid chromatography
ECN	Equivalent carbon number
GC	Gas chromatography
C11C11C11	1,2,3-triundecanoylglycerol
DHA	Docosahexaenoic acid
EPA	Eicosapentaenoic acid
PPBu	1,2-dipalmitoyl-3-butyroyl glycerol
LOQ	Limit of quantification
LOD	Limit of detection
RSD	Residual standard deviation
RF	Response factor
D	Diffusion coefficient
K	Boltzmann constant

Chapter 1

Introduction

1.1 Triacylglycerols

Triacylglycerols are a class of lipids. Lipids are heterogeneous group of biological compounds that are soluble in organic solvents such as chloroform and methanol but insoluble in water. Triacylglycerols also known as triglycerides are non-polar, water insoluble triesters of glycerol and fatty acids. Triacylglycerols have different types based on their identity and placement of three fatty acid residues in the glycerol back bone. (Gurr, MI; James, 1975; Voet, Donald, Voet, 1999) Triacylglycerols are present in nature as animal fats and vegetable oils. Animal fats like butter and lard are solids at room temperature since they contain saturated fatty acids in the triacylglycerol back bone. The vegetable oils are liquids at room temperature due to the presence of mono- or poly-unsaturated fatty acids in the triacylglycerols of vegetable oils. Usually, triacylglycerols with unsaturated fatty acids have cis (Z) geometry at double bond in the fatty acid chain. Triacylglycerols are triesters of three long chain carboxylic acids i.e., fatty acids and glycerol. Glycerol and three fatty acids are yielded upon hydrolysis of a fat or oil (triacylglycerol). (Figure 1.1) (McMurry, 2004)

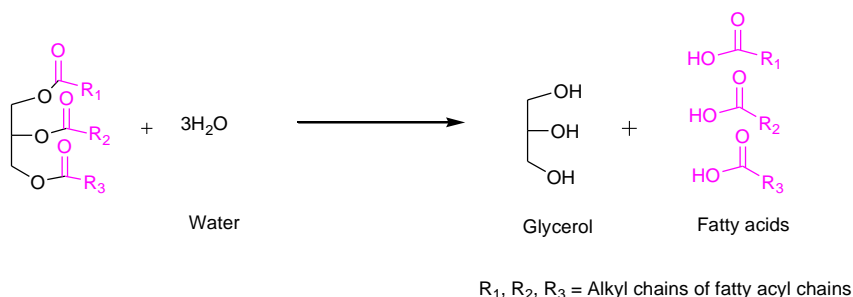


Figure 1.1 Triacylglycerol hydrolyze into its components (fat and glycerol)

Fatty acids are the main constituents of triacylglycerols. Triacylglycerols have different properties depending upon the presence of either saturated or unsaturated fatty acids in their structure. More than 100 different fatty acids have been identified and 40 of them occur most abundantly. Palmitic acid (C₁₆) and stearic acid (C₁₈) are the most abundant fatty acids in nature while oleic and linoleic acid (both C₁₈) are the most abundant unsaturated fatty acids in natural triacylglycerols. Linoleic and linolenic acids occur in cream and are very important for growth of children. If the infants are fed with non-fat milk for prolonged time, then they grow weak and develop skin lesions.

Table 1.1 Structures of common fatty acids

Symbol ^a	Common name	Systematic name	Structure	Melting point (°C)
Saturated fatty acids				
12:0	Lauric acid	Dodecanoic acid	$\text{CH}_3(\text{CH}_2)_{12}\text{COOH}$	44.2
14:0	Myristic acid	Tetradecanoic acid	$\text{CH}_3(\text{CH}_2)_{14}\text{COOH}$	52.0
16:0	Palmitic acid	Hexadecanoic acid	$\text{CH}_3(\text{CH}_2)_{16}\text{COOH}$	63.1
18:0	Stearic acid	Octadecanoic acid	$\text{CH}_3(\text{CH}_2)_{18}\text{COOH}$	69.1
20:0	Arachidic acid	Eicosanoic acid	$\text{CH}_3(\text{CH}_2)_{20}\text{COOH}$	75.4
22:0	Behenic acid	Docosanoic acid	$\text{CH}_3(\text{CH}_2)_{22}\text{COOH}$	81.0
24:0	Lignoceric acid	Tetracosanoic acid	$\text{CH}_3(\text{CH}_2)_{24}\text{COOH}$	84.2
26:0	Cerotic acid	n-Hexacosanoic acid	$\text{CH}_3(\text{CH}_2)_{26}\text{COOH}$	57.7
28:0	Montanic acid	n-Octacosanoic acid	$\text{CH}_3(\text{CH}_2)_{28}\text{COOH}$	90.9
Unsaturated fatty acids				
Monoenoic acids				
16:1	Palmitoleic acid	cis-9-hexadecanoic acid	$\text{CH}_3(\text{CH}_2)_5\text{CH}=\text{CH}(\text{CH}_2)_7\text{COOH}$	-0.5
18:1	Oleic acid	cis-9-octadecanoic acid	$\text{CH}_3(\text{CH}_2)_5\text{CH}=\text{CH}(\text{CH}_2)_7\text{COOH}$	13.2
22:1	Vaccenic acid	cis-11-octadecenoic acid	$\text{CH}_3(\text{CH}_2)_9\text{CH}=\text{CH}(\text{CH}_2)_9\text{COOH}$	13.0
24:1	Nervonic acid	15-tetracosenic acid	$\text{CH}_3(\text{CH}_2)_7\text{CH}=\text{CH}(\text{CH}_2)_{13}\text{COOH}$	39.0
Dienoic acids				
18:2	Linoleic acid	cis-9, 12-octadecadienoic acid	$\text{CH}_3(\text{CH}_2)_4(\text{CH}=\text{CHCH}_2)_2(\text{CH}_2)_7\text{COOH}$	-9.0
Trienoic acids				
18:3	α -Linoleic acid	cis-9, 12,15-octadecadienoic acid	$\text{CH}_3\text{CH}_2(\text{CH}=\text{CHCH}_2)_3(\text{CH}_2)_6\text{COOH}$	-17.0
18:3	γ -Linoleic acid	cis-6,9, 12-octadecadienoic acid	$\text{CH}_3(\text{CH}_2)_4(\text{CH}=\text{CHCH}_2)_3(\text{CH}_2)_3\text{COOH}$	
Tetraenoic acids				
20:4	Arachidonic acid	cis-5,8,11,14-Eicosatetraenoic acid	$\text{CH}_3(\text{CH}_2)_4(\text{CH}=\text{CHCH}_2)_4(\text{CH}_2)_2\text{COOH}$	-49.5
Pentaenoic acids				
20:5	EPA	cis-5,8,11,14,17-Eicosapentaenoic acid	$\text{CH}_3\text{CH}_2(\text{CH}=\text{CHCH}_2)_5(\text{CH}_2)_2\text{COOH}$	-54.0

^aNumber of carbon atoms, Number of double bonds

Triacylglycerols possess positional and regioisomeric isomerism. This is due to different position of fatty acids at one of the three carbon atoms of glycerol backbone. TAGs are classified into different categories based on carbon numbers, position of fatty acids, geometrical configuration (cis or trans) of double bonds in the fatty acyl chain and stereospecific positions i.e., sn-1 (α), sn-2 (β), sn-3 (γ) of the fatty acids on the glycerol backbone. The central carbon atom in the glycerol is pro-S i.e., prochiral. If

three acyl groups attached to glycerol in the TAGs are the same, then the TAG is achiral and possess a plane of symmetry. The presence of three different fatty acyl chains in TAG results in enantiomeric pairs of TAGs. (Grossert et al., 2014) The three binding positions of fatty acids on the glycerol backbone result in the positional isomers of triacylglycerols. The binding positions of fatty acids sn-1 (α), sn-2 (β) and sn-3 (γ) on glycerol backbone in TAG and positional isomers and enantiomeric forms of TAGs are given in figure 1.2. The specific position of fatty acid in TAGs molecule is very important in the food absorption and function in both animals and human beings. The presence of palmitic acid at β -position in human milk, helps infant to digest the milk easily and get energy. In food chemistry, the digestion, absorption and physiology of animals and humans is strongly affected by the positional isomerism of triacylglycerols. (Beppu et al., 2013; Yoshinaga, 2021)

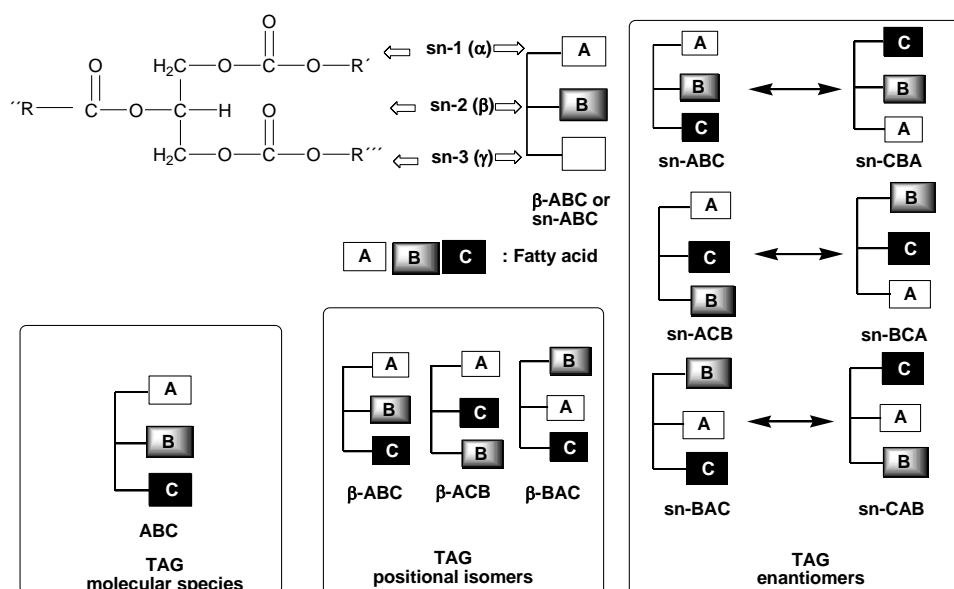


Figure 1.2 Structures of TAGs molecular species, positional isomers, and enantiomers

Triacylglycerols exhibit the property of polymorphism in their structure. They crystallize into three main polymorphs by an increased order of stability as; α polymorphs have hexagonal unit cell (H), β' polymorphs have orthorhombic unit cell (O_{\perp}) and β polymorphs have triclinic unit cell ($T_{//}$). (Maynard-Casely et al., 2019) The sub cell structures of triacylglycerols have been determined by the single crystal X-ray diffraction, high-resolution X-ray powder diffraction and differential scanning calorimetry techniques. (Langevelde et al., 2000; Rousset et al., 1998) The crystal structure also differs according to the chain length structures. The chain length structure produces a repetitive sequence of the fatty acyl chains in the unit cell lamella along the long chain axes. A double chain structure is formed when the chemical properties of three fatty acyl chains are similar or very close to each other, e.g., tricaprins β -form. When the chemical properties of one or two of the three fatty acyl chains are largely different from each other, then a triple chain structure is formed. Triple chain structure of triacylglycerol is due

to the chain sorting and steric hindrance. e.g., 1,2-dipalmitoyl-3-acetyl glycerol (PP2) β -form has triple chain structure. The chain length structure ranges from double (DCL) to triple (TCL), quarto (QCL) or hexa (HCL) structure when the fatty acid chains become more complex. (Figure 1.3) (Sasaki et al., 2012; Sato, 2001)

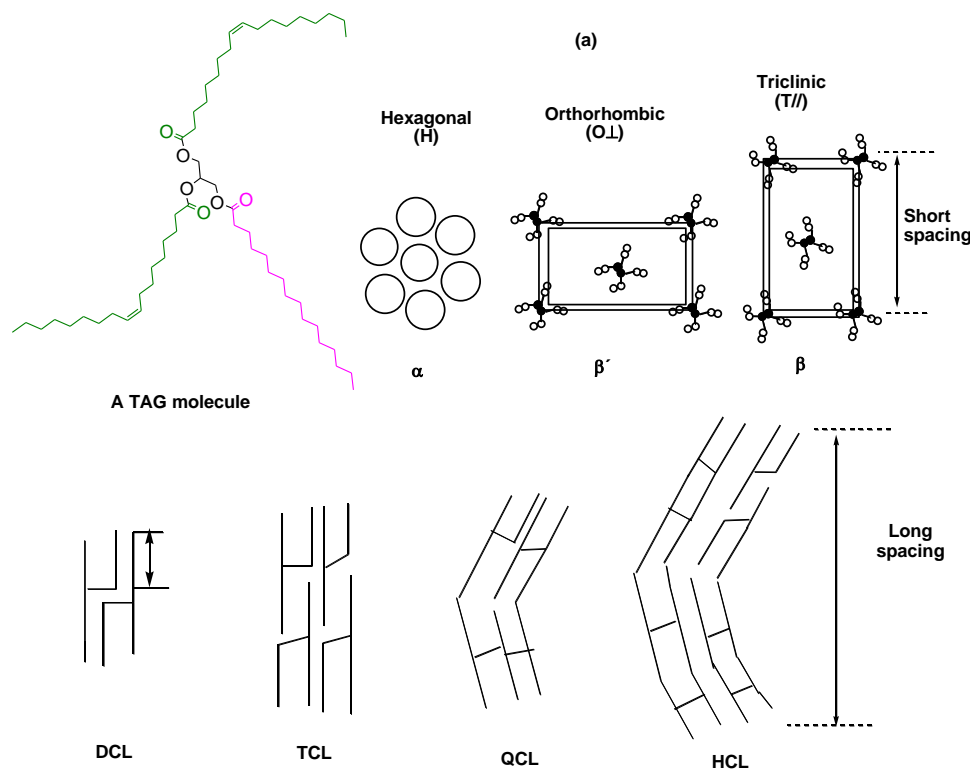


Figure 1.3 Sub cell structures and (b) chain length structures of triacylglycerol

Table 1.2 Characteristics of triacylglycerol polymorphs

Polymorphs	d-spacing value	Sub cell lattice	Chain orientation	Symbol
α	4.15	Hexagonal	Random	H
β	3.80, 4.20	Orthorhombic	Orthogonal	O_{\perp}
γ	3.65, 3.85, 4.57	Triclinic	Parallel	T_{\parallel}

The stability of the polymorphs of triacylglycerol depends upon the angle of tilt at which the double or the triple chains pack together. The hexagonal structure (H) has no tilt angle and Orthorhombic and triclinic structures have angle of tilt between 50° and 70° . (Himawan et al., 2006) The α -polymorph is the least stable, β' is metastable and β is the most stable.

In addition to chain length, triacylglycerols have two conformations i.e., bent, or tuning fork and chair structures. The molecular configuration of triacylglycerol is determined by the conformation of the glycerol backbone. The saturated triacylglycerols have β -phase consisting of two straight chains attached at sn-1 and sn-2 and a bent chair attached at the sn-3 position. The bent fatty acid chain at

sn-2 position has a gauche bond in the vicinity of ester group bonded to the glycerol. This results in a chair conformation. (Figure 1.4) (Akita et al., 2006) Van Langevelde proposed a tuning fork asymmetric configuration for β crystal structure of tripalmitin. (Van Langevelde et al., 1999)

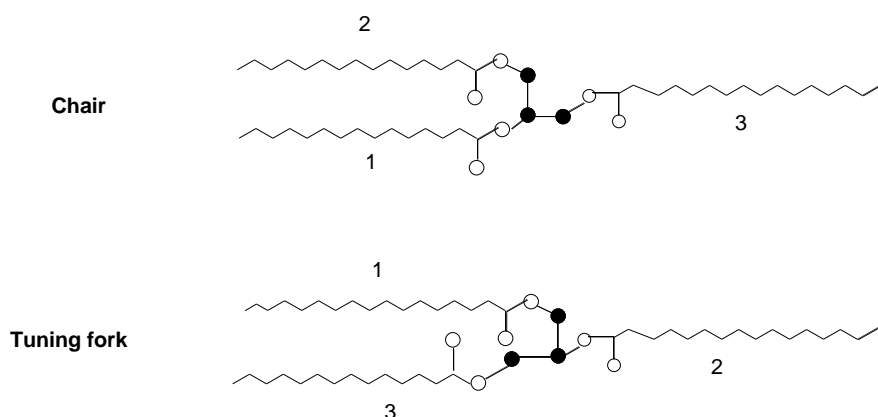


Figure 1.4 Conformation of glycerol group in triacylglycerol (White circles= oxygen atoms, Black circles= glycerol carbon atoms, Zig-zag lines= hydrocarbon chains)

Triacylglycerols with unsaturated fatty acid in sn-2 position and saturated fatty acids at sn-1 and sn-3 positions are present in many vegetable oils and cocoa butter. The acyl chain interactions in biological membranes also have the saturated and unsaturated interactions. The study of the polymorphs of Sat-U-Sat triacylglycerols is very important to quantify fats and oils in food like cocoa butter, margarine etc. and in pharmaceuticals. The most important TAGs are 1-palmitoyl-2-oleoyl-3-palmitoyl glycerol [POP], 1-palmitoyl-2-oleoyl-3-stereoyl glycerol [POS] and 1-stereoyl-2-oleoyl-3-stereoyl glycerol [SOS]. (Yano et al., 1993; Yano & Sato, 1999) In these TAGs for β and β' forms, a triple chain structure is formed from the double bond of oleic acid. The oleic acid chain pack together and separately from the saturated acid chains. This results a kink in the molecular structure. The exception to this is the β' form of POP which has double chain structure. These differences in the polymorphic properties of triacylglycerols affect the melting and crystallization properties of the TAGs and in return the taste and physiological properties of food and pharmaceuticals. (Himawan et al., 2006; Rousset et al., 1998)

The monounsaturated triacylglycerols i.e., Sat-U-Sat possess a large diversity in chain length structure, methyl end packing, sub cell structure and glycerol group conformation. The cis double bond in the olefinic acyl chain of triacylglycerols has SCS' (skew-cis-skew') and SCS (skew-cis-skew) conformations. S has an internal rotational angle of +120 and S' has an internal rotational angle of -120. (M. Kobayashi & Kaneko, 1989) The structure of different polymorphs has been investigated by NMR techniques. The proton peaks for the glycerol carbons in TAG are different for the α , β and γ polymorphs. The signals for the carbonyl carbons and olefinic carbons appear differently for the different sub cells of the TAGs polymorphs. (Arishima et al., 1996) These NMR studies are very useful to study the mobility and passive diffusion of TAG across biological membranes. (Eads et al., 1992)

1.2 Biological significance of Triacylglycerols

Triacylglycerols are the main source of energy reservoirs in animals. (Yano et al., 1993) Triacylglycerols are a source to store the metabolic energy in biological tissues. Triacylglycerols are less oxidized than carbohydrates or proteins and provide more energy per unit mass on complete oxidation. The non-polar fats are stored in anhydrous form inside the cytosol of the cell. In contrast to triacylglycerol, the glycogen binds twice its weight of water molecules with them under physiological conditions. This makes triacylglycerols to provide 6 times more energy of an equal weight of hydrated glycogen. In animals triacylglycerols are stored in the adipose cells. Adipose tissue is the most abundant in a subcutaneous layer and in the abdominal cavity. The fat reservoirs in the cells of normal humans (21 % for men and 26 % for women) helps them to survive under starvation for 2 or 3 months. (Voet, Donald, Voet, 1999) The adipose tissues which store fat droplets are called adipocytes. The adipocytes are classified into two types i.e., white, and brown adipocytes with different physiological functions. The adipocytes are believed to be heterogeneous in their physiological function. Some function as long-term energy stores and others e.g., perinodal adipocytes adjacent to lymphoid cells in mammals, function as short-term stores of energy for TAGs. The subcutaneous layer provides thermal insulation to warm blooded aquatic animals whales, seals, geese, and penguins. (Murphy, 2001)

In most of the animals the cytosolic lipid bodies are present in all animal tissues. These contain neutral lipids i.e., TAGs within the small droplets of 1 μm diameter. The mobile acyl chains of the TAGs are recognized by specific resonance signals in the ^1H NMR. These NMR signals have been used in the diagnosis and prognosis of human brain tumor and other malignant stages. (Murphy, 2001) However, there is a little doubt about that either these NMR signals originate from TAG microdomains in the membrane or the cytosolic lipid bodies. The cytosolic lipid bodies are still agreed to give the NMR signals despite all these controversies. (Schmitz & Muller, 1991; Wennerberg et al., 2001)

The plant seeds store triacylglycerols in the form of lipid droplets (LD) in the cytosol of the seed cell. Germination of plant seed and growth of new plant is mobilized by the energy from these lipid droplets of the triacylglycerols. Lipid droplets (LD) of triacylglycerols are present in almost every cell of the plant and they help in many important processes inside the plant like stress responses, pathogen resistance and hormone signaling during plant growth. (Chapman et al., 2012) Triacylglycerol LDs provide hydrophobic barrier as protective covering to the pollen coat in the plant fruit during the gradual death of the cell. These also provide hydrophobic protective barrier in the outer covering of the mammalian skin. (Schwartz & Wolins, 2007) The protein molecules are associated with lipid droplets (LDs) in the plants and play important role in several physiological and biogenetic functions. Oleosins proteins are small sized and most abundant in seeds of plants. These bind to LDs and prevent the coalescence of LDs during seed desiccation. Oleosins regulate the size and stability of LDs in the seed. Upon the seed imbibition and germination, TAGs in these LDs produce fatty acids upon mobilization. Sucrose is

produced during mobilization of lipid droplets. The second type of proteins associated with LDs are caleosins. Caleosins are important to serve for the structural and functional roles in the LDs life cycle. The third type of LDs-associated protein in plants are steroleosins. Steroleosins have N-terminal hydrophobic part that attaches with LDs and a C-terminal HSD part. (Figure 1.5) (Murphy, 2001)

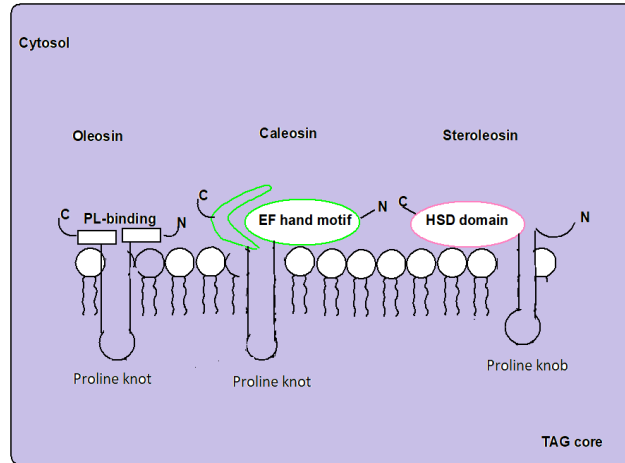


Figure 1.5 Structural representation of oleosins, caleosins and steroleosins at the surface of a TAG-filled lipid droplets (LD)

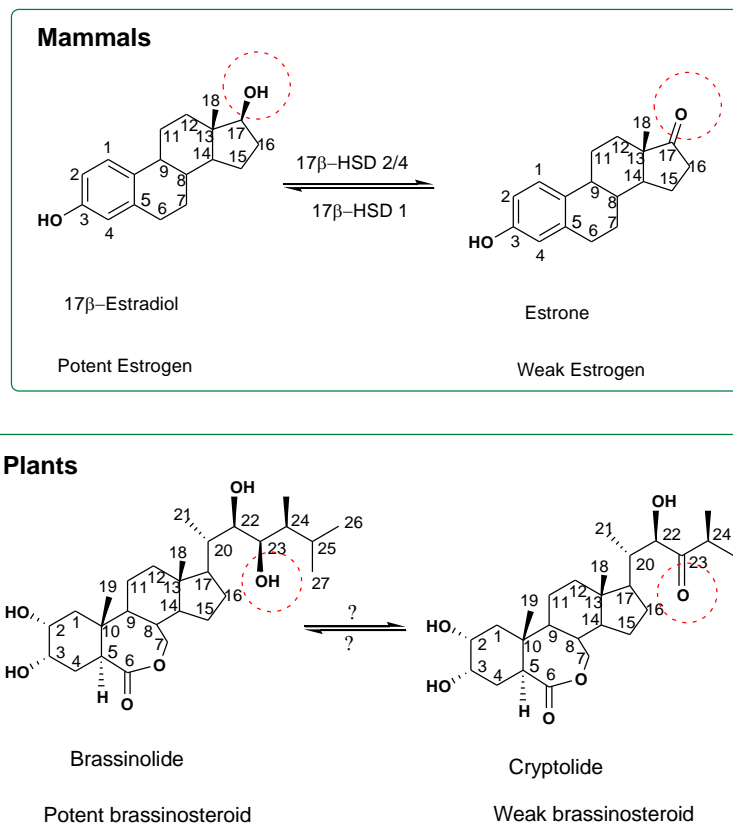


Figure 1.6 Structure and interconversion of steroid hormones in animals and plants (Mammals= 17 β estradiol; plants= brassinolide)

In mammals, the concentration of biologically active and less active forms of many steroid hormones is regulated by the HSD class of enzymes. For example, 17 β -estradiol a potent estrogen hormone in mammals is dehydrogenated by 17- β -HSD 2/4 and a less active ketone-containing estrone derivative

is formed. In plants brassinosteroids (BR) is metabolized by steroleosins. BRs play an important role in growth, development, fertility, and stress responses in the plants. (Figure 1.6)

Triacylglycerols play many important biological and physiological roles in living organisms. Lipids are an essential component of biological membranes. They help in lipid mobilization, trafficking at endoplasmic reticulum, cell signaling and lipid biogenesis. Plasma membrane is composed of lipid bilayer. In plasma membrane the lipids are attached at the upper and lower layers with the polar heads towards outside and hydrophobic hydrocarbon chains towards the inside. The protein molecules are embedded in the lipid bilayer.

Lipid intake in diet regulates the lipid composition of the membrane. Although triacylglycerols do not form the lipid bilayer, triacylglycerols and fatty acids can change the phospholipid mesomorphism. The molecular mechanisms involved for these interactions are not well discovered yet. (Prades et al., 2003) In biological membranes, the most commonly present fatty acids are palmitic, oleic, linoleic, and stearic acids. Almost one half of the fatty acids in the membranes are unsaturated and are called polyunsaturated. The double bond in these unsaturated fatty acids has cis configuration and a rigid bent structure at 30°. Unsaturated fatty acids pack less closely than saturated fatty acids. This results in reduced van der Waals interactions of unsaturated fatty acids. As a result, the melting points of the fatty acid decreases with increase of unsaturation and fluidity of lipid bilayer increase. On the other hand, the saturated fatty acids are highly flexible molecules due to reduced or saturated structure. The C-C bond is freely rotating and has least steric hinderance. The melting points of saturated fatty acids increase with an increase in the molecular weight. (Pérez-Gil, 2008)

The fluidity of biological membranes is an important physiological aspect in the life of living organisms. It is useful to describe the fluidity of lipid bilayer in terms of its melting point and the transition temperature from an ordered crystalline form to a fluid liquid crystal. When the lipid bilayer cools down below the transition temperature, it undergoes phase transition into a gel like solid and its fluidity is decreased. Above the transition temperature, mobile lipids attain an ordered liquid crystal state. The lipid bilayer is then less thick and fluidity of the biological membrane increases. The transition temperature of most biological membranes is between 10 to 40 °C. (Mansilla et al., 2004; Voet, Donald, Voet, 1999) The fluidity of the biological membranes is associated with the chemical structure of fatty acids in them. The transition temperature of the lipid bilayer increases with the increase in the chain length and degree of unsaturation of fatty acid residues and vice versa. Similarly, the melting points of the bilayer increase. Bacteria and cold-blooded animals such as fish, control and reduce the fluidity of the membranes with increase in the production of shorted chain and less unsaturated fatty acids. (Marsh, 2010) X-ray diffraction studies have shown that unsaturated triacylglycerols i.e., triolein (OOO), trilinolein (LLL) and trilinolenin (LnLnLn) undergo phase transition changes with the change in temperature in the liposomes. (Prades et al., 2003)

The lipid bilayer is selectively permeable. It regulates the flow of less viscous liquids across the cell boundary. The fluidity of the biological membrane is very important to facilitate the absorption of the drugs. (Cocucci et al., 2017) The interphases at the lipid are heterogenous in chemical composition and polarity. The position of the protein at the bilayer determines the kinetics and energetics of the membrane interactions during membrane trafficking and cell signaling. (Cho & Stahelin, 2005) The lipid-protein interactions provide transient and dynamic microdomains for the vesicle formation. These interactions are useful in membrane trafficking and signaling of the drugs. The diffusion permeability coefficient of a molecule is calculated for developing the suitable drugs in pharmacokinetics and therapeutics. (Figure 1.7) (T. Kobayashi et al., 1998; Wadhwa et al., 2021)

Lipid bilayer membrane possesses the unique property of diffusion. The hydrocarbon fatty acid chain of the lipid bilayer and neutral TAGs are in constant random motion. This Brownian movement of the fatty acid chains results in the diffusion across the biological membranes. The rates of diffusion depend upon the temperature of the viscous fluid, molecular density, and the random forces of collision. The limited motion of the lipid's bilayer and the restriction of lateral mobility increases the viscosity of the bilayer. This diffusion in the lipid bilayer is quantified by the diffusion coefficient D . (S. Block, 2018; Marguet et al., 2006) The diffusion coefficients are larger for the small-sized molecules, less viscous fluid, and the higher temperature. The diffusion coefficients of membranes can be calculated by measuring viscosity of the membrane. From the viscosity and diffusion coefficient, it is possible to determine the amount of lipids in the membrane. The increase in phospholipid content in the membranes results in the increase of membrane viscosity. As a result, the diffusion coefficients are decreased. (Mika et al., 2016) The diffusion is involved in several biochemical processes e.g., protein aggregation and transportation in intercellular systems. The main processes involved are shown in fig. 1.7. So, the development of analytical methods to measure the diffusion coefficients of biological molecules such as proteins, TAGs is very important. (Wang & Hou, 2011)

Triacylglycerols are mobilized from the adipose tissues and transferred to the blood plasma for energy utilization. In humans the rate of mobilization of fatty acids decreases in the order as, $C20:5, n-3 > C20:4, n-6 > C18:3, n-3 > C18:2, n-6 > C22:6, n-3$. Interestingly, the TAGs which are respectively precursors of the 3- and 2-series of prostaglandins i.e., $C20:5, n-3$ and $C20:4, n-6$, had been observed to mobilize preferentially. The chemical structure of triacylglycerols is very crucial in their mobility across adipose tissues. The chain length of fatty acids and degree of unsaturation alter the rate of mobilization. Increase in the chain length of fatty acid chain for a given degree of unsaturation decreases the relative rate of mobilization. On the other hand, the rate increases with increase in the unsaturation for the same chain length. (Lafontan & Langin, 2009) The mobilization of triacylglycerols is an important phenomenon in the life of humans and other living organisms. The abnormalities in the intracellular TAG mobilization causes inherited metabolic disorder such as Wolman's disease (WD)

and neutral lipid storage disease (NLSD). The TAGs lipolysis occurs in the presence of enzymes. It is very important in the metabolism of living organisms including humans. The non-esterified fatty acids (NEFA) and glycerol are formed during the lipolysis. Some of the NEFA are re-esterified into intracellular TAGs and glycerol is not re-utilized by the fat cells. An increased rate of lipolysis can result in metabolic disorders such as obesity. The obesity in human beings results in many diseases such as cardiovascular diseases, type II diabetes and cancer. The increase in lipolysis leads to weight loss. (Grönke et al., 2007) These studies are very important in drug discovery to develop new therapeutics that can develop antilipolytic pathways. The study of lipogenesis and lipolysis is important to develop new chemical entities for the treatment of obesity-related problems such as insulin resistance, dyslipidemia, and cardiovascular risk. (Gibbons et al., 2000)

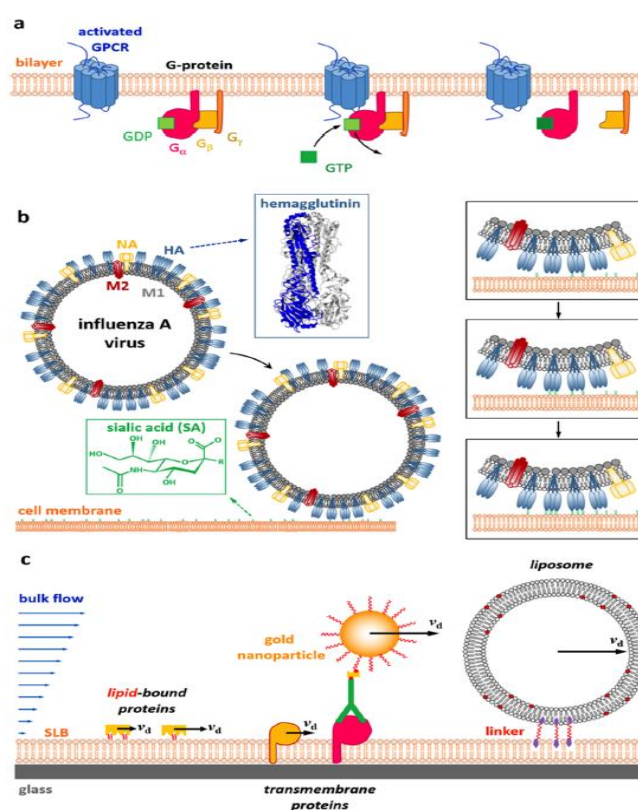


Figure 1.7 Diffusion of bilayer membrane (a) Cell signaling via complex formation (b) Receptor-mediated virus diffusion (c) Differences in the mobility or size of the membrane-associated objects (e.g., proteins, lysosomes) (S. Block, 2018)

Characteristic physical properties of TAG mixtures such as solidification, melting and polymorphic behavior give each product its own characteristics (Sato, 1996). For example, the spread ability of butter and lipstick, hardness of chocolate, quality of ointments, and the consistency of whipped cream are all determined by the polymorphic phase of the fat component. Likewise, temperature-dependent polymorphic phase transitions are held responsible for product degradation, e.g., fat-bloom formation at the chocolate surface. To understand the complex crystallization processes and totally control the

manufacturing processes, crystal-structure information of various TAG polymorphs is indispensable. (Langevelde et al., 2000)

During storage, several post crystallization processes occur, which can affect properties of TAGs such as hardness, which often noticeably increases. This is due to sintering, i.e., the formation of solid bridges between crystals to form a network. Polymorphic transformation towards more stable phases and changes in size distribution via Ostwald ripening may occur. The study of fat crystallization is thus a valuable activity as a greater understanding of fat crystallization enables fractionation and food processes to operate more efficiently and the functional effectiveness of fats in food products to be optimized. (Minato et al., 1996)(Himawan et al., 2006)

1.3 Biosynthesis of Triacylglycerol

Triacylglycerols are composed of fatty acids and glycerol back bone. Fatty acids are synthesized in every cell of the plant. During photosynthesis light energy is converted into chemical energy and carbohydrates are synthesized during Krebs cycle. As a result of this reaction triose phosphate are produced (TPs). (Figure 1.8) These TPs are then used to synthesize lipids (TAGs), starch and amino acid. (Schnurr et al., 2004; Xu & Shanklin, 2016)

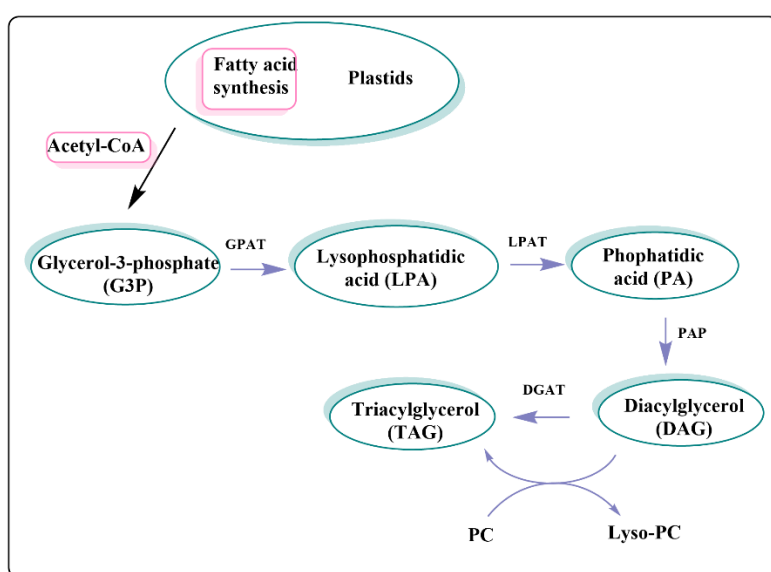


Figure 1.8 Schematic representation of biosynthesis of TAGs

Fatty acid biosynthesis takes place through condensation of C_2 units, and it is reverse of the β -oxidation process. David Rittenberg and Konrad Bloch in 1945, demonstrated with isotopic labelling techniques that these C_2 condensation units are derived from acetic acid. Later research showed that both acetyl-CoA and bicarbonate are needed and a C_3 unit, malonyl-CoA is an intermediate in the biosynthesis of fatty acids. (Bloch, 1976)

The starting material for the fatty acid synthesis i.e., Acetyl-CoA is produced in the mitochondrion via the oxidative decarboxylation of pyruvate in the presence of pyruvate dehydrogenase enzyme. (Bloch, 1976) Fatty acids are biosynthesized in the cytosol and later they are transported to the endoplasmic reticulum for the synthesis of triacylglycerols (TAGs). (M. A. Block & Jouhet, 2015)

Acetyl-CoA passes through impermeable mitochondrial membrane and enters the cytosol through the tricarboxylate transport system. (Figure 1.9) ATP-citrate lyase catalyzes the conversion of citrate into oxaloacetate. (Somerville et al., 2008)



Oxaloacetate is then reduced to malate by the malate dehydrogenase. Malate is decarboxylated to pyruvate by malic enzyme and returns to mitochondria in this state. The NADPH produced during these processes is utilized in the reductive processes of fatty acid biosynthesis. (Hele, 1958)

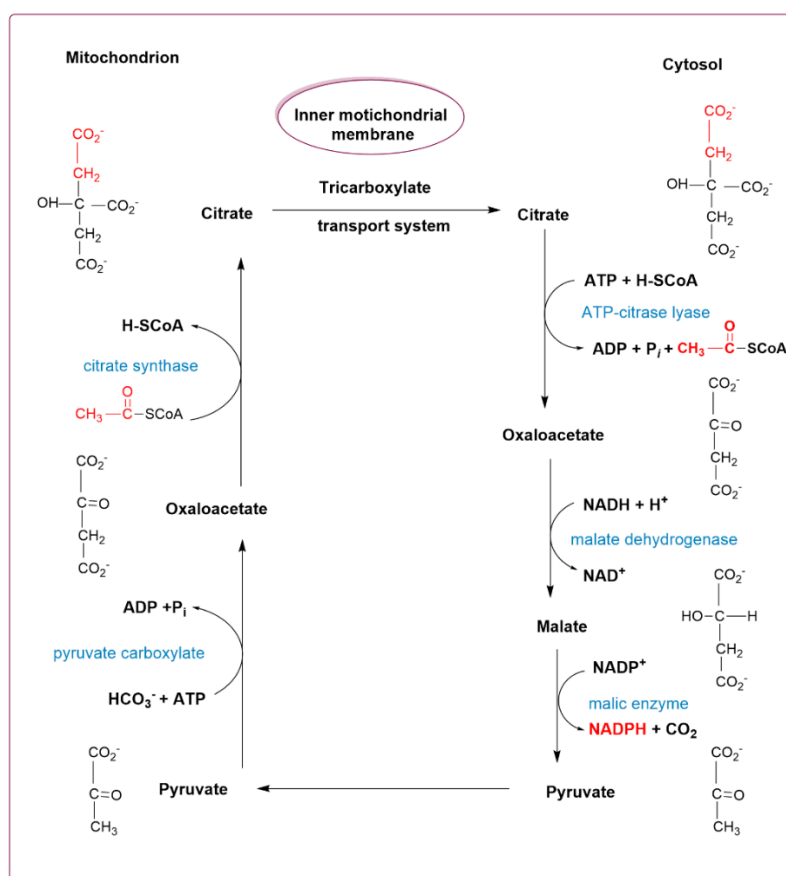
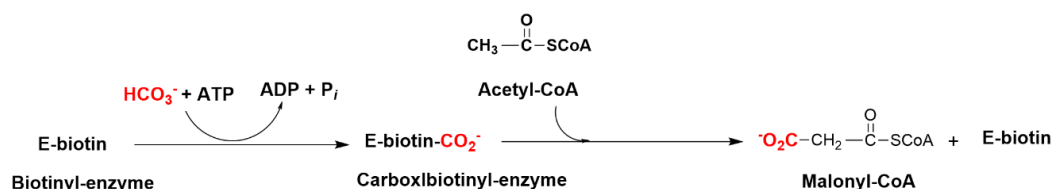


Figure 1.9 The tricarboxylate transport system to transfer acetyl-CoA from the mitochondrion to the cytosol

Acetyl-CoA carboxylase catalyzes the first step of fatty acid biosynthesis which is one of the rate-controlling steps. It involves two steps, a CO_2 activation, and a carboxylation. (Figure 1.10) (Xu & Shanklin, 2016)

Figure 1.10 CO₂ activation by Biotin-enzyme and formation of malonyl-CoA

In mammals, the acetyl-CoA carboxylase is a 230-kD polypeptide. It is responsible for allosteric and hormonal control in mammals. The enzymatic activity of acetyl-CoA carboxylase is stimulated by citrate. It involves the biotin prosthetic group and increase in V_{\max} . Acetyl-CoA carboxylase is a substrate for many kinases. It has 6 phosphorylation sites but only Ser-79 phosphorylation results in enzyme inactivation. Glucagon and epinephrine both promote the phosphorylation of Ser-79 and inhibit its dephosphorylation. (Voet, Donald, Voet, 1999) In contrast to this insulin activates dephosphorylation of acetyl-CoA carboxylase and activates the enzyme. In *E. coli*, the acetyl-CoA carboxylase is a multisubunit protein. The guanine nucleotide regulates its activity and fatty acid synthesis has been coordinated with cell growth. Prokaryotes do not synthesize TAGs for energy storage and fatty acids are used as primary phospholipid precursors. (Alvarez, 2016)

The proteins mainly involved in the synthesis of fatty acids are 2500-kD multifunctional enzyme in yeast with the composition $\alpha_6\beta_6$ and in animals it is 534-kD multifunctional enzyme with two identical polypeptide chains.

The synthesis of fatty acids starts from acetyl-CoA and malonyl-CoA, and it involves seven enzymatic steps. These reactions were first studied in *E. coli*. The growing fatty acid is attached with acyl-carrier protein (ACP). (Rawlings, 1998) ACP has a phosphopantetheine group and forms a thioester group with an acyl group. In CoA, the phosphopantetheine group is attached with adenosine monophosphate (AMP) and in ACP the phosphopantetheine group is esterified with the Ser OH group. (Figure 1.11) (Voelker & Kinney, 2001)

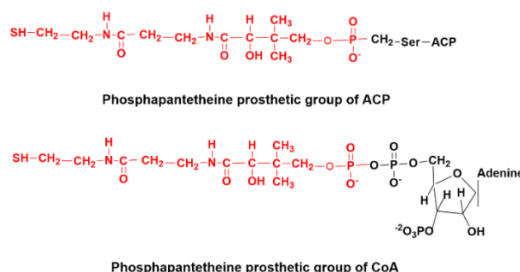


Figure 1.11 The phosphopantetheine group in acyl-carrier protein (ACP) and in CoA

In *E. coli* ACP is a 10-kD polypeptide and in animals ACP is a part of multifunctional polypeptide chain. The reaction sequences for the biosynthesis of fatty acids are given in figure 1.12. The biosynthesis of fatty acids involves a series of condensation and reduction processes. Reactions 1 and 2 are

transacylation reaction in which synthase enzyme is loaded for the condensation reaction. (Rock & Cronan, 1996)

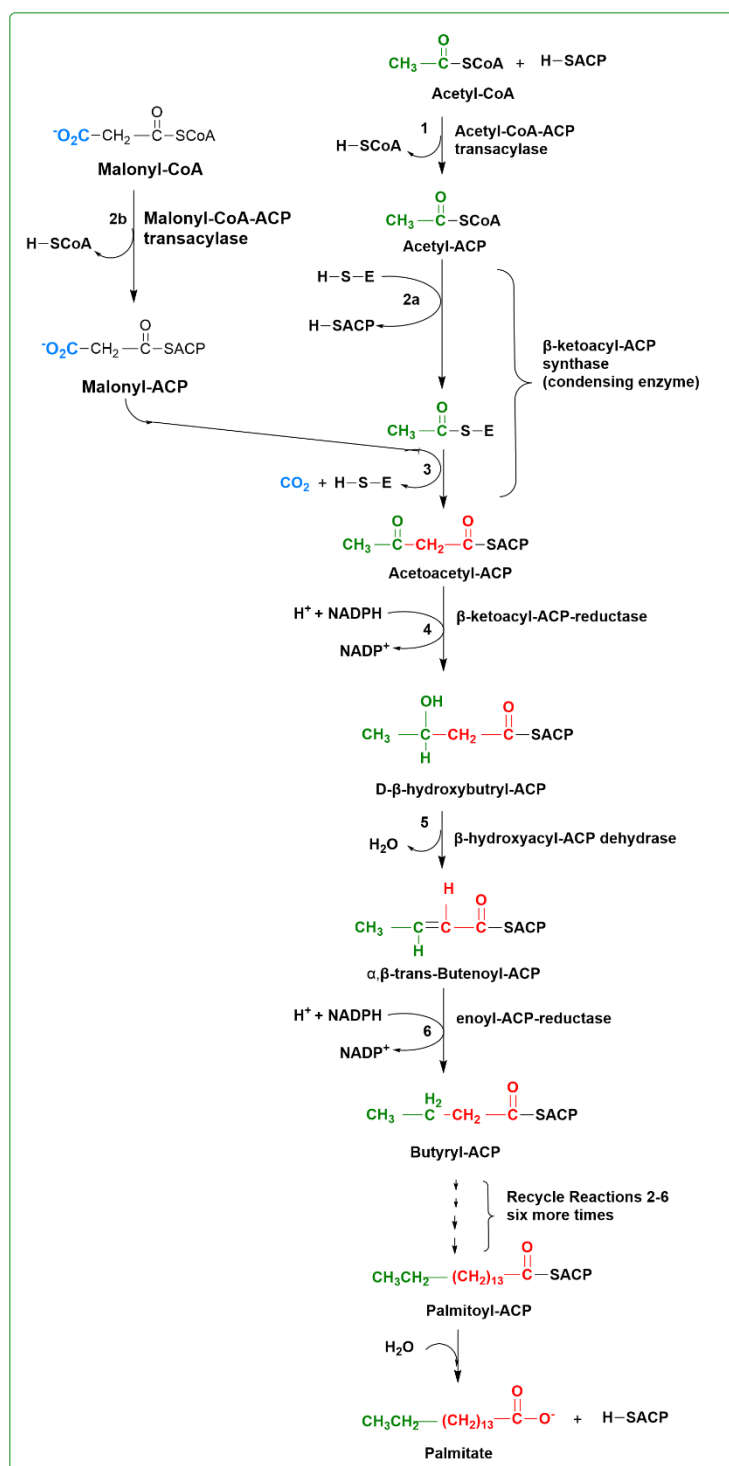
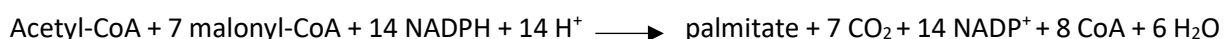


Figure 1.12 The reactions involved in the biosynthesis of fatty acids

In the reaction-3 the decarboxylation of malonyl-CAP results in the formation of a carbanion and C2 attack of the acetyl group is facilitated. The basic chemistry in the carboxylation of acetyl group into malonyl group is to create a reactive site by the carbanion formation. The formation of C-C bond is an

endergonic process in which an active precursor is needed. Exergonic decarboxylation of malonyl-CoA provides acetyl-CoA carbanion. The β -keto group has been converted to an alkyl group in two reductions and a dehydration step. The NADPH acts as a coenzyme for the two reduction processes (reactions 4 and 6). The final products of fatty acid synthesis are 16:0-ACP and 18:0-ACP and unsaturated 18:1-ACP. These newly synthesized fatty acids are then utilized for biosynthesis of triacylglycerols in two ways i.e., either in the chloroplast by prokaryotic way or by eukaryotic way in the endoplasmic reticulum.

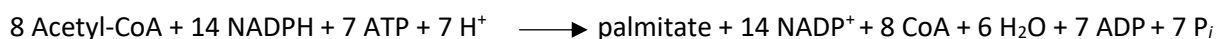
The stoichiometry of palmitate synthesis is as:



The 7 malonyl-CoA are derived from acetyl-CoA as:



The overall stoichiometry of palmitate biosynthesis is as:



After the synthesis of fatty acid, which is mainly palmitic acid, the elongation and unsaturation take place in the fatty acyl chains. After the de-novo synthesis, the fatty acids are distributed among different tissues, e.g., in plants to form wax and cutin coverings. For example, 18:0 fatty acid is used in wax biosynthesis and 16:0 and 18:1 for cutin biosynthesis. (Schnurr et al., 2004) The palmitic acid, stearic acid, oleic acid (18:1), linoleic acid (18:2) and linolenic acid (18:3) are the main fatty acid that are present in seed oils and in the membrane lipids. These are called as common acids. (Millar et al., 2000)

Triacylglycerols are synthesized from fatty acyl-Co-A and glycerol-3-phosphate or dihydroxyacetone phosphate. The most common and quantitative pathway for the biosynthesis of triacylglycerols is the Kennedy or glycerol phosphate pathway. (GURR, 1980) The glycerol-3-phosphate is converted to lysophosphatidic acid by glycerol-3-phosphate acyltransferase enzyme either in mitochondria or in endoplasmic reticulum. The conversion of dihydroxyacetone phosphate to lysophosphatidic acid occurs in two steps. (STYMNE & STOBART, 1987) First dihydroxyacetone phosphate is converted into acyl-dihydroxyacetone phosphate by the enzyme dihydroxyacetone phosphate acyltransferase. In the next step acyl-dihydroxyacetone phosphate is reduced by NADPH-dependent acyl-dihydroxyacetone phosphate reductase to lysophosphatidic acid. The lysophosphatidic acid is then converted into triacylglycerols via a series of steps. (Cagliari et al., 2011) Each step is catalyzed by an enzyme. 1-acylglycerol-3-phosphate acyltransferase catalyzes the formation of phosphatidic acid from lysophosphatidic acid. Phosphatidic acid is converted into diacylglycerol by the action of phosphatidic acid phosphatase and diacylglycerol into triacylglycerol by diacylglycerol acyltransferase. The acyltransferases are not specific for the addition of fatty acyl-CoAs either in the chain length or degree

of unsaturation, but palmitate adds to position 1 and oleate at position 2 in the triacylglycerols. (Figure 1.13) (Lehner & Kuksis, 1996)

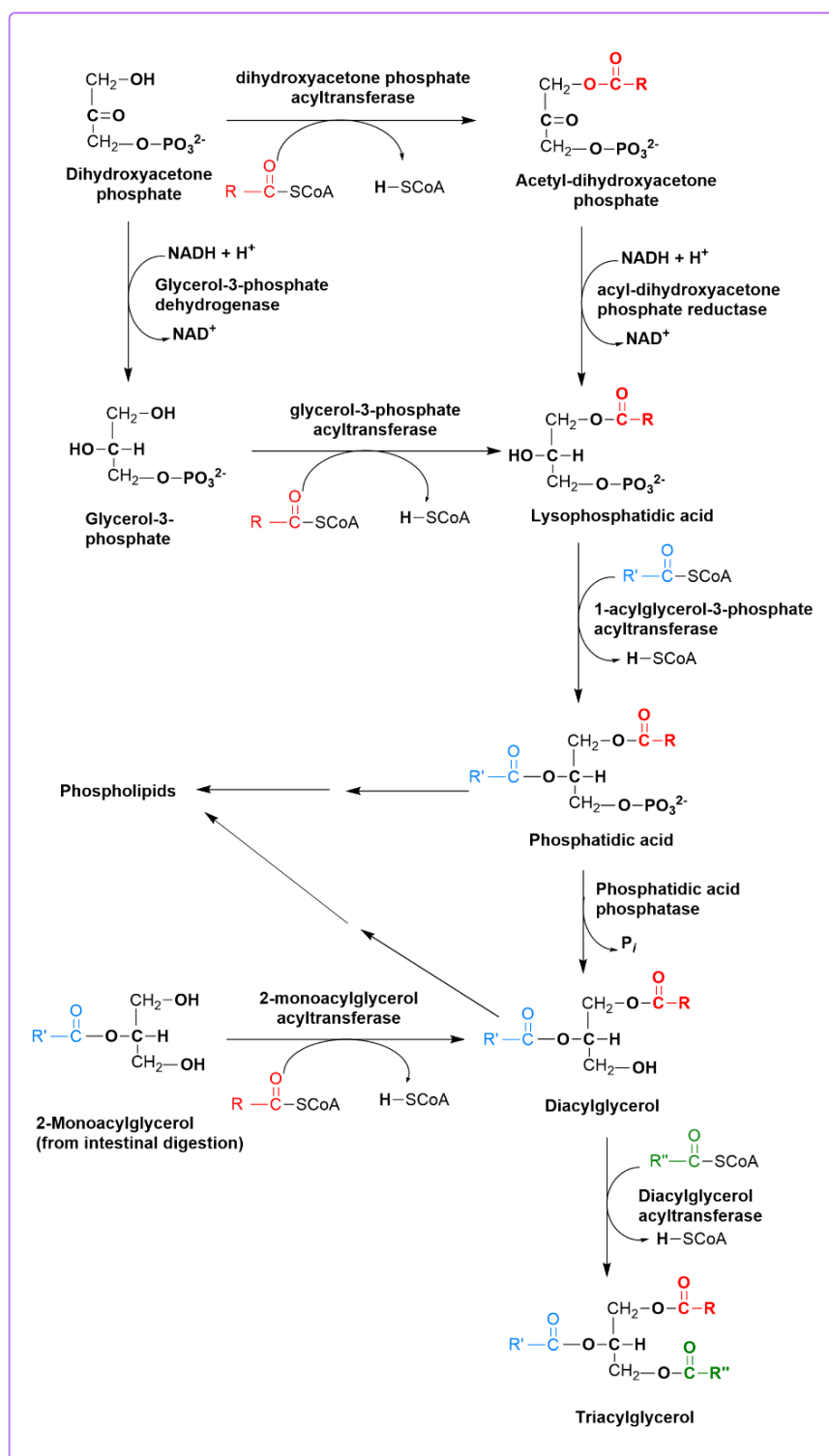


Figure 1.13 Chemical reactions of the biosynthesis of TAGs

1.4 Biomolecules in nature

Living organisms contain many molecules known as biomolecules. These are very important in the life of living organisms as they maintain biological processes such as cell division, morphogenesis, or development. Biomolecules are either large sized i.e., macromolecules or small sized i.e., micromolecules. Macromolecules include proteins, carbohydrates, lipids, nucleotides, and nucleic acids while micromolecules include primary metabolites, secondary metabolites, and natural products. (TAKADA, 2013) Edwin Haslam named the biomolecules as the 'children of nature'. He used this term for mainly the secondary metabolites. (Haslam, 1989) The summary of the structure, function and biological importance of these biomolecules has been given.

1.4.1 Nucleotides and nucleic acids

Nucleotides are naturally occurring molecules that contain a nitrogenous base, sugar and a phosphate. The nucleoside contains a base and a sugar only. The bases are planar, heterocyclic derivatives of either purine or pyrimidine. The purines bases are bicyclic and are adenine (A) and guanine (G). The pyrimidines are composed of one nitrogen ring and include cytosine (C), uracil (U) and thymine (T). the sugar is either ribose or deoxyribose. The deoxyribose sugar lacks a hydroxyl group at 2' position. The phosphate group is attached to the either 2', 3' or 5' carbon of the sugar. Nucleotides are the basic units of ribonucleic acid (RNA) and deoxyribonucleic acid (DNA). Free form of nucleotides are energy molecules that perform important functions in biochemical processes. The common examples are adenosine triphosphate (ATP), adenosine diphosphate (ADP), flavin adenine dinucleotide (FAD) and nicotine adenine dinucleotide (NAD⁺). (Kit, 1967) The chemical structures of ATP and ADP are given in figure 1. 14.

ATP provides energy for the biochemical reactions, ion transport and cell movement by transferring its phosphate group to another molecule. In addition to energy transfer, nucleotides also help in metabolic reactions. They do this by transferring some substituent instead of the phosphate group. In plants, the repeated addition of glucose during starch synthesis is proceeded by the ADP-glucose. (Figure 1.15) Flavin adenine dinucleotide (FAD) and nicotine adenine dinucleotide (NAD⁺) are derivatives of nucleotides. They both facilitate oxidation-reduction processes in biological systems. Coenzyme A is a nucleotide derivative and helps in metabolism process. It does not take part in oxidation-reduction processes. It is derived from pantothenic acid (vitamin B₃). (Huang et al., 2000) Nucleotides join via 3' and 5' positions of their phosphate end and form polymers named as nucleic acids. The phosphates of the polynucleotides are acidic and at physiological pH nucleic acids are polyanions. (FILIPOWICZ, 1956)

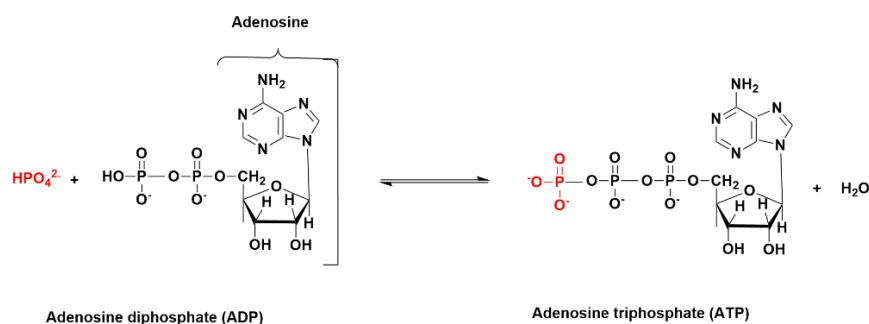


Figure 1. 14 The chemical structures of ATP and ADP

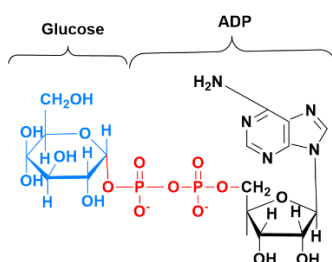


Figure 1.15 ADP-glucose. The glucose (blue) is attached to adenosine by two phosphate groups (red)

1.4.2 Amino acids, peptides, and proteins

Amino acids are building blocks of proteins. In 1939, the Dutch chemist G.J. Mulder used the term 'protein' for the nitrogen containing, molecules essential for the life of living organisms. The first amino acid was isolated in 1830. (Voet, Donald, Voet, 1999) Amino acids are found in both free form and bound by amide linkage in peptides and proteins. Amino acids contain a basic amino ($-\text{NH}_2$) group and an acidic carboxylic group ($-\text{COOH}$) in their molecule. So, they exist in the form of a zwitterion. (Figure 1.16) The α -carboxylic group has pK values in the small range of 2.2 and the α -amino group has pK near 9.2. in the living organisms, at the physiological pH (~ 7.4), the protonation of the amino groups takes place while the carboxylic group exist in the protonated conjugated form. (Hall, 1985)

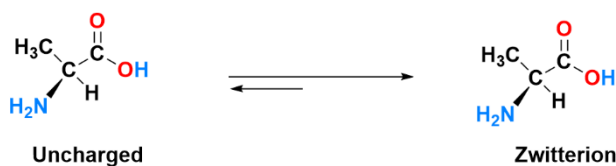


Figure 1.16 Uncharged and Zwitterionic form of alanine

There are 20 amino acids that are present in protein. The configuration of α - carbon atom in amino acid is either L- or D- these are assigned in chemical correlation with D- or L-serine or with D- or L- glyceraldehyde. All amino acids except glycine are optically active because α - carbon atoms of these amino acids are asymmetric. (Neuberger, 1948) The amino acids link together through amide bond to form peptides. The polymeric amino acid chains consisting of two, three and many amino acids are called dipeptide, tripeptide, and polypeptide. The proteins are made up of one or more polypeptide

chains. Proteins are very important in the physiological and biological functions of living organisms. They are a part of many enzyme catalysts and coenzyme that take part in biochemical processes. (Chothia, 1984)

Free amino acids and peptide produce taste in food. Ikeda in 1908, discovered that monosodium glutamate has the essential taste component of Japanese seasoners such as tangle. All free amino acids possess some of the tastes among sweetness, bitterness, sourness, and umami. Peptides and amino acids also contribute to the taste of vegetables. The specific taste of peptides depends on the sequence of amino acids and is an important scenario in food chemistry. (Kato et al., 1989)

1.4.3 Glycolipids

Glycolipids are the lipids that are linked to the carbohydrates by a glycosidic linkage. The glycosidic linkage is a covalent bond. Glycolipids are present in the plasma membrane where they facilitate the interactions of particles across the membrane. Glycolipids are important in immune function and growth control. (C. Jarrell, Harold; C. P. Smith, 1990)

Unlike proteins, carbohydrates do not catalyze the metabolic and biochemical reaction. They are a source of 40-50 % energy in living organisms. (Asp, 1994) The carbohydrates include raffinose, stachyose and dietary fiber like cellulose. When linked to lipids by the glycosidic covalent bond, they serve important functions in plants, animals, and bacteria. (Hans Englyst & Hudson, 1996) The carbohydrates are classified into different categories depending on the number of monosaccharide units present in them, degree of polymerization and the type of glycosidic linkage. Upon ring closure or cyclisation, the carbonyl carbon becomes chiral center and a pair of α and β anomers are formed for a particular monosaccharide. Conformations related to six carbon atom sugars become very important aspects. The furanoses and hexoses can adopt different chair conformations. The stabilities of these conformers differ depending upon the presence of bulky groups at either axial or equatorial positions. (Lichtenthaler, 2010) The complex carbohydrates i.e., polysaccharide is made up of three and more monosaccharide units joined together by glycosidic linkages. (Blaak & Saris, 1995)

Glycolipids are divided into two major classes which is based upon the hydrophobic nature of the linkage. Bacteria and plants consist of glycolipids which are made up of mono- and oligo saccharides linked glycosidically with glycerol-3 position of 1,2-diacylglycerols. The second class of glycolipids is present in animals and consists of carbohydrates glycosidically linked to ceramide glycosphingolipids. (Curatolo, 1943)

The main functions of glycolipids in the membrane are stabilization, shape determination, recognitions, and ion binding. The corynebacteria, mycobacteria and nocardia contain a variety of phosphoglycolipids such as diacyltrehalose which carry out the formation of long filamentous chains. Glycolipids are present in the brush borders of the intestinal wall and help in ion mobility. (Curatolo, 1987)

1.4.4 Terpenes

Terpenes are a class of natural products which are produced by a variety of plants and animals. These have been known as essential oils for centuries, produced by the steam distillation of plant materials. Over the centuries, these plant extracts have been used as medicines, spices, and perfumes. Chemically the plant essential oils consist of mixtures of lipids called as terpenes. These are known as secondary metabolites as these are derived from primary metabolites such as amino acids, sugars, and vitamins. (Perveen, 2018)

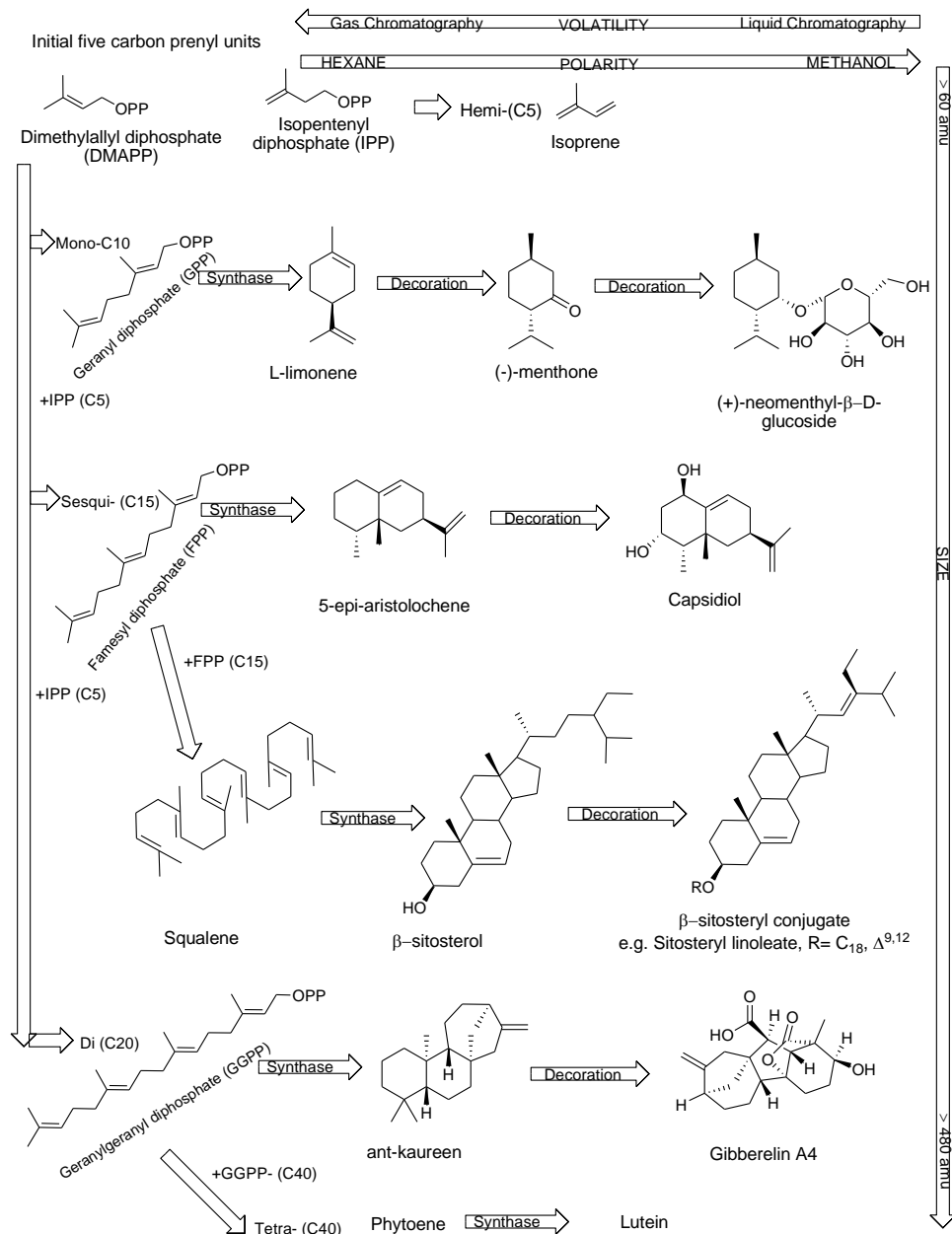


Figure 1.17 The scheme for the terpene metabolism. A presentation of different classes of terpenoid compounds and their classification based on volatility and polarity

The term terpenes have been used by the German chemist, August Kekule in 1866. (August 1866) Terpenes are simple hydrocarbons and some of them consist of oxygen. They are either open chain,

acyclic or cyclic molecules. The basic structural unit of terpenes is a 5-carbon isoprene unit. They are classified into different classes based on number of isoprene units present in their structures. These include hemiterpenes, (C₅), diterpenes (C₁₀), sesquiterpenes (C₁₅), sesterterpenes (C₂₅), triterpenes (C₃₀) and polyterpenes (\geq C₃₀). (Figure 1.17) (Jiang et al., 2016)

The chirality exists in the terpenes and different enantiomeric forms have different properties. For example, R- and S- stereoisomers of limonene have different flavor properties. R- (+)-limonene has an orange like odor whereas S-(-)-limonene has an odor like turpentine. (Figure 1. 18) (Pichersky & Gershenzon, 2002)

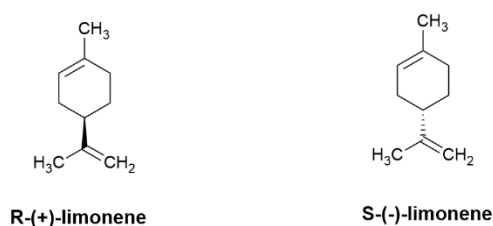


Figure 1.18 The chemical structures of R- and S- limonene

The diversity in the physiological and biological properties of terpenes has made them useful as flavor additives in foods, fragrances in perfumery and medicines aromatherapy. (Tholl, 2006) In nature, isopentenyl diphosphate as a precursor for the biosynthesis of terpenes. Isopentenyl diphosphate is synthesized either by the mevalonate pathway or the deoxyxylulose pathway. The mevalonate pathway synthesizes the isopentenyl diphosphate by a series of Claisen condensation, Aldol condensation, reduction, and phosphorylation processes. (Loreto et al., 2004)

Terpenes play important role as anti-inflammatory, antioxidants, and anticancer therapeutic agents in human beings. Paclitaxel and docetaxel are effective drugs for cancer chemotherapy. (Kiyama, 2017)

1.4.5 Steroids

Steroids are a class of secondary metabolites which are derived from triterpenes upon cyclisation. Steroids contain a basic cyclopentanoperhydrophenanthrene structure consisting of four rings. The four rings are designated as A, B, C and D. (Figure 1. 19) All steroids are a class of cholesterol. (McMurry, 2004)

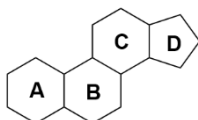


Figure 1. 19 Cyclopentanoperhydrophenanthrene

The steroids have a non-flat molecular structure due to the stereochemistry of the rings. The six membered rings (A to C) adopt a chair conformation in either cis or trans manner. In cis-decalin the groups at the junction of the two rings (angular group) are on the same side of the two rings. In trans-decalin the groups at the ring junction are on the opposite side of the two rings. An A-B trans steroid has C₁₉ angular methyl group directed in the upward direction and is said to be β -position. The C₅

hydrogen atom in the A-B trans steroid points down and is said to be in α -position. An A-B cis steroid has both C19 angular methyl group and the C5 hydrogen atom in the same direction i.e., the β -position. (Sultan, 2015) The steroids include sterols, bile acids, several hormones, and some hydrocarbons. In humans the steroids function as hormones and neurosteroids that act as chemical messengers and cholesterol. Cholesterol is the main component of plasma membrane. Cholesterol decreases the fluidity of membrane as the rigid ring system interacts with the fatty acid side chains in the other membrane lipids. Cholesterol optimizes the Vander Walls interactions of the phospholipids in the lipid bilayer. (Bloch, 1976) plants contain small amount of cholesterol. Other steroids present in humans include sex steroids, corticosteroids, anabolic steroids, and vitamin D. The plants contain sterols with 28 and 29 carbon atoms mostly ergosterol, sitosterol and stigmasterol. Some insects also contain C27 sterols. (Heftmann, 1975)

All steroid classes and their metabolites play important roles in the physiology and biochemistry of living organisms in which these are found. Several synthetic steroids are being extensively used as anti-hormones, contraceptive drugs, anti-cancer agents, cardiovascular agents, osteoporosis drugs anti-biotics, anesthetics, anti-inflammatories, and anti-asthmatics. Cortisone has good therapeutic ability in treatment of rheumatoid arthritis. Several steroids have shown many physiological properties. Now-a-days steroids have been used as anti-tumor agents, as sedatives and in cardiovascular therapy. (Sedlacek & Smith, 1988)

1.4.6 Polyketides

Polyketides are a group of natural products with biosynthetic origin. They are synthesized from carbonyl building blocks i.e., acetyl-CoA and malonyl-CoA with polyketones as intermediates. Polyketides are important therapeutic agents in clinical uses and many polyketides are infamous food-spoiling toxins. There is a large diversity in the structure of the polyketide group of compounds. These include polyphenols, macrolides, polyenes, enediynes, and polyether. Polyketides play important biological activities as antibiotics, immunosuppressants, antiparasitic, cholesterol-lowering, and antitumoral agents. Due to their complex structures and importance as therapeutic agents, the polyketides are considered important precursors for the synthesis of natural drugs. The biosynthetic pathway of a polyketide is given in figure 1.20. An understanding of the biosynthetic pathways is thought to be useful to develop new drugs. Polyketides are biosynthesized by a Claisen condensation mechanism. This biosynthesis occurs in the presence of Co-enzyme A with the gradual addition of alkyl acyl moieties (via a). The second pathway is by β -keto processing (via a). Figure 1. 20 (Hertweck, 2009) Polyketides are divided into three types i.e., type I PKSs, type II PKSs and type III PKSs. The type I PKSs are basically multifunctional proteins with many functional domains. These are found in bacteria and fungi. The type II PKSs particularly present in bacteria, are formed by separate catalytic structures. The type III PKSs are mainly present in plants and bacteria. These are chemically simpler chalcone synthase

type enzymes and catalyze the formation of the product within a single active site. The understanding and study of assembly-line PKSs is important to study the biosynthesis of secondary metabolites, the evolution of genes that encode multiple homologous but functionally distinct units and expand the therapeutic perspective. (Nivina et al., 2019)

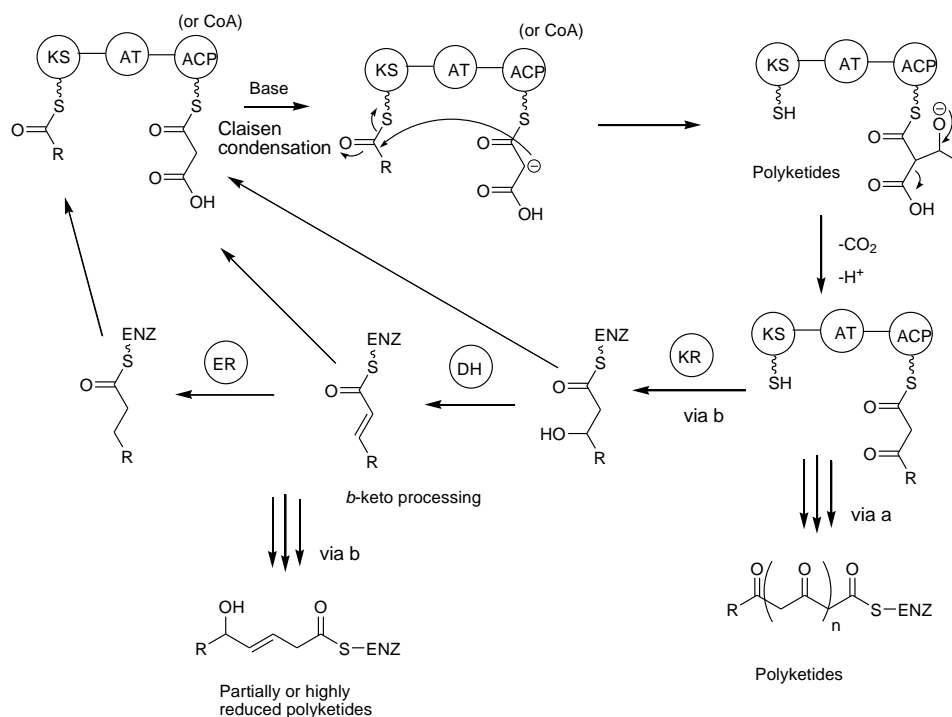


Figure 1. 20 The basic mechanism of biosynthesis of polyketides

1.4.7 Glycerophospholipids

Glycerophospholipids or phosphoglycerides are the major components of biological membranes. Glycerophospholipids are synthesized from by a de novo pathway in which phosphatidic acid (PA) and diacylglycerol (DAG) or cytidine diphosphate-DAG (CDP-DAG) are synthesized in the first step. The glycerophospholipids are the glycerol-3-phosphate molecules which consist of long chain fatty acids at sn-1 and sn-2 positions and a phosphoryl group at sn-3 position. The phosphoryl group is linked to another polar group i.e., X. due to the presence of non-polar hydrocarbon chains and polar phosphoryl-X groups, the glycerophospholipids are amphiphilic molecules. (Figure 1.21) (Hishikawa et al., 2014)

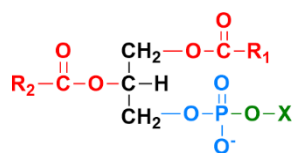


Figure 1.21 Glycerophospholipid

The glycerophospholipids are classified into various classes based on the type of polar head group present at sn-3 position of the glycerol back bone. These include phosphatidylcholine (PC), phosphatidylethanolamine (PE), phosphatidylserine (PS), phosphatidylinositol (PI), phosphatidylglycerol (PG) and cardiolipin (CL). The chemical structure of glycerophospholipids can be determined by the hydrolytic reduction of glycerophospholipids by the phospholipases enzymes.

(Yamashita et al., 2014) The chemical structures of the common glycerophospholipids are shown in figure 1.22.

The composition of glycerophospholipid is different in different cells, organelles, and inner and outer membranes. This is responsible for various physiological and biological functions of lipids such as signal transduction, vesicle trafficking, and membrane fluidity. A glycerophospholipid containing two palmitoyl chains at sn-1 and sn-2 position is an important component of lung surfactant. Some glycerophospholipids contain polyunsaturated fatty acids (PUFA) such as arachidonic acid, linoleic acid, EPA, and DHA. These glycerophospholipids are the major sources of fatty acid-derived lipid mediators and endocannabinoids. The unsaturated fatty acids in glycerophospholipids contribute to the phase behavior of all the lipid membranes. All membrane can adopt either solid or liquid phases depending upon the fatty acid component, the lateral diffusion coefficient and order parameter of saturated fatty acyl chain. (Van Meer et al., 2008)

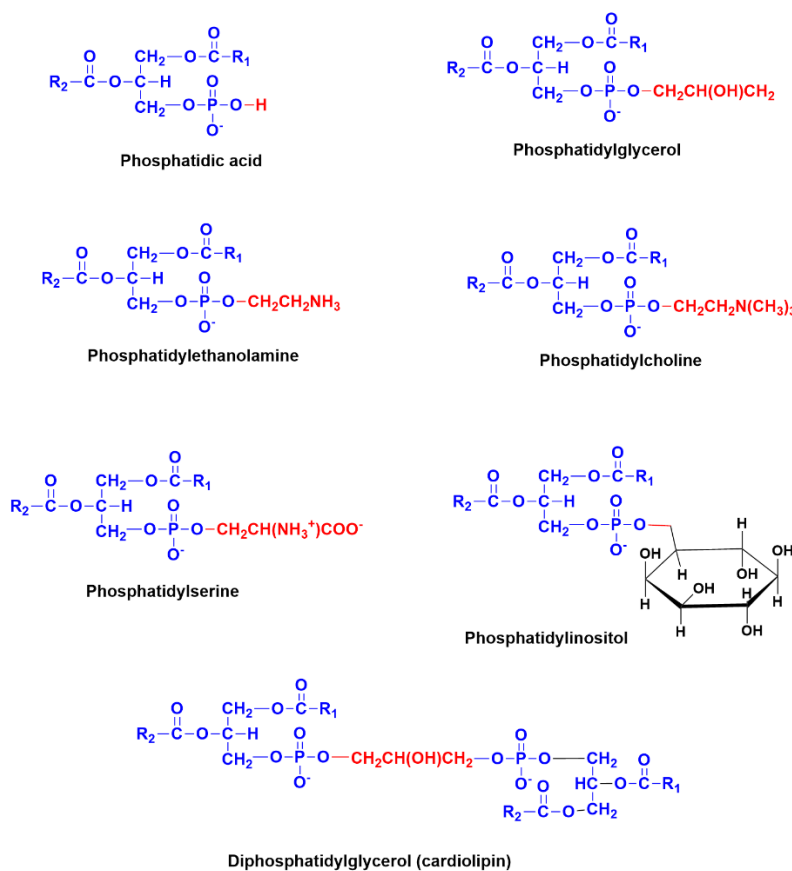


Figure 1.22 Common classes of glycerophospholipids

Mitochondria synthesize large amount of lipids which are then utilized in the biosynthesis of triacylglycerols. the most important are phosphatidylcholine (PC) and cardiolipin (CL) which help to accommodate membrane proteins. (Daum, 1985) The glycerophospholipids are arranged in an asymmetric pattern over the lipid bilayer forming micelles. The asymmetric distribution of lipids is important. For example, upon exposed on the cell surface, phosphatidylserine (PS) acts as a susceptibility signal for phagocytosis and as a propagation signal in blood coagulation. The translocation of lipids in the cytosolic bodies imbalances the lipid quantity and this causes the bending of the membrane for vesicle formation. Cone-shaped glycerophospholipids with small polar heads and bulky acyl chains (mono-unsaturated fatty acid-containing glycerophospholipids) are known to have important roles in membrane fusion and fission steps during endocytosis, exocytosis, cytokinesis, and vesicle trafficking. (Figure 1.23) (Pomorski & Menon, 2006)

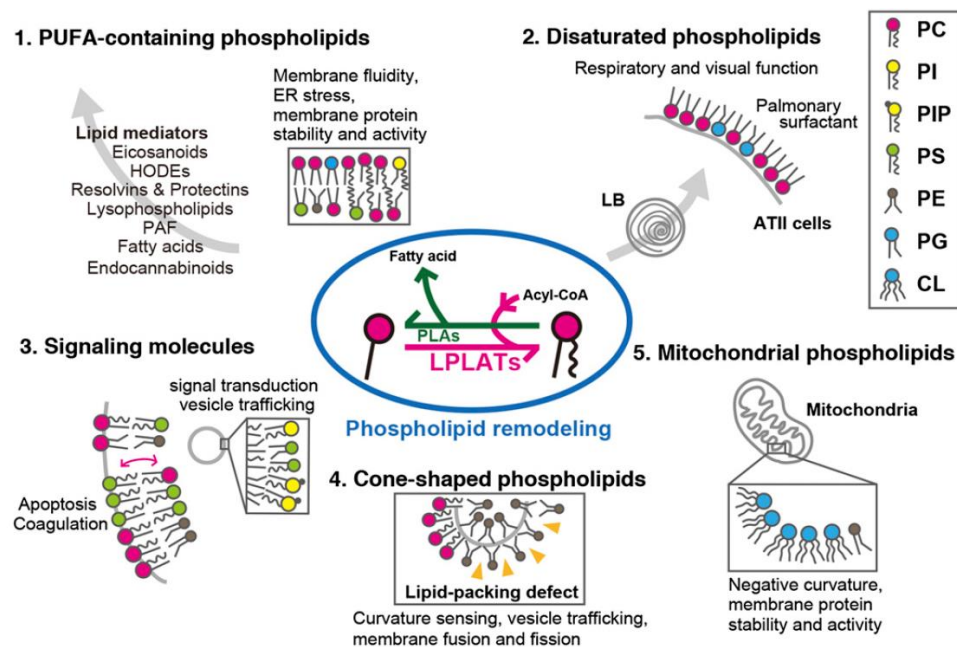


Figure 1.23 Cellular functions of glycerophospholipids. (PC = phosphatidylcholine, PE = phosphatidylethanolamine, PS = phosphatidylserine, PI = phosphatidylinositol, PG = phosphatidylglycerol, CD = cardiolipin, LB = lipid bodies, LPLATs = lysophospholipid acyltransferases) (Hishikawa et al., 2014)

1.4.8 Sphingolipids

Sphingolipids are a class of lipids that are the major components of membranes. These are mostly derivatives of sphingosine which is a C₁₈ amino alcohol with a trans double bond. Sphingolipids includes mainly ceramide (Cer), sphingosine (Sph), sphingosine -1-phosphate (S1P) and ceramide-1-phosphate (C1P) as bioactive molecules. Ceramides are the N-acyl derivatives of sphingosine. Ceramides are the parent compounds of sphingomyelins, cerebroside and gangliosides. The chemical structures of sphingomyelin, sphingosine and ceramide are shown in figure 1.24. (Hannun et al., 2009)

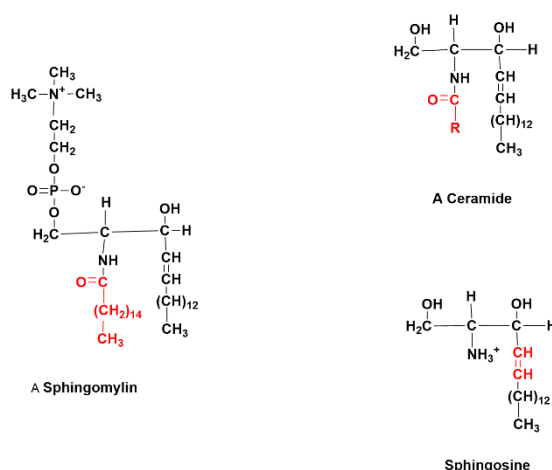


Fig. 1.24 Chemical structures of sphingomyelin, sphingosine, and ceramide

Sphingolipids play important role in cell metabolism and are important in cell signaling. Lipid membranes modify and control the phase behaviors due to the lipid–lipid interactions. The lipids of biological membranes can exist in multiple possible phase states. The most common are the lamellar states that are related to bio membranes. Non-bilayer lipid phases, such as hexagonal and cubic phases are related to transient bio membrane aspects, such as fusion, fission and pore formation. The adopted phase depends on lipid structure. The sphingomyelin (SM) contains long, saturated hydrocarbon chains. So, SM-rich mixtures usually adopt solid-like phases unlike unsaturated hydrocarbon chains in most bio membrane glycerophospholipids which tend to be enriched in liquid phases. (Hannun et al., 2009)

Accumulation of sphingomyelins (SM) and decrease in ceramide levels are implicated in tumor initiation, immune evasion, growth, and metastasis. Additionally, reports document SM roles in atherosclerosis, Alzheimer, and diseases caused by human immunodeficiency virus and prion invasion. Interactions of sphingolipid metabolism of numerous parasites, such as Plasmodium, Trypanosoma, Toxoplasma, Schistosoma with that of the host contribute to parasite survival and host defense. (Hannun & Obeid, 2018)

1.5 Dietary Oil composition

Dietary fats and oils are important constituents of human diet. Chemically vegetable oils and animal fats are triacylglycerols also called triglycerides. Mostly triacylglycerols consist of C16 and C 18 fatty acids. The most common are palmitic acid (16:0), stearic acid (18:0), linoleic acid (18:1) and linolenic acid (18:2). Among these fatty acids, and linolenic acid (18:2) is the essential fatty acid. Human body cannot synthesize and linolenic acid (18:2) and they need to take it in diet. Arachidonic acid (20:4) is the most common precursor of regulatory compounds. Unsaturated fatty acids have two conformations i.e., either cis or trans. The cis form is the most common in naturally occurring fatty acids. The presence of double bond in fatty acid chain produces a kink or bent in the fatty acyl chain.

This kink results in loose packing of fatty acid chains in triacylglycerols and lowers their melting points and increases the fluidity of the plasma membrane. (Alabi et al., 2015)

Fatty acids in fats and oils have positional isomerism regarding the position of double bond in the fatty acid chain. The different position of double bond in the fatty acid chain causes different metabolic rates in living organisms. Dietary trans fatty acids are found naturally in meat and dairy products due to anaerobic bacterial fermentation in ruminant animals. An intake of trans fatty acids increases cholesterol-HDL level and increases the risk of cardiovascular diseases. (Foster et al., 2009)

Triacylglycerols are composed of 90% by weight of fatty acids. The stereochemical distribution of fatty acids and their degree of unsaturation greatly affects the physiological properties of triacylglycerols. Triacylglycerols are hydrolyzed into free fatty acids and monoacylglycerols after consumption as food. In the intestinal cell, lipids are associated with nascent triacylglycerol-rich lipoprotein particle, called chylomicron. First the chylomicrons are secreted directly into the lymph then they enter the bloodstream. After entering the blood circulation, triacylglycerol is hydrolyzed before crossing the plasma membrane of peripheral cells for further metabolism. The lipoprotein lipase enzyme hydrolyzes triacylglycerol in plasma. (Dijkstra, 2015)

Phospholipids are a sub-type of fatty acids that are present in dietary fats and oils. These consist of fatty acid chains in sn-1 and sn-2 positions and a polar head group at sn-3 position. The amphipathic structure of phospholipids helps to store unsaturated fatty acids and fluidity of the plasma membrane. In the small intestine, they facilitate emulsification and absorption of fat and fat-soluble vitamin due to their amphipathic structure. Cholesterol is a constituent of animal food. It is also a component of plasma membrane with phospholipids. Cholesterol is an amphipathic molecule consisting of steroid nucleus and a branched hydrocarbon chain. Cholesterol decreases the fluidity of lipid bilayer by interacting with the phospholipids and restricting the mobility of the fatty acyl chains. The high intake of Cholesterol causes a risk for cardiovascular diseases. (Frérot & Lichtenstein, 2012)

High intake of triacylglycerols with saturated fatty acids results in heart diseases. Monounsaturated fatty acids are a source for lipid droplets known as adiposomes and help in cell signaling, regulation of lipid metabolism and control of the synthesis and secretion of inflammatory mediators. Now-a-days essential fatty acids have been considered as functional food components. A regular intake of food with unsaturated fatty acids is recommended for good health and to avoid disease risk. According to the National Health and Nutrition Examination Survey (NHANES) recall data from 1999–2000, the 10 major dietary sources of saturated fatty acids in US diets are regular cheese (6.0% of the total grams of saturated fatty acids consumed), whole milk (4.6%), regular ice cream (3.0%), 2% low-fat milk (2.6%), pizza with meat (2.5%), French fries (2.5%), Mexican dishes with meat (2.3%), regular processed meat (2.2%), chocolate candy (2.1%), and mixed dishes with beef (2.1%). Hence, most saturated fatty acids are contributed by regular dairy products (16%), and the top 10 sources contribute 30% of the total

saturated fatty acids consumed. A total intake of 10% energy contribution (% ERDI) saturated fatty acids has been recommended by the World Health Organization for a healthy life. (Orsavova et al., 2015)

1.6 Health effects of fats and oils

Dietary fats and oils have good, bad, and ugly effects on human health. Dietary fats and oils are composed of triacylglycerols, fatty acids, phospholipids, and cholesterol. These serve as good components for human life as they help to carry soluble vitamins (A, E, K and D). Fats and oils are good because these increase the bioavailability of fat-soluble nutrients and facilitate the synthesis of metabolically active compounds by providing them with the essential substrates. Fats and oils are components of biological membranes and lipoprotein particles where they help in intercellular and intracellular movement of substrates across the plasma membranes. They help in cell signaling via lipid trafficking and preventing carbohydrate-induced hypertriglyceridemia. (Chong et al., 2006)

The bad effects of fats and oils include the storage of fat-soluble toxic compounds in the human body. This results in several diseases. The accumulation of adipose tissues under the skin or in and around the organs causes obesity. The accumulation of excess metabolic bodies or decrease in the fatty acid component due to abnormalities in the lipolytic rates are the ugly aspects of fats and oils. This also includes the accumulation of saturated and trans fatty acids in the body. (DiNicolantonio & O'Keefe, 2017)

The animal fat contains a large amount of saturated fatty acids and cholesterol. A high intake of saturated fatty acids and cholesterol increases the risk of heart diseases. Plants oils and fats contain mostly unsaturated fatty acids i.e., monounsaturated fatty acids and polyunsaturated fatty acids. The tropical oils are an exception as they contain saturated fatty acids and are liquid at room temperature due to presence of short chain fatty acids. The risk of coronary diseases increases with the high intake of trans fatty acids in the diet. The intake of diet with saturated and trans fatty acids increases the level of low-density lipoproteins (LDL) and plasma low density proteins-cholesterol level. This results in a decrease in the concentration level of high-density lipoproteins (HDL). (Vicario et al., 2003) The accumulation of LDL-cholesterol causes the thickening of the arterial walls known as atherosclerosis. Atherosclerotic plaques are diagnosed at the later stage. These results in several health risks such as obesity, diabetes, and insulin resistance syndrome. (Badimon & Llorente-corte, 2004)

The cardiovascular diseases, Alzheimer disease, type 2 diabetes mellitus, obesity is related to an imbalanced food and energy intake. Hippocrates in the 4th BC proposed a direct relationship between human diet and human health. (Mozaffarian, 2016)

1.7 Quantitative and qualitative analysis

The chromatographic, spectrometric, and spectroscopic methods are usually used for the analysis of lipids and triacylglycerols. These methods are used for identification, quantification and regiospecific analysis of triacylglycerols in diets.

1.7.1 Ultraviolet spectroscopy (UV)

Ultraviolet spectroscopy (UV) referred to as absorption spectroscopy involves the absorption of ultraviolet radiation in the visible region of the spectrum. It is usually used for identification of transition metals and organic molecules containing conjugated systems. The energy differences between electronic levels in most molecules vary from 125 to 650 kJ/mol. UV/HPLC spectroscopy is used for the analysis of triacylglycerols (TAGs) in edible oils. In UV/HPLC a UV lamp is used to detect the TAGs separated by HPLC column. (Stübiger et al., 2003) UV spectroscopy is also used for adulteration of virgin olive oil with refined olive oil or olive residue oil based on the presence of conjugated polyene systems in the adulterated oils. UV absorption spectra have been observed for the adulterated oils, but the sensitivity is low since the virgin olive oils themselves show a wide range of absorptivity. (Li-Chan, 1994)

1.7.2 Infrared spectroscopy

Infrared spectroscopy (IR) is used to determine the functional groups in a molecule. It involves absorption of infrared radiation by a molecule in a quantized way. The absorption of infrared radiation corresponds to energy changes in the order of 8 to 40 kJ/mol. Radiation in this energy range cause stretching and bending vibrational frequencies of the bonds in most covalent molecules. IR spectroscopic data is useful to elucidate the structure of TAGs. Since TAG molecule contains C=O, hydrocarbon chain (CH₂-, CH₃- groups) and C=C for unsaturated fatty acids. IR spectroscopy has been used to determine the presence of trans double bonds in TAGs, but it does not help to locate the position of double bond in fatty acid chain. (Christie et al., 2007) Fourier-transform infrared spectroscopy (FTIR) is very useful to distinguish between TAGs of different origins. FTIR gives quantitative analysis of TAGs in edible oils and fats as intensities of the spectral bands are proportional to the concentration. (Lerma-García et al., 2010)

1.7.3 Mass spectrometry

Mass spectrometry (MS) is used to determine the molecular ion peaks of individual TAGs in a sample. The MS spectrum of individual TAG can be achieved with the ionized molecular ion peak M⁺ and ionized fragments of the molecule. Different ionization techniques have been used in mass spectrometry for analysis of different kinds of samples. Vegetable oils and fats are being analyzed by coupling mass spectrometry with high-performance liquid chromatography HPLC, gas chromatography GC and capillary gas chromatography CGC. (Řezanka & Mareš, 1991) The ionization techniques in mass spectrometry include electron ionization (EI) by a beam of high energy electrons (Hites & Hites, 1970),

chemical ionization of ionized reagent gas (Marai et al., 1994), secondary ion mass spectrometry (SIMS), fast atom bombardment (FAB) and matrix-assisted laser desorption ionization (MALDI). (Lamberto & Saitta, 1995) MALDI-MS has been used for lipid analysis in cellular membrane systems and for some edible oils. It provides a better analytical data than GC. (Lay et al., 2006)

1.7.4 High performance liquid chromatography

HPLC is the most important technique used for analysis of lipids. HPLC-MS (or simply LC-MS) couples an HPLC instrument to a mass spectrometer through a special interface. The components of a sample are separated by HPLC and detected by the mass spectrometer. The flow of eluting solvents is usually isocratic or gradient in modes. HPLC can be either normal phase or reverse phase. Usually reverse phase HPLC (RP-HPLC) has been used for the analysis of triacylglycerols. AS, in normal phase HPLC (NR-HPLC) TAG peaks overlap. (Rhodes & Netting, 1988) The use of silver ion HPLC (Ag-HPLC) techniques has been useful in the study of regioisomers of TAGs and to separate cis-trans isomers. (Zeitoun et al., 1991)

1.7.5 Nuclear Magnetic spectroscopy

High resolutions ^1H -NMR was first used for determination of degree of unsaturation in TAGs and average molecular weight of natural fats. (Johnson & Shoolery, 1962) ^1H -NMR spectroscopy has limited use in fatty acid analysis as it gives small range of chemical shifts for protons. ^{13}C -NMR complements ^1H -NMR technique in TAGs analysis. ^{13}C -NMR can be used to determine positional distribution of fatty acids in TAGs based on chemical shifts of esterified fatty acids in all three positions. Different stereoisomers can be isolated by different chemical shifts for 1-, 2- and 3- positions of fatty acyl chains in glycerol backbone. ^{13}C -NMR spectra of TAGs provide a wide range of chemical shifts which provide more information about structures of TAGs. (Lie Ken Jie & Mustafa, 1997) NMR spectroscopic techniques has been used for the qualitative and quantitative analysis of the compounds and mixtures. But now its application has become vaster. Two new techniques emerged in NMR spectroscopy. First is HPLC-NMR and is used to identify the components of complex mixtures eluted directly from HPLC column. The second NMR technique i.e., diffusion ordered spectroscopy (DOSY) allows to calculate the diffusion coefficients of components of mixture based on their molecular weights. DOSY is also useful in identification of unknown compounds in a mixture. (Morris, 2009)

1.8 Synthesis

The chemical synthesis of organic compounds is an old art. Earlier chemist used to synthesize inorganic compound sin the laboratory. There was an idea of vital force theory that organic compounds cannot be synthesized in the laboratory by chemical methods. The chemists at that time used to believe that the organic compounds are synthesized in nature by a super nature force. Due this believes the organic chemistry synthesis did not flourish until a century. In 1828, Friedrich Wohler synthesized urea, a natural fertilizer from an inorganic compound. So, this was the end of vital force and later many organic

compounds started synthesizing in the laboratory. (Schoch et al., 1947) the chemical synthesis can be either semi synthesis or total synthesis. Semi synthesis is a kind of partial synthesis that involves the synthesis of novel compounds from the chemical compounds separated from the natural sources. Usually, drugs are synthesized by the method of semi synthesis. On the other hand, total synthesis involves the synthesis of simpler and complex compounds from available chemical compounds. (Murakami et al., 2020)

References:

- Akita, C., Kawaguchi, T., & Kaneko, F. (2006). Structural study on polymorphism of cis-unsaturated triacylglycerol: Triolein. *Journal of Physical Chemistry B*, 110(9), 4346–4353. <https://doi.org/10.1021/jp054996h>
- Alabi, T. D., Olabiyi, F. A., Oguntibeju, O. O., Aguila, M. B., Mandarim-De-Lacerda, C. A., Dijkstra, A. J., Badimon, L., Llorente-corte, V., Frérot, E., Lichtenstein, A. H., Orsavova, J., Misurcova, L., Vavra Ambrozova, J., Vicha, R., Mlcek, J., Foster, R., Williamson, C. S., Lunn, J., Mani, V., ... Gabler, N. K. (2015). Fats and Oils. *Springer Handbooks*, 10(1), 1–9. <https://doi.org/10.1186/1743-7075-10-6>
- Alvarez, H. M. (2016). Triacylglycerol and wax ester-accumulating machinery in prokaryotes. *Biochimie*, 120, 28–39. <https://doi.org/10.1016/j.biochi.2015.08.016>
- Arishima, T., Sugimoto, K., Kiwata, R., Mori, H., & Sato, K. (1996). ¹³C cross-polarization and magic-angle spinning nuclear magnetic resonance of polymorphic forms of three triacylglycerols. *JAOCS, Journal of the American Oil Chemists' Society*, 73(10), 1231–1236. <https://doi.org/10.1007/BF02525451>
- Asp, N. G. (1994). Nutritional classification and analysis of food carbohydrates. *American Journal of Clinical Nutrition*, 59(3 SUPPL.), 679–681. <https://doi.org/10.1093/ajcn/59.3.679Sa>
- August, K. (1866). *Lehrbuch der organischen Chemie[Textbook of Organic Chemistry] (in German)* (Vol. 2). Enke, Ferdinand.
- Badimon, L., & Llorente-corte, V. (2004). *Atherogenesis*. 1, 278–287
- Beppu, F., Nagai, T., Yoshinaga, K., Mizobe, H., Kojima, K., & Gotoh, N. (2013). Quantification of triacylglycerol molecular species in cocoa butter using high-performance liquid chromatography equipped with nano quantity analyte detector. *Journal of Oleo Science*, 62(10), 789–794. <https://doi.org/10.5650/jos.62.789>
- Blaak, E. E., & Saris, W. H. M. (1995). Health aspects of various digestible carbohydrates. *Nutrition Research*, 15(10), 1547–1573. [https://doi.org/10.1016/0271-5317\(95\)02027-S](https://doi.org/10.1016/0271-5317(95)02027-S)

Bloch, K. (1976). On the Evolution of Biosynthetic Pathway. In *Reflections on Biochemistry* (pp. 143–146, 146a, 147–150). <https://doi.org/https://doi.org/10.1016/C2013-0-02804-6>

Block, M. A., & Jouhet, J. (2015). Lipid trafficking at endoplasmic reticulum-chloroplast membrane contact sites. *Current Opinion in Cell Biology*, 35, 21–29. <https://doi.org/10.1016/j.ceb.2015.03.004>

Block, S. (2018). Brownian motion at lipid membranes: A comparison of hydrodynamic models describing and experiments quantifying diffusion within lipid bilayers. *Biomolecules*, 8(2). <https://doi.org/10.3390/biom8020030>

C. Jarrell, Harold; C. P. Smith, I. (1990). NMR Applications in Biopolymers. In *Basic Life Sciences, Book series* (pp. 303–313). Springer, Boston, MA. https://doi.org/DOI : 10.1007/978-1-4684-5868-8_17

Cagliari, A., Margis, R., Dos Santos Maraschin, F., Turchetto-Zolet, A. C., Loss, G., & Margis-Pinheiro, M. (2011). Biosynthesis of triacylglycerols (TAGs) in plants and algae. *International Journal of Plant Biology*, 2(1), 40–52. <https://doi.org/10.4081/pb.2011.e10>

Chapman, K. D., Dyer, J. M., & Mullen, R. T. (2012). Biogenesis and functions of lipid droplets in plants: Thematic review series: Lipid droplet synthesis and metabolism: From yeast to man. *Journal of Lipid Research*, 53(2), 215–226. <https://doi.org/10.1194/jlr.R021436>

Cho, W., & Stahelin, R. V. (2005). Membrane-protein interactions in cell signaling and membrane trafficking. *Annual Review of Biophysics and Biomolecular Structure*, 34, 119–151. <https://doi.org/10.1146/annurev.biophys.33.110502.133337>

Chong, E. W. T., Sinclair, A. J., & Guymer, R. H. (2006). Facts on fats. *Clinical and Experimental Ophthalmology*, 34(5), 464–471. <https://doi.org/10.1111/j.1442-9071.2006.01250.x>

Chothia, C. (1984). Principles that determine the structure of proteins. *Annual Review of Biochemistry*, 53, 537–572. <https://doi.org/10.1146/annurev.bi.53.070184.002541>

Christie, W. W., Dobson, G., & Adlof, R. O. (2007). A practical guide to the isolation, analysis and identification of conjugated linoleic acid. *Lipids*, 42(12), 1073–1084. <https://doi.org/10.1007/s11745-007-3107-8>

- Cocucci, E., Kim, J. Y., Bai, Y., & Pabla, N. (2017). Role of Passive Diffusion, Transporters, and Membrane Trafficking-Mediated Processes in Cellular Drug Transport. *Clinical Pharmacology and Therapeutics*, 101(1), 121–129. <https://doi.org/10.1002/cpt.545>
- Curatolo, W. (1943). The Physical Properties of Nylon. *Textile Research Journal*, 13(7), 24–27. <https://doi.org/10.1177/004051754301300706>
- Curatolo, W. (1987). Glycolipid function. *BBA - Reviews on Biomembranes*, 906(2), 137–160. [https://doi.org/10.1016/0304-4157\(87\)90009-8](https://doi.org/10.1016/0304-4157(87)90009-8)
- Daum, G. (1985). Lipids of mitochondria. *BBA - Reviews on Biomembranes*, 822(1), 1–42. [https://doi.org/10.1016/0304-4157\(85\)90002-4](https://doi.org/10.1016/0304-4157(85)90002-4)
- Dijkstra, A. J. (2015). Vegetable Oils: Composition and Analysis. In *Encyclopedia of Food and Health* (1st ed.). Elsevier Ltd. <https://doi.org/10.1016/B978-0-12-384947-2.00708-X>
- DiNicolantonio, J. J., & O’Keefe, J. H. (2017). Good Fats versus Bad Fats: A Comparison of Fatty Acids in the Promotion of Insulin Resistance, Inflammation, and Obesity. *Missouri Medicine*, 114(4), 303–307
- Eads, T. M., Blaurock, A. E., Bryant, R. G., Roy, D. J., & Croasmun, W. R. (1992). Molecular motion and transitions in solid tripalmitin measured by deuterium nuclear magnetic resonance. *Journal of the American Oil Chemists’ Society*, 69(11), 1057–1068. <https://doi.org/10.1007/BF02541038>
- FILIPOWICZ, B. (1956). Structure of nucleic acids. *Postepy Biochemii*, 2(1), 15–60
- Foster, R., Williamson, C. S., & Lunn, J. (2009). Culinary oils and their health effects. *Nutrition Bulletin*, 34(1), 4–47. <https://doi.org/10.1111/j.1467-3010.2008.01738.x>
- Frérot, E., & Lichtenstein, A. H. (2012). Fats and Oils. *Springer Handbooks*, 2–4, 201–208. <https://doi.org/10.1016/B978-0-12-375083-9.00097-0>
- Gibbons, G. F., Islam, K., & Pease, R. J. (2000). Mobilisation of triacylglycerol stores. *Biochimica et Biophysica Acta - Molecular and Cell Biology of Lipids*, 1483(1), 37–57. [https://doi.org/10.1016/S1388-1981\(99\)00182-1](https://doi.org/10.1016/S1388-1981(99)00182-1)

Grönke, S., Müller, G., Hirsch, J., Fellert, S., Andreou, A., Haase, T., Jäckle, H., & Kühnlein, R. P. (2007). Dual lipolytic control of body fat storage and mobilization in *Drosophila*. *PLoS Biology*, 5(6), 1248–1256. <https://doi.org/10.1371/journal.pbio.0050137>

Grossert, J. S., Herrera, L. C., Ramaley, L., & Melanson, J. E. (2014). Studying the chemistry of cationized triacylglycerols using electrospray ionization mass spectrometry and density functional theory computations. *Journal of the American Society for Mass Spectrometry*, 25(8), 1421–1440. <https://doi.org/10.1007/s13361-014-0917-9>

GURR, M. I. (1980). The Biosynthesis of Triacylglycerols. In *Lipids: Structure and Function* (Vol. 4). ACADEMIC PRESS, INC. <https://doi.org/10.1016/b978-0-12-675404-9.50014-x>

Gurr, MI; James, A. (1975). *Lipid Biochemistry* (2nd ed.)

Hall, C. and. (1985). *Chemistry and Biochemistry of the Amino Acids* (G. C. Barret, Ed.; 1st ed.). <https://doi.org/10.1007/978-94-009-4832-7>

Hannun, Y. A., & Obeid, L. M. (2018). Sphingolipids and their metabolism in physiology and disease. *Nature Reviews Molecular Cell Biology*, 19(3), 175–191. <https://doi.org/10.1038/nrm.2017.107>

Hannun, Y. A., Obeid, L. M., Futerman, A. H., Hannun, Y. A., Bartke, N., & Hannun, Y. A. (2009). The complex life of simple sphingolipids. *Journal of Lipid Research*, 5(3), 777–782. <https://doi.org/10.1038/sj.embor.7400208>

Hans Englyst, carbohydrates N., & Hudson, G. J. (1996). The classification and measurement of dietary. *Food Chemisrry*, 57(1), 15–21

Haslam, E. (1989). *Plant polyphenols: Vegetable tennins revisited* (1st ed.)

Heftmann, E. (1975). Functions of steroids in plants. *Phytochemistry*, 14(4), 891–901. [https://doi.org/10.1016/0031-9422\(75\)85156-9](https://doi.org/10.1016/0031-9422(75)85156-9)

Hele, P. (1958). Biosynthesis of fatty acids. *British Medical Bulletin*, 14(3), 201–206. <https://doi.org/10.1093/oxfordjournals.bmb.a069684>

Hertweck, C. (2009). The biosynthetic logic of polyketide diversity. *Angewandte Chemie - International Edition*, 48(26), 4688–4716. <https://doi.org/10.1002/anie.200806121>

Himawan, C., Starov, V. M., & Stapley, A. G. F. (2006). Thermodynamic and kinetic aspects of fat crystallization. *Advances in Colloid and Interface Science*, 122(1–3), 3–33. <https://doi.org/10.1016/j.cis.2006.06.016>

Hishikawa, D., Hashidate, T., Shimizu, T., & Shindou, H. (2014). Diversity and function of membrane glycerophospholipids generated by the remodeling pathway in mammalian cells. *Journal of Lipid Research*, 55(5), 799–807. <https://doi.org/10.1194/jlr.R046094>

Hites, R. A., & Hites, R. A. (1970). Quantitative Analysis of Triglyceride Mixtures by Mass Spectrometry. *Analytical Chemistry*, 42(14), 1736–1740. <https://doi.org/10.1021/ac50160a041>

Huang, F., Bugg, C. W., & Yarus, M. (2000). RNA-catalyzed CoA, NAD, and FAD synthesis from phosphopantetheine, NMN, and FMN. *Biochemistry*, 39(50), 15548–15555. <https://doi.org/10.1021/bi002061f>

Jiang, Z., Kempinski, C., & Chappell, J. (2016). Extraction and Analysis of Terpenes/Terpenoids. *Current Protocols in Plant Biology*, 1(2), 345–358. <https://doi.org/10.1002/cppb.20024>

Johnson, L. F., & Shoolery, J. N. (1962). Determination of Unsaturation and Average Molecular Weight of Natural Fats by Nuclear Magnetic Resonance. *Analytical Chemistry*, 34(9), 1136–1139. <https://doi.org/10.1021/ac60189a033>

Kato, H., Rhue, M. R., & Nishimura, T. (1989). *Role of Free Amino Acids and Peptides in Food Taste*. 158–174. <https://doi.org/10.1021/bk-1989-0388.ch013>

Kit, S. (1967). *Metabolic pathways* (D. Greenberg, Ed.; Third). University of Michigan

Kiyama, R. (2017). Estrogenic terpenes and terpenoids: Pathways, functions, and applications. *European Journal of Pharmacology*, 815(September), 405–415. <https://doi.org/10.1016/j.ejphar.2017.09.049>

Kobayashi, M., & Kaneko, F. (1989). Molecular and crystal structures of lipids and related compounds. *Journal of Dispersion Science and Technology*, 10(4–5), 319–350. <https://doi.org/10.1080/01932698908943179>

Kobayashi, T., Gu, F., & Gruenberg, J. (1998). Lipids, lipid domains and lipid-protein interactions in endocytic membrane traffic. *Seminars in Cell and Developmental Biology*, 9(5), 517–526. <https://doi.org/10.1006/scdb.1998.0257>

Lafontan, M., & Langin, D. (2009). Lipolysis and lipid mobilization in human adipose tissue. *Progress in Lipid Research*, 48(5), 275–297. <https://doi.org/10.1016/j.plipres.2009.05.001>

Lamberto, M., & Saitta, M. (1995). Principal component analysis in fast atom bombardment-mass spectrometry of triacylglycerols in edible oils. *Journal of the American Oil Chemists' Society*, 72(8), 867–871. <https://doi.org/10.1007/BF02542062>

Langevelde, A. Van, Malssen, K. Van, Driessen, R., Goubitz, K., Hollander, F., Peschar, R., Zwart, P., & Schenk, H. (2000). research papers Structure of C_nC_n+2C_n-type (n=even) beta-triacylglycerols. *Acta Crystallographica Section B*, 56, 1103–1111

Lay, J. O., Liyanage, R., Durham, B., & Brooks, J. (2006). Rapid characterization of edible oils by direct matrix-assisted laser desorption/ionization time-of-flight mass spectrometry analysis using triacylglycerols. *Rapid Communications in Mass Spectrometry*, 20(6), 952–958. <https://doi.org/10.1002/rcm.2394>

Lehner, R., & Kuksis, A. (1996). Biosynthesis of triacylglycerols. *Progress in Lipid Research*, 35(2), 169–201. [https://doi.org/10.1016/0163-7827\(96\)00005-7](https://doi.org/10.1016/0163-7827(96)00005-7)

Lerma-García, M. J., Ramis-Ramos, G., Herrero-Martínez, J. M., & Simó-Alfonso, E. F. (2010). Authentication of extra virgin olive oils by Fourier-transform infrared spectroscopy. *Food Chemistry*, 118(1), 78–83. <https://doi.org/10.1016/j.foodchem.2009.04.092>

Li-Chan, E. (1994). Developments in the detection of adulteration of olive oil. *Trends in Food Science and Technology*, 5(1), 3–11. [https://doi.org/10.1016/0924-2244\(94\)90042-6](https://doi.org/10.1016/0924-2244(94)90042-6)

Lichtenthaler, F. W. (2010). Carbohydrates: Occurrence, Structures and Chemistry. *Ullmann's Encyclopedia of Industrial Chemistry*. https://doi.org/10.1002/14356007.a05_079.pub2

Lie Ken Jie, M. S. F., & Mustafa, J. (1997). High-resolution nuclear magnetic resonance spectroscopy - Applications to fatty acids and triacylglycerols. *Lipids*, 32(10), 1019–1034. <https://doi.org/10.1007/s11745-997-0132-y>

Loreto, F., Pinelli, P., Manes, F., & Kollist, H. (2004). Impact of ozone on monoterpene emissions and evidence for an isoprene-like antioxidant action of monoterpenes emitted by *Quercus ilex* leaves. *Tree Physiology*, 24(4), 361–367. <https://doi.org/10.1093/treephys/24.4.361>

Mansilla, M. C., Cybulski, L. E., Albanesi, D., & De Mendoza, D. (2004). Control of membrane lipid fluidity by molecular thermosensors. *Journal of Bacteriology*, 186(20), 6681–6688. <https://doi.org/10.1128/JB.186.20.6681-6688.2004>

Marai, L., Kuksis, A., & Myher, J. J. (1994). Reversed-phase liquid chromatography-mass spectrometry of the uncommon triacylglycerol structures generated by randomization of butteroil. *Journal of Chromatography A*, 672(1–2), 87–99. [https://doi.org/10.1016/0021-9673\(94\)80596-2](https://doi.org/10.1016/0021-9673(94)80596-2)

Marguet, D., Lenne, P. F., Rigneault, H., & He, H. T. (2006). Dynamics in the plasma membrane: How to combine fluidity and order. *EMBO Journal*, 25(15), 3446–3457. <https://doi.org/10.1038/sj.emboj.7601204>

Marsh, D. (2010). Structural and thermodynamic determinants of chain-melting transition temperatures for phospholipid and glycolipids membranes. *Biochimica et Biophysica Acta - Biomembranes*, 1798(1), 40–51. <https://doi.org/10.1016/j.bbamem.2009.10.010>

Maynard-Casely, H. E., Booth, N., Leung, A. E., Stuart, B. H., & Thomas, P. S. (2019). Potential of neutron powder diffraction for the study of solid triacylglycerols. *Food Structure*, 22, 100124. <https://doi.org/10.1016/j.foostr.2019.100124>

McMurry, J. (2004). *Organic chemistry* (6th ed.). Belmont, CA: Thomson-Brooks/Cole

Mika, J. T., Thompson, A. J., Dent, M. R., Brooks, N. J., Michiels, J., Hofkens, J., & Kuimova, M. K. (2016). Measuring the Viscosity of the Escherichia coli Plasma Membrane Using Molecular Rotors. *Biophysical Journal*, 111(7), 1528–1540. <https://doi.org/10.1016/j.bpj.2016.08.020>

Millar, A. A., Smith, M. A., & Kunst, L. (2000). All fatty acids are not equal: Discrimination in plant membrane lipids. *Trends in Plant Science*, 5(3), 95–101. [https://doi.org/10.1016/S1360-1385\(00\)01566-1](https://doi.org/10.1016/S1360-1385(00)01566-1)

Minato, A., Ueno, S., Yano, J., Wang, Z. H., Seto, H., Amemiya, Y., & Sato, K. (1996). Synchrotron radiation x-ray diffraction study on phase behavior of PPP-POP binary mixtures. *JAACS, Journal of the American Oil Chemists' Society*, 73(11), 1567–1572. <https://doi.org/10.1007/BF02523526>

Morris, G. A. (2009). Diffusion-Ordered Spectroscopy. *Encyclopedia of Magnetic Resonance*, 1–13. <https://doi.org/10.1002/9780470034590.emrstm0119.pub2>

Mozaffarian, D. (2016). Dietary and Policy Priorities for Cardiovascular Disease, Diabetes, and Obesity. *Circulation*, 133(2), 187–225. <https://doi.org/10.1161/CIRCULATIONAHA.115.018585>

Murakami, K., Toma, T., Fukuyama, T., & Yokoshima, S. (2020). Total Synthesis of Tetrodotoxin. *Angewandte Chemie - International Edition*, 59(15), 6253–6257. <https://doi.org/10.1002/anie.201916611>

Murphy, D. J. (2001). The biogenesis and functions of lipid bodies in animals, plants and microorganisms. *Progress in Lipid Research*, 40(5), 325–438. [https://doi.org/10.1016/S0163-7827\(01\)00013-3](https://doi.org/10.1016/S0163-7827(01)00013-3)

Neuberger, A. (1948). Stereochemistry of Amino Acids. *Advances in Protein Chemistry*, 4(C), 297–383. [https://doi.org/10.1016/S0065-3233\(08\)60009-1](https://doi.org/10.1016/S0065-3233(08)60009-1)

Nivina, A., Yuet, K. P., Hsu, J., & Khosla, C. (2019). Evolution and Diversity of Assembly-Line Polyketide Synthases. *Chemical Reviews*, 119(24), 12524–12547. <https://doi.org/10.1021/acs.chemrev.9b00525>

Orsavova, J., Misurcova, L., Vavra Ambrozova, J., Vicha, R., & Mlcek, J. (2015). Fatty acids composition of vegetable oils and its contribution to dietary energy intake and dependence of

cardiovascular mortality on dietary intake of fatty acids. *International Journal of Molecular Sciences*, 16(6), 12871–12890. <https://doi.org/10.3390/ijms160612871>

Pérez-Gil, J. (2008). Structure of pulmonary surfactant membranes and films: The role of proteins and lipid-protein interactions. *Biochimica et Biophysica Acta - Biomembranes*, 1778(7–8), 1676–1695. <https://doi.org/10.1016/j.bbamem.2008.05.003>

Perveen, S. (2018). Introductory Chapter: Terpenes and Terpenoids. *Terpenes and Terpenoids*, 1–12. <https://doi.org/10.5772/intechopen.79683>

Pichersky, E., & Gershenzon, J. (2002). The formation and function of plant volatiles: Perfumes for pollinator attraction and defense. *Current Opinion in Plant Biology*, 5(3), 237–243. [https://doi.org/10.1016/S1369-5266\(02\)00251-0](https://doi.org/10.1016/S1369-5266(02)00251-0)

Pomorski, T., & Menon, A. K. (2006). Lipid flippases and their biological functions. *Cellular and Molecular Life Sciences*, 63(24), 2908–2921. <https://doi.org/10.1007/s00018-006-6167-7>

Prades, J., Funari, S. S., Escribá, P. V., & Barceló, F. (2003). Effects of unsaturated fatty acids and triacylglycerols on phosphatidylethanolamine membrane structure. *Journal of Lipid Research*, 44(9), 1720–1727. <https://doi.org/10.1194/jlr.M300092-JLR200>

Rawlings, B. J. (1998). Biosynthesis of fatty acids and related metabolites. *Natural Product Reports*, 15(3), 275–308. <https://doi.org/10.1039/a815275y>

Řezanka, T., & Mareš, P. (1991). Determination of plant triacylglycerols using capillary gas chromatography, high-performance liquid chromatography and mass spectrometry. *Journal of Chromatography A*, 542(C), 145–159. [https://doi.org/10.1016/S0021-9673\(01\)88755-0](https://doi.org/10.1016/S0021-9673(01)88755-0)

Rhodes, S. H., & Netting, A. G. (1988). Normal-phase high-performance liquid chromatography of triacylglycerols. *Journal of Chromatography A*, 448(C), 135–143. [https://doi.org/10.1016/S0021-9673\(01\)84572-6](https://doi.org/10.1016/S0021-9673(01)84572-6)

Rock, C. O., & Cronan, J. E. (1996). *Escherichia coli* as a model for the regulation of dissociable (type II) fatty acid biosynthesis. *Biochimica et Biophysica Acta - Lipids and Lipid Metabolism*, 1302(1), 1–16. [https://doi.org/10.1016/0005-2760\(96\)00056-2](https://doi.org/10.1016/0005-2760(96)00056-2)

Rousset, P., Rappaz, M., & Minner, E. (1998). Polymorphism and solidification kinetics of the binary system POS-SOS. *JAACS, Journal of the American Oil Chemists' Society*, 75(7), 857–864. <https://doi.org/10.1007/s11746-998-0237-y>

Sasaki, M., Ueno, S., & Sato, K. (2012). Polymorphism and Mixing Phase Behavior of Major Triacylglycerols of Cocoa Butter. In *Cocoa Butter and Related Compounds*. AOCS Press. <https://doi.org/10.1016/B978-0-9830791-2-5.50009-8>

Sato, K. (2001). Crystallization behaviour of fats and lipids - A review. *Chemical Engineering Science*, 56(7), 2255–2265. [https://doi.org/10.1016/S0009-2509\(00\)00458-9](https://doi.org/10.1016/S0009-2509(00)00458-9)

Schmitz, G., & Muller, G. (1991). Structure and function of lamellar bodies, lipid-protein complexes involved in storage and secretion of cellular lipids. *Journal of Lipid Research*, 32(10), 1539–1570. [https://doi.org/10.1016/s0022-2275\(20\)41642-6](https://doi.org/10.1016/s0022-2275(20)41642-6)

Schnurr, J., Shockey, J., & Browse, J. (2004). The Acyl-CoA synthetase encoded by LACS2 is essential for normal cuticle development in arabidopsis. *Plant Cell*, 16(3), 629–642. <https://doi.org/10.1105/tpc.017608>

Schoch, E. P., Felsing, W. A., Watt, G. W., & Okell, F. L. (1947). General chemistry. *The Analyst*, 72(854), 226–227. <https://doi.org/10.2307/3468263>

Schwartz, D. M., & Wolins, N. E. (2007). A simple and rapid method to assay triacylglycerol in cells and tissues. *Journal of Lipid Research*, 48(11), 2514–2520. <https://doi.org/10.1194/jlr.D700017-JLR200>

Sedlacek, L., & Smith, L. L. (1988). Biotransformations of steroids. *Critical Reviews in Biotechnology*, 7(3), 187–236. <https://doi.org/10.3109/07388558809146602>

Somerville, C., Browse, J., Durrett, T. P., Benning, C., Ohlrogge, J., STYMNE, S., & STOBART, A. K. (2008). Plant triacylglycerols as feedstocks for the production of biofuels. *Lipids: Structure and Function*, 54(Table I), 175–214. <https://doi.org/10.1126/science.252.5002.80>

Stübiger, G., Pittenauer, E., & Allmaier, G. (2003). Characterisation of Castor Oil by On-line and performance Liquid Chromatography – Mass Spectrometry (APCI and UV / MALDI). *Phytochem. Anal.*, 346(January), 337–346

STYMNE, S., & STOBART, A. K. (1987). Triacylglycerol Biosynthesis. In *Lipids: Structure and Function* (Vol. 9, Issue Table I). ACADEMIC PRESS, INC. <https://doi.org/10.1016/b978-0-12-675409-4.50014-9>

Sultan, A. (2015). Steroids: A Diverse Class of Secondary Metabolites. *Medicinal Chemistry*, 5(7). <https://doi.org/10.4172/2161-0444.1000279>

TAKADA, S. (2013). Molecular Dynamics Simulations of Biomolecules. *Journal of the Society of Mechanical Engineers*, 116(1131), 78–80. https://doi.org/10.1299/jsmemag.116.1131_78

Tholl, D. (2006). Terpene synthases and the regulation, diversity, and biological roles of terpene metabolism. *Current Opinion in Plant Biology*, 9(3), 297–304. <https://doi.org/10.1016/j.pbi.2006.03.014>

Van Langevelde, A., Van Malssen, K., Sonneveld, E., Peschar, R., & Schenk, H. (1999). Crystal packing of a homologous series β' -stable triacylglycerols. *JAOCs, Journal of the American Oil Chemists' Society*, 76(5), 603–609. <https://doi.org/10.1007/s11746-999-0010-x>

Van Meer, G., Voelker, D. R., & Feigenson, G. W. (2008). Membrane lipids: Where they are and how they behave. *Nature Reviews Molecular Cell Biology*, 9(2), 112–124. <https://doi.org/10.1038/nrm2330>

Vicario, I. M., Griguol, V., & León-Camacho, M. (2003). Multivariate characterization of the fatty acid profile of spanish cookies and bakery products. *Journal of Agricultural and Food Chemistry*, 51(1), 134–139. <https://doi.org/10.1021/jf0258297>

Voelker, T., & Kinney, A. J. (2001). Variations in the Biosynthesis of Seed Storage Lipids. *Lipids*, 42, 358–365

Voet, Donald, Voet, J. G.; P. C. W. (1999). *Fundamentals of Biochemistry*. John Wiley & Sons, Inc.

Wadhwa, R., Yadav, N. S., Katiyar, S. P., Yaguchi, T., Lee, C., Ahn, H., Yun, C. O., Kaul, S. C., & Sundar, D. (2021). Molecular dynamics simulations and experimental studies reveal differential permeability of withaferin-A and withanone across the model cell membrane. *Scientific Reports*, 11(1), 1–15. <https://doi.org/10.1038/s41598-021-81729-z>

Wang, J., & Hou, T. (2011). Application of molecular dynamics simulations in molecular property prediction II: Diffusion coefficient. *Journal of Computational Chemistry*, 32(16), 3505–3519. <https://doi.org/10.1002/jcc.21939>

Wennerberg, A. B. A., Jonsson, T., Forssberg, H., & Li, T. Q. (2001). Mobile lipid production after confluence and pH stress in perfused C6 cells. *NMR in Biomedicine*, 14(1), 33–40. <https://doi.org/10.1002/nbm.688>

Xu, C., & Shanklin, J. (2016). Triacylglycerol Metabolism, Function, and Accumulation in Plant Vegetative Tissues*. In *Annual Review of Plant Biology* (Vol. 67). <https://doi.org/10.1146/annurev-arplant-043015-111641>

Yamashita, A., Hayashi, Y., Nemoto-Sasaki, Y., Ito, M., Oka, S., Tanikawa, T., Waku, K., & Sugiura, T. (2014). Acyltransferases and transacylases that determine the fatty acid composition of glycerolipids and the metabolism of bioactive lipid mediators in mammalian cells and model organisms. *Progress in Lipid Research*, 53(1), 18–81. <https://doi.org/10.1016/j.plipres.2013.10.001>

Yano, J., & Sato, K. (1999). FT-IR studies on polymorphism of fats: Molecular structures and interactions. *Food Research International*, 32(4), 249–259. [https://doi.org/10.1016/S0963-9969\(99\)00079-4](https://doi.org/10.1016/S0963-9969(99)00079-4)

Yano, J., Ueno, S., Sato, K., Arishima, T., Sagi, N., Kaneko, F., & Kobayashi, M. (1993). FT-IR study of polymorphic transformations in SOS, POP, and POS. *Journal of Physical Chemistry*, 97(49), 12967–12973. <https://doi.org/10.1021/j100151a053>

Yoshinaga, K. (2021). Development of analytical methods and nutritional studies using synthetic fatty acids and triacylglycerols. *Journal of Oleo Science*, 70(1), 1–9. <https://doi.org/10.5650/jos.ess20196>

Zeitoun, M. A. M., Neff, W. E., Selke, E., & Mounts, T. L. (1991). Analyses of vegetable oil triglyceride molecular species by reversed phase high performance liquid chromatography. *Journal of Liquid Chromatography*, 14(14), 2685–2698.
<https://doi.org/10.1080/01483919108049348>

Chapter 2

Synthesis of symmetrical and unsymmetrical triacylglycerols & their diffusion NMR studies

2.1 Introduction

The biomimetic synthesis of triacylglycerol (TAGs) has been practiced in the laboratories by using enzymes. Lipase catalyzed synthesis of TAGs started in 1911. (Jahrgang, 1911) The chemists developed the enzyme catalyzed biosynthesis of TAGs under different conditions. The role of an organic solvent, the immobilization of water and the type of enzyme are important factors in the enzymatic synthesis of TAGs. (Janssen et al., 1993) Lipases are the biocatalysts with regioselectivity in their ability for the synthesis of TAGs. Lipases have the capability to esterify or trans esterify fatty acids at either sn-1 and sn-2 position of the glycerol and 1,3-diacylglycerols have been obtained with regioselectivity. (Haraldsson et al., 2000; Wei et al., 2015) Synthesis of mono- and di-unsaturated triacylglycerols has been achieved by using immobilized lipase enzymes. (Duan et al., 2015; Ergan et al., 1990)

Triacylglycerols can be chemically prepared by three methods i.e. (a) the glycerolysis of vegetable oils (b) the hydrolysis of triglycerides (c) the direct esterification of fatty acids with glycerol. The chemical synthesis of TAGs by esterification reaction developed progressively. (Kotwal et al., 2011) In the late nineteenth century, the chemists started to synthesize the TAGs from esterification of carboxylic acids (fatty acids) and alcohol. The earliest attempt has been made by Wolfgang Steglich in 1978. The esterification of carboxylic acids has been carried out using N, N'-dicyclohexylcarbodiimide (DCC) as condensation reagent. The dimethyl amino pyridine has been proved to be good reagent for accelerating the reaction rate. (Neises & Steglich, 1978)

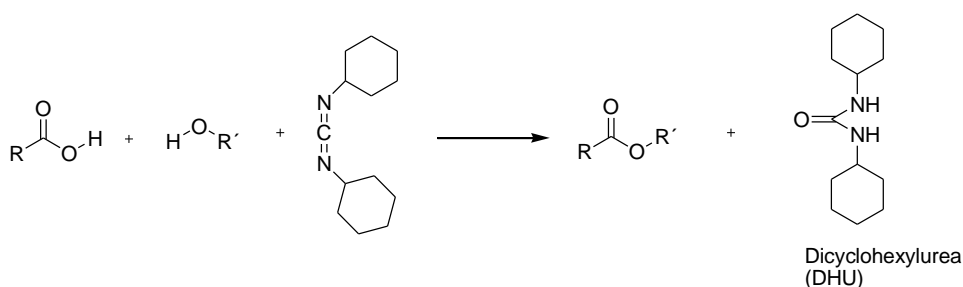


Figure 2.1 A general scheme for the esterification reaction

Later alkoxy and phospho- derivatives of lipids have been synthesized. (Paulsen, 1982) There are different methods for esterification of carboxylic acids. The most important have been the Kodali synthesis, Fischer esterification and Hassner esterification. In Kodali synthesis the carbon tetrachloride (CCl_4) had been used for the TAGs synthesis with 4-dimethyl amino pyridine (4-DMAP) and N, N'-dicyclohexylcarbodiimide (DCC) as condensation reagents. (Adlof & List, 2003; Kodali et al., 1987) Later on, the Kodali synthesis was modified by using different catalysts e.g., *p*-toluene sulfonic acid to

improve the yield of the reaction and avoid formation of side products. (Adlof & List, 2008) Alfred Hassner further improved the esterification reaction for TAGs synthesis by introduction of aminopyridines as acylation catalysts. He introduced 4-dimethylamino pyridine, 4-pyrrolidinopyridine and N, N-bis ((dimethyl amino) methyl) pyridine-4-amine as catalysts for esterification of hindered alcohols. The anhydride formation and pyridinium species 1 with the aminopyridine catalysts reduces the formation of side products. The presence of β -protons in aminopyridines are shown to have more catalytic activity and the proton shifts of β -H also varied. The steric hindrance due to substituents at β -atom of amino pyridines also reduces their catalytic activity. (Hassner et al., 1978; Hassner & Alexanian, 1978)

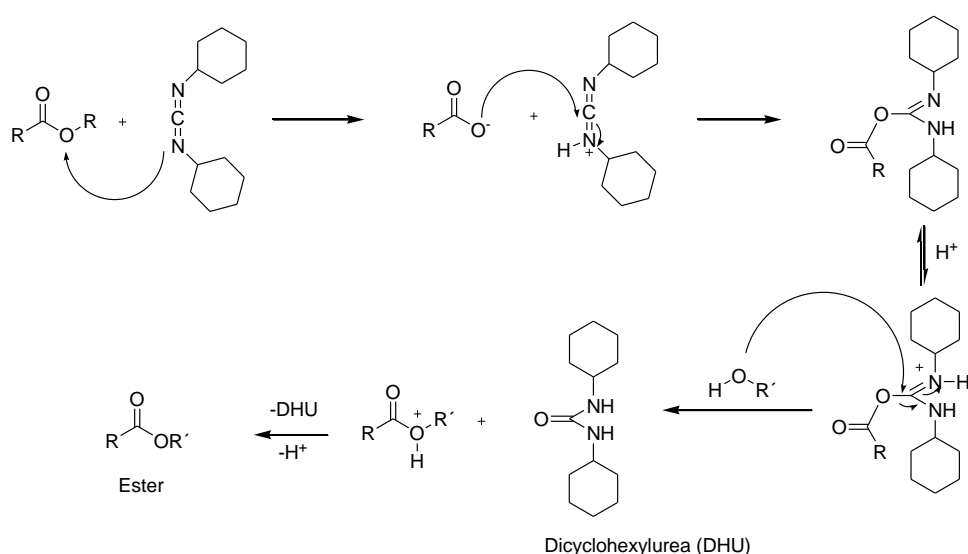


Figure 2.2 The mechanism of the esterification reaction

Hassner esterification led a way to the synthesis of TAGs with ^{14}C radiolabeled nuclei in the fatty acid chains. These radio-labelled TAGs have been useful in clinical diagnosis e.g., breath-test. (Elbert, 1989) The synthesis of TAGs was then reported with acyl bromides. The use of acyl bromides for the esterification proved to be less time consuming with excellent yields of the reaction. (Saroja & Kaimal, 1986) Fischer esterification with sulfuric acid as catalysts has been used to synthesize tri-ester i.e., TAGs. Thermal energy storage properties of TAGs have been estimated by DSC which showed sharp phase transition and high enthalpy values. The TAGs possess high stability at high temperature and do not undergo sharp degradation. This makes them good thermal energy storage material for energy storage devices. (Sar et al., 2010; Sari et al., 2009) Recently, environmentally friendly silica supported sulfonic acid heterogeneous catalysts have been synthesized for esterification of fatty acids with glycerol. These heterogeneous immobilized mesoporous catalysts have greater selectivity than the homogeneous catalyst i.e., *p*-toluene sulfonic acid. Furthermore, these silicas supported catalysts are easily recyclable at the end of the reaction. (Alrouh et al., 2017; Jeenpadiphat et al., 2015) The use of

metal oxides catalysts develops the field of esterification for TAGs for more efficient and environmentally friendly. Triacylglycerols (TAGs) can be synthesized in high conversion and good yield by using zinc fluoride, zinc oxide and iron oxide as catalysts. These metal oxide catalysts are recyclable five to six times without loss of catalytic activity. (Guner et al., 1996; Singh et al., 2013; Z.I. Takai, 2018)

2.2 Experimental

All NMR experiments for measuring 2D NOESY and 2D ROESY were undertaken on a Bruker Avance III Ultra shield 600 MHz spectrometer (Kingston University, London) operating at 600.13 MHz frequency and at 298 K probe temperature. TMS was used as an internal reference standard. CDCl_3 was obtained from Merck. All spectra were acquired and processed using Bruker Topspin 4.06 with diffusion constants determined using Bruker Dynamics Centre. The 1D ^1H spectra were acquired using fid of size 65,536; number of scans 16; spectral width 20.555 ppm; relaxation delay 1.000 s; acquisition time 2.656 s; pulse width 30°C (zg30). 1D ^1H spectra were processed using an EM windows apodization (LB = 0.3 Hz). The ^1H NMR and ^{13}C -NMR spectra were run on JEOL ECS- 400 MHz NMR spectrometer (Eching, Germany) operating at 400 MHz and 100 MHz respectively at room temperature in CDCl_3 solution, using a 5mm probe and number of scans 16. The IR spectra were recorded on Bruker spectrophotometer (Vektor 33, Bremen, Germany).

2.2.1 LC-MS analysis

LC-tandem MS was carried out using an ion trap detector in positive ion mode equipped with an ESI source. The LC equipment (Agilent 1100/1260 series, Bremen, Germany) comprised a binary pump, an auto sampler with a 20 μL loop, and a DAD detector with a light-pipe flow cell (recording at 210 and 320 nm and scanning from 200 to 380 nm) (Bruker Daltonics HCT Ultra, Bremen, Germany) operating in full scan, auto MS^n mode to obtain fragment ion m/z . As necessary, MS^2 , MS^3 and MS^4 fragments were also obtained. HPLC separation was achieved on a 3.0 x 150 mm i.d. Agilent Poroshell 120 column 4.0 μm and 3.0 x 5 mm i.d. guard column of the same material (Agilent, Germany). Solvent (DCM: Ethanol 20:80) was delivered at a total flow rate of 800 $\mu\text{L}/\text{min}$ by 37 min gradient.

2.2.2 HPLC:

Separation was achieved on a 3.0 x 150 mm i.d. Agilent Poroshell 120 column 4.0 μm and 3.0 x 5 mm i.d. guard column of the same material (Agilent, Germany). Solvent (DCM: Ethanol 20:80) was delivered at a total flow rate of 800 $\mu\text{L}/\text{min}$ by 37 min gradient.

2.2.3 Thin layer chromatography:

The progress of the reactions was monitored by thin layer chromatography using precoated silica gel plates (Merck, Kieselgel 60 F₂₅₄ silica) using 9.5:0.5 petroleum ether/ ethyl acetate as a solvent system. Chromatograms were developed with phosphomolybdic acid anhydrate ethanolic solution.

Melting points of the compounds were determined on a BüCHI B-545 melting point apparatus.

2.3 Synthesis of Symmetrical triacylglycerols (TAGs)

Several symmetrical triacylglycerols (TAGs) have been synthesized by the procedure already described by the Hassner. The experimental conditions in the reported procedure have been modified. (Hassner et al., 1978; Hassner & Alexanian, 1978)

2.3.1 Synthesis of 1,2,3-Tripalmitoyl glycerol [Tripalmitin (PPP)] (1)

In a two-neck round, bottomed flask filled with nitrogen (N_2), propane-1,2,3-triol (glycerol) (MW = 92.09 gmol^{-1} , 0.23g, 0.182 mL, 2.5 mmol, 1 equiv.) was added to a stirred solution of n-hexadecenoic acid (palmitic acid) (MW = 256.42 gmol^{-1} , 1.923g, 7.5 mmol, 3 equiv.) in 75 mL of DCM, followed by 4-dimethylamino pyridine (4-DMAP) (MW = 122.17 gmol^{-1} , 0.091g, 0.75 mmol, 0.3 equiv.) at room temperature. The solution was stirred continuously and then cooled to 0°C in an ice bath. To this solution, N, N'-dicyclohexylcarbodiimide (DCC) (MW = 206.33 gmol^{-1} , 1.70g, 8.25 mmol, 3.3 equiv.) was added at 0°C in small portions over 30 minutes. The reaction mixture was stirred at 0°C for 10 minutes and then at room temperature for 24 hrs. The solution was filtered, and the organic layer was washed with 0.5N HCl (2 x 50 mL) and then saturated NaHCO_3 solution (2 x 50 mL). The solution was dried over anhydrous MgSO_4 , filtered and the solvent was removed under vacuum. The product was purified by silica gel (SiO_2) column chromatography with petroleum ether/ethyl acetate as eluents. 1,2,3-Tripalmitoyl glycerol [Tripalmitin (PPP)] (1) has been obtained as white solid. (MW = 807.32 gmol^{-1} , % Yield= 45%; R_f = 0.8; m.p. 68.2°C).

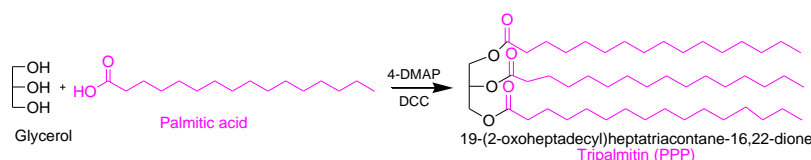


Figure 2.3 Reaction scheme for the synthesis of 1,2,3-Tripalmitoyl glycerol [Tripalmitin (PPP)] (1)

ν_{max} (ATR mode) / cm^{-1} 1728.8 (C=O), 2953.9 (C-H stretch), 1300.6 (C-O), 1471.6 ($-\text{CH}_2$), 1390 ($-\text{CH}_3$)
 δ_{H} (400 MHz; CDCl_3) 5.18-5.21 (m, 1H), 4.08-4.09 (dd, 2H), 4.21-4.24 (dd, 2H), 2.22-2.26 (m, 6H), 1.48-1.57 (m, 6H), 1.18-1.57 (m, 73H), 0.80-0.82 (t, 9H)
 δ_{C} (100 MHz; CDCl_3) 172.06, 172.48 ($-\text{C}=\text{O}$), 68.04 ($-\text{CH}-\text{O}$), 61.28 ($-\text{CH}_2-\text{O}$), 33.40, 33.24, 31.11, ($-\text{CH}_2-\text{C}=\text{O}$), 28.89.1-28.27 ($-\text{CH}_2-$), 24.09, 24.05, 21.88 ($-\text{CH}_2$), 13.30 ($-\text{CH}_3$); m/z (HR-MS) 824.82 $[\text{M} + \text{NH}_4]^+$.

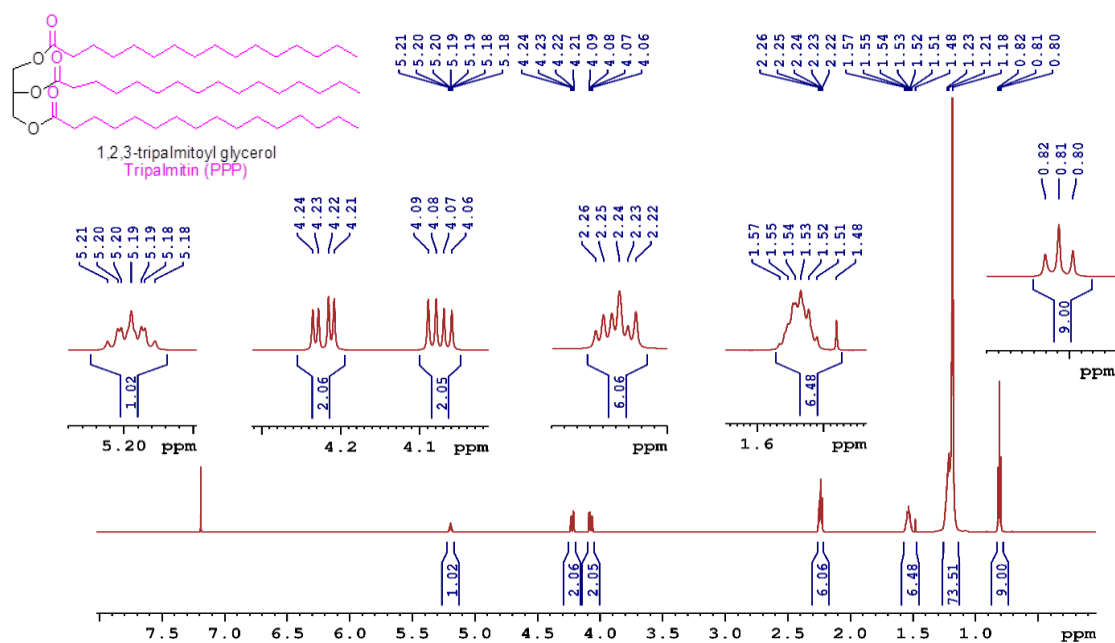


Figure 2.4 $^1\text{H-NMR}$ (400 MHz, CDCl_3) spectrum of 1,2,3-tripalmitoyl glycerol [Tripalmitin (PPP)] (1)

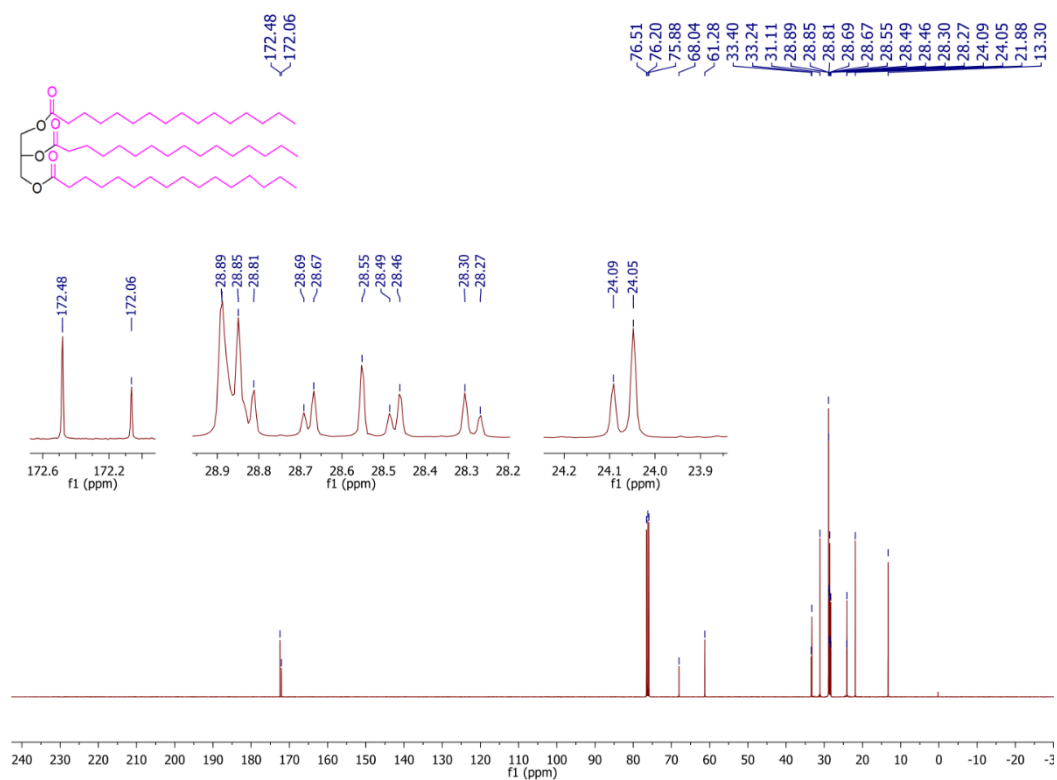


Figure 2.5 $^{13}\text{C-NMR}$ (100 MHz, CDCl_3) spectrum of 1,2,3-tripalmitoyl glycerol [Tripalmitin PPP] (1)

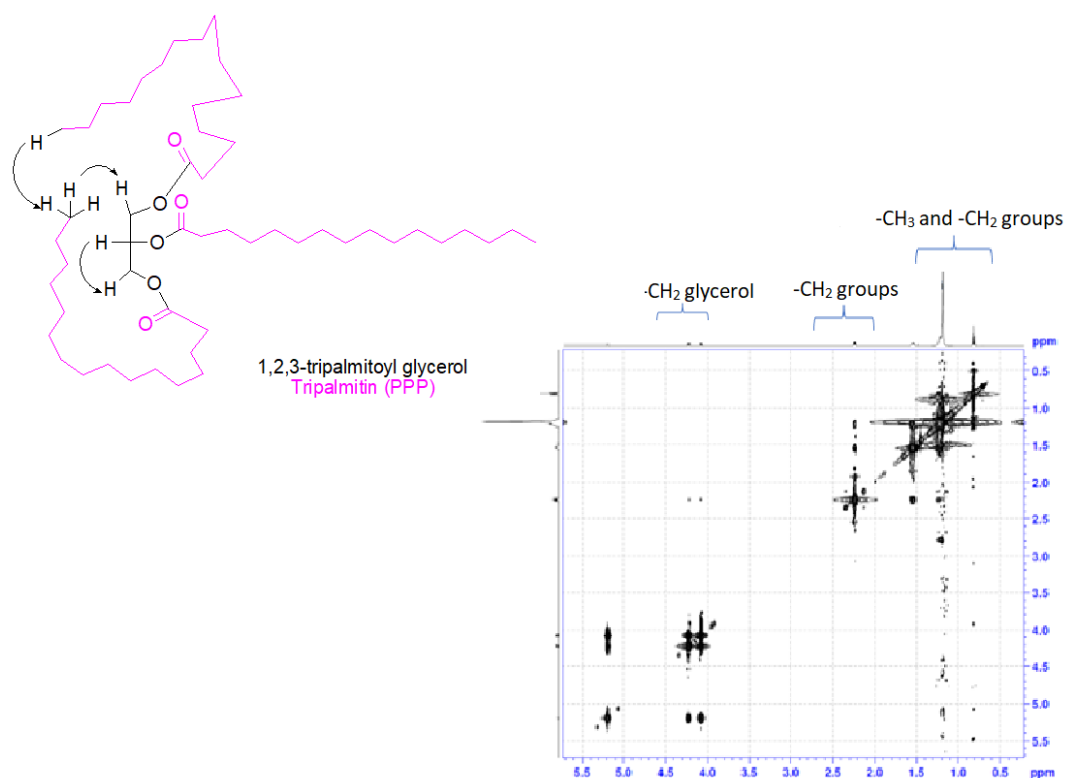


Figure 2.6 2D NOESY of 1,2,3-tripalmitoyl glycerol [Tripalmitin PPP] (1)

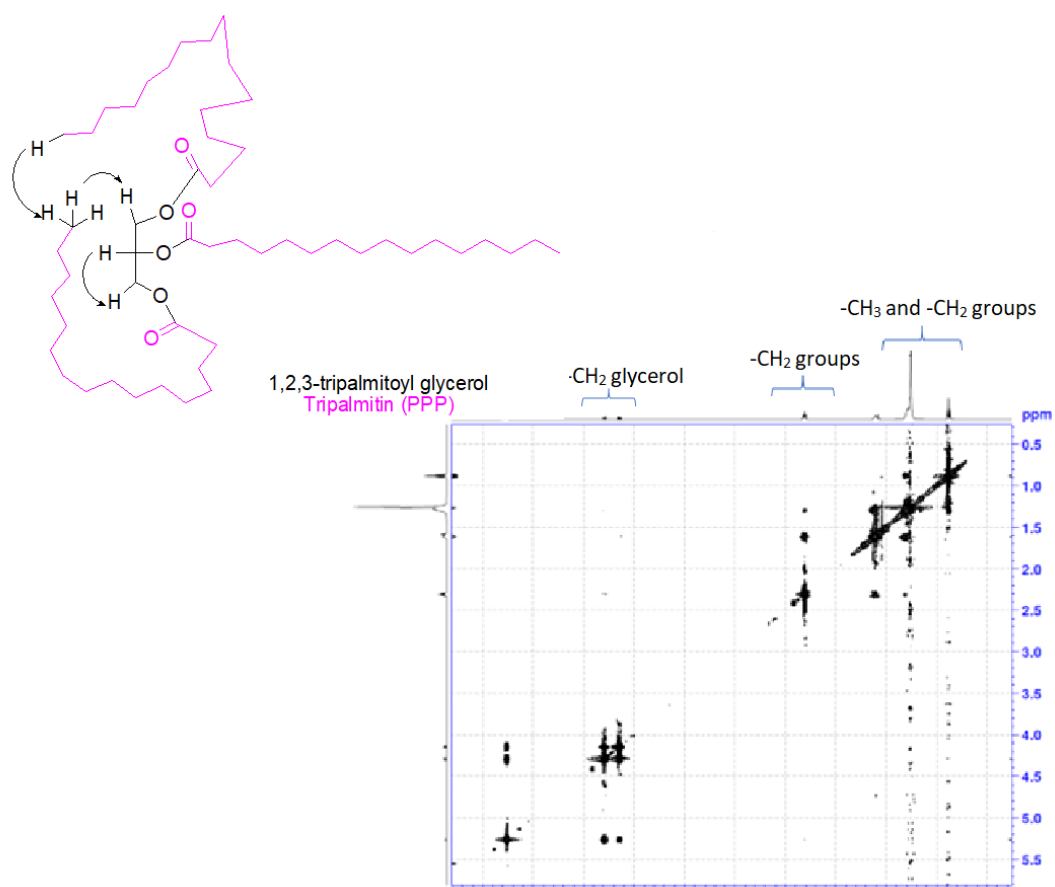


Figure 2.7 2D ROESY of 1,2,3-tripalmitoyl glycerol [Tripalmitin PPP] (1)

2.3.2 Synthesis of 1,2,3-Tristearoyl glycerol [Tristearin (SSS)] (2)

1,2,3-Tristearoyl glycerol [Tristearin (SSS)] (2) has been synthesized in two ways with different reaction times and slight change in the steps of reaction.

a) In a two-neck oven dried, round bottomed flask filled with nitrogen (N_2), a stirred solution of n-octadecanoic acid (stearic acid) ($MW = 284.48 \text{ g mol}^{-1}$, 1.0668g, 3.75 mmol, 3 equiv.) in 120 mL of DCM was obtained. A turbid solution was obtained with partially soluble stearic acid. This solution was made clear by gentle heating for 5-10 minutes. Propane-1,2,3-triol (glycerol) ($MW = 92.09 \text{ g mol}^{-1}$, 0.09 mL, 0.115g, 1.25 mmol, 1 equiv.) was added to the above clear solution at room temperature, followed by 4-dimethylamino pyridine (4-DMAP) ($MW = 122.17 \text{ g mol}^{-1}$, 0.0458g, 0.375 mmol, 0.3 equiv.) at room temperature. To this solution, N, N'-dicyclohexylcarbodiimide (DCC) ($MW = 206.33 \text{ g mol}^{-1}$, 0.851g, 4.125 mmol, 3.3 equiv.) was added at room temperature, in small portions over 30 minutes. The reaction mixture was stirred at room temperature for 4 hrs. The solution was filtered, and the organic layer was washed with 0.5N HCl (2 x 50 mL) and then saturated $NaHCO_3$ solution (2 x 50 mL). The solution was dried over anhydrous $MgSO_4$, filtered and the solvent was removed under vacuum. The product was purified by silica gel (SiO_2) column chromatography with petroleum ether/ethyl acetate as eluents. 1,2,3-Tristearoyl glycerol [Tristearin (SSS)] (2) has been obtained as white crystalline solid. ($MW = 981.48 \text{ g mol}^{-1}$, % Yield= 11.4%; $R_f = 0.5$; m.p. $73.6^\circ C$)

b) In a two-neck round, bottomed flask filled with nitrogen (N_2), propane-1,2,3-triol (glycerol) ($MW = 92.09 \text{ g mol}^{-1}$, 0.115g, 0.09 mL, 1.25 mmol, 1 equiv.) was added to a stirred solution of n-octadecanoic acid (stearic acid) ($MW = 284.48 \text{ g mol}^{-1}$, 1.0668g, 3.75 mmol, 3 equiv.) in 120 mL of DCM, followed by 4-dimethylamino pyridine (4-DMAP) ($MW = 122.17 \text{ g mol}^{-1}$, 0.0458g, 0.375 mmol, 0.3 equiv.) at room temperature for 10-15 minutes. The solution was cooled to $0^\circ C$ in an ice bath with continuous stirring. To this solution, N, N'-dicyclohexylcarbodiimide (DCC) ($MW = 206.33 \text{ g mol}^{-1}$, 0.851g, 4.125 mmol, 3.3 equiv.) was added at $0^\circ C$ in small portions over 30 minutes. The reaction mixture was stirred at $0^\circ C$ for 10 minutes and then at room temperature for 25 hrs. The solution was filtered, and the filtrate solution (organic layer) was washed with 0.5N HCl (2 x 50 mL) and then saturated $NaHCO_3$ solution (2 x 50 mL). The solution was dried over anhydrous $MgSO_4$, filtered and the solvent was removed under vacuum. The product was purified by silica gel (SiO_2) column chromatography with petroleum ether/ethyl acetate as eluents. 1,2,3-Tristearoyl glycerol [Tristearin (SSS)] (2) has been obtained as white crystalline solid. ($MW = 891.48 \text{ g mol}^{-1}$, % Yield= 18.7%; $R_f = 0.5$; m.p. $73.6^\circ C$)

ν_{max} (ATR mode) / cm^{-1} 1728.53 (C=O), 2954.08 (C-H stretch), 1271.37 (C-O), 1471.70 ($-CH_2$), 1391.9 ($-CH_3$)

δ_H (400 MHz; $CDCl_3$) 5.20-5.25 (m, 1H), 4.08-4.12 (dd, 2H), 4.23-4.27 (dd, 2H), 2.25-2.29 (ddd, 6H), 1.55-1.56 (m, 7H), 1.21-1.24 (m, 83H), 0.82-0.85 (t, 9H)

δ_c (100 MHz; $CDCl_3$) 172.29, 171.87 (-C=O), 67.84 (-CH-O), 61.08 (-CH₂-O), 33.21, 33.04, 30.92, (-CH₂-C=O), 28.07-28.70 (-CH₂-), 23.90, 23.85, 21.68 (-CH₂), 13.11 (-CH₃); m/z (HR-MS) 908.89 [M + NH₄]⁺.

2.3.3 Synthesis of 1,2,3-Trioleoyl glycerol [Triolein (OOO)] (3)

To a stirred solution of (9Z)-octadecenoic acid (oleic acid) (MW = 282.46 gmol⁻¹, 1.059g, 3.75 mmol, 3 equiv.) in 110 mL of DCM, propane-1,2,3-triol (glycerol) (MW = 92.09 gmol⁻¹, 0.115g, 0.09 mL, 1.25 mmol, 1 equiv.) was added followed by 4-dimethylamino pyridine (4-DMAP) (MW = 122.17 gmol⁻¹, 0.0458g, 0.375 mmol, 0.3 equiv.) at room temperature. The solution was stirred continuously and then cooled to 0°C in an ice bath. To this solution, N, N'-dicyclohexylcarbodiimide (DCC) (MW = 206.33 gmol⁻¹, 0.851g, 4.125 mmol, 3.3 equiv.) was added at room temperature in small portions over 30 minutes. The reaction mixture was stirred at 0°C for 10 minutes and then at room temperature for 22 hrs. The solution was filtered, and the organic layer was washed with 0.5N HCl (2 x 50 mL) and then saturated NaHCO₃ solution (2 x 50 mL). The solution was dried over anhydrous MgSO₄, filtered and the solvent was removed under vacuum. The product was purified by silica gel (SiO₂) column chromatography with petroleum ether/ethyl acetate as eluents. 1,2,3-Trioleoyl glycerol [Triolein (OOO)] (3) was obtained as colorless liquid. (MW = 885.43 gmol⁻¹, % Yield= 32%. R_f= 0.7)

ν_{max} (ATR mode) / cm⁻¹ 1744.4 (C=O), 2923 (sp³ C-H stretch), 1160 (C-O), 1463 (-CH₂), 1237 (-CH₃), 1653 (C=C), 3073 (sp² =C-H stretch) δ_H (400 MHz; $CDCl_3$) 5.18-5.31 (m, 7H, m), 4.20-4.24 (dd, 2H), 4.05-4.1 (dd, 2H), 2.22-2.26 (dt, 6H), 1.92-1.95 (m, 11H), 1.52-1.54 (d, 7H), 1.20-1.23 (d, 58H), 0.79-0.83 (m, 9H) δ_c (100 MHz; $CDCl_3$) 172.71, 172.29 (-C=O), 129.4 129.1 (-CH=CH-), 68.3 (-CH-O), 61.5 (-CH₂-O), 33.6, 33.4 (-CH₂-C=O), 31.3, 31.22, 29.2, 29.1 (-CH₂), 28.9, 28.7, 28.6, 28.5, 28.4, 26.6, 24.2, 22.1 (-CH₂-), 13.5 (-CH₃); m/z (HR-MS) 902.89 [M + NH₄]⁺.

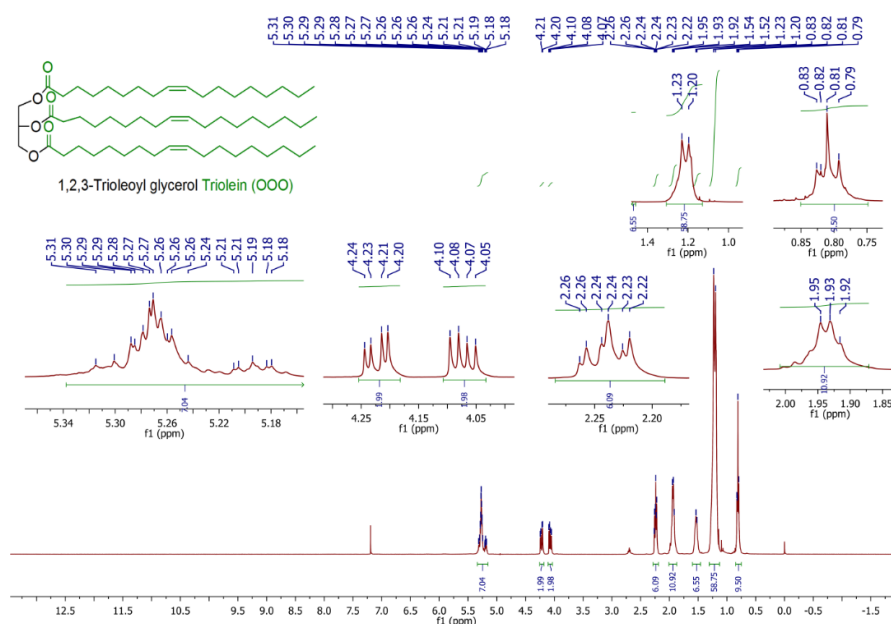


Figure 2.8 ¹H-NMR (600 MHz, $CDCl_3$) spectrum of 1,2,3-trioleoyl glycerol [Triolein OOO] (3)

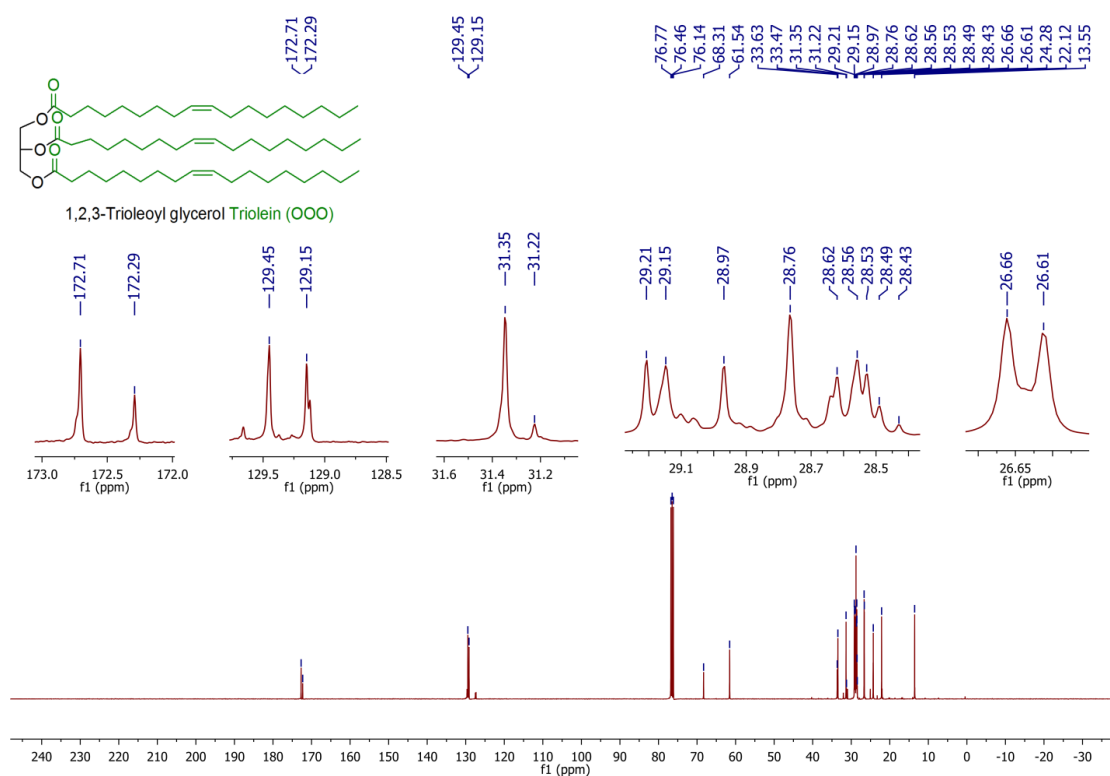


Figure 2.9 ^{13}C -NMR (100 MHz, CDCl_3) spectrum of 1,2,3-Trioleoyl glycerol [Triolein OOO] (3)

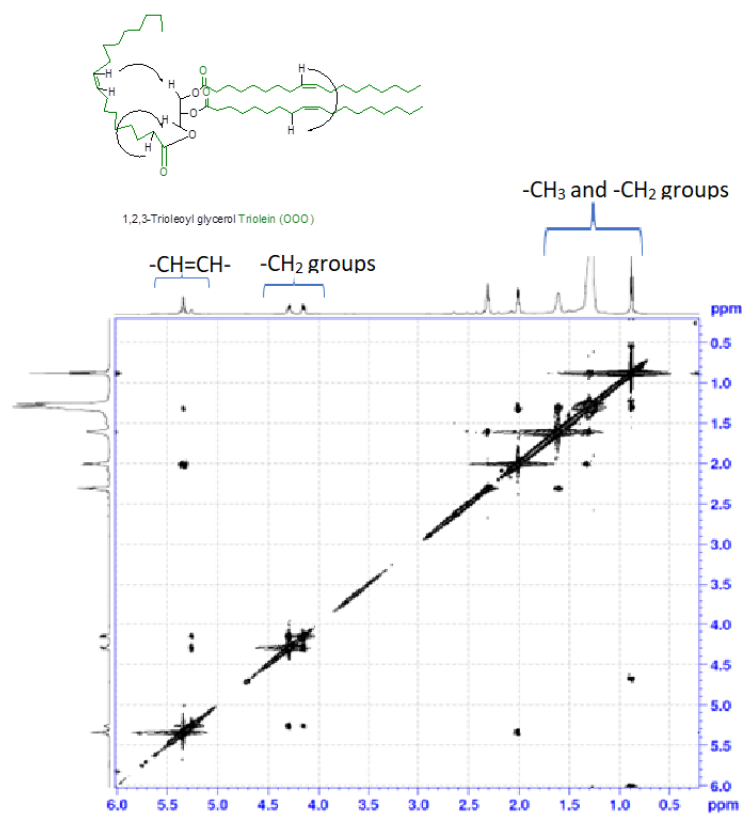


Figure 2.10 2D NOESY of 1,2,3-Trioleoyl glycerol [Triolein OOO] (3)

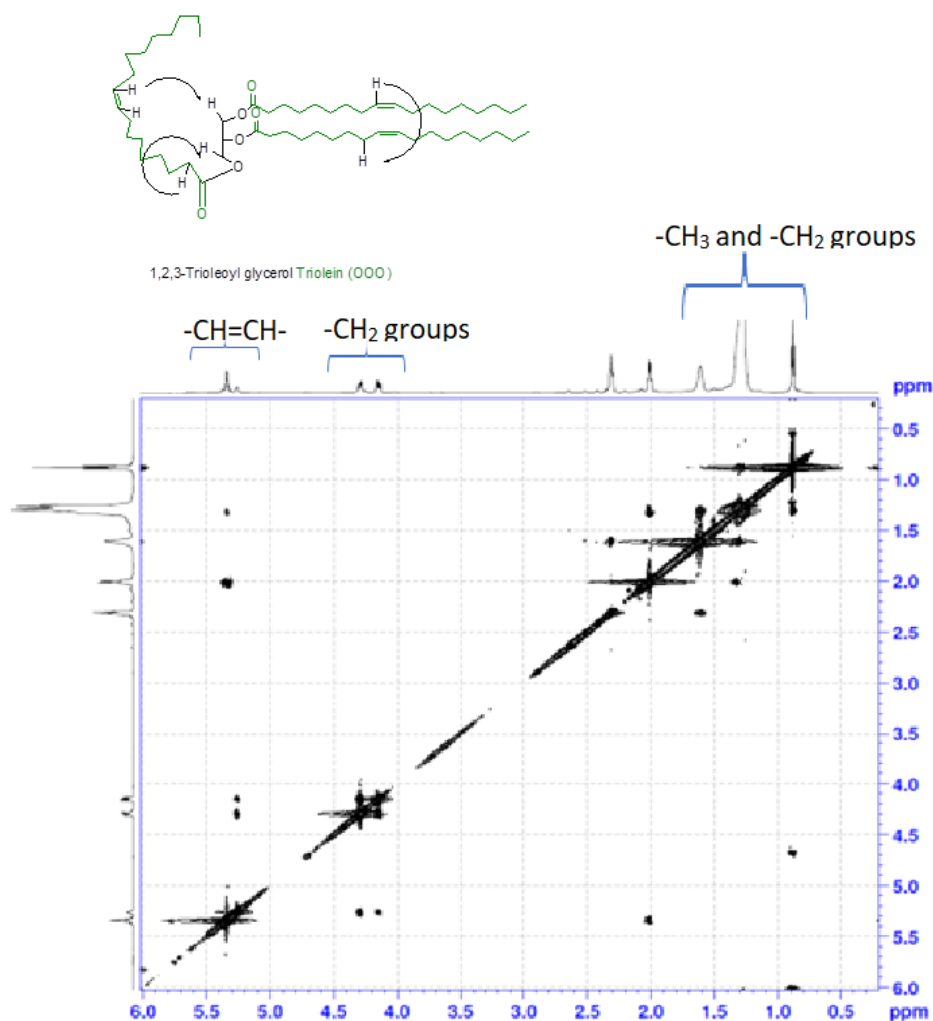


Figure 2.11 2D ROESY of 1,2,3-Triooleyl glycerol [Triolein OOO] (3)

2.3.4 Synthesis of 1,2,3-Trilinoleoyl glycerol [Trilinolein (LLL)] (4)

In the same way as for compound (1), 0.42g (9Z,12Z)-octadecadienoic acid (linoleic acid) (MW = 280.45 gmol^{-1} , 0.465 mL, 1.5 mmol, 3 equiv.) in 5 mL of DCM, 0.036 mL propane-1,2,3-triol (glycerol) (MW = 92.09 gmol^{-1} , 0.46g, 0.036 mL, 0.5 mmol, 1 equiv.) 0.018g 4-dimethylamino pyridine (4-DMAP) (MW = 122.17 gmol^{-1} , 0.15 mmol, 0.3 equiv.) and 0.34g N, N'-dicyclohexylcarbodiimide (DCC) (MW = 206.33 gmol^{-1} , 1.65 mmol, 3.3 equiv.). The reaction mixture was stirred at 0°C for 10 minutes and then at room temperature for 27 hrs. The reaction mixture was processed and purified in the same way as compound (1). 1,2,3-Trilinoleoyl glycerol [Trilinolein (LLL)] (4) was obtained as colorless liquid. (MW = 879.38 gmol^{-1} , % Yield= 41.2%, R_f = 0.7)

ν_{max} (ATR mode) / cm^{-1} 1744.4 (C=O), 2855 (sp^3 C-H stretch), 1160 (C-O), 1459 (CH_2), 1237 (CH_3), 1655 (C=C), 2925 (sp^2 =C-H stretch)

δ_H (400 MHz; $CDCl_3$) 5.2-5.37 (m, 7H, m), 4.20-4.24 (dd, 2H), 4.07-4.12 (dd, 2H), 2.71-2.74 (t, 6H), 2.24-2.28 (m, 6H), 1.97-2.02 (q, 12H), 1.17-1.31 (m, 43H), 0.82-0.86 (m, 9H)

δ_C (100 MHz; $CDCl_3$) 173.34, 172.9 (-C=O), 130.31, 130.1, 130.06, 128.1 127.9 (-CH=CH-), 68.9 (-CH-O), 62.2 (-CH₂-O), 34.2, 34.1 (-CH₂-C=O), 31.6, 29.7, 29.4, 29.2, 29.1 (-CH₂), 27.2, 25.7, 24.9, 22.6 (-CH₂-), 14.2 (-CH₃); m/z (HR-MS) 896.81 [M + NH₄]⁺.

2.3.5 Synthesis of 1,2,3-Trioctanoyl glycerol [Trioctanein (OcOcOc)] (5)

In the same way as for compound (1), 0.423 g n-octanoyl chloride (MW = 162.66 gmol⁻¹, 0.44 mL, 2.60 mmol, 3 equiv.) in 50 mL of DCM, 0.0634 mL propane-1,2,3-triol (glycerol) (MW = 92.09 gmol⁻¹, 0.088g, 0.868 mmol, 1 equiv.), 0.0318g 4-dimethylamino pyridine (4-DMAP) (MW = 122.17 gmol⁻¹, 0.2604 mmol, 0.3 equiv.) and 0.59g N, N'-dicyclohexylcarbodiimide (DCC) (MW = 206.33 gmol⁻¹, 2.86 mmol, 3.3 equiv.). The reaction mixture was stirred at 0°C for 10 minutes and then at room temperature for 20 hrs. The reaction mixture was filtered, and the filtrate was washed with 0.5N HCl (2 x 60 mL) and then saturated NaHCO₃ solution (2 x 60 mL). After this, the filtrate was washed with distilled H₂O (2 x 60 mL). The solution was dried over anhydrous MgSO₄, filtered and the solvent was removed under vacuum. The product was purified by silica gel (SiO₂) column chromatography with petroleum ether/ethyl acetate as eluents. 1,2,3-Trioctanoyl glycerol [Trioctanein (OcOcOc)] (5) was obtained as colorless liquid. (MW = 470.68 gmol⁻¹, % Yield= 16.2%. R_f= 0.4)

δ_H (400 MHz; $CDCl_3$) 5.2-5.29 (m, 1H), 4.23-4.35 (m, 4H), 3.94-3.97 (m, 1H), 3.71-3.77 (m, 3H), 3.15-3.16 (s, 1 H), 2.64-2.72 (m, 3H), 1.55-2.07 (m, 35H), 1.19-1.31 (m, 41H), 0.80-0.82 (m, 9H)

δ_C (100 MHz; $CDCl_3$) 175.58, 170.9 (-C=O), 153.56 (-CH-), 63.9 (-CH-O), 56.5 (-CH₂-O), 30.99, 30.95 (-CH₂-C=O), 29.35, 28.51, 28.4, 25.7 (-CH₂), 24.9, 24.8, 24.7, 24.6, 24.5, 23.5, 21.8 (-CH₂-), 13.3 (-CH₃); m/z (HR-MS) 488.35 [M + NH₄]⁺.

2.3.6 Synthesis of 1,2,3-Trilauroyl glycerol [Trilaurein (LaLaLa)] (6)

In the same way as for compound (1), 1.42 g lauryl chloride (MW = 218.76 gmol⁻¹, 1.5 mL, 6.512 mmol, 4 equiv.) in 65 mL of DCM, 0.0634 mL, propane-1,2,3-triol (glycerol) (MW = 92.09 gmol⁻¹, 0.15 g, 0.12 mL, 1.628 mmol, 1 equiv.), 0.079 g 4-dimethylamino pyridine (4-DMAP) (MW = 122.17 gmol⁻¹, 0.651 mmol, 0.4 equiv.) and 1.108 g N, N'-dicyclohexylcarbodiimide (DCC) (MW = 206.33 gmol⁻¹, 5.372 mmol, 3.3 equiv.). The reaction mixture was stirred at 0°C for 1 hour and then at room temperature for 43 hrs. The reaction mixture was washed with 0.5N HCl (2 x 100 mL) and then saturated NaHCO₃ solution (2 x 100 mL). After this, the filtrate was washed with distilled H₂O (2 x 60 mL). The solution was dried over anhydrous MgSO₄, filtered and the solvent was removed under vacuum. The product was purified by silica gel (SiO₂) column chromatography with trichloro methane/methanol (99:01 / 1%) as eluents. 1,2,3-Trilauroyl glycerol [Trilaurein (LaLaLa)] (6) was obtained as a gel. (MW = 639 gmol⁻¹, % Yield= 36.3%. R_f= 0.4)

δ_H (400 MHz; $CDCl_3$) 5.23-5.27 (m, 1H), 4.26-4.29 (dd, 2H), 4.12-4.14 (dd, 2H), 2.28-2.31 (m, 6H), 1.58-1.6 (m, 7H), 1.24-1.28 (m, 49H), 0.85-0.88 (t, 9H)
 δ_C (100 MHz; $CDCl_3$) 172.4, 172 (-C=O), 68.01, (-CH-O), 61.25 (-CH₂-O), 33.3, 33.21, 31 (-CH₂-C=O), 28.6, 28.5, 28.4, 28.2 (-CH₂), 24, 24, 21.8 (-CH₂-), 12.3 (-CH₃); m/z (HR-MS) 656.6 $[M + NH_4]^+$.

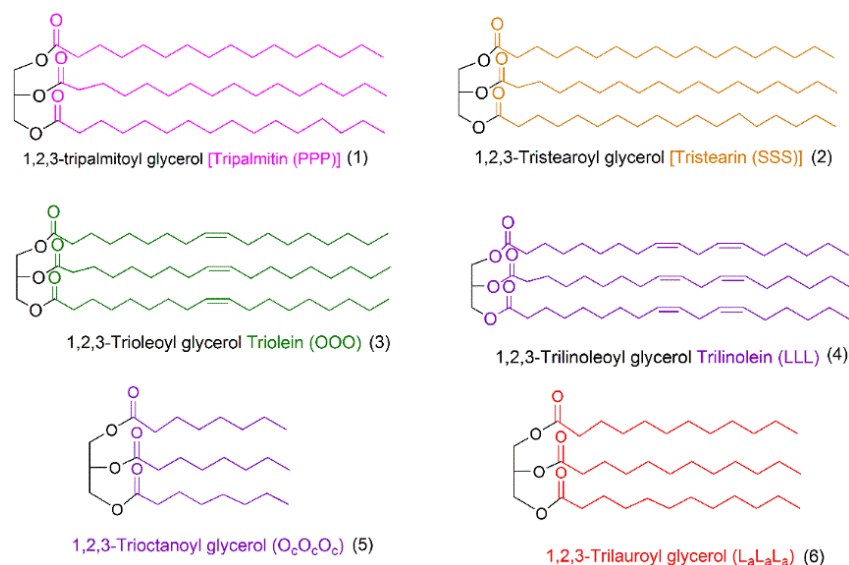


Figure 2.12 Structures of symmetrical triacylglycerols synthesized

2.4 Synthesis of unsymmetrical triacylglycerols (TAGs)

2.4.1 Synthesis of 1-Palmitoyl-2,3-isopropylidene glycerol (7) (Hui et al., 2003)

The 2,2-dimethyl-1,3-dioxolane-4-methanol (1,2-Isopropylidene glycerol or Solketal) (MW = 132.16 $gmol^{-1}$, 0.25 g, 0.23 mL, 1.88 mmol, 1 equiv.) was dissolved in 3 mL of pyridine at room temperature and then cooled to 0°C in an ice bath with continuous stirring. The n-hexadecanoyl chloride (palmitoyl chloride) (MW = 274.87 $gmol^{-1}$, 0.516 g, 0.569 mL, 1.88 mmol, 1 equiv.) was dissolved in 80 mL of DCM at room temperature and this solution was added drop wise to the above solution of 2,2-dimethyl-1,3-dioxolane-4-methanol (1,2-Isopropylidene glycerol or Solketal) in pyridine at 0°C over a time span of 30 minutes. To this reaction solution, 4-dimethylamino pyridine (4-DMAP) (MW = 122.17 $gmol^{-1}$, 0.023 g, 0.118 mmol, 0.1 equiv.) was added at 0°C. The reaction mixture was stirred for 1 hour at 0°C and then at room temperature for 27 hours. The reaction mixture was poured into ice-cold water (50 mL) and was extracted with chloroform (2 x 50 mL). The organic layer (chloroform extract) was washed with ice-cold HCl (2 N) (2 x 50 mL), saturated $NaHCO_3$ solution (2 x 50 mL) and then ice-cold distilled H_2O (2 x 50 mL). The organic layer was dried over Na_2SO_4 , and the solvent was removed under vacuum. The product was purified by silica gel (SiO_2) column chromatography with petroleum ether/ethyl

acetate (95:05 / 5%) as eluents. 1-palmitoyl-2,3-Isopropylidene glycerol (7) was obtained as white waxy solid (MW = 370.3 gmol⁻¹, % Yield= 82%, R_f= 0.3)

δ_H (400 MHz; CDCl₃) 4.22-4.28 (m, 1H), 4.08-4.12 (dd, 2H), 3.99-4.01 (dd, 1H), 3.65-3.69 (dd, 1H), 2.25-2.29 (t, 2H), 1.52-1.57 (m, 2H), 1.3-1.37 (d, 6H), 1.18-1.21 (m, 25H), 0.79-0.83 (t, 3H)

δ_C (100 MHz; CDCl₃) 172.64 (-C=O), 108.80 (-C-), 65.4, (-CH-O), 63.5 (-CH₂-O), 33.1, (-CH₂-C=O), 28.6, 28.4, 28.2 (-CH₂), 25.7, 25.5, 24.4, 24.2, 23.8 (-CH₂-), 13.1, 13 (-CH₃).

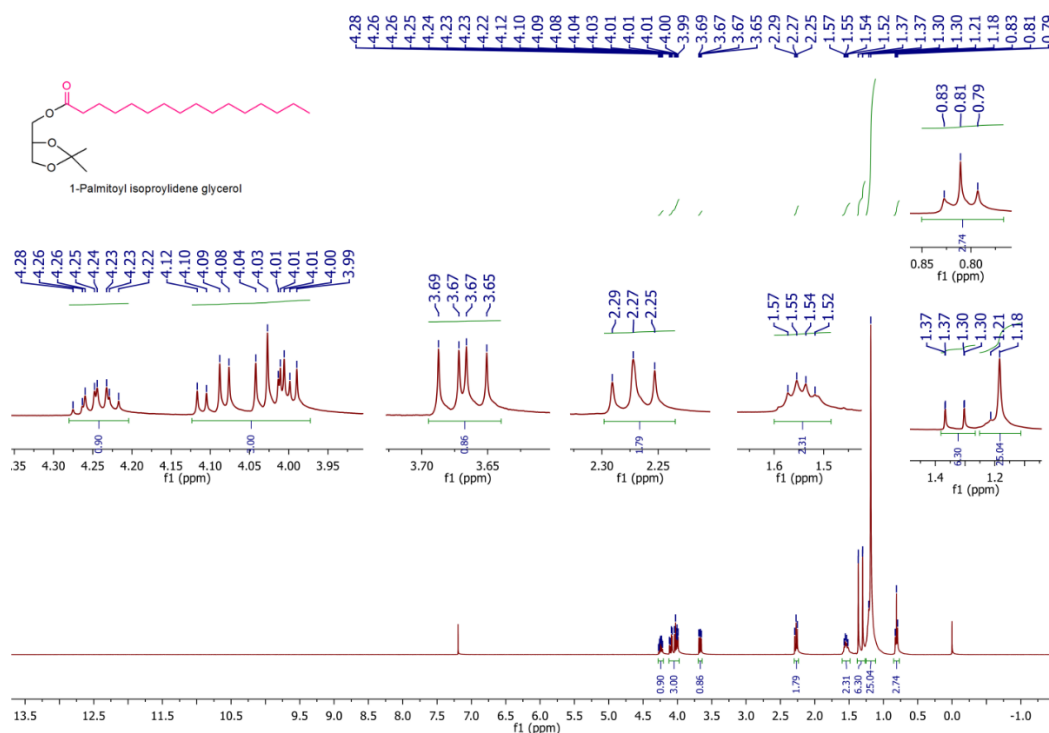


Figure 2.13 ¹H-NMR (400 MHz, CDCl₃) spectrum of 1-Palmitoyl isopropylidene glycerol (7)

2.4.2 Synthesis of 1-Palmitoyl glycerol (8) (J., 1994)

1-palmitoyl-2,3-Isopropylidene glycerol (7) (MW = 370.3 gmol⁻¹, 0.566 g, 1.528 mmoles, 1 equiv.) was dissolved in 9 mL of methanol (MW = 32.04 gmol⁻¹) at room temperature. To this solution HCl (0.09 mL, 32%, 10.2 N) was added at room temperature and reaction mixture was stirred for 2 hours at room temperature. The reaction was monitored by TLC until 1-palmitoyl-2,3-Isopropylidene glycerol was deprotected into 1-palmitoyl glycerol (8). The reaction mixture was dissolved in 50 mL of trichloroethane (chloroform) and the solution was washed with saturated NaHCO₃ solution (1 x 15 mL) and then distilled water (1 x 50 mL). The solution was dried over MgSO₄ the solvent was removed under vacuum. The product was purified by silica gel (SiO₂) column chromatography with petroleum ether/ethyl acetate (95:05 / 5%) as eluents. 1-Palmitoyl glycerol (8) was obtained as white crystalline solid (MW = 330.2 gmol⁻¹, % Yield= 75.6%, R_f= 0.01).

δ_H (400 MHz; $CDCl_3$) 4.08-4.18 (m, 2H), 3.78-3.91 (m, 1H), 3.63-3.67 (dd, 1H), 3.53-3.57 (dd, 1H), 2.28-2.32 (t, 2H), 2.22 (s, 2H), 1.54-1.59 (m, 2H), 1.2-1.24 (d, 25H), 0.81-0.85 (t, 3H)
 δ_C (100 MHz; $CDCl_3$) 173.62 (-C=O), 69.5, (-CH-O), 64.4, 62.5 (-CH₂-O), 33.3, (-CH₂-C=O), 28.9, 28.8, 28.6, 28.5, 28.4, 28.3 (-CH₂), 13.4, 13.2 (-CH₃); m/z (HR-MS) 353.2 [M + Na]⁺.

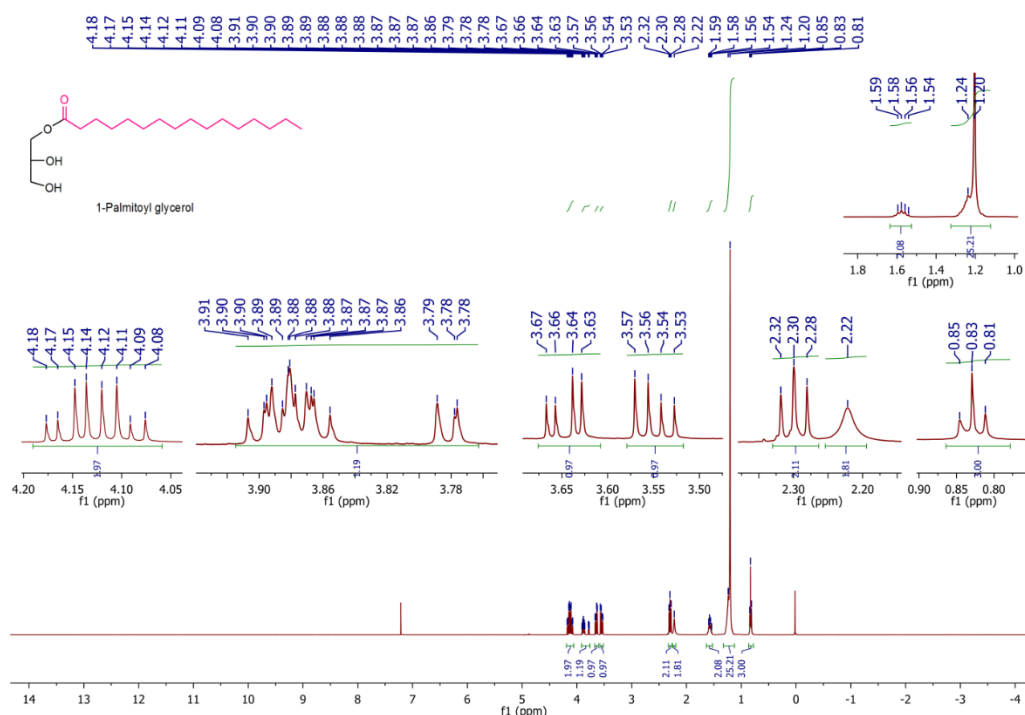
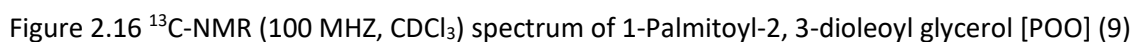
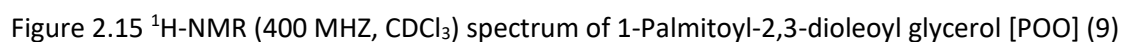


Figure 2.14 ¹H-NMR (400 MHz, $CDCl_3$) spectrum of 1-Palmitoyl glycerol (8)

2.4.3 Synthesis of 1-Palmitoyl-2,3-dioleoyl glycerol [POO] (9) (Hui et al., 2003)

The 1-palmitoyl glycerol (8) (MW = 330.2 $gmol^{-1}$, 0.1 g, 0.302 mmol, 1 equiv.) was dissolved in 5 mL of pyridine at room temperature and then this solution was cooled to 0°C in an ice bath with continuous stirring. The (9Z)-octadecenoyl chloride (oleoyl chloride) (MW = 300.91 $gmol^{-1}$, 0.227 g, 0.25 mL, 0.775 mmol, 2.5 equiv.) was dissolved in 8 mL of DCM at room temperature and this solution was added drop wise to the above solution of 1-palmitoyl glycerol in pyridine at 0°C over a time span of 30 minutes. To this reaction solution, 4-dimethylamino pyridine (4-DMAP) (MW = 122.17 $gmol^{-1}$, 0.0074 g, 0.0604 mmol, 0.2 equiv.) was added at 0°C. The reaction mixture was stirred for 2 hours at 0°C and then at room temperature for 26 hours. The reaction mixture was poured into ice-cold distilled water (30 mL) and was extracted with chloroform (2 x 60 mL). The organic layer (chloroform extract) was washed with ice-cold HCl (2 N) (2 x 60 mL) and then ice-cold distilled H₂O (2 x 60 mL). The organic layer was dried over Na₂SO₄, and the solvent was removed under vacuum. The product was purified by silica gel (SiO₂) column chromatography with petroleum ether/ethyl acetate (95:05 / 5%) as eluents. 1-palmitoyl-2,3-dioleoyl glycerol (9) was obtained as colorless liquid (MW = 859.39 $gmol^{-1}$, % Yield= 21%, R_f = 0.4).



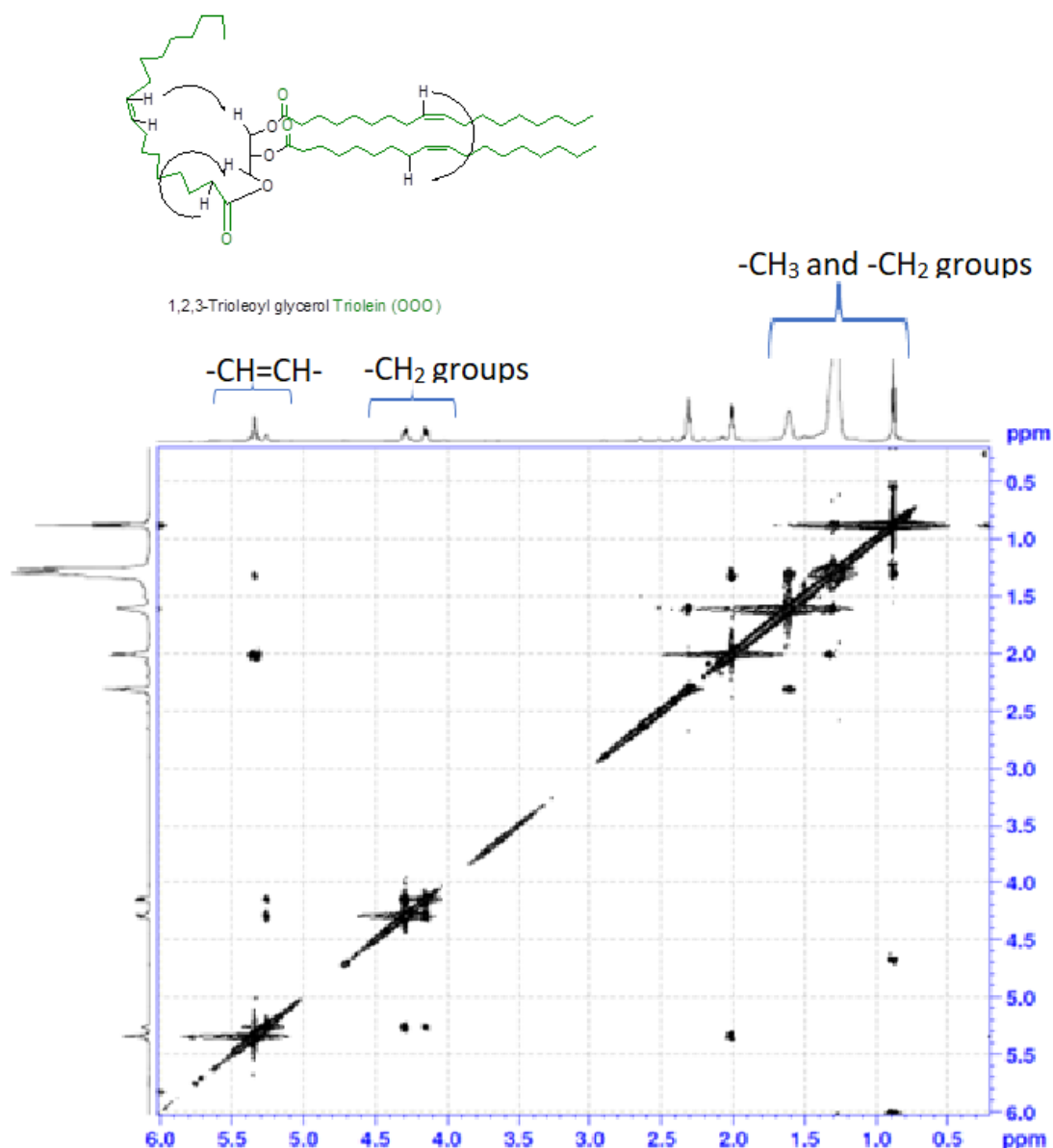


Figure 2.17 2D NOESY of 1-Palmitoyl-2,3-dioleoyl glycerol [POO] (9)

2.4.4 Synthesis of 1-Palmitoyl-2,3-distearoyl glycerol [PSS] (10) (Hui et al., 2003)

In the same way as compound (9). 1-palmitoyl glycerol (8) (MW = 330.2 gmol⁻¹, 0.1 g, 0.302 mmol, 1 equiv.) was dissolved in 5 mL of pyridine, n-octadecanoyl chloride (stearoyl chloride) (MW = 302.92 gmol⁻¹, 0.274 g, 0.305 mL, 0.906 mmol, 3 equiv.) in 8 mL of DCM and 4-dimethylamino pyridine (4-DMAP) (MW = 122.17 gmol⁻¹, 0.0074 g, 0.0604 mmol, 0.2 equiv.). The reaction steps were followed as above for compound (9). The reaction mixture was stirred for 2 hours at 0°C and then at room temperature for 25 hours. The reaction mixture was poured into ice-cold distilled water (50 mL) and was extracted with chloroform (2 x 60 mL). The organic layer (chloroform extract) was washed with ice-cold HCl (2 N) (2 x 60 mL) and then ice-cold distilled H₂O (2 x 60 mL). The organic layer was dried over Na₂SO₄, and the solvent was removed under vacuum. The product was purified by silica gel (SiO₂)

column chromatography with petroleum ether/ethyl acetate (95:05 / 5%) as eluents. 1-palmitoyl-2,3-distereoyl glycerol (9) was obtained as colorless liquid (MW = 863.43 gmol⁻¹, % Yield= 43.7%, R_f= 0.4). δ_H (400 MHz; CDCl₃) 5.18-5.21 (m, 1H), 4.21-4.24 (dd, 2H), 4.06-4.09 (dd, 1H), 2.23-2.26 (m, 6H), 1.51-1.57 (m, 6H), 1.18-1.23 (m, 81H), 0.80-0.82 (t, 9H)

δ_C (100 MHz; CDCl₃) 172.04, 171.6 (-C=O), 67.6, (-CH-O), 60.8 (-CH₂-O), 32.7, 30.6 (-CH₂-C=O), 28.4, 28.2, 28 (-CH₂), 27.9, 27.8, 25.9, 24.4, 23.6, 21.4 (-CH₂-), 12.8 (-CH₃); m/z (HR-MS) 880.83 [M + Na]⁺.

2.4.5 Synthesis of 1-Palmitoyl-2,3-dilinoleoyl glycerol [PLL] (11) (Hui et al., 2003)

In the same way as compound (9). 1-palmitoyl glycerol (8) (MW = 330.2 gmol⁻¹, 0.1 g, 0.302 mmol, 1 equiv.) was dissolved in 5 mL of pyridine, 9Z,12Z-octadeca-9,12-dienoyl chloride (linoleoyl chloride) (MW = 298.89 gmol⁻¹, 0.270 g, 0.290 mL, 0.906 mmol, 3 equiv.) in 8 mL of DCM and 4-dimethylamino pyridine (4-DMAP) (MW = 122.17 gmol⁻¹, 0.0074 g, 0.0604 mmol, 0.2 equiv.). The reaction steps were followed as above for compound (9). The reaction mixture was stirred for 2 hours at 0°C and then at room temperature for 26 hours. The reaction mixture was poured into ice-cold distilled water (50 mL) and was extracted with chloroform (2 x 60 mL). The organic layer (chloroform extract) was washed with ice-cold HCl (2 N) (2 x 60 mL) and then ice-cold distilled H₂O (2 x 60 mL). The organic layer was dried over Na₂SO₄, and the solvent was removed under vacuum. The product was purified by silica gel (SiO₂) column chromatography with petroleum ether/ethyl acetate (gradient elution up to 1-10 %) as eluents. 1-palmitoyl-2,3-dilinoleoyl glycerol (10) was obtained as colorless liquid (MW = 854.36.43 gmol⁻¹, % Yield= 20.5%, R_f= 0.3).

δ_H (400 MHz; CDCl₃) 5.23-5.33 (m, 7H), 4.01-4.14 (m, 5H), 2.69-2.72 (t, 6H), 1.96-1.99 (m, 6H), 1.54-1.56 (m, 7H), 1.19-1.23 (m, 55H), 0.79-0.82 (m, 9H)

δ_C (100 MHz; CDCl₃) 173.18 (-C=O), 129.47, 129.2, 127.3, 127.1, (-CH=CH-), 67.6, (-CH-O), 64.2 (-CH₂-O), 33.3, 31, 30.7 (-CH₂-C=O), 28.9, 28.5, 28.3 (-CH₂), 26.4, 24.8, 24.1, 21.8 (-CH₂-), 13.3 (-CH₃).

2.4.6 Synthesis of 1-Stearoyl-2,3-isopropylidene glycerol (12) (Hui et al., 2003)

In the same way as compound (7). The 2,2-dimethyl-1,3-dioxolane-4-methanol (1,2-Isopropylidene glycerol or Solketal) (MW = 132.16 gmol⁻¹, 0.25 g, 0.23 mL, 1.885 mmol, 1 equiv.) was dissolved in 3 mL of pyridine, n-octadecanoyl chloride (stearoyl chloride) (MW = 302.92 gmol⁻¹, 0.571 g, 0.636 mL, 1.88 mmol, 1 equiv.) in 80 mL of DCM and 4-dimethylamino pyridine (4-DMAP) (MW = 122.17 gmol⁻¹, 0.023 g, 0.118 mmol, 0.1 equiv.). The reaction steps were followed as above for compound (7). The reaction mixture was stirred for 1 hour at 0°C and then at room temperature for 19 hours. The reaction mixture was poured into ice-cold water (50 mL) and was extracted with chloroform (2 x 50 mL). The organic layer (chloroform extract) was washed with ice-cold HCl (2 N) (2 x 50 mL), saturated NaHCO₃ solution (1 x 50 mL) and then ice-cold distilled H₂O (2 x 50 mL). The organic layer was dried over Na₂SO₄, and the solvent was removed under vacuum. The product was purified by silica gel (SiO₂) column

chromatography with petroleum ether/ethyl acetate (96:04 / 4%) as eluents. 1-stearoyl-2,3-Isopropylidene glycerol (12) was obtained as white crystalline solid (MW = 398.2 gmol⁻¹, % Yield= 58%, R_f= 0.4)

δ_H (400 MHz; CDCl₃) 4.22-4.27 (m, 1H), 4.08-4.12 (dd, 2H), 3.99-4.01 (dd, 1H), 3.65-3.69 (dd, 1H), 2.25-2.29 (t, 2H), 1.52-1.57 (m, 2H), 1.3-1.37 (d, 6H), 1.18-1.21 (m, 30H), 0.79-0.83 (t, 3H)

δ_C (100 MHz; CDCl₃) 172.8 (-C=O), 109.05 (-C-), 72.9, (-CH-O), 65.6, 63.7 (-CH₂-O), 33.3, 31.1 (-CH₂-C=O), 28.9, 28.8, 28.6, 28.5-28.3 (-CH₂), 25.9, 24.6, 24.1, 21.9 (-CH₂-), 13.3 (-CH₃).

2.4.7 Synthesis of 1-Stearoyl glycerol (13) (J., 1994)

In the same way as compound (8). 1-Stearoyl-2,3-isopropylidene glycerol (12) (MW = 398.2 gmol⁻¹, 0.432g, 1.084 mmoles, 1 equiv.) was dissolved in 7 mL of methanol (MW = 32.04 gmol⁻¹) and dichloromethane (MW = 85.0 gmol⁻¹, 2 mL); HCl (MW = 36.5 gmol⁻¹, 0.07 mL, 32%, 10.2 N). The reaction steps were followed as above for compound (8). The reaction mixture was stirred for 2 hours at room temperature. The reaction mixture was processed in the same way as above for compound (8). The product was purified by silica gel (SiO₂) column chromatography with petroleum ether/ethyl acetate (95:05 / 5%) as eluents. 1-Stearoyl glycerol (13) was obtained as white crystalline solid (MW = 358.56 gmol⁻¹, % Yield= 63 %, R_f= 0.01).

δ_H (400 MHz; CDCl₃) 4.08-4.18 (m, 2H), 3.78-3.91 (m, 1H), 3.63-3.67 (dd, 1H), 3.53-3.57 (dd, 1H), 2.28-2.32 (t, 2H), 2.22 (s, 2H), 1.54-1.6 (m, 2H), 1.2-1.24 (d, 30H), 0.81-0.85 (t, 3H)

δ_C (100 MHz; CDCl₃) 174.46 (-C=O), 65.2, (-CH-O), 63.5, 63.4 (-CH₂-O), 34.2, (-CH₂-C=O), 29.7, 29.5, 29.4, 29.3, 29.2, 24.9, 22.7 (-CH₂), 14.2, 14.1 (-CH₃); m/z (HR-MS) 379.31[M + Na]⁺.

2.4.8 Synthesis of 1-Stearoyl-2,3-dipalmitoyl glycerol [SPP] (14 a and 14 b) (Hui et al., 2003)

In the same way as compound (9). 1-Stearoyl glycerol (13) (MW = 358.56 gmol⁻¹, 0.1 g, 0.278 mmol, 1 equiv.) was dissolved in 5 mL of pyridine, n-hexadecanoyl chloride (palmitoyl chloride) (MW = 274.87 gmol⁻¹, 0.229 g, 0.252 mL, 0.834mmol, 3 equiv.) in 8 mL of DCM and 4-dimethylamino pyridine (4-DMAP) (MW = 122.17 gmol⁻¹, 0.0068 g, 0.0556 mmol, 0.2 equiv.). The reaction steps were followed as above for compound (9). The reaction mixture was stirred for 2 hours at 0°C and then at room temperature for 23 hours. The reaction mixture was poured into ice-cold distilled water (60 mL) and was extracted with chloroform (2 x 70 mL). The organic layer (chloroform extract) was washed with ice-cold HCl (2 N) (2 x 70 mL), saturated NaHCO₃ solution (1 x 70 mL) and then ice-cold distilled H₂O (2 x 70 mL). The organic layer was dried over Na₂SO₄, and the solvent was removed under vacuum. The product was purified by silica gel (SiO₂) column chromatography with petroleum ether/ethyl acetate (95:05 / 5%) as eluents. Two conformational isomers have been isolated from the same reaction mixture by column chromatography.

1- Stearoyl -2,3- palmitoyl glycerol [SPP] (14 a) was the upper fraction in the TLC of the reaction mixture and was obtained as white crystalline solid (MW = 835.37 gmol⁻¹, % Yield= 22.4%, R_f= 0.5). the second fraction (14 b) was lower than the [SPP] (14 a) and was also obtained as white crystalline solid (MW = 835.37 gmol⁻¹, % Yield= 87.6%, R_f= 0.2).

[SPP] (14 a)

δ_H (400 MHz; CDCl₃) 5.18-5.21 (m, 1H), 4.21-4.24 (dd, 2H), 4.06-4.09 (dd, 1H), 2.23-2.26 (m, 6H), 1.49-1.55 (m, 6H), 1.18-1.24 (m, 78H), 0.80-0.82 (t, 9H)

δ_C (100 MHz; CDCl₃) 172.3 (-C=O), 67.9, (-CH-O), 61.1 (-CH₂-O), 33.2, 33.1, 30.9 (-CH₂-C=O), 28.7, 28.5, 28.4, 28.3, 28 (-CH₂), 23.9, 21.7 (-CH₂-), 13.1 (-CH₃); m/z (HR-MS) 852.908[M + NH₄]⁺.

[SPP-isomer] (14 a)

δ_H (400 MHz; CDCl₃) 4.01-4.13 (m, 4H), 2.26-2.29 (t, 6H), 1.54-1.57 (m, 6H), 1.19-1.24 (m, 77H), 0.80-0.82 (t, 9H)

δ_C (100 MHz; CDCl₃) 177.7, 172.8 (-C=O), 67.3, (-CH-O), 63.9 (-CH₂-O), 32.7, 30.8 (-CH₂-C=O), 28.6, 28.5, 28.3, 28.1 (-CH₂), 21.6 (-CH₂-), 13.06 (-CH₃); m/z (HR-MS) 845.4[M + Li]⁺.

2.4.9 Synthesis of 1-Stearoyl-2,3-dioleoyl glycerol [SOO] (15) (Hui et al., 2003)

The 1- Stearoyl glycerol (13) (MW = 358.56 gmol⁻¹, 0.1 g, 0.278 mmol, 1 equiv.) was dissolved in 5 mL of pyridine at room temperature and then this solution was cooled to 0°C in an ice bath with continuous stirring. To this reaction solution, 4-dimethylamino pyridine (4-DMAP) (MW = 122.17 gmol⁻¹, 0.0068 g, 0.0556 mmol, 0.2 equiv.) was added at 0°C and the whole solution was stirred for 30 minutes at 0°C. The (9Z)-octadecenoyl chloride (oleoyl chloride) (MW = 300.91 gmol⁻¹, 0.418 g, 0.459 mmol, 1.39 mmol, 5 equiv.) was dissolved in 8 mL of DCM at room temperature and this solution was added drop wise to the above solution of 1-stearoyl glycerol in pyridine and 4-DMAP at 0°C over a time span of 30 minutes. The reaction mixture was stirred for 2 hours at 0°C and then at room temperature for 52 hours. The reaction mixture was poured into ice-cold distilled water (60 mL) and was extracted with chloroform (2 x 70 mL). The organic layer (chloroform extract) was washed with ice-cold HCl (2 N) (2 x 70 mL), saturated NaHCO₃ solution (1 x 70 mL) and then ice-cold distilled H₂O (2 x 70 mL). The organic layer was dried over Na₂SO₄, and the solvent was removed under vacuum. The product was purified by silica gel (SiO₂) column chromatography with petroleum ether/ethyl acetate (95:05 / 5%) as eluents. 1- Stearoyl-2,3-dioleoyl glycerol (15) was obtained as colorless liquid (MW = 887.45 gmol⁻¹, % Yield= 46 %, R_f= 0.45).

δ_H (400 MHz; CDCl₃) 5.21-5.34 (m, 4H), 4.23-4.27 (dd, 2H), 4.08-4.12 (dd, 2H), 2.25-2.29 (m, 6H), 1.96-1.97 (m, 7H), 1.51-1.57 (m, 11H), 1.21-1.26 (m, 71H), 0.82-0.85 (t, 9H)

δ_c (100 MHz; $CDCl_3$) 173.3, 172.9 (-C=O), 130.12, 129.8 (-CH=CH-), 69, (-CH-O), 62.2 (-CH₂-O), 34.1, 32.01 (-CH₂-C=O), 29.8, 29.6, 29.4, 29.2, 27.3 (-CH₂), 24.9, 22.7 (-CH₂-), 14.2 (-CH₃); m/z (HR-MS) 904.83 $[M + NH_4]^+$.

2.4.10 Synthesis of 1-Stearoyl-2,3-dilinoleoyl glycerol [SLL] (16) (Hui et al., 2003)

In the same way as compound (15). The 1- Stearoyl glycerol (13) (MW = 358.56 $gmol^{-1}$, 0.05 g, 0.139 mmol, 1 equiv.) was dissolved in 3 mL of pyridine, 4-dimethylamino pyridine (4-DMAP) (MW = 122.17 $gmol^{-1}$, 0.0426 g, 0.3475 mmol, 2.5 equiv.), (9Z,12Z)-octadecadienoyl chloride (linoleoyl chloride) (MW = 298.89 $gmol^{-1}$, 0.124 g, 0.13 mL, 0.417 mmol, 3 equiv.) in 4 mL of DCM. The reaction steps were followed as above for compound (15). The reaction mixture was stirred for 2 hours at 0°C and then at room temperature for 24 hours. The reaction mixture was poured into ice-cold distilled water (50 mL) and was extracted with chloroform (2 x 50 mL). The organic layer (chloroform extract) was washed with ice-cold HCl (2 N) (2 x 50 mL), saturated $NaHCO_3$ solution (2 x 50 mL) and then ice-cold distilled H_2O (2 x 50 mL). The organic layer was dried over Na_2SO_4 , and the solvent was removed under vacuum. The product was purified by silica gel (SiO_2) column chromatography with petroleum ether/ethyl acetate (95:05 / 5%) as eluents. 1- Stearoyl-2,3-dilinoleoyl glycerol (16) was obtained as colorless liquid (MW = 883.42 $gmol^{-1}$, % Yield= 24.3 %, R_f = 0.3).

δ_H (400 MHz; $CDCl_3$) 5.19-5.37 (m, 9H), 4.22-4.26 (dd, 2H), 4.07-4.12 (dd, 2H), 2.24-2.28 (dt, 6H), 1.97-2.02 (m, 7H), 1.56 (s, 7H), 1.20-1.26 (m, 62H), 0.81-0.86 (t, 8H)

δ_c (100 MHz; $CDCl_3$) 173.3, 172.9 (-C=O), 130.3, 130.1, 130, 128.1, 127.9 (-CH=CH-), 68.9, (-CH-O), 62.1 (-CH₂-O), 34.2, 34.1, 32.02, 31.6 (-CH₂-C=O), 29.7, 29.5, 29.4, 29.3, 29.2, 29.1, 27.2 (-CH₂), 25.7, 24.9, 22.7, 22.6 (-CH₂-), 14.2, 14.1 (-CH₃); m/z (HR-MS) 904.84 $[M + NH_4]^+$.

2.4.11 Synthesis of 1-Oleoyl glycerol (17) (Hui et al., 2003)

In the same way as compound (7). The 2,2-dimethyl-1,3-dioxolane-4-methanol (1,2-Isopropylidene glycerol or Solketal) (MW = 132.16 $gmol^{-1}$, 1 g, 0.93 mL, 7.541 mmol, 1 equiv.) was dissolved in 13 mL of pyridine, (9Z)-octadecenoyl chloride (oleoyl chloride) (MW = 300.91 $gmol^{-1}$, 3.403 g, 3.74 mL, 11.3115 mmol, 1.5 equiv.) in 35 mL of DCM and 4-dimethylamino pyridine (4-DMAP) (MW = 122.17 $gmol^{-1}$, 0.0925 g, 0.7541 mmol, 0.1 equiv.). The reaction steps were followed as above for compound (7). The reaction mixture was stirred for 1 hour at 0°C and then at room temperature for 24 hours. The reaction mixture was poured into ice-cold water (200 mL) and was extracted with chloroform (4 x 70 mL). The organic layer (chloroform extract) was washed with ice-cold HCl (2 N) (3 x 75 mL), saturated $NaHCO_3$ solution (1 x 100 mL) and then ice-cold distilled H_2O (3 x 100 mL). The organic layer was dried over Na_2SO_4 , and the solvent was removed under vacuum. The product was purified by silica gel (SiO_2) column chromatography with petroleum ether/ethyl acetate (96:04 / 4%) as eluents. 1- oleoyl glycerol (17) was obtained as colorless liquid (MW = 356.6 $gmol^{-1}$, % Yield= 66.8 %, R_f = 0.01)

δ_H (400 MHz; $CDCl_3$) 5.29 (m, 2H), 3.85-4.18 (m, 3H), 3.53-3.79 (m, 2H), 2.28-2.32 (t, 2H), 1.97-2.02 (m, 7H), 1.58-1.6 (d, 2H), 1.22-1.25 (m, 20H), 0.81-0.84 (t, 3H)

δ_C (100 MHz; $CDCl_3$) 173.58 (-C=O), 129.26, 128.9 (-CH=CH-), 69.4, (-CH-O), 64.3, 62.5 (-CH₂-O), 33.3, 31.1 (-CH₂-C=O), 28.9, 28.7, 28.5-28.3 (-CH₂), 26.5, 24.1, 21.8 (-CH₂-), 13.3 (-CH₃); m/z (HR-MS) 379.3 [M + Na]⁺.

2.4.12 Synthesis of 1-Oleoyl-2,3-dipalmitoyl glycerol [OPP] (18) (Hui et al., 2003)

In the same way as compound (15). The 1- Oleoyl glycerol (17) (MW = 356.54 gmol⁻¹, 0.1 g, 0.28 mmol, 1 equiv.) was dissolved in 5 mL of pyridine, 4-dimethylamino pyridine (4-DMAP) (MW = 122.17 gmol⁻¹, 0.09 g, 0.7 mmol, 2.5 equiv.), n-hexadecanoyl chloride (palmitoyl chloride) (MW = 274.87 gmol⁻¹, 0.23 g, 0.252 mL, 0.84 mmol, 3 equiv.) in 8 mL of DCM. The reaction steps were followed as above for compound (15). The reaction mixture was stirred for 2 hours at 0°C and then at room temperature for 22 hours. The reaction mixture was processed as above for compound (15). The product was purified by silica gel (SiO₂) column chromatography with petroleum ether/ethyl acetate (95:05 / 3%) as eluents. 1-Oleoyl-2,3-dipalmitoyl glycerol (18) was obtained as white waxy solid (MW = 833.36 gmol⁻¹, % Yield= 9 %, R_f= 0.25).

δ_H (400 MHz; $CDCl_3$) 5.16-5.28 (m, 3H), 4.19-4.23 (dd, 2H), 4.04-4.09 (dd, 2H), 2.21-2.25 (dt, 6H), 1.92-1.94 (m, 4H), 1.53-1.54 (m, 7H), 1.18-1.22 (m, 69H), 0.78-0.82 (t, 9H)

δ_C (100 MHz; $CDCl_3$) 172.7 (-C=O), 129.4, 129.1 (-CH=CH-), 68.2, (-CH-O), 61.5 (-CH₂-O), 33.6, 33.4, 31.3 (-CH₂-C=O), 29.08, 28.9, 28.7, 28.5, 26.5, 24.2, 22 (-CH₂), 13.5 (-CH₃); m/z (HR-MS) 850.89 [M + NH₄]⁺.

2.4.13 Synthesis of 1-Oleoyl-2,3-dilinoleoyl glycerol [OLL] (19) (Hui et al., 2003)

In the same way as compound (15). The 1- Oleoyl glycerol (17) (MW = 356.54 gmol⁻¹, 0.1 g, 0.28 mmol, 1 equiv.) was dissolved in 5 mL of pyridine, 4-dimethylamino pyridine (4-DMAP) (MW = 122.17 gmol⁻¹, 0.09 g, 0.7 mmol, 2.5 equiv.), (9Z,12Z)-octadecadienoyl chloride (linoleoyl chloride) (MW = 298.89 gmol⁻¹, 0.25 g, 0.27 mL, 0.84 mmol, 3 equiv.) in 8 mL of DCM. The reaction steps were followed as above for compound (15). The reaction mixture was stirred for 2 hours at 0°C and then at room temperature for 22 hours. The reaction mixture was processed as above for compound (15). The product was purified by silica gel (SiO₂) column chromatography with petroleum ether/ethyl acetate (95:05 / 5 %) as eluents. 1-Oleoyl-2,3-dilinoleoyl glycerol (19) was obtained as white waxy solid (MW = 881.4 gmol⁻¹, % Yield= 11 %, R_f= 0.34).

δ_H (400 MHz; $CDCl_3$) 5.30 (m, 10H), 4.10-4.25 (m, 4H), 2.26-2.28 (m, 10H), 1.56 (m, 8H), 1.25 (s, 49H), 0.84 (m, 9H)

δ_C (100 MHz; $CDCl_3$) 173.3 (-C=O), 130.2, 130.02, 128.08, 127.9 (-CH=CH-), 68.8, (-CH-O), 62.1 (-CH₂-O), 34.02, 31.9, 31.5 (-CH₂-C=O), 29.6, 29.3, 29.1, 27.1 (-CH₂), 25.6, 24.8, 22.5 (-CH₂-), 14 (-CH₃); m/z (HR-MS) 898.78 [M + NH₄]⁺.

2.4.14 Synthesis of 1-Linoleoyl-2,3-isopropylidene glycerol (20) (Hui et al., 2003)

In the same way as compound (7). The 2,2-dimethyl-1,3-dioxolane-4-methanol (1,2-Isopropylidene glycerol or Solketal) (MW = 132.16 gmol⁻¹, 0.1856 g, 0.17 mL, 1.4 mmol, 1 equiv.) was dissolved in 3 mL of pyridine, (9Z,12Z)-octadecadienoyl chloride (linoleoyl chloride) (MW = 298.89 gmol⁻¹, 0.4185 g, 0.45 mL, 1.4 mmol, 1 equiv.) in 10 mL of DCM and 4-dimethylamino pyridine (4-DMAP) (MW = 122.17 gmol⁻¹, 0.017 g, 0.14 mmol, 0.1 equiv.). The reaction steps were followed as above for compound (7). The reaction mixture was stirred for 1 hour at 0°C and then at room temperature for 24 hours. The reaction mixture was worked-up as above for compound (7). The product was purified by silica gel (SiO₂) column chromatography with petroleum ether/ethyl acetate (96:04 / 4 %) as eluents. 1-Linoleoyl-2,3-Isopropylidene glycerol (20) was obtained as white crystalline solid (MW = 394.59 gmol⁻¹, % Yield= 54.7 %, R_f= 0.3)

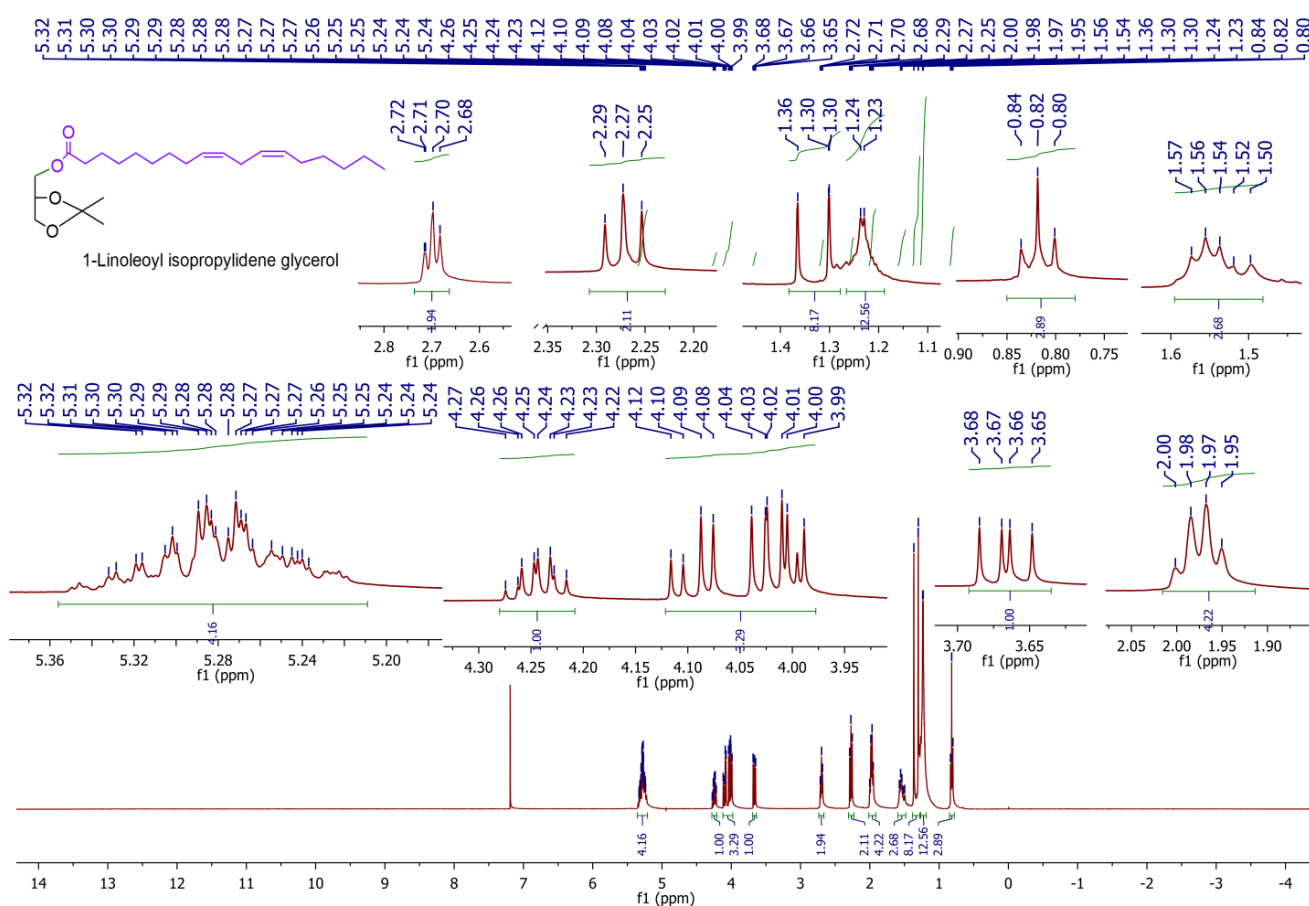


Figure 2.18 ¹H-NMR (400 MHz, CDCl₃) spectrum of 1-Linoleoyl-2,3-Isopropylidene glycerol (20)

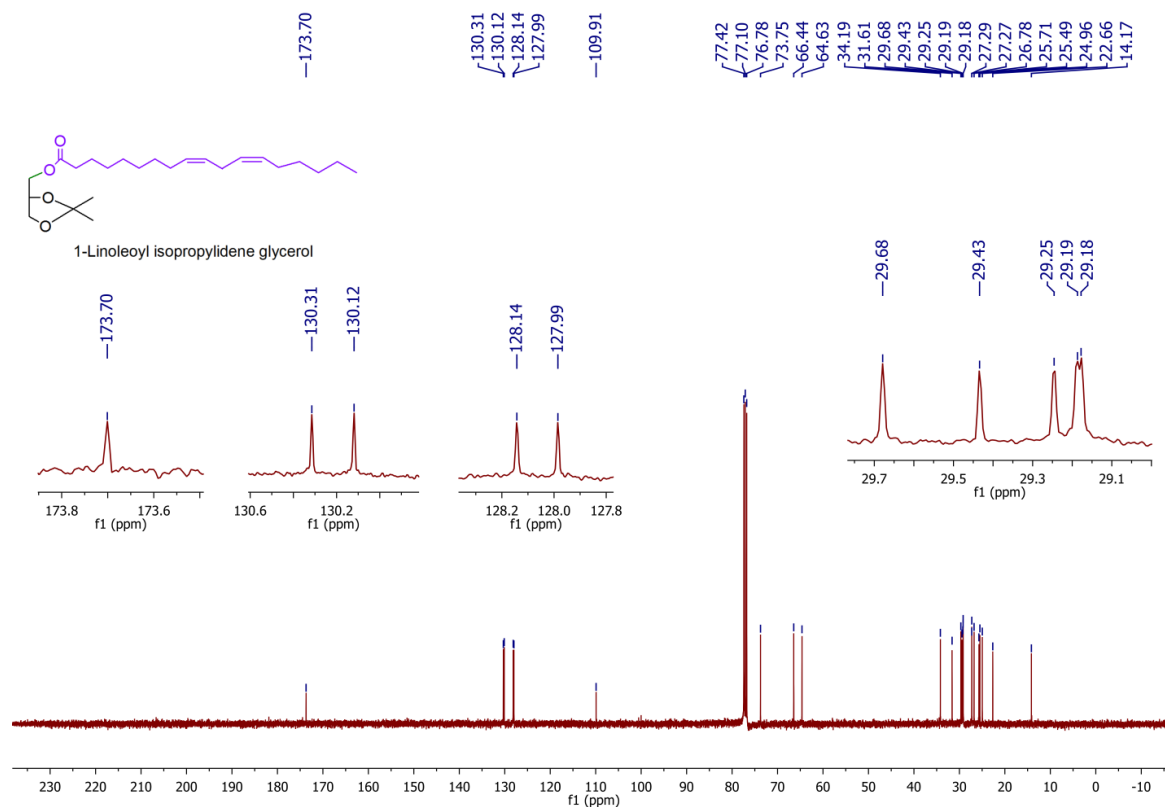


Figure 2.19 ^{13}C -NMR (100 MHz, CDCl_3) spectrum of 1-Linoleoyl-2,3-Isopropylidene glycerol (20)

δ_{H} (400 MHz; CDCl_3) 5.24-5.32 (m, 4H), 4.22-4.27 (m, 1H), 4.08-4.12 (dd, 2H), 3.99-4.04 (dd, 1H), 3.65-3.68 (dd, 1H), 2.68-2.72 (t, 2H), 2.25-2.29 (t, 2H), 1.95-2.0 (m, 4H), 1.50-1.57 (m, 3H), 1.3-1.36 (d, 8H), 1.23-1.24 (d, 13H), 0.80-0.84 (t, 3H)

δ_{C} (100 MHz; CDCl_3) 173.7 (-C=O), 130.3, 130.1, 128.1, 127.9 (-CH=CH-), 73.7, (-CH-O), 66.4, 64.6 (-CH₂-O), 34.1, 31.6 (-CH₂-C=O), 29.6, 29.4, 29.2, 29.1-27.2 (-CH₂), 26.7, 25.7, 25.4, 24.9, 22.6 (-CH₂-), 14.1 (-CH₃).

2.4.15 Synthesis of 1-Linoleoyl glycerol (21) (J., 1994)

In the same way as compound (8). 1-Linoleoyl-2,3-isopropylidene glycerol (20) (MW = 394.59 g mol^{-1} , 0.30 g, 0.76 μmoles , 1 equiv.) was dissolved in 6 mL of methanol (MW = 32.04 g mol^{-1}) and HCl (MW = 36.5 g mol^{-1} , 0.06 mL, 32%, 10.2 N). The reaction steps were followed as above for compound (8). The reaction mixture was stirred for 2.5 hours at room temperature. The reaction mixture was processed in the same way as above for compound (8). The product was purified by silica gel (SiO_2) column chromatography with petroleum ether/ethyl acetate (95:05 / 5%) as eluents. 1-Linoleoyl glycerol (21) was obtained as colorless solid (MW = 354.52 g mol^{-1} , % Yield= 62 %, R_f = 0.01).

δ_{H} (400 MHz; CDCl_3) 5.24-5.33 (m, 4H), 4.06-4.16 (m, 2H), 3.76-3.89 (m, 2H), 3.61-3.65 (dd, 1H), 3.51-3.55 (dd, 1H), 2.26-2.30 (t, 2H), 2.16 (s, 2H), 1.95-2.01 (q, 5H), 1.54-1.58 (m, 16H), 0.80-0.84 (t, 3H)

δ_c (100 MHz; $CDCl_3$) 173.7 (-C=O), 129.6, 129.4, 127.5, 127.1 (-CH=CH-), 69.6, (-CH-O), 64.6, 62.7 (-CH₂-O), 33.5, 30.9 (-CH₂-C=O), 29, 28.7, 28.5 (-CH₂), 26.6, 25, 24.3, 22 (-CH₂-), 13.5 (-CH₃); m/z (HR-MS) 377.30 [M + Na]⁺.

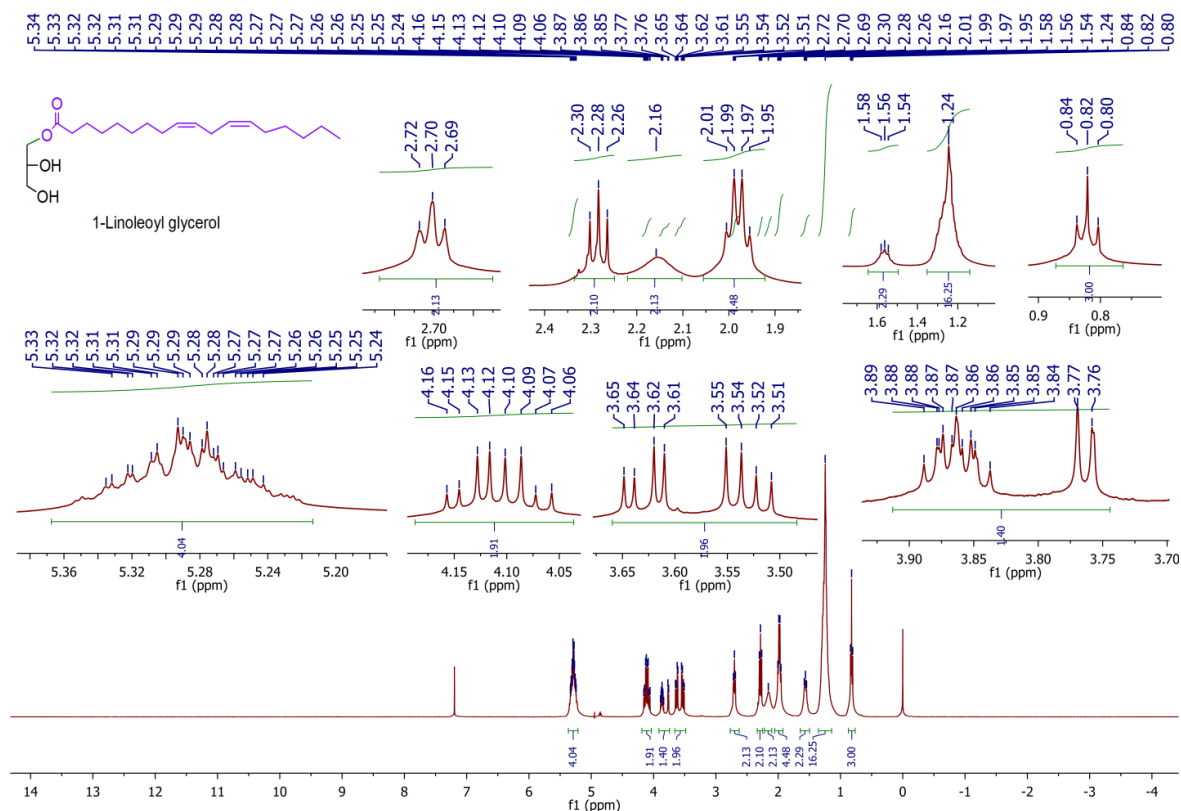


Figure 2.20 ¹H-NMR (400 MHz, $CDCl_3$) spectrum of 1-Linoleoyl glycerol (21)

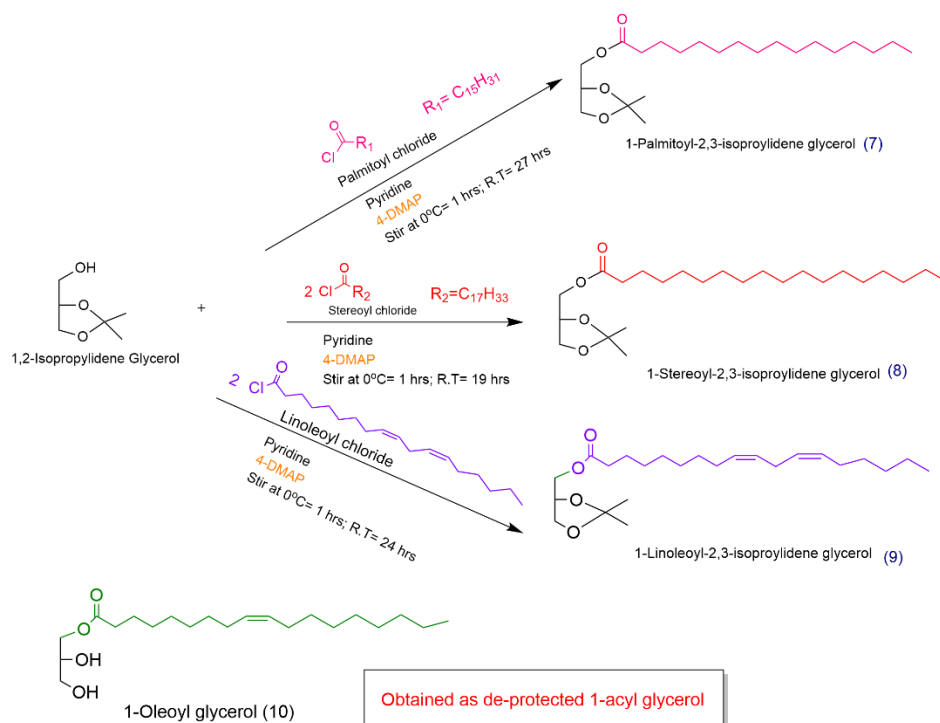
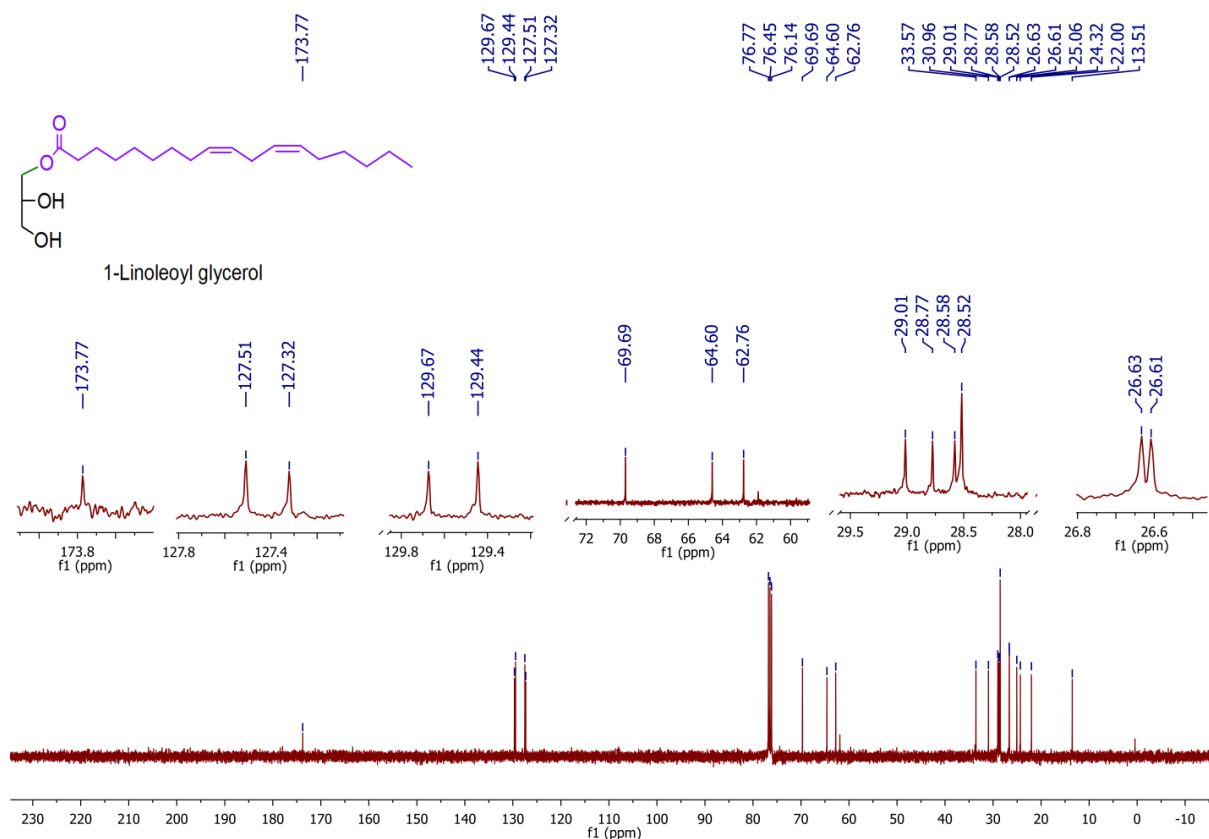


Figure 2.22 Synthesis of 1-acyl isopropylidene glycerols

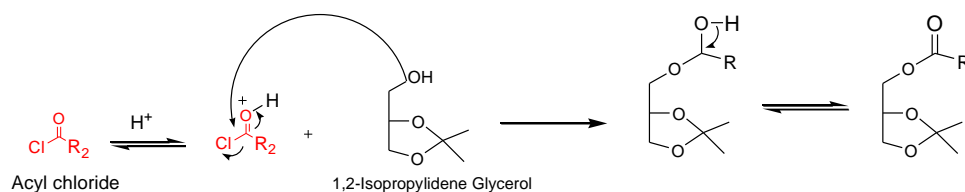


Figure 2.23 Mechanism of formation of 1-acyl isopropylidene glycerol

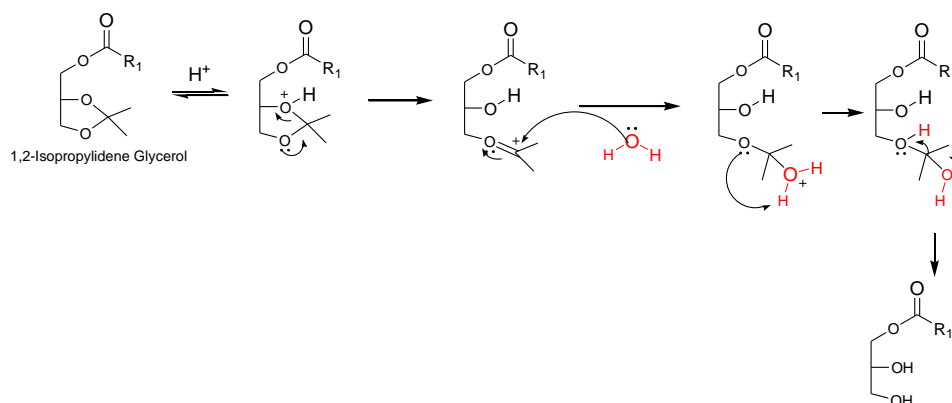


Figure 2.24 Mechanism of hydrolysis of 1-acyl isopropylidene glycerol

2.4.16 Synthesis of 1-Linoleoyl-2,3-dipalmitoyl glycerol [LPP] (22) (Hui et al., 2003)

In the same way as compound (15). The 1-Linoleoyl glycerol (21) (MW = 354.52 gmol⁻¹, 0.1 g, 0.282 mmol, 1 equiv.) was dissolved in 5 mL of pyridine, 4-dimethylamino pyridine (4-DMAP) (MW = 122.17 gmol⁻¹, 0.0865 g, 0.705 mmol, 2.5 equiv.), n-hexadecanoyl chloride (palmitoyl chloride) (MW = 274.87 gmol⁻¹, 0.232 g, 0.25 mL, 0.846 mmol, 3 equiv.) in 4 mL of DCM. The reaction steps were followed as above for compound (15). The reaction mixture was stirred for 2 hours at 0°C and then at room temperature for 21 hours. The reaction mixture was poured into ice-cold distilled water (60 mL) and was extracted with chloroform (2 x 60 mL). The organic layer (chloroform extract) was washed with ice-cold HCl (2 N) (2 x 50 mL), saturated NaHCO₃ solution (2 x 50 mL) and then ice-cold distilled H₂O (2 x 60 mL). The organic layer was dried over Na₂SO₄, and the solvent was removed under vacuum. The product was purified by silica gel (SiO₂) column chromatography with petroleum ether/ethyl acetate (95:05 / 5%) as eluents. 1- Linoleoyl-2,3-dipalmitoyl glycerol (22) was obtained as colorless liquid (MW = 831.34 gmol⁻¹, % Yield= 21 %, R_f= 0.32).

δ_H (400 MHz; CDCl₃) 5.20-5.36 (m, 5H), 4.23-4.27 (dd, 2H), 4.08-4.13 (dd, 2H), 2.71-2.75 (t, 2H), 1.98-2.03 (m, 4H), 1.52-1.56 (m, 7H), 1.21-1.26 (m, 63H), 0.82-0.87 (m, 9H)

δ_C (100 MHz; CDCl₃) 172.1 (-C=O), 129.2, 129, 127, 126.8 (-CH=CH-), 67.8, (-CH-O), 61.1 (-CH₂-O), 33.2, 33, 30.9, 30.5 (-CH₂-C=O), 28.7, 28.6, 28.4, 28.3, 28.2, 28.1, 26.2 (-CH₂), 24.6, 23.9, 23.8, 21.7, 21.5 (-CH₂-), 13.1, 13 (-CH₃); m/z (HR-MS) 848.77 [M + NH₄]⁺.

2.4.17 Synthesis of 1-Linoleoyl-2,3-dioleoyl glycerol [LOO] (23) (Hui et al., 2003)

In the same way as compound (15). The 1-Linoleoyl glycerol (21) (MW = 354.52 gmol⁻¹, 0.1 g, 0.282 mmol, 1 equiv.) was dissolved in 5 mL of pyridine, 4-dimethylamino pyridine (4-DMAP) (MW = 122.17 gmol⁻¹, 0.0865 g, 0.705 mmol, 2.5 equiv.), (9Z)-octadecenoyl chloride (oleoyl chloride) (MW = 300.91 gmol⁻¹, 0.424 g, 0.47 mL, 1.42 mmol, 5 equiv.) in 8 mL of DCM. The reaction steps were followed as above for compound (15). The reaction mixture was stirred for 2 hours at 0°C and then at room temperature for 21 hours. The reaction mixture was worked-up as above for compound (22). The product was purified by silica gel (SiO₂) column chromatography with petroleum ether/ethyl acetate (95:05 / 5%) as eluents. 1- Linoleoyl-2,3-dipalmitoyl glycerol (22) was obtained as colorless liquid (MW = 883.42 gmol⁻¹, % Yield= 65.8 %, R_f= 0.4).

δ_H (400 MHZ; CDCl₃) 5.27 (m, 9H), 4.07-4.23 (m, 4H), 1.54-2.70 (m, 27H), 1.53-1.54 (m, 56H), 0.80-0.81 (m, 9H)

δ_C (100 MHZ; CDCl₃) 1723.3, 172.9 (-C=O), 130.3, 130.1, 129.79, 129.77, 128.1, 127.9 (-CH=CH-), 68.9, (-CH-O), 62.1 (-CH₂-O), 334.2, 34.1, 31.9, 31.6 (-CH₂-C=O), 29.8, 29.7, 29.6, 29.4, 29.2, 29.1 (-CH₂), 27.3, 27.2, 25.7, 24.9, 22.7, 22.6, (-CH₂-), 14.2, 14.1 (-CH₃); m/z (HR-MS) 900.80 [M + NH₄]⁺.

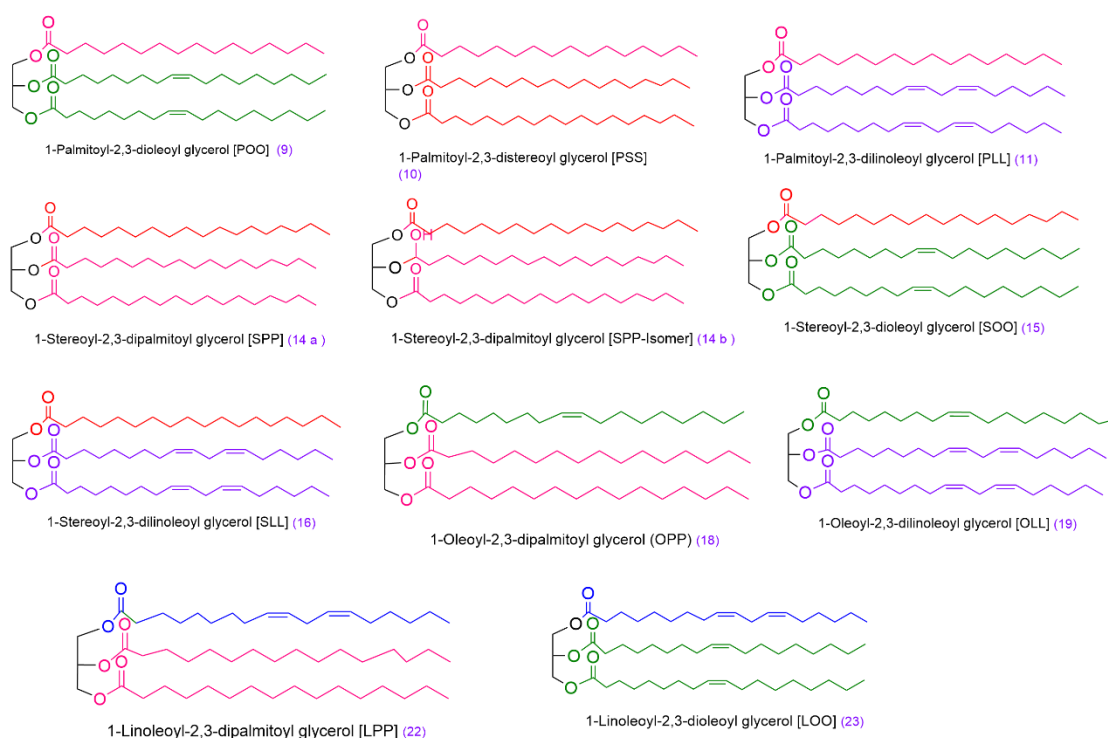


Figure 2.25 Chemical structures of unsymmetrical triacylglycerols synthesized by a multistep synthesis (15-23)

2.5 Results & Discussion

Chemical synthesis of triacylglycerols (TAGs) has been reported in the literature since long time ago. However, the methods of the synthesis of TAGs had been tedious and produced poor yields. (Kotwal et al., 2011) The first synthesis of TAGs at room temperature was reported by Alfred Hassner. The chemical synthesis of synthetic TAGs has been carried out by using Hassner esterification method with 4-dimethyl amino pyridine (4-DMAP) and N, N'-dicyclohexylcarbodiimide (DCC) as a catalyst. (Hassner & Alexanian, 1978) The use of 4-DMAP increases the rate of reaction by 20% and reduces the production of side products i.e., N-acylureas. (Elbert, 1989) Tripalmitin has been synthesized earlier by using triphenylphosphine as a catalyst. (Saroja & Kaimal, 1986) Recently the enantiomeric synthesis of tripalmitin [PPP], tristearin [SSS], triolein [OOO], trilinolein [LLL], trilinolenin [LnLnLn] and some unsymmetrical TAGs has been reported by the randomization reaction method. The unsymmetrical TAGs synthesized by these randomization reactions include 1-stereoyl-2,3-dipalmitoyl glycerol [SLL], 1-stereoyl-2,3-dioleoyl glycerol [SOO], 1-oleoyl-2,3-distereoyl glycerol [OSS], 1-oleoyl-2,3-dipalmitoyl glycerol [OPP], 1-oleoyl-2,3-dilinoleoyl glycerol [OLL], 1-linoleoyl-2,3-dioleoyl glycerol [LOO], 1-linoleoyl-2,3-distereoyl glycerol [LSS], 1-linoleoyl-2,3-dipalmitoyl glycerol [LPP] and 1-palmitoyl-2,3-dioleoyl glycerol [POO]. The trifluoroacetic acid has been used in this method for the deprotection step. (Lísa & Holčápek, 2013)

The synthesis of all the TAGs in this research work follows the mild method of esterification for the synthesis of TAGs at room temperature. The unsymmetrical TAGs have been synthesized in a multistep synthesis from a reported method for the synthesis of TAGs. (Hui et al., 2003) The synthesis of 1-monoacylglycerol has been achieved enantiomerically. The deprotection step uses mild hydrochloric acid and at room temperature. The reaction at room temperature reduces the chances of acyl migration and enantiomeric TAGs are synthesized. (Lísa & Holčápek, 2013) These conditions are also a green chemistry approach. The optimization of reaction conditions for temperature, time of reaction and use of catalyst has also been observed on short scale. It has been observed that longer reaction times result in significant increase of % yield of the TAGs. The esterification reaction is more favorable at room temperature. Increase in temperature and heating of the reaction mixture results in the reduction of % yield. The reagents used as catalysts for the reaction, catalyze the reaction when freshly purchased. The esterification reactions of all the TAGs have been carried out by blowing inert nitrogen gas through the reaction mixture. This is applicable to reduce the accumulation of water molecules produced during the esterification reaction. The room temperature is useful to avoid the polymerization of unsaturated fatty acid TAGs and increase in the rate of reaction. (Cox, 1944)

The chemical structures of synthesized triacylglycerols have been confirmed by ^1H NMR and ^{13}C NMR. In ^1H NMR of the TAGs with three saturated fatty acid chains the $-\text{CH}_2\text{CH}_3$ appeared with large line

intensities in the range on 0.9-2.0 ppm. The glycerol protons showed a multiplet at approximately 4.0-4.4 ppm. In the case of unsaturated fatty acid chain, in addition to usual peaks, a multiplet has been observed at 5.0-5.4 ppm. Some diacylglycerols (DAGs) have been isolated as a fraction from the reaction mixture of these esterification reactions. These DAGs showed the same types of peaks with less intensity. A comparison of the ^1H NMR of some TAGs, diacylglycerol and a monoacylglycerol has been shown in Figure 2.24. The ^{13}C NMR of the TAGs showed carbonyl ($-\text{C}=\text{O}$) peak at 170-173 ppm. The $-\text{CH}=\text{}$ peaks for unsaturated fatty acid chains appeared at 118-130 ppm. These NMR studies of synthetic TAGs are important to study and correlate the structures and conformation of TAGs in natural food and drugs. (Broadhurst et al., 2004)

The usual TAGs present in the biological membranes are OOO, LLL and LnLnLn. The meat and fish contain trans fatty acids but a small amount of short chain fatty acids. The synthesis of these TAGs is useful to provide synthetic standard for the analysis of TAGs in food, pharmaceuticals, and perfumes. (Prades et al., 2003)

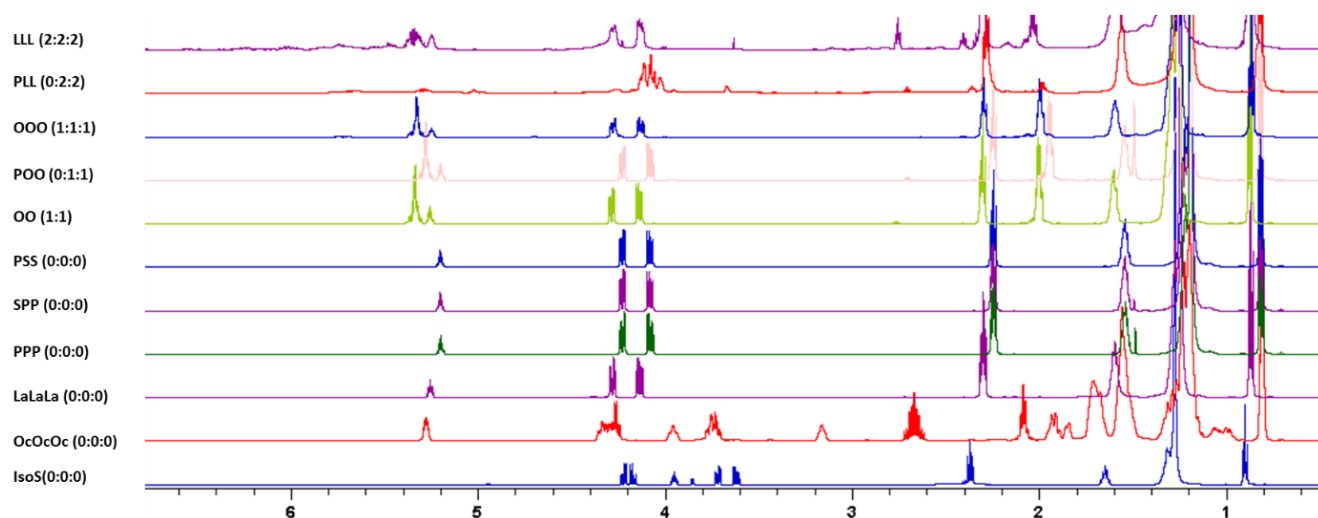


Figure 2.26 Comparison of 1D ^1H NMR spectra of triacylglycerols and diacylglycerols referenced to TMS in CDCl_3 , NS = 16

Triacylglycerols (TAGs) exist in two different conformations naturally i.e., a chair and a bent or tuning fork conformation. It is suggested that the synthesis of TAGs can result in different conformers of TAGs. (Sasaki et al., 2012) The synthesis of tripalmitin [PPP] was carried out with different reaction times. The two different products for the same esterification reaction showed a difference in their ^1H NMR spectra. For PPP-isomer the peaks appeared at 1.99-2.0 ppm. This suggest that there is a dynamic interchange between different conformations. The same has been observed for the 1-stereoyl-2,3-dipalmitoyl glycerol [SPP].

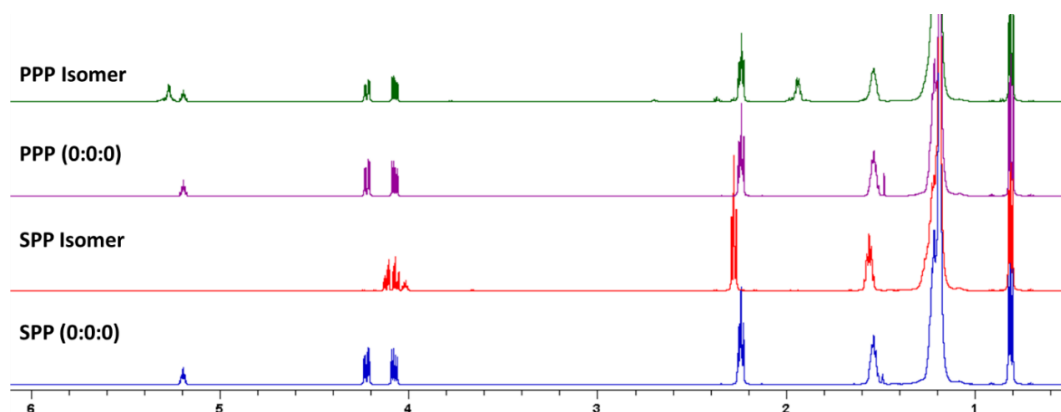


Figure 2.27 comparison of 1D ^1H NMR spectra of tripalmitin [PPP] and 1-stereoyl-2,3-dipalmitoyl glycerol [SPP] and their isomeric fraction separated from the esterification reaction mixtures referenced to TMS in CDCl_3 , NS = 16

2.5.1 2D NOESY and 2D ROESY NMR measurements

The 2D NOESY spectra of TAGs with unsaturated fatty acyl chains showed an in-space coupling between the methylene ($-\text{CH}_2$) and $\text{C}=\text{C}$ protons. Such in-space couplings were absent for TAGs with saturated fatty acyl chains. In the 2D NOESY of TAGs with saturated fatty acyl chains the glycerol protons show in-space coupling with the adjacent methylene ($-\text{CH}_2$) protons. This suggests a bent conformation in the saturated TAGs. (Lameiras & Nuzillard, 2016)

The conformation of TAGs with saturated fatty acyl chains and TAGs with unsaturated fatty acyl chains can be determined with NOESY and ROESY. TAGs with unsaturated fatty acyl chains are more rigid due to $\text{C}=\text{C}$ and a bent structure at 30° . This is seen in the 2D NOESY of unsaturated TAGs. The van der Waals interactions are less in unsaturated TAGs. (Pérez-Gil, 2008)

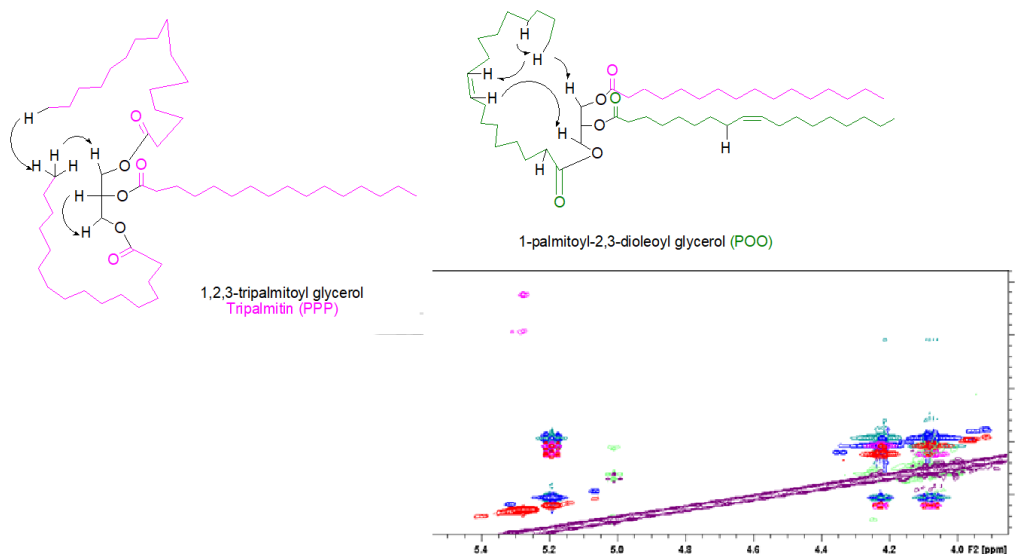


Figure 2.28 Comparison of PLL (Purple), PPP (Blue) and POO (Red), 2D NOESY spectra referenced to TMS in CDCl_3 , NS = 32.

Box highlights peaks of interest showing long range NOESY peaks between glycerol and mono-unsaturated and aliphatic fatty acyl chains. (Figure 2.28) The peaks suggest a folded over structure due to presence of double bonds bringing polar and non-polar protons into closer proximity. Peaks are seen for the long-range coupling between the $-CH_2-$ of the fatty acyl chain (2.0-2.2 ppm) and the protons from the glycerol backbone (5.2-5.4 ppm) for PPP (blue) and POO (red) and these are absent for 2D NOESY of PLL (purple). It is suggested that a greater number of double bonds in TAGs have different activation energy than the monounsaturated TAG. This suggests a different conformation for polyunsaturated TAGs as compared to monounsaturated TAG. PPP shows peaks in 2D NOESY due to its small length of fatty acyl chain. It is suggested that smaller chain length in saturated TAGs favours folding of the fatty acyl chain. The cross peaks in 2D NOESY and 2D ROESY of TAGs, DAGs and monoacylglycerols appear due to proximity of protons in space.

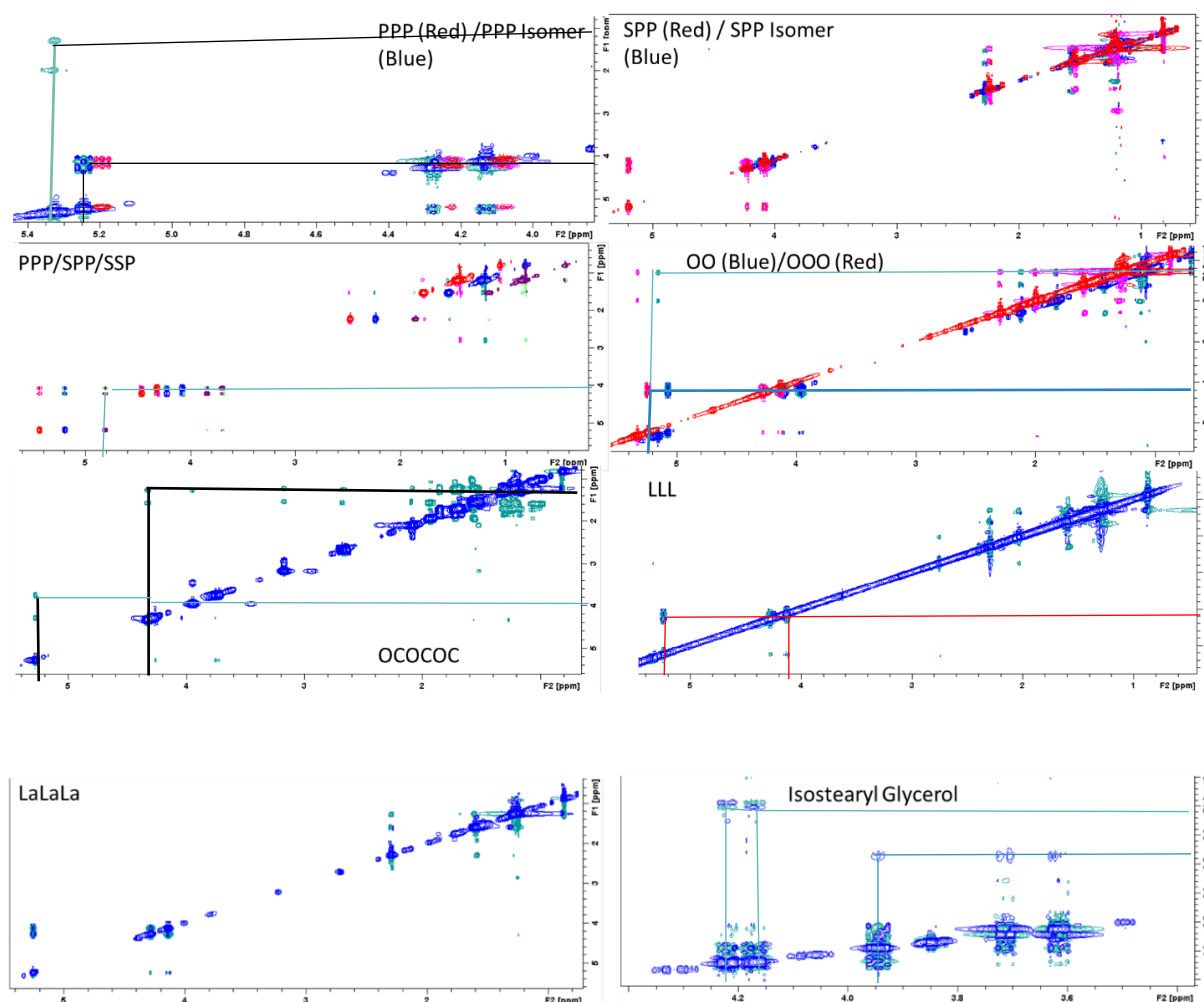


Figure 2.29 Comparison of 2D NOESY spectra triacylglycerols (TAGs), diacylglycerol (DAG) and a monoacylglycerol referenced to TMS in $CDCl_3$, NS = 32 (peaks for the coupling of the $-CH_2-$ and $-CH_3-$ protons of the fatty acyl chain with the protons of glycerol backbone of the TAGs are indicated by the lines in the 2D NOESY spectra)

In figure Figure 2.29 2D NOESY spectra show important information about the conformational features of saturated and unsaturated TAGs. TAGs with smaller molecular weight i.e., 1, 2,3-trioctanoyl glycerol ($O_cO_cO_c$) peaks are seen in the 2D NOESY spectrum. It suggests that fatty acyl chain with small chain length tend to fold and have a folded or bent conformation. This difference between the 2D NOESY spectra of PPP and SPP. 2D NOESY spectrum of PPP shows peaks for the coupling of protons of $-CH_2-$ of fatty acyl chain with the protons of glycerol. These peaks are absent in SPP. This suggests that the saturated TAGs differ in their conformation based on the length of the fatty acyl chain and molecular weight. 1,2,3-triolein (OOO) and diolein (OOX) differ in the number of double bonds and degree of unsaturation. 2D NOESY spectra of OOO and OOX show peaks for the coupling of the $-CH_2-$ and $-CH_3-$ protons of the fatty acyl chain with the protons of glycerol backbone. These coupling of the protons do not appear in the 2D NOESY of LLL.

NOESY and 2D ROESY provide useful information about the conformation of triacylglycerols. this is very important to understand the polymorphism of drugs, cosmetics, and perfumes. (Khodov et al., 2013)

2.6 Conclusion

The synthesis of triacylglycerols provides a mild method of synthesis at room temperature and feasible method of deprotection. The NMR studies are useful to study the triacylglycerol conformations in natural foods. These are important for the studies of metabolite and identification of known and unknown triacylglycerols in complex mixtures from natural products. NOESY and ROESY spectra show long range coupling between methylene $-CH_2$ groups of the glycerol backbone and the $-CH_3$ groups of the fatty acyl chains of TAGs. This is suggested that the TAGs possess a bent conformation. This is determined experimentally for the first time for the synthetic TAGs. The diffusion coefficient shows an increase in the chain length of fatty acyl chain and the number of double bonds. It reveals the activation energies at the different stereochemical positions at the glycerol backbone in TAG molecule. There are several biological phenomena associated with the conformation and diffusion coefficients of the TAGs. The movement of food molecules, salts and drugs is facilitated by the diffusion coefficient of the molecules. The study of diffusion coefficient and NOESY and ROESY of the synthetic TAGs can be helpful in metabolomics, pharmacokinetics, and biochemical studies. The diffusion coefficient determination of TAGs during metabolomics can trace the TAGs components and to know about the diseases in humans. NOESY and ROESY spectra can provide information about the unknow TAGs present in nature.

References

- Adlof, R. O., & List, G. R. (2003). Synthesis and analysis of symmetrical and nonsymmetrical disaturated/monounsaturated triacylglycerols. *Journal of Agricultural and Food Chemistry*, 51(7), 2096–2099. <https://doi.org/10.1021/jf021085l>
- Adlof, R. O., & List, G. R. (2008). Synthesis and physical properties of symmetrical and non-symmetrical triacylglycerols containing two palmitic fatty acids. *JAACS, Journal of the American Oil Chemists' Society*, 85(2), 99–104. <https://doi.org/10.1007/s11746-007-1173-y>
- Alrouh, F., Karam, A., Alshaghel, A., & El-Kadri, S. (2017). Direct esterification of olive-pomace oil using mesoporous silica supported sulfonic acids. *Arabian Journal of Chemistry*, 10, S281–S286. <https://doi.org/10.1016/j.arabjc.2012.07.034>
- Belloque, J., & Ramos, M. (1999). Application of NMR spectroscopy to milk and dairy products. *Trends in Food Science and Technology*, 10(10), 313–320. [https://doi.org/10.1016/S0924-2244\(00\)00012-1](https://doi.org/10.1016/S0924-2244(00)00012-1)
- Broadhurst, C. L., Schmidt, W. F., Crawford, M. A., Wang, Y., & Li, R. (2004). ¹³C nuclear magnetic resonance spectra of natural undiluted lipids: Docosahexaenoic-rich phospholipid and triacylglycerol from fish. *Journal of Agricultural and Food Chemistry*, 52(13), 4250–4255. <https://doi.org/10.1021/jf0353178>
- Cox, R. P. (1944). Esterification of U n s a t u r a t e d Fatty Acids 1. *Society*, 57–60
- Duan, Z. Q., Fang, X. L., Wang, Z. Y., Bi, Y. H., & Sun, H. (2015). Sustainable Process for 1,3-Diolein Synthesis Catalyzed by Immobilized Lipase from *Penicillium expansum*. *ACS Sustainable Chemistry and Engineering*, 3(11), 2804–2808. <https://doi.org/10.1021/acssuschemeng.5b00720>
- Elbert, T. (1989). Near-quantitative conversion of labelled acids to esters by modified Hassner esterification. Synthesis of labelled triglycerides. *Journal of Labelled Compounds and Radiopharmaceuticals*, XXVI, No.1, 107–116
- Ergan, F., Trani, M., & André, G. (1990). Production of glycerides from glycerol and fatty acid by immobilized lipases in non-aqueous media. *Biotechnology and Bioengineering*, 35(2), 195–200. <https://doi.org/10.1002/bit.260350210>

Guner, F. S., Sirkecioglu, A., Yilmaz, S., Erciyes, A. T., & Erdem-Senatalar, A. (1996). Esterification of oleic acid with glycerol in the presence of sulfated iron oxide catalyst. *JAACS, Journal of the American Oil Chemists' Society*, 73(3), 347–351. <https://doi.org/10.1007/BF02523429>

Haraldsson, G. G., Halldorsson, A., & Kuls, E. (2000). Chemoenzymatic synthesis of structured triacylglycerols containing eicosapentaenoic and docosahexaenoic acids. *JAACS, Journal of the American Oil Chemists' Society*, 77(11), 1139–1145. <https://doi.org/10.1007/s11746-000-0179-1>

Hassner, A., & Alexanian, V. (1978). R: Me 2, R:(CH₂14 3, R:C (NMe₂)₂. *New York*, 46, 0–3

Hassner, A., Krepski, L. R., & Alexanian, V. (1978). Aminopyridines as acylation catalysts for tertiary alcohols. *Tetrahedron*, 34(14), 2069–2076. [https://doi.org/10.1016/0040-4020\(78\)89005-X](https://doi.org/10.1016/0040-4020(78)89005-X)

Hui, S. P., Murai, T., Yoshimura, T., Chiba, H., & Kurosawa, T. (2003). Simple Chemical Syntheses of TAG Monohydroperoxides. *Lipids*, 38(12), 1287–1292. <https://doi.org/10.1007/s11745-003-1191-9>

J., Kocienski. P. (1994). *Protecting Groups* (2nd ed.). Georg Thieme Verlag Stuttgart

Jahed, V., Zarrabi, A., Bordbar, A. K., & Hafezi, M. S. (2014). NMR (1H, ROESY) spectroscopic and molecular modelling investigations of supramolecular complex of β -cyclodextrin and curcumin. *Food Chemistry*, 165, 241–246. <https://doi.org/10.1016/j.foodchem.2014.05.094>

Jahrgang, X. (1911). p z e x t s e Angewandte Chemie. 767(1903)

Janssen, A. E. M., Van der Padt, A., & Riet, K. V. t. (1993). Solvent effects on lipase-catalyzed esterification of glycerol and fatty acids. *Biotechnology and Bioengineering*, 42(8), 953–962. <https://doi.org/10.1002/bit.260420806>

Jeenpadiphat, S., Björk, E. M., Odén, M., & Tungasmita, D. N. (2015). Propylsulfonic acid functionalized mesoporous silica catalysts for esterification of fatty acids. *Journal of Molecular Catalysis A: Chemical*, 410, 253–259. <https://doi.org/10.1016/j.molcata.2015.10.002>

Khodov, I. A., Nikiforov, M. Y., Alper, G. A., Blokhin, D. S., Efimov, S. V., Klochkov, V. V., & Georgi, N. (2013). Spatial structure of felodipine dissolved in DMSO by 1D NOE and 2D NOESY NMR spectroscopy. *Journal of Molecular Structure*, 1035, 358–362. <https://doi.org/10.1016/j.molstruc.2012.11.040>

Kodali, D. R., Atkinson, D., Redgrave, T. G., & Small, D. M. (1987). Structure and polymorphism of 18-carbon fatty acyl triacylglycerols: Effect of unsaturation and substitution in the 2-position. *Journal of Lipid Research*, 28(4), 403–413. [https://doi.org/10.1016/s0022-2275\(20\)38692-2](https://doi.org/10.1016/s0022-2275(20)38692-2)

Kotwal, M., Deshpande, S. S., & Srinivas, D. (2011). Esterification of fatty acids with glycerol over Fe-Zn double-metal cyanide catalyst. *Catalysis Communications*, 12(14), 1302–1306. <https://doi.org/10.1016/j.catcom.2011.05.008>

Lameiras, P., & Nuzillard, J. M. (2016). Highly Viscous Binary Solvents: DMSO-d₆/Glycerol and DMSO-d₆/Glycerol-d₈ for Polar and Apolar Mixture Analysis by NMR. *Analytical Chemistry*, 88(8), 4508–4515. <https://doi.org/10.1021/acs.analchem.6b00481>

Lísa, M., & Holčápek, M. (2013). Characterization of triacylglycerol enantiomers using chiral HPLC/APCI-MS and synthesis of enantiomeric triacylglycerols. *Analytical Chemistry*, 85(3), 1852–1859. <https://doi.org/10.1021/ac303237a>

Neises, B., & Steglich, W. (1978). Simple Method for the Esterification of Carboxylic Acids. *Angewandte Chemie International Edition in English*, 17(7), 522–524. <https://doi.org/10.1002/anie.197805221>

Paulsen, H. (1982). International Edition in English. *Angewandte Chemie International Edition in English*, 21(3), 155–173

Pérez-Gil, J. (2008). Structure of pulmonary surfactant membranes and films: The role of proteins and lipid-protein interactions. *Biochimica et Biophysica Acta - Biomembranes*, 1778(7–8), 1676–1695. <https://doi.org/10.1016/j.bbamem.2008.05.003>

Prades, J., Funari, S. S., Escribá, P. V., & Barceló, F. (2003). Effects of unsaturated fatty acids and triacylglycerols on phosphatidylethanolamine membrane structure. *Journal of Lipid Research*, 44(9), 1720–1727. <https://doi.org/10.1194/jlr.M300092-JLR200>

Sar, A., Bier, A., Karaipekli, A., Alkan, C., & Karadag, A. (2010). Synthesis, thermal energy storage properties and thermal reliability of some fatty acid esters with glycerol as novel solidliquid phase change materials. *Solar Energy Materials and Solar Cells*, 94(10), 1711–1715. <https://doi.org/10.1016/j.solmat.2010.05.033>

Sari, A., Biçer, A., & Karaipekli, A. (2009). Synthesis, characterization, thermal properties of a series of stearic acid esters as novel solid-liquid phase change materials. *Materials Letters*, 63(13–14), 1213–1216. <https://doi.org/10.1016/j.matlet.2009.02.045>

Saroja, M., & Kaimal, T. N. B. (1986). A convenient method of esterification of fatty acids. Preparation of alkyl esters, sterol esters, wax esters and triacylglycerols. *Synthetic Communications*, 16(11), 1423–1430. <https://doi.org/10.1080/00397918608056391>

Sasaki, M., Ueno, S., & Sato, K. (2012). Polymorphism and Mixing Phase Behavior of Major Triacylglycerols of Cocoa Butter. In *Cocoa Butter and Related Compounds*. AOCS Press. <https://doi.org/10.1016/B978-0-9830791-2-5.50009-8>

Singh, D., Patidar, P., Ganesh, A., & Mahajani, S. (2013). Esterification of oleic acid with glycerol in the presence of supported zinc oxide as catalyst. *Industrial and Engineering Chemistry Research*, 52(42), 14776–14786. <https://doi.org/10.1021/ie401636v>

Wei, W., Feng, Y., Zhang, X., Cao, X., & Feng, F. (2015). Synthesis of structured lipid 1,3-dioleoyl-2-palmitoylglycerol in both solvent and solvent-free system. *LWT - Food Science and Technology*, 60(2), 1187–1194. <https://doi.org/10.1016/j.lwt.2014.09.013>

Z.I.Takai. (2018). Ournal of. *Asian Journal of Chemistry*, 30(18), 2424–2430

Chapter 3

Absolute quantification of triacylglycerols (TAGs)

3.1 Introduction

Triacylglycerols (TAGs) are an important constituents of all kinds of natural food. They are a source of energy for the living organisms. They play important role for maintaining the biological and physiological functions of human beings and biological organisms. (F.D. Gunstone, 2006) TAGs occur naturally in plant oils and animal fats. Most commonly, the TAGs in plant oils consist of oleic (O), linoleic (L), Linolenic (Ln), stearic (S) and palmitic (P) acids. These saturated and unsaturated fatty acids are attached in different ways to one of the three stereochemical positions sn-1, sn-2 and sn-3 on the glycerol backbone which results in a large variety of triacylglycerols in nature. (Small, 1991) Several analytical techniques have been used to study the structure and composition of TAGs in complex natural lipid mixtures. Among these techniques, non-aqueous reverse phase high-performance liquid chromatography (NARP-HPLC) is the most widely used technique. NARP-HPLC separates TAGs in an increasing order of equivalent carbon number (ECN). (Řezanka et al., 2016) ECN is equal to number of the total acyl chain carbons minus two times the number of double bonds ($ECN = CN - 2 D.B$). NARP-HPLC is also useful for the separation of critical pairs of TAGs i.e. TAGs with the same molecular weight but different fatty acyl chains. The polymeric ODS column has been used for the separation of positional isomers of TAGs. The ODS stationary phase recognizes the differences among the positional TAGs isomers. The ODS column facilitates the separation of the TAGs positional isomers at low temperature. (Kuroda, 2008) The silver ion HPLC has been used for the separation of regioisomers and cis/trans isomers of TAGs. (Dugo et al., 2004)

Mass spectrometry allows the separation of organic molecules according to their chemical masses and helps in the detection and quantification of organic molecules with high selectivity. (Sargent et al., 2013) The quantification of TAGs has been achieved with NARP-HPLC or gas chromatography (GC). In GC the fully saturated TAGs are eluted first then followed by monounsaturated and polyunsaturated TAGs. However, the baseline resolution between the unsaturated fatty acid methyl esters with the same carbon skeleton is absent in GC chromatography of TAGs. (Hlongwane et al., 2001) TAGs are separated in GC on the basis of their partition number (PN) or TCN. Positional isomers of TAGs known as critical pairs can not be separated by simple GC using chiral stationary phase. These are separated in the GC-flame ionization detector (FID) with a non-polar stationary phase. This is useful for the identification of critical pairs of TAGs in cocoa butter and chocolate. In GC-FID the correction factors (CFs) of TAGs are calculated relative to internal standards and used for the quantification of TAGs in cocoa butter, palm oil and other fats and oils. (Yoshinaga et al., 2017) Several analytical methods, i.e. HPLC, APCI-MS, LC-MS have been developed to study the TAGs composition in natural food such as vegetable oils. (Lísa & Holčápek, 2008) Earlier Kuhnert et. al. have reported the

presence of mixtures of complex molecules and some unknown compounds in fermented cocoa beans by Fourier-transform ion cyclotron resonance (FTICR). (Kuhnert et al., 2013) Later on, Kuhnert et. al. extended their analytical work to detect the unknown TAGs in cocoa butter by HPLC-ESI mass spectrometry. (Sirbu et al., 2018) The quantitative analysis of TAGs is achieved with the HPLC coupled with atmospheric pressure chemical ionization mass spectrometry on the basis of relative abundance of the fragment ions of positional isomers of TAGs. The calibration curves developed for the different fragment ions allow the quantification of the TAGs positional isomers. The regression technique establishes a relationship between the standard concentration (y) and their response (x). The least square regression analysis can be used for the statistical analysis and quantification of TAGs. (Fauconnot et al., 2004)

Tandem mass spectrometry coupled with RP-HPLC is a reliable method for the quantitative analysis of the positional isomers of TAGs adducts. Duffin, first of all reported the electrospray ionization tandem mass spectrometry ESI-MS/MS for diacylglycerols (DAGs) after collision-induced dissociation (CID) of $[M + NH_4]^+$ in triple quadrupole mass spectrometer (QqQ). The quantification of TAGs in ESI-LC-MS/MS is achieved by a neutral loss of the fatty acyl chain. The quantification of TAGs is affected by the carbon chain length of the fatty acyl chain, degree of unsaturation and position of the fatty acyl chain on the glycerol backbone. (Li et al., 2014) For quantitative analysis of TAGs by the calibration curve data, three types of ionization techniques are used. These are atmospheric pressure chemical ionization (APCI), electrospray ionization of TAGs in positive mode and negative ion chemical ionization (NICI) with ammonia. These all are used for the quantification of TAGs. (Ramaley et al., 2013)

A number of analytical techniques have been developed for the quantification of TAGs in food such as oils and fats. These are used to identify and quantify positional isomers with identical fatty acyl content. The palm oil and lard both contain oleic acid (O) and palmitic acid (P) in different positions. Different isomers in palm oil and lard such as sn-OPP/sn-OPO/sn-OOP/sn-POO can be separated by quantification. RP-HPLC with the chiral column is used to separate the positional isomers. Later on, RP-HPLC was coupled with the chiral HPLC to separate positional isomers and enantiomers. But this combination of two analytical techniques posed some complications in the analysis. Now, chiral HPLC is very successful for the separation of TAGs positional isomers and enantiomers such as sn-OPP/sn-OPO/sn-OOP/sn-POO. (Nagai et al., 2020) Fatty acids are widely distributed in vegetable oils. The nutritional, biochemical and quality level of vegetable oils depends on the relative distribution of fatty acids of TAGs in vegetable oils. TAGs in most of the vegetable oils contain linoleic acid (L) and oleic acid (O). The relative ratio of positional isomers i.e. LOL and LLO has been determined by quantification using calibration curves. The variation in the data shows that linoleic acid (L) and oleic acid (O) are randomly distributed in nature. (Jakab et al., 2003) These analytical methods are of

practical importance in food industry, pharmacokinetics and metabolic studies in human beings and living organism. The metabolism of fatty acid or TAGs is affected by the molecular structure of TAGs. These studies can help to access the food quality and develop new food products. The quantitative measurement of drugs in biological fluids is helpful in pharmacokinetics and control diseases. (Yoshinaga, 2021) Microalgae are rich in TAGs and are important to be used as biofuels. The quantification of TAGs in microalgae has been observed during different stages of nitrogen stress. The reference compound for the TAGs quantification was a single fatty acid. (Schwartz & Wolins, 2007) The standard TAGs containing docosahexaenoic acid (DHA, D), eicosapentaenoic acid (EPA, E), Oleic acid (O) and palmitoleic acid (Po) have been used as standards for TAGs quantification in fish oils. (Gotoh et al., 2006) The interesterification of TAGs in milk affects the flavor and nutritional value of milk. The 1,2-dipalmitoyl-3-butyroyl glycerol (PPBu) has been used as a reference compound to quantify TAGs in milk. (Yoshinaga et al., 2013)

The analysis of biological fluids and matrix cause complexity in the analytical measurements. This is caused by the matrix effect of the biological fluids. The matrix effects can be either rotational or translational. The rotational matrix effect occurs when the components of the test solution affect the signal of the analyte. In this case the slope of the calibration function is changed. The translational matrix effect is caused by the concomitant substances present in the solution and not by the analyte. This changes the intercept of the calibration function. In the cocoa beans analysis the translational matrix effects are usually observed. (Belo et al., 2017) Matrix effect occurs in GC-MS and HPLC-MS/MS. The matrix effect in the analytical methods leads to analytical errors. Different vegetables and pesticides show matrix effect during HPLC analysis. (Karmakar, 2020) The development of analytical methods was further improved by multiple reaction monitoring. The salts, sugars and amino acids in the biological fluids cause matrix effects in the quantification of biomolecules. This has been observed in the quantification of hydroxyproline content of collagen in the muscles. MRM differentiates between different isomers of hydroxyproline (Hyp.) by giving different MRM transitions for 3-Hyp and 4-Hyp. (Colgrave et al., 2012) The quantification of biomolecules by tandem mass spectrometry is very important in pharmacokinetics. The drugs can be determined in the patient blood at low concentration with high sensitivity and low energy CID. (Keevil et al., 2002) A very lower limit of detection is required for the quantification of drugs in human blood. (Chen & Hsu, 2013) The development of the analytical methods coupled with MRM for the quantification of TAGs and biomolecules allows the study of biomolecules in the solvent rather than biological fluids. The use of calibration curves for absolute quantification decrease the possibility of the loss of sensitivity and the matrix effect during the ionization process. Calibration curves in solvent have less matrix effect as compared to the calibration curves prepared in the biological fluids. The optimization of LC-MS conditions i.e. selection of positive ionization mode (PIM) and acquisition of fragmentation spectra

with appropriate multiple reaction monitoring (MRM) transitions acquired the calibration curves in solvent and with negligible matrix effect. This kind of quantification is obtained for the LC-MS quantification of caffeine and theobromine in blood plasma. (Mendes et al., 2019)

During the quantitative LC-MS the calibration curve range is set up. The lower limit of quantification LLOQ and upper limit of quantification ULOQ are important to allow the pharmacokinetics and toxicokinetics of the analyte in the sample. A general recommendation for the anticipated C_{max} is 10 % LLOQ. The EMA guidance suggest LLOQ to be 5% of the expected C_{max} for the study of biological samples. The expected analyte concentration and the linearity of the calibration curves determine the ULOQ. (Marsin Sanagi et al., n.d.) The detection across the dynamic range is directly affected by the ionization properties of the analyte. If the analyte has low ionization efficiency, it leads to poor accuracy and precision at low concentration. The calibrators are prepared by two methods i.e. serial dilution and point-to-point dilution. The US FDA and EMA guidelines on 'Bioanalytical Method Validation' state that the calibration standards should be prepared in the same biological matrix as the sample under study. Multiple reaction monitoring (MRM) allows the specific determination of multiple analytes in the same analytical fluid. (Fu et al., 2019) The LOQ and LOD determine the sensitivity of analytical method and the detector used for the analysis. The lower values of LOQ and LOD are useful to detect analytes with high sensitivity. Different detectors are used for the analysis of TAGs in RP-HPLC. These are evaporative light scattering detector (ELSD), ultraviolet-visible (UV-Vis.) detector and nano quality analyte detector (NAQD). Nano quality analyte detector (NQAD) has been used in HPLC to quantify TAGs in cocoa butter. The internal standard used was 1,2,3-triundecanoylglycerol (C11C11C11). The special property of chocolate melting in mouth known as mouth feel is due to three main TAGs i.e. β -1-palmitoyl-2-oleoyl-3-stereoyl glycerol (β -POS), β -1-palmitoyl-2-oleoyl-3-palmitoyl glycerol (β -POP) and β -1-stereoyl-2-oleoyl-3-stereoyl glycerol (β -SOS). It is difficult to identify and quantify these positional isomers of TAGs with less sensitive analytical method. LOQ and LOD determine the sensitivity of analytical method and the detector used for the analysis. The lower values of LOQ and LOD are obtained with NAQD which shows that NAQD shows more sensitivity and accuracy than the other detectors. This is very useful for the quantification of TAGs in food such as fats, oils, milk and chocolate. (Beppu et al., 2013) The analysis of positional isomers of TAGs in cocoa butter detects the level of cocoa butter equivalents in the chocolate. A new European legislation (2000/36CE) has allowed the use of vegetable fats other than cocoa butter in chocolate up to 5% in the product. (Lipp & Adam, 1998) These are known as cocoa butter equivalents (CBE) and cocoa butter replacer (CBR). The cocoa butter equivalents (CBE) include non-lauric plant fats. These are similar in physical and chemical composition with the cocoa butter and can be mixed easily. Cocoa butter replacer (CBR) are non-lauric fats with a distribution of fatty acid like cocoa butter but have a completely different structure of the triglycerides. These are compatible to cocoa

butter only in small ratios. Cocoa butter substitutes (CBSs) are lauric acid containing plant fats but chemically totally different from cocoa butter. CBSs have some physical similarities that are suitable only to substitute cocoa butter to 100%. The quantification of cocoa butter TAGs i.e. POS, POP and PLS and the ratios of POP/PLS, POS/PLP are biomarker to discriminate cocoa butter from the cocoa butter equivalents (CBE) and cocoa butter replacer (CBR). (Dionisi et al., 2004)

Calibration curve in bioanalytical method is a linear relation between concentration of the analyte and response of the instrument. This is useful to determine the unknown concentration of a compound in an analytical sample. The relationship between the analyte concentration 'x' and the instrument response i.e. signal 'y' is given by the general formula $y = ax + b$ where a and b are slope and intercept respectively. (Marsin Sanagi et al., n.d.) Linear calibration graph for a range of concentration of analyte provides information about the validation of the analytical method. The linearity of the calibration graph is expressed by the correlation coefficient (R^2). In linear calibration, the errors occur in the y-direction. The y-direction errors are normally distributed. In linear calibration, the least square line is subject to uncertainty so the y-values are subject to uncertainty. In the analytical works, the calibration graph is used in the inverse way. In this case, the experimental value of 'y' i.e. the instrument response is the input and the corresponding value of 'x' i.e. concentration of the sample is subject to error. (Miller, 1991) The linear calibration is important in the analytical determinations based on the linearity in the calibration range. The linearity is proved by the visual inspection of the calibration curves i.e. the regression analysis, the residual plots (RPs) and the response factors (RFs). Linearity plots with the response factors versus concentration level indicate the range of sensitivity for the confidence limit of 5%. Linearity also consider other parameters such as correlation coefficient (R), standard deviation of regression, standard deviation of slope, quality coefficients and back-calculated concentration expressed as percentage of relative errors (%RE). Residual plots are important in several chemometric and quality control measurements. Residual plots help to detect outliers, influence points, lack of fit or uneven variance. The response factors plots are obtained by plotting signal-to-noise ratio (the so called response factor) versus concentration of the analytes. Positive and negative deviations from the linearity in the RF plots are related to the low and high concentration levels of the analyte. The difference between the calculated concentration and predicted concentration gives the relative error (RE). The recommended linear range of RE is $\pm 15\%$ for the calibration range and $\pm 20\%$ for the LOQ. (Jurado et al., 2017)

Absolute quantification of TAGs is important to study the TAGs metabolism and genetic breeding in human beings. The regioisomeric analysis of TAGs is the main step-stone in the lipid biochemistry and provides criteria to understand the involvement of lipids in diseases and nutrition. The quantitative study of TAGs in solvents is achieved with RP-HPLC-MRMS. This allows the quantification

of drugs in blood plasma and to quantify TAGs in food such as chocolate, milk, fats and oils. Calibration curve studies of LC-MS analysis of TAGs set up standards for ULOQ, LLOQ, precision and accuracy. These are important in food authentication, detection of adulteration and to develop new food varieties. It is suggested to study of the peaks of crystallization curves of TAGs positional isomers by differential scanning calorimeter (DSC). This can provide new criteria to differentiate TAGs isomers in food and biological fluids.

3.2 Experimental

3.2.1 Chemicals and Reagents

All the chemicals and solvents have been purchased from Sigma Aldrich, TCI Germany and OmniLab. The solvents used for LC-MS and calibration studies are of HPLC grade and purchased from Merck and Rotislov.; ammonium formate was used as an internal standard and purchased from Sigma Aldrich. The TAGs used for the calibration curves have been synthesized by a modification in the reported procedure for the esterification. For this symmetrical Triacylglycerols i.e , 1,2,3-tripalmitoyl glycerol [PPP], 1,2,3-tristearoyl glycerol [SSS], 1,2,3-trioleoyl glycerol [OOO] and 1,2,3-trilinolein glycerol [LLL] and unsymmetrical triacylglycerol i.e. 1-palmitoyl-2,3-dioleoyl glycerol [POO], 1-palmitoyl-2,3-distearoyl glycerol [PSS], 1-stearoyl-2,3-dioleoyl glycerol [SOO], 1-stearoyl-2,3-dilinoleoyl glycerol [SLL], 1-stearoyl-2,3-dipalmitoyl glycerol [SPP], 1-linoleoyl-2,3-dipalmitoyl glycerol [LPP], 1-oleoyl-2,3-dilinoleoyl glycerol [OLL] have been synthesized in purity.

3.2.2 LC-MS conditions

LC-MS was carried out using an Ion-Trap mass detector in positive ion mode equipped with an ESI source (Bruker Daltonics UHT Ultra, Bremen, Germany). The full scan mass spectra were recorded in the range m/z 200-1200 operating in positive ion mode. Capillary temperature was set to 350 °C, drying gas flow rate of 10L/ min and nebulizer pressure of 10 psi. Tandem mass spectra were acquired in Auto MSⁿ (smart fragmentation) using a ramping of the collision energy.

3.2.3 Sample preparation for the calibration curves and limit of detection

The stock solutions of all synthetic TAGs standards were prepared by measuring 2 mg of the TAGs and dissolving it in 2 mL of HPLC grade chloroform. The purity of the TAGs was established by HPLC and retention times of the pure individual TAGs have been determined. These retention times of the individual TAGs were set up as a standard parameter to identify TAGs in the calibration curves studies and in the cocoa butter. The column used in this study was Agilent Poroshell 120 column 4.0 μ m and 3.0 x 5 mm i.d. guard column of the same material (Agilent, Germany).

A set of two calibration mix with six synthetic TAGs in each mix were made. One set of calibration mix consisted of six TAGs i.e. SPP, PSS, OOO, LOO, PPP, LLL. The second calibration mix consisted of six TAGs namely POO, SOO, LPP, OLL, SLL, SSS. The standard solutions of the synthetic TAGs for the calibration curves have been prepared in the concentration of 1 mg/ 1 mL. For calibration curves

measurement, a serial dilutions 1:10, 1:25, 1:50, 1:75, 1:100, 1:150, 1:200 and 1:500 were used and an eight point calibration was established. The LOD was determined by running the samples in triplicate. The sequence was started with the highest dilution. In total 12 synthetic TAGs were used to make calibration mixes of two with six TAGs in each calibration mix.

3.3 Results & Discussion

The retention times of the synthetic TAGs have been determined by LC-MS. The retention times of the synthetic TAGs with unsaturated fatty acid in sn-1 and sn-2 positions are lower. This suggests that the unsaturated fatty acids in the triacylglycerols possess less Vander Waals forces. The TAGs with saturated fatty acids in sn-2 and sn-3 positions i.e. PSS and SPP have higher retention times. It is suggested that the saturated fatty acyl chains are straightened and have greater Vander Waals interactions in the column. The calibration mix of six TAGs each show the usual trend that LLL has the lowest retention time. Furthermore, a pair of TAGs coelute closely as LOO and LPP, then OOO and POO and SPP and SOO pairs. This suggests that the stereochemical position and degree of saturation and unsaturation affects the physical and physiological properties of TAGs. The saturated fatty acid on the glycerol back bone in TAGs is suggested to possess a linear structure. The unsaturated fatty acyl chains possess a bent structure due to the presence of double bond and π - electrons. So, it is suggested that they cause less interaction and experience more degree of freedom to move in the HPLC column.

Table 3.1 The retention times and $[M+NH_4]^+$ masses of the synthetic triacylglycerols

S. No.	Triacylglycerol	Retention time (t_R)	$[M+NH_4]^+$
1	PSS	27.6	880.842
2	SPP	23.3	852.813
3	SOO	22	904.841
4	PPP	19.4	824.776
5	POO	18.2	876.813
6	OOO	17.7	902.824
7	LPP	15.4	848.785
8	SLL	14.5	900.812
9	OLL	11.7	898.797
10	LLL	9.4	896.767
11	SSS	32.3	908.863
12	LOO	14.9	900.8

TAGs show different absorbance coefficient at 210 nm with UV-Vis detector. The magnitude of the absorbance coefficient depends upon the number of double bonds in unsaturated TAGs. The greater

the number of double bonds in the TAG, the higher is the absorbance coefficient. This phenomenon has been observed in the synthetic TAGs. (Table 3.1)

Earlier the absorbance of TAGs in the natural products has been studied with different detectors in the HPLC-LC-MS. A shift in the retention time of the synthetic TAGs is observed with the change in the concentration of the synthetic TAGs solution. The retention time shifts to higher value with the decrease in the concentration. (Figure 3.1) A shift in the peak of the synthetic TAGs predicts the relationship between the range of concentration from higher to lower level and the retention time of TAGs. It is suggested that low energy is required for the collision-induced dissociation (CID) of the TAGs. This is useful for the quantitative LC-MS analysis of TAGs in bio-samples.

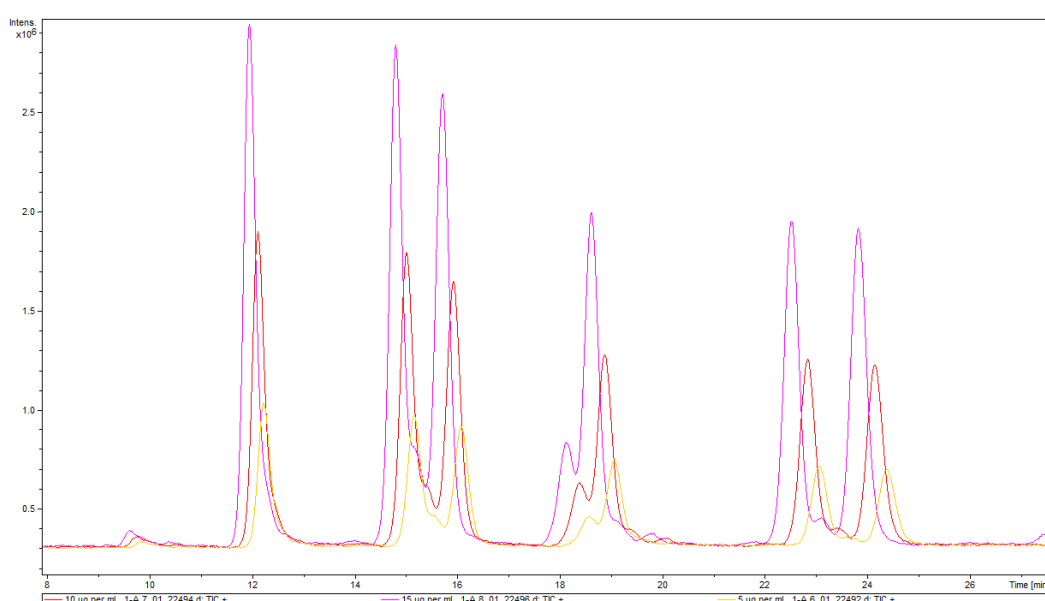


Figure 3.1 Chromatogram of TAGs adducts $[M+NH_4]^+$ for different concentrations showing a shift in the retention time with the change in the concentration

Calibration curves of the synthetic TAGs have been obtained by 8 point calibration methods with a serial dilution. The calibration curves were developed for different concentrations by measuring the instrument response (y_i), for a given set of calibrants with higher to lower concentration of the analyte (Synthetic TAGs). The peak areas of the chromatograms increase with the increase in the concentration. 5 µg/L was the lowest possible concentration to detect the signals of TAGs in the calibration curve mixtures. Calibration curves are obtained by plotting the peak area (y_i) of the chromatogram for each TAGs against concentrations of the analyte samples in excel using data analysis function. The correlation coefficient R^2 values of all the calibration curves for the synthetic TAGs showed a value in the range of 0.993-0.999. This establishes a linear relation between the TAGs concentration and the instrument response. The value of the residual standard deviation (RSD) range from 2.04 E+04 to 1.08 E+08. The value of the residual standard deviation (RSD) for the PPP is 8.01 E+04 and for the LLL is 8.55 E+06. The RSD of PPP and LLL are different from the other TAGs. The LOD

for all the synthetic TAGs is in the range of 1.738 µg/L to 14.425µg/L. This is smallest detection limit for the TAGs detection. It is suggested to be useful for the quantification of TAGs in the blood plasma to study TAGs metabolism and in food authentication. The LOD for all the synthetic TAGs is in the range of 5.267 µg/L to 43.712 µg/L. Calibration curve data and correlation coefficient (R^2) for synthetic TAGs are shown in table 3.2.

Table 3.2 The statistical data for R^2 , residual standard deviation (RSD), LOQ and LOD of the synthetic TAGs by ANOVA table.

S. No.	TAG	$y = mx + c$	R^2	RSD $\sqrt{\sum (y_i - \hat{y}_i)^2 / n - 2}$	LOQ µg/L	LOD µg/L
1	PSS	$y = 2E+06x - 1E+07$	0.9965	6.66E+06	12.299	4.058
2	SPP	$y = 1E+06x - 8E+06$	0.9999	2.19E+05	5.267	1.738
3	SOO	$y = 2E+06x - 9E+06$	0.998	1.19E+06	10.351	3.416
4	PPP	$y = 25047x - 294841$	0.9699	8.01E+04	43.712	14.425
5	POO	$y = 1E+06x - 8E+06$	0.9983	1.08E+08	11.389	3.758
6	OOO	$y = 651098x - 8E+06$	0.9716	2.04E+04	42.767	14.113
7	LPP	$y = 2E+06x - 7E+06$	0.9943	1.97E+06	16.288	5.375
8	SLL	$y = 2E+06x - 5E+06$	0.9935	2.03E+06	17.07	6.658
9	OLL	$y = 1E+06x - 2E+06$	0.9896	2.13E+06	21.683	7.155
10	LLL	$y = 301905x - 286392$	0.9773	8.55 E+06	36.237	11.958
11	SSS	$y = 1E+06x - 2E+07$	0.9963	2.06 E+06	19.787	6.529

The regression lines are linear with the correlation coefficient ranging from 0.993 to 0.999. The intercept in the calibration curves of the TAGs is a higher negative value. The intercept of a linear calibration curve is normally zero or very close to zero. In linear regression the intercept is zero when the analyte's concentration is $x=0$. In HPLC analysis zero intercept corresponds to analyte's signal ($y=0$). The negative intercept shows that the LOD does not lie at $x=0$. The calibration measurements of the TAGs standards were then adjusted to bring the LOD at $x=0$ and standard error was set to 2%.

The different synthetic TAGs $[M + NH_4]^+$ adduct ions produced slopes from 25047 to $2E+06$ and y-intercept - 286392 to - $2E+07$. The higher values of the slope suggest that the TAGs can be precisely quantified in the smaller amounts in biological fluids and in food. These regression data show that the position of the fatty acid, number of double bonds and stereochemical arrangement of fatty acyl

chains affect the fragmentation behavior of TAGs. In addition to these effects, the length of the fatty acid chain is suggested to be important in the quantification of TAGs. This depends on the relative abundance of the DAGs fragments. (Herrera et al., 2010)

The regression analysis data for residual standard deviation of the synthetic TAGs and cocoa butter are given in the supplementary information.

The TAGs have been quantified in cocoa butter from different origins by using the calibration curves of the synthetic triacylglycerols. The quantity of cocoa butter TAGs per 100 g of the cocoa butter is calculated from the peak area of the chromatogram and retention time. The retention times and $[M+NH_4]^+$ molecular ion peaks of the synthetic triacylglycerols have been used as a reference standards to identify and quantify the triacylglycerols LPP, OPP, POO, SOO, OOO, PPP in the cocoa butter from Ghana, Ecuador and Cameroon. The calibration curves of the TAGs in cocoa butter from Ghana, Cameroon and Ecuador are plotted from the concentration of TAGs in cocoa butter and peak areas.

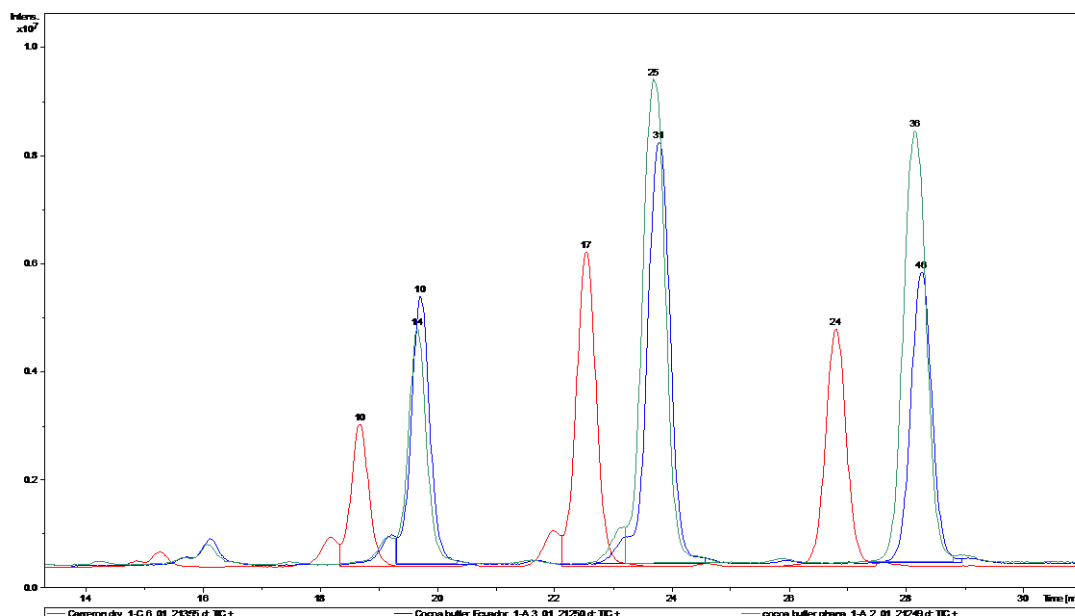


Figure 3.2 Chromatograms of the cocoa butters from Cameroon, Ecuador and Ghana

The relative amount of cocoa butter from different regions is quantified per 100g for the first time. (Table 3.3)

Table 3.3 Relative quantity of cocoa butter TAGs from different origins as calculated per 100 g

S. No.	Triacylglycerol (TAG)	Ecuador (g)	Ghana (g)	Cameron dry (g)	Cameron wet (g)	Ghana dry (g)	Ghana wet (g)
1	LPP	0.5148	0.4875	0.4683	0.4677	0.4509	0.4402
2	OPP	7.0387	6.1356	3.8885	4.2348	3.8835	3.8542
3	POO	0.7371	0.7183	0.7538	0.7659	0.6888	0.6698
4	SOO	0.7148	0.7753	0.7787	0.8256	0.7027	0.6706
5	OOO	1.1616	1.1608	1.1408	1.1750	1.1633	1.1535
6	PPP	1.3411	1.327	1.1408	1.0710	1.3246	1.3508
7	SOS	8.4481	13.3451	6.9633	7.9435	8.5558	8.2153
8	SOA	0.6294	0.6995	0.6454	0.6517	0.6729	0.6381
9	PLO	0.6183	0.6072	0.6128	0.6124	0.6087	0.6063
10	POS	13.1624	14.9720	8.7444	9.6522	9.4463	9.2688
11	SOMa	0.6129	0.6168	0.6116	0.6137	0.6105	0.6145
12	SPP	-	-	-	-	0.5206	0.5210
	Total	34.972	27.975	25.748	28.013	28.628	28.003

3.4 Conclusion

The calibration studies of the synthetic TAGs, the intercept, the slope values and response factors are very useful for the quantification of TAGs in food such as fats, oils and chocolate. It is suggested that metabolism of TAGs in human and drug functions can be determined with the quantification of TAGs with high sensitivity.

The calibration curves have important application to quantify triacylglycerols in food, pharmaceutical drugs, and cosmetics. LOD and LOQ values are important in the forensic measurements. The US department of Health and Human Services (HHS) National Laboratory Certification Program (NLCP) requires the determination of LOD and LOQ to prove the analyte concentration below the administrative cutoff. (Arinbruster, et al., 1994) The determination of LOD and LOQ of the synthetic TAGs is important in pharmacokinetics and food quality assessment. The clinical laboratory tests in the metabolic studies of TAGs in humans require the fully characterization with LOD, LOQ and LoB.

The official methods for quantification of TAGs in fats and oils are usually applicable to quantify TAGs in the cocoa butter or chocolate. The absolute quantification of these synthetic TAGs is applicable to TAGs quantification in the chocolate, natural fats, and oils. Absolute quantification require high quality authentic reference molecules and low LOQ. Since TAGs authentic standards are only available for few compounds a little data on the absolute quantities in dietary materials is available. For the first time absolute quantities of selected TAGs have been determined in the cocoa butter by using the synthetic TAGs standards. The absolute quantification and statistical analysis of these synthetic TAGs can serve as standard for more analytical work of TAGs in dietary foods, metabolism of TAGs in human and pharmacokinetics.

References:

- ‘Gotoh, N., Aoki, T., ‘Nakayaso, K., & ‘Tokairin, S. (2006). Quantification Method for Triglyceride Molecular Species in Fish Oil with High Performance Liquid Chromatography-Ultraviolet Detector. *Journal of Oleo Science*, 55(9), 457–463.
- ‘Kuroda, I. ‘Nagai, T. ‘, ‘Mizobe, H. ‘Yoshimura, N. ‘Gotoh, N. ‘Wada, S. (2008). HPLC Separation of Triacylglycerol Positional Isomers on a Polymeric ODS Column. *ANALYTICAL SCIENCES; The Japan Society for Analytical Chemistry*, 24, 865–869.
- Arinbruster, ‘, D. A., Tillman, M. D., & Hubbs, L. M. (1994). Limit of Detection (LOD)/Limit of Quantitation (LOQ): Comparison of the Empirical and the Statistical Methods Exemplified with GC-MS Assays of Abused Drugs. In *Laboratory Management and Utilization CLINICAL CHEMISTRY* (Vol. 40, Issue 7). <https://academic.oup.com/clinchem/article-abstract/40/7/1233/5647851>
- Belo, R. F. C., Pissinatti, R., de Souza, S. V. C., & Junqueira, R. G. (2017). Evaluating Matrix Effects in the Analysis of Polycyclic Aromatic Hydrocarbons from Food: Can These Interferences Be Neglected for Isotope Dilution? *Food Analytical Methods*, 10(5), 1488–1499. <https://doi.org/10.1007/s12161-016-0706-0>
- Beppu, F., Nagai, T., Yoshinaga, K., Mizobe, H., Kojima, K., & Gotoh, N. (2013). Quantification of Triacylglycerol Molecular Species in Cocoa Butter Using High-Performance Liquid Chromatography Equipped with Nano Quantity Analyte Detector. In *J. Oleo Sci* (Vol. 62, Issue 10). <http://www.jstage.jst.go.jp/browse/jos/http://mc.manuscriptcentral.com/jjocs>
- Chen, Y. A., & Hsu, K. Y. (2013). Development of a LC-MS/MS-based method for determining metolazone concentrations in human plasma: Application to a pharmacokinetic study. *Journal of Food and Drug Analysis*, 21(2), 154–159. <https://doi.org/10.1016/j.jfda.2013.05.004>
- Colgrave, M. L., Allingham, P. G., Tyrrell, K., & Jones, A. (2012). Multiple reaction monitoring for the accurate quantification of amino acids: Using hydroxyproline to estimate collagen content. *Methods in Molecular Biology*, 828, 291–303. https://doi.org/10.1007/978-1-61779-445-2_23
- Dionisi, F., Golay, P. A., Hug, B., Baumgartner, M., Callier, P., & Destailats, F. (2004). Triacylglycerol Analysis for the Quantification of Cocoa Butter Equivalents (CBE) in Chocolate: Feasibility Study and Validation. *Journal of Agricultural and Food Chemistry*, 52(7), 1835–1841. <https://doi.org/10.1021/jf035391q>

Dugo, P., Favoino, O., Tranchida, P. Q., Dugo, G., & Mondello, L. (2004). Off-line coupling of non-aqueous reversed-phase and silver ion high-performance liquid chromatography-mass spectrometry for the characterization of rice oil triacylglycerol positional isomers. *Journal of Chromatography A*, 1041(1–2), 135–142. <https://doi.org/10.1016/j.chroma.2004.04.063>

Fauconnot, L., Hau, J., Aeschlimann, J. M., Fay, L. B., & Dionisi, F. (2004). Quantitative analysis of triacylglycerol regioisomers in fats and oils using reversed-phase high-performance liquid chromatography and atmospheric pressure chemical ionization mass spectrometry. *Rapid Communications in Mass Spectrometry*, 18(2), 218–224. <https://doi.org/10.1002/rcm.1317>

F.D. Gunstone. (2006). *Modifying lipids for use in food* (1st edition). Wood publishing limited.

Fu, Y., Li, W., & Flarakos, J. (2019). Recommendations and best practices for calibration curves in quantitative LC-MS bioanalysis. In *Bioanalysis* (Vol. 11, Issue 15, pp. 1375–1377). Future Medicine Ltd. <https://doi.org/10.4155/bio-2019-0149>

Herrera, L. C., Potvin, M. A., & Melanson, J. E. (2010). Quantitative analysis of positional isomers of triacylglycerols via electrospray ionization tandem mass spectrometry of sodiated adducts. *Rapid Communications in Mass Spectrometry*, 24(18), 2745–2752. <https://doi.org/10.1002/rcm.4700>

Hlongwane, C., Delves, I. G., Wan, L. W., & Ayorinde, F. O. (2001). Comparative quantitative fatty acid analysis of triacylglycerols using matrix-assisted laser desorption/ionization time-of-flight mass spectrometry and gas chromatography. *Rapid Communications in Mass Spectrometry*, 15(21), 2027–2034. <https://doi.org/10.1002/rcm.462>

Jakab, A., Jablonkai, I., & Forgács, E. (2003). Quantification of the ratio of positional isomer dilinoleoyl-oleoyl glycerols in vegetable oils. *Rapid Communications in Mass Spectrometry*, 17(20), 2295–2302. <https://doi.org/10.1002/rcm.1193>

Jurado, J. M., Alcázar, A., Muñoz-Valencia, R., Ceballos-Magaña, S. G., & Raposo, F. (2017). Some practical considerations for linearity assessment of calibration curves as function of concentration levels according to the fitness-for-purpose approach. *Talanta*, 172, 221–229. <https://doi.org/10.1016/j.talanta.2017.05.049>

Karmakar, R. (2020). Evaluation of Matrix Effect of Chilli, Cabbage and Bitter Gourd in Multiclass Multi-pesticide Residue Analysis Using Gas Chromatography Mass Spectrometry (GC-MS).

International Journal of Agriculture Environment and Biotechnology, 13(1).
<https://doi.org/10.30954/0974-1712.1.2020.15>

Keevil, B. G., Tierney, D. P., Cooper, D. P., & Morris, M. R. (2002). Rapid liquid chromatography-tandem mass spectrometry method for routine analysis of cyclosporin A over an extended concentration range. *Clinical Chemistry*, 48(1), 69–76.
<https://doi.org/10.1093/clinchem/48.1.69>

Kuhnert, N., Dairpoosh, F., Yassin, G., Golon, A., & Jaiswal, R. (2013). What is under the hump? Mass spectrometry based analysis of complex mixtures in processed food-lessons from the characterisation of black tea thearubigins, coffee melanoidines and caramel. In *Food and Function* (Vol. 4, Issue 8, pp. 1130–1147). <https://doi.org/10.1039/c3fo30385c>

Li, M., Butka, E., & Wang, X. (2014). Comprehensive quantification of triacylglycerols in soybean seeds by electrospray ionization mass spectrometry with multiple neutral loss scans. *Scientific Reports*, 4. <https://doi.org/10.1038/srep06581>

Lipp, M., & Adam, E. (1998). Review of cocoa butter and alternative fats for use in chocolate- Part A. Compositional data. In *Analytical. Nutritional and Clinical Method Section* (Vol. 62, Issue 1).

Lísa, M., & Holčapek, M. (2008). Triacylglycerols profiling in plant oils important in food industry, dietetics and cosmetics using high-performance liquid chromatography-atmospheric pressure chemical ionization mass spectrometry. *Journal of Chromatography A*, 1198–1199(1–2), 115–130. <https://doi.org/10.1016/j.chroma.2008.05.037>

Marsin Sanagi, M., Nasir, Z., Ling, S. L., Hermawan, D., Aini Wan Ibrahim, W., & Abu Naim, A. (n.d.). *A Practical Approach for Linearity Assessment of Calibration Curves Under the International Union of Pure and Applied Chemistry (IUPAC) Guidelines for an In-House Validation of Method of Analysis*. <https://academic.oup.com/jaoac/article/93/4/1322/5655698>

Mendes, V. M., Coelho, M., Tomé, A. R., Cunha, R. A., & Manadas, B. (2019). Validation of an LC-MS/MS Method for the quantification of caffeine and theobromine using non-matched matrix calibration curve. *Molecules*, 24(16). <https://doi.org/10.3390/molecules24162863>

Miller, J. N. (1991). Basic Statistical Methods for Analytical Chemistry Part 2. Calibration and Regression Methods* A Review. In *ANALYST* (Vol. 116).

Nagai, T., Kinoshita, T., Kasamatsu, E., Yoshinaga, K., Mizobe, H., Yoshida, A., Itabashi, Y., & Gotoh, N. (2020). Simultaneous quantification of mixed-acid triacylglycerol positional isomers and enantiomers in palm oil and lard by chiral high-performance liquid chromatography coupled with mass spectrometry. *Symmetry*, 12(9). <https://doi.org/10.3390/SYM12091385>

Ramaley, L., Herrera, L. C., & Melanson, J. E. (2013). Applicability of non-linear versus linear fractional abundance calibration plots for the quantitative determination of triacylglycerol regioisomers by tandem mass spectrometry. *Rapid Communications in Mass Spectrometry*, 27(11), 1251–1259. <https://doi.org/10.1002/rcm.6569>

Řezanka, T., Řezanka, M., & Sigler, K. (2016). Regioisomeric Analysis of Triacylglycerols. In *Encyclopedia of Lipidomics* (pp. 1–11). Springer Netherlands. https://doi.org/10.1007/978-94-007-7864-1_113-1

Sargent, M., Wolff, C., Mussell, C., Neville, D., Lord, G., Saeed, M., Lad, R., Godfrey, R., Hird, S., & Barwick, V. (2013). *Guide to achieving reliable quantitative LC-MS measurements RSC Analytical Methods Committee First Edition 2013 Editor.*

Schwartz, D. M., & Wolins, N. E. (2007). A simple and rapid method to assay triacylglycerol in cells and tissues. *Journal of Lipid Research*, 48(11), 2514–2520. <https://doi.org/10.1194/jlr.D700017-JLR200>

Sirbu, D., Corno, M., Ullrich, M. S., & Kuhnert, N. (2018). Characterization of triacylglycerols in unfermented cocoa beans by HPLC-ESI mass spectrometry. *Food Chemistry*, 254, 232–240. <https://doi.org/10.1016/j.foodchem.2018.01.194>

Small, D. M. (1991). *THE EFFECTS OF GLYCERIDE STRUCTURE ON ABSORPTION AND METABOLISM*. www.annualreviews.org

Yoshinaga, K. (2021). Development of analytical methods and nutritional studies using synthetic fatty acids and triacylglycerols. In *Journal of Oleo Science* (Vol. 70, Issue 1, pp. 1–9). Japan Oil Chemists Society. <https://doi.org/10.5650/jos.ess20196>

Yoshinaga, K., Nagai, T., Mizobe, H., Kojima, K., & Gotoh, N. (2013). Simple method for the quantification of milk fat content in foods by LC-APCI-MS/MS using 1,2-dipalmitoyl-3-butyroyl-glycerol as an indicator. In *J. Oleo Sci* (Vol. 62, Issue 3). <http://www.jstage.jst.go.jp/browse/jos/http://mc.manuscriptcentral.com/jjocs>

Yoshinaga, K., Obi, J., Nagai, T., Iioka, H., Yoshida, A., Beppu, F., & Gotoh, N. (2017). Quantification of triacylglycerol molecular species in edible fats and oils by gas chromatography-flame ionization detector using correction factors. *Journal of Oleo Science*, 66(3), 259–268. <https://doi.org/10.5650/jos.ess16180>

Chapter 4

Diffusion NMR of dietary triacylglycerols (TAGs)

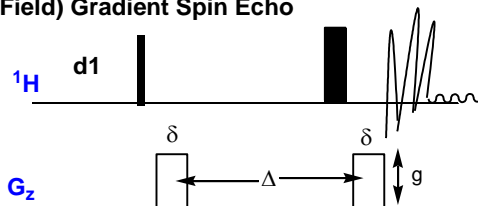
4.1 Introduction

Diffusion ordered spectroscopy is an NMR technique which measures the diffusion coefficient of molecules. It is basically used to distinguish the components of a mixture based on molecular diffusion of different molecules in a mixture. Molecular diffusion in solution is affected by the molecular size, shape and aggregation states of the molecules and is expressed as the hydrodynamic radius of a molecule. In diffusion NMR the field gradients are applied across a sample area in the NMR instrument and as a result each molecule gets accelerated and moves with a specific diffusion coefficient. After the delay Δ the dephasing of the spin echo takes place. This is followed by rephrasing by applying an opposite gradient. If the molecule possesses a diffusion coefficient, then the deviation from spin echo has been observed. (Claridge, 1999) The basic principle of diffusion NMR is that the pulsed field gradient (PFG) spin echo is applied across the sample. In the absence of gradient pulses, the chemical shift signal is attenuated only by the transverse relaxation T_2 during $2 T_2$ period. During the pulsed field gradients, the molecules give the same signal for the chemical shift if they remain in the same physical location during the delay with PFG. If the molecules possess diffusion coefficient, then they will diffuse away from their initial position during diffusion delay Δ . The chemical shift signal will be attenuated by an amount equivalent to the diffusion coefficient of the molecule. The diffusion rates of the molecule can be measured at different length of the gradient pulses and with different strength of the gradient pulses. (Morris, 2009) However, the delay time has been kept constant. The observed intensity I , for the basic PFG spin-echo experiment is given by:

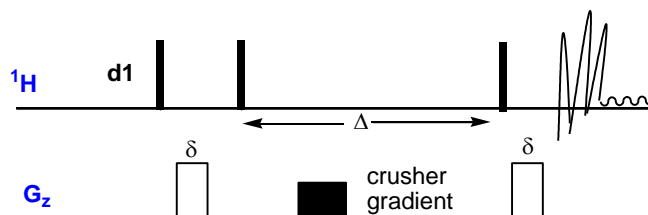
$$\bar{I} = I_0 \exp(-2\tau / T_2^2 - (\gamma \delta G)^2 x^4 - \delta / 31J) \quad \text{Eq. 5.1}$$

This shows that the diffusion coefficient D and intensity I and strength of the magnetic field G (Gradient strength) are inversely proportional. (Kuchel et al., 1997; Nilsson et al., 2004) Diffusion NMR data can be processed in either univariate or multivariate manner to observe the difference in the molecular dimensions. It is possible to plot the diffusion NMR within a pseudo 2D spectrum with the conventional 1D ¹H NMR along horizontal axis and the diffusion coefficients along the vertical dimension. High resolution 2D DOSY spectra have now been achieved by pure shift extraction and spin echo evolution. (Dumez, 2018; Nilsson, 2009) In high resolution DOSY, the diffusion dependent 1D NMR spectra are plotted in high resolution manner i.e., the peaks are well resolved and assigned to individual constituents. The exponential curve fitting on the attenuation of these resolved peaks helps to calculate diffusion coefficients and corresponding errors to produce high resolution diffusion domain with the resolution of the order of 1 % difference. (Nicolay et al., 2001)

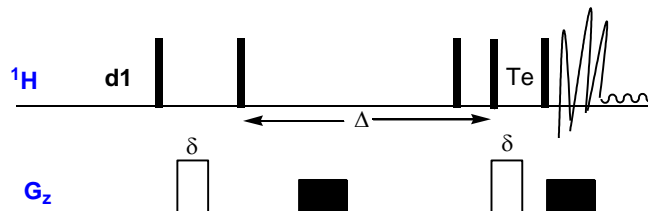
(A) PSGE Pulsed (Field) Gradient Spin Echo



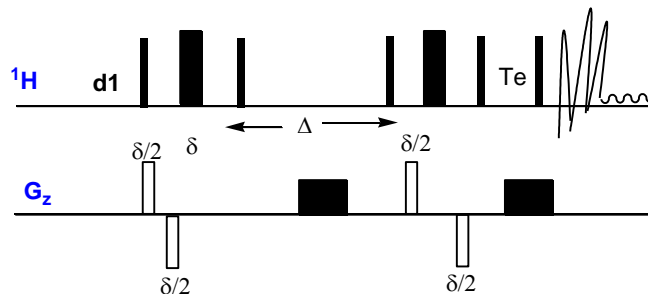
(B) STE Stimulated Echo



(C) STE-LTE Longitudinal Eddy current delay



(D) STE + LTE +BP BiPolar Gradients



(E) STE + LTE +BP + CC convection compensation

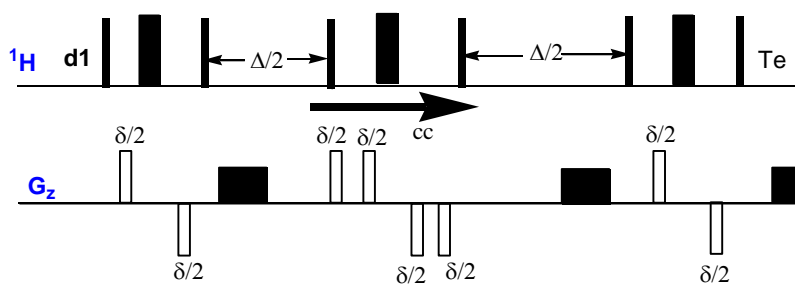


Figure 4.1 Pulse sequence for the DOSY experiment

1D proton NMR spectra used in DOSY measurements suffer from spectral congestion and peak overlap in mixtures due to the limited range of proton chemical shifts and the complexity of J coupling multiplet patterns. The external domain extension from 1D to 2D by encoding the diffusion element to existing 2D NMR pulse sequences has provided a solution to enhance the resolution of NMR peaks. This results in 3D DOSY variants i.e., DOSY-COSY involving external diffusion and 2D J -iDOSY with internal diffusion encoding. (Li et al., 2019)

The first pulse sequence in the diffusion NMR is composed of spin Echo or gradient echo (PGSE). (Figure 4.1 A) Diffusion experiment requires quantitative intensities so preparation along enough d_1 is important. If chemical shift differences are large, then gradient pulses cannot be asymmetric with 180° pulse. The issue with PGSE is solved by splitting 180° pulse into two 90° pulses. (Figure 4.1 B) Magnetization is stored longitudinally which produces a longer delay Δ (d_{20}). All constant velocity effects are cancelled by double stimulated echo (STE) in the convection stimulated sequences. (Figure 4.1 C) Magnetization is once again stored longitudinally along (z-axis) at the end of STE sequence. This is longitudinal eddy current delay (LED). Bipolar gradients reduce the eddy current by phasing and dephasing the magnetization. (Figure 4.1 D) Convection compensation reduces the magnetization decay due to the translational motion caused by the convection current. (Figure 4.1 E) (Kerssebaum, 2002)

Diffusion of the molecules is a random translation motion. It is known as Brownian movement. Molecules are distributed in space and in the biological systems by the translational diffusion processes. Mathematically, the diffusion processes are described by the Fick's first and second law of diffusion. (Nicolay et al., 2001) Diffusion of the molecules is the area per unit time and is expressed in m^2s^{-1} . Diffusion is related to the size of the molecules by the Stokes-Einstein equation.

$$D = (kT) / f \quad \text{Eq. 5.2}$$

D = Diffusion coefficient

T = Absolute temperature

K = Boltzmann constant

f = Friction coefficient

For spherical molecules the friction coefficient is given by:

$$f = 6\pi\eta R_H \quad \text{Eq. 5.3}$$

In this equation η is the viscosity and R_H is the hydrodynamic radius of the molecule. The diffusion coefficients measurement provides information about the shape of the molecules, hydrodynamic radius, and the interactions of the molecules in the biological systems. The diffusion is related non-

linearly with the temperature. The change in the temperature changes the viscosity of the system. The exponential dependence of the diffusion coefficient (D) on temperature (T) is as:

$$D = D_0 e^{-E_a/kT} \quad \text{Eq. 5.4}$$

E_a is the activation energy associated with the translational diffusion of the molecule. (Yeh & Hummer, 2004)

Diffusion is the main phenomenon occurring in biological membranes and biochemical systems. The calculation of diffusion coefficient is applicable in the determination of molecular weights of the molecules. The diffusion coefficient of a molecule is directly related to its shape and formula weight. (Neufeld & Stalke, 2015) The chemical reactions proceed with the identification of the new product. The diffusion coefficient calculations are useful for the detection of the products and to determine structural conformations. (Kuhnert et al., 2005; Kuhnert & Le-Gresley, 2005)

The diffusion is related to the chemical structures and conformations of the biological molecules. The plasma membrane is composed of lipids bilayer. The diffusion coefficient in the membrane depends upon the viscosity and hydrodynamic radii of the molecules. The change in temperature changes the viscosity of the membrane. (Block, 2018) The saturated or unsaturated structure of the fatty acyl chain, changes the conformational arrangement. This affects the diffusion coefficient and permeability of the membranes. (Prades et al., 2003)

The diffusion coefficient is very important in pharmacokinetics. The passive diffusion of a drug is proportional to the partition coefficient of biomolecules between plasma membrane and cytosol. The membrane permeability of the drugs is determined, and structure is selected depending upon the suitable diffusion coefficient. (Cocucci et al., 2017) The DOSY has become an important tool for the separation of the mixtures. The components can be separated with the different diffusion coefficients based on the viscosity and molecular size. (Gresley et al., 2012)

4.2 Experimental

All the diffusion NMR experiments were undertaken on a Bruker Avance III Ultrashield 600 MHz spectrometer (Kingston University, UK) operating at 600.13 MHz frequency and at 298 K probe temperature. TMS was used as an internal reference standard. CDCl_3 was obtained from Merck. All spectra were acquired and processed using Bruker Topspin 4.06 with diffusion constants determined using Bruker Dynamics Centre.

The acquisition parameters for the 1D ^1H spectra were as follows, size of fid 65,536; number of scans 16; spectral width 20.555 ppm; relaxation delay 1.000 s; acquisition time 2.656 s; pulse width 30°C (zg30). 1D ^1H spectra were processed using an EM windows apodization (LB = 0.3 Hz).

The acquisition parameters for the Diffusion experiments were as follows; size of fid 65,536; number of scans 16; spectral width 15.021 ppm; relaxation delay 5.000 s; acquisition time 2.656 s; $\delta = 600 \mu\text{s}$,

$\Delta = 200\text{ms}$, Led pulse sequence (ledbpgp2s). Diffusion data was preprocessed using an EM windows apodization (LB = 0.3 Hz) and polynomial (5) baseline correction.

All the triacylglycerols used for the diffusion NMR studies have been synthesized by the experimental procedure described above.

4.3 Results & Discussion

The diffusion coefficients of the synthetic TAGs show a variance depending upon the shape and conformation of the TAG molecule, its molecular weight, degree of unsaturation, length of fatty acyl chain and hydrodynamic radius.

The diffusion coefficient and hydrodynamic radii of TAGs have been calculated in two different ways by using two values of Gyromagnetic ratio (γ) one value is 4257.7000 Hz/ G (for ^1H) and the second value is 26770.7000 Hz/ G in diffusion spectra processing on Topspin. The hydrodynamic radii increase with more value of Gyromagnetic ratio (γ). The errors in the diffusion coefficients are calculated from the individual atoms data produced from the Topspin.

The average diffusion coefficients of all triacylglycerols are determined from the diffusion coefficients of each individual peak in the TAGs molecule. (Table 4.1) The highest value of diffusion coefficient is obtained for the monounsaturated diacylglycerol i.e., diolein (OOX). The diolein is the fastest with the larger diffusion coefficient. (Hishikawa et al., 2014) Tripalmitin [PPP] has lower diffusion coefficient than the tristearin [SSS]. The hydrodynamic radius of PPP shows much smaller value than the SSS. It is suggested that the length of the fatty acyl chains is directly related to the diffusion coefficient of the TAGs. This is seen in larger diffusion coefficient of the SSS than the PPP. In the diffusion NMR spectra, there a difference in the distribution of signals for the methylene ($-\text{CH}_2-$) group of the PPP and LLL. It is suggested that the double bonds increase the diffusion coefficient in the TAG molecule. (Figure 4.2 & 4.3) This has been seen that for symmetrical TAGs with the saturated fatty acyl chains, the high molecular weight tristearin (SSS) shows higher diffusion coefficient and decrease in hydrodynamic radii than the less molecular weight tripalmitin (PPP) and 1-stereoyl-2,3-dipalmitoyl glycerol (SPP). It is suggested that the high molecular weight TAGs have more diffusion coefficient than those of small molecular weight.

It has been observed that in the case of asymmetrical TAGs i.e., 1-stereoyl-2,3-dipalmitoyl glycerol [SPP] and 1-palmitoyl-2,3-distereoyl glycerol [PSS], the deviation of diffusion coefficients is less in comparison to that in PPP and SSS. This reflects the fact that the free activation energies associated with the palmitic acid and stearic acid are different. The change in the stereochemical position also does not affect the diffusion coefficient of the individual TAGs. It is the molecular weight of the TAG that is important in the diffusion coefficient of TAGs. The smaller and larger molecular weight and different sized TAGs can be identified and isolated based on their diffusion coefficients. (Le Gresley et al., 2015)

The TAGs exhibit different polymorphic forms in nature. The fish and meat consist of trans fatty acids, but their nutritional value is balanced by the presence of small molecular weight TAGs. (Mozaffarian, 2016) The diffusion coefficients of smaller molecular weight TAGs i.e., trioctanein [OcOcOc] and trilaurein [LaLaLa] show comparable diffusion coefficients as that of the higher molecular weight symmetrical TAGs i.e., SSS and PPP. The smaller sized TAGs are thought to be more folded and possess free energies to move faster in the diffusion field gradient.

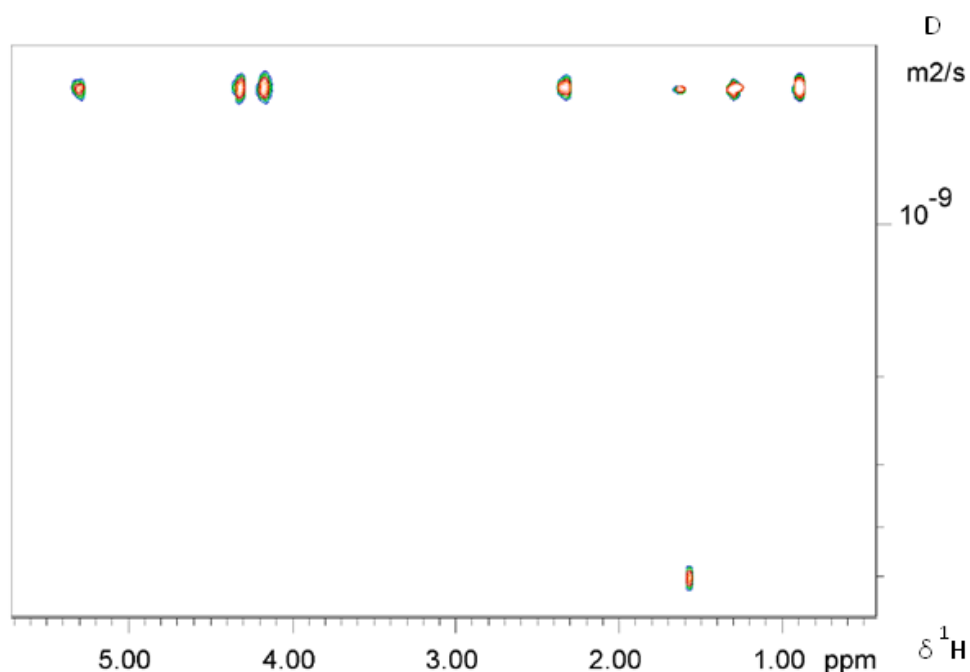


Figure 4.2 2D DOSY of 1,2,3-tripalmitoyl glycerol [Tripalmitin PPP] (1)

The larger diffusion coefficients have been observed for monosaturated-diunsaturated TAGs i.e., 1-palmitoyl-2,3-dioleoyl glycerol [POO] and 1-palmitoyl-2,3-dilinoleoyl glycerol [PLL] and for polyunsaturated TAGs i.e., trilinolein [LLL] and triolein [OOO]. On the other hand, the diacylglycerol diolein OOX has the largest diffusion coefficient than the TAGs. It is suggested that the distribution of unsaturated fatty acyl chains at sn-1, sn-2 and sn-3 positions has different activation energy.

The diffusion coefficient of monoacylglycerols with unsaturated fatty acyl chains have been observed to have more diffusion coefficient than the ones with saturated fatty acid chain. It is suggested that the unsaturated fatty acyl chains in TAGs have bent conformation. The higher diffusion coefficients suggest that the unsaturated fatty acyl chains have cis- conformation. As the cis- double bond is suggested to tilt at an angle of 120° in unsaturated TAGs. (Fr  rot & Lichtenstein, 2012) This results in close packing of the TAGs molecule and the rate of the diffusion is increased. The diffusion coefficient of OOO is larger than LLL. The glycerol conformation in OOO is proposed to have bent conformation and C=C bond produces a kink in the structure. This reduces the friction coefficient of the molecule.

(Akita et al., 2006) It is suggested that two C=C bonds in LLL cause more Vander Waals interactions of the fatty acyl chains with the solvent and slower diffusion of the molecule.

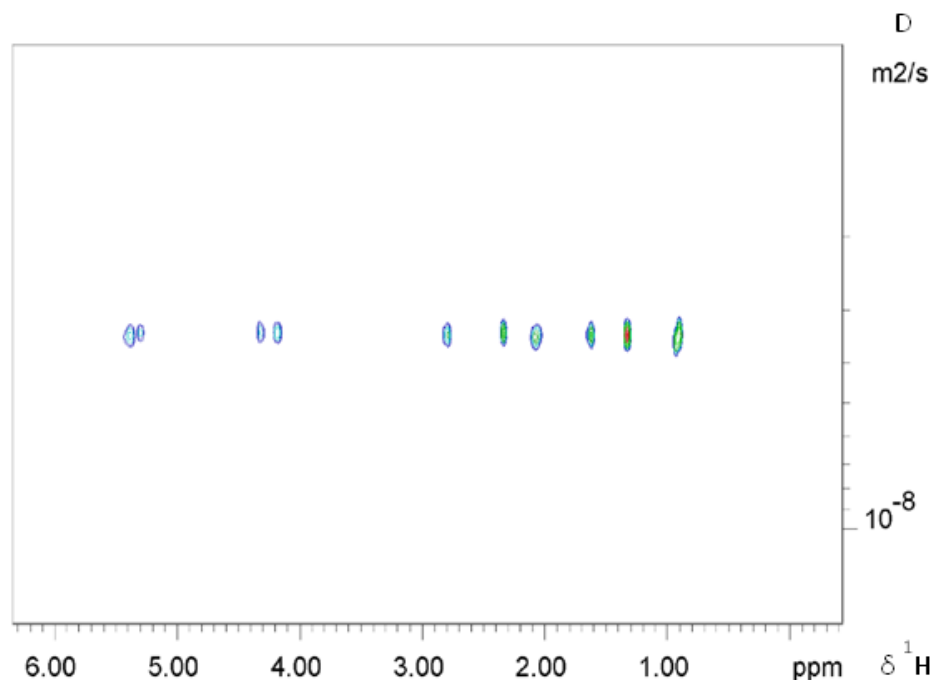


Figure 4.3 2D DOSY of 1,2,3-Trilinoleoyl glycerol [Trilinolein LLL] (4)

In the diffusion spectra of the LLL the diffusion coefficients of the individual ^1H signals within the molecule lie linearly along F2 axis. It has been suggested that the double bonds of polyunsaturated TAGs have different interactions in the solvent. The difference in the diffusion coefficients of PPP and LLL is due to the difference in the degree of unsaturation and symmetry of the fatty acyl chain. (Figure 4.3)

For 1-monoacylglycerols (MAG), the 1-stereoyl glycerol has smaller diffusion coefficient than 1-oleoyl glycerol. This is due to the cis C=C bond and a kink structure of the oleoyl chain. From the DOSY data we see that PLL and POO have a distinctly smaller hydrodynamic radii than PPP which is supported by the fact that the POO has the partial overlap of polar and non-polar groups of molecules. (Figure 4.4 and Figure 4.5) The larger diffusion coefficients of the PLL and POO suggest that the double bonds produce folding in the TAG. Figure 4.4 (B) shows a comparison of the DOSY spectra of POO, PLL and PPP. The POO is suggested to possess more dynamic energy and smaller hydrodynamic radius. The presence of two double bonds in PLL causes rigidity in the molecule. This suggests a non-folded structure of the PLL and larger hydrodynamic radius.

The usual order of diffusion coefficient of the mono-, di- and triacylglycerols with either saturated or unsaturated fatty acids has been calculated as: (Table 4.1 & 4.2)

1-stereoyl glycerol \leq PPP-isomer \leq LaLaLa \leq PPP \leq SPP \leq PSS \leq OcOcOc \leq PLL \leq SPP-Isomer \leq 1-oleoyl glycerol \leq SSS \leq POO \leq LLL \leq OOO \leq OOX

The diffusion coefficient phenomenon is important in the lipid immobilization and diffusion across plasma membrane. Earlier this has been observed that the rate of fatty acid mobility in human adipose tissues increases with the increase in the chain length and increase in degree of unsaturation of fatty acids. This is suggested that this is due to the folded structure of the unsaturated TAGs and closed packing in the higher molecular weight TAGs. This is seen in the diffusion efficient of the synthetic TAGs.

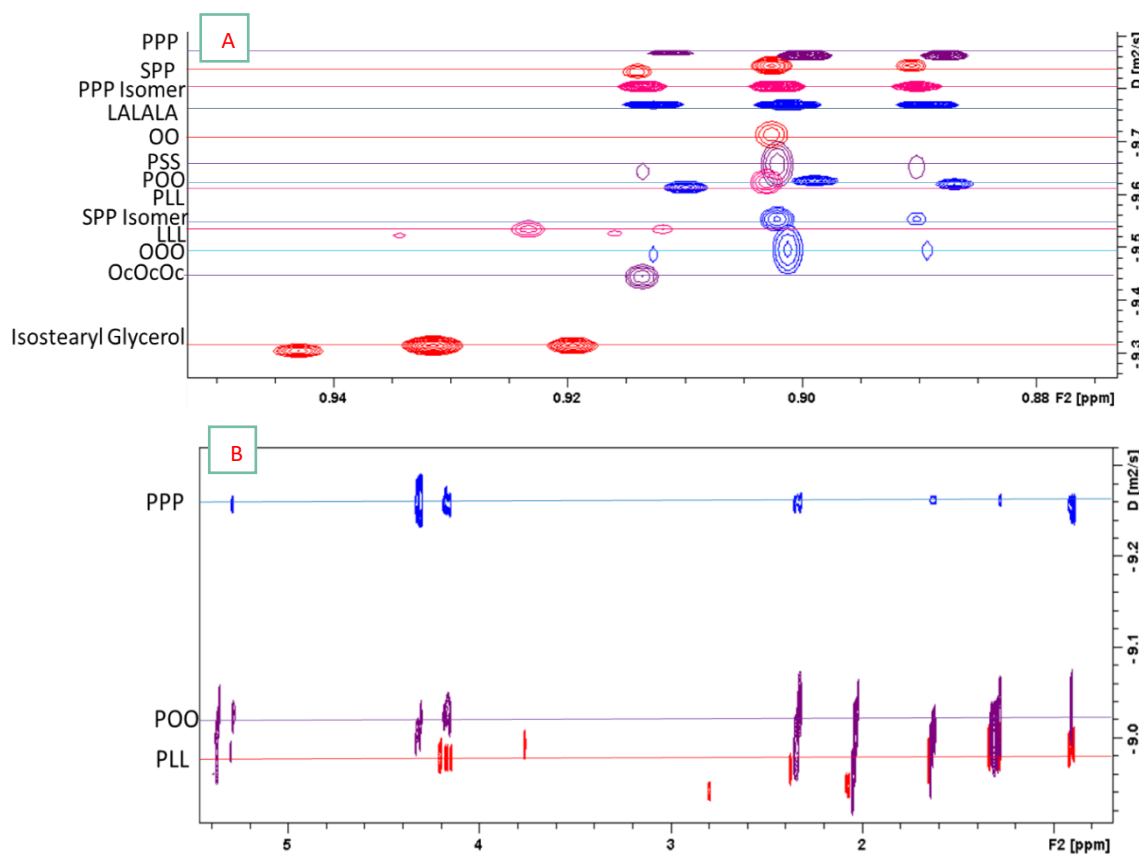


Figure 4.4 (A) 1D DOSY spectra referenced to TMS in CDCl_3 , $D_{20} = 0.2\text{s}$, $P_{30} = 600\mu\text{s}$. DOSY increments = 16, NS = 64 for labelled DAGs. (B) Comparison of PLL (Red), PPP (Blue) and POO (Purple) DOSY spectra referenced to TMS in CDCl_3 , $D_{20} = 0.2\text{s}$, $P_{30} = 600\mu\text{s}$. DOSY increments = 16, NS = 64.

The x-ray diffraction and neutron powder diffraction studies have shown that close chain packing also occurs in saturated triacylglycerols e.g., SSS. The TAGs exist in three polymorphic forms i.e., α (hexagonal unit cell), β' (orthorhombic unit cell) and β (triclinic unit cell). This arrangement of TAGs into packed structure, brings the distant protons close to glycerol protons and they undergo long range coupling. This is seen in diffusion coefficients of PPP and other saturated TAGs. The similar opposite cross peaks have been observed in 2D ROESY spectra of TAGs. (Maynard-Casely et al., 2019) The diffusion coefficients of the unsaturated TAGs have been greater than the monosaturated-diunsaturated TAGs. The unsaturation in TAGs has been responsible to create folding of the TAG

molecule and more activation energy for the molecule which causes them to spin more in the field gradient. Because of this TAGs with unsaturated fatty acid chain in their molecule, have higher diffusion coefficients. (Birker et al., n.d.)

Table 4.1 Diffusion coefficients of TAGs with Gyromagnetic ratio 4257.7000 gamma HZ/ G

S. No.	Triacylglycerol	Diffusion coefficient (m ² /s) E-10	Average error E-10	Hydrodynamic radius (m) E-10
1	1- Stereoyl glycerol	0.157	0.3114	263.3
2	1- Oleoyl glycerol	19.68	2.10	0.9336
3	LaLaLa	6.145	0.051	6.72
4	OcOcOc	9.0618	0.5121	4.563
5	PPP	6.7258	0.1287	6.146
6	PPP-Isomer	5.0503	0.0834	8.185
7	SSS	22.069	1.7787	1.873
8	PSS	8.7041	0.4115	4.749
9	POO	26.028	3.255	1.588
10	PLL	11.06	0.2533	3.735
11	OOO	36.78	4.568	1.124
12	LLL	31.93	1.6475	1.294
13	OOX	53.23	1.017	0.0776
14	SPP	7.9353	0.3896	5.209
15	SPP-Isomer	14.088	0.5122	2.934

This phenomenon suggests the conformational and structural rearrangements in the natural molecules is associated with the diffusion coefficient of the molecules. It is suggested that the conformation of TAGs depends upon the degree of saturation, length of the fatty acyl chain and number of double bonds in the mono- and polyunsaturated TAGs and stereochemical conformation of the fatty acyl chains. Diffusion coefficient increases with the increase in the chain length of the fatty acyl chain of saturated TAGs. The change in diffusion coefficient is not regular for the polyunsaturated TAGs. It is suggested that the double bonds in polyunsaturated TAGs interact differently at different stereochemical positions on the glycerol back bone.

This difference in the diffusion efficient of the TAGs across biological membranes changes with the change in the viscosity of the membrane and is related to the radius of the longitudinal cross section

of the membrane. The translational and rotational diffusion of the lipids and lipo-proteins controls the permeability of the biological membranes in living organisms. (Mika et al., 2016)

The diffusion of the diunsaturated TAGs has been greater than the symmetrical and unsymmetrical saturated TAGs. The double bond in the acyl chain of TAG is thought to have different the hydrodynamic energies in the TAG molecule. (Marguet et al., 2006)

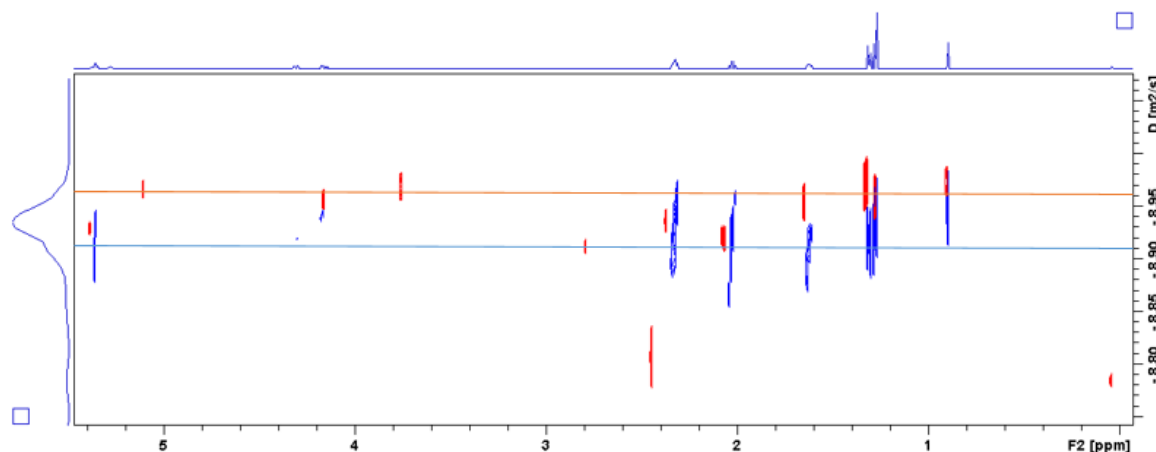


Figure 4.5 Comparison of PLL (Red) and POO (Blue) DOSY spectra referenced to TMS in CDCl_3 , $\text{D}_2\text{O} = 0.2\text{s}$, $\text{P30} = 600\mu\text{s}$. DOSY increments = 16, NS = 64. POO has a smaller hydrodynamic than PLL which demonstrates a more rigid structure with two double bonds.

The average errors in the diffusion coefficients show a non-linear trend. The average errors are slightly larger for the OOO, 1-oleoyl glycerol and SSS. This suggests that the TAGs molecular size and hydrodynamic radii are important in the error related to diffusion coefficient. This suggests that the potential energy is associated with the TAG having larger size and more unsaturated structure.

The diffusion NMR of the TAGs have been measured in chloroform-d solvent. The alignment of TAGs in the diffusion filed gradient is consistent. The acyl groups in the glycerol back bone of TAGs develop hydrophilic interaction with water. The chloroform-d solvent is non-polar and has shown good signal intensity. (Kuchel et al., 1997) The hydrodynamic radii of all the mono- di- and triacylglycerols have been calculated by using Stokes-Einstein equation $D = KT/6\pi\eta r$. The processing of the diffusion NMR spectra on Topspin with different gyromagnetic ratio showed a change in the average diffusion coefficients of the TAGs and their hydrodynamic radii. The change in the gyromagnetic ratio produces different values of the diffusion coefficients and average errors. This predicts the fact that TAGs possess molecular simulations in their structure. The computational model of restricted translational diffusion of TAGs can be built to study the biological systems. (Hyslop & Lauterbur, 1991)

Table 4.2 Diffusion coefficients of TAGs with Gyromagnetic ratio 26770.7000 gamma HZ/ Gauss

S. No.	Triacylglycerol	Diffusion coefficient (m ² /s)	Average error	Hydrodynamic radius (m)
1	1- Stearoyl glycerol	0.397 E-10	0.0075 E-10	104.135 E-10
2	1-Palmitoyl glycerol	0.3083 E-10	0.00539 E-10	134 E-10
3	LaLaLa	0.1605 E-10	0.00167 E-10	257.57 E-10
4	OcOcOc	0.2271 E-10	0.0125 E-10	182.03 E-10
5	PPP	0.1707 E-10	0.003222 E-10	242.19 E-10
6	PPP-Isomer	0.1282 E-10	0.002089 E-10	322.49 E-10
7	SSS	0.5581 E-10	0.05001 E-10	74.07 E-10
8	PSS	0.2181 E-10	0.0109 E-10	189.55 E-10
9	POO	0.6805 E-10	0.1119 E-10	60.75 E-10
10	PLL	0.2798 E-10	0.0064 E-10	147.752 E-10
11	OOO	0.9362 E-10	0.1081 E-10	44.158 E-10
12	LLL	0.728 E-10	0.0375 E-10	56.78 E-10
13	OOX	0.2525 E-10	0.0210 E-10	163.72 E-10
14	SPP	0.2032 E-10	0.00852 E-10	203.453 E-10
15	SPP-Isomer	0.3563 E-10	0.01295 E-10	116.02 E-10

4.4 Conclusion

The diffusion coefficient is important in determining the molecular weight of unknown compounds in natural food stuffs and in industry. The lipids are important constituents of plasma membrane and control the movement of substances by the translational diffusion mechanism. The diffusion coefficient is important to describe the movement of particles across the membrane. The drugs molecule is designed with the specific chemical structures which possess the suitable diffusion coefficient to cross the cell membrane and enter the cell. The chemical structure of triacylglycerol is important in the phase behavior of the plasma membrane. The study of the diffusion coefficients of these synthetic triacylglycerols is useful to understand the physical properties of foods containing triacylglycerols e.g., the mouth melting and taste. The diffusion coefficient provides information of about the hydrodynamic radii of the TAGs and the average errors associated with the diffusion coefficients. Further computational studies are suggested for these synthetic triacylglycerols to study and understand the potential and hydrodynamic energies associated with the triacylglycerol molecules. The diffusion coefficients of saturated and unsaturated TAGs show irregular change in the values of the diffusion coefficients. It is suggested that further studies on the diffusion coefficients of

the synthetic and natural TAGs can reveal the stereochemical structure of TAGs and the mystery of activation energies involved at sn-1, sn-2, and sn-3 positions. It is important too to develop new drugs and to study metabolic pathways in humans.

References

- Akita, C., Kawaguchi, T., & Kaneko, F. (2006). Structural study on polymorphism of cis-unsaturated triacylglycerol: Triolein. *Journal of Physical Chemistry B*, 110(9), 4346–4353. <https://doi.org/10.1021/jp054996h>
- Birker, P. J. M. W. L., de Jong, S., Roijers, E. C., & van Soest, T. C. (n.d.). *Structural Investigations of/3' Triacylglycerols: An X-Ray Diffraction and Microscopic Study of Twinned/3' Cwstals*.
- Block, S. (2018). Brownian motion at lipid membranes: A comparison of hydrodynamic models describing and experiments quantifying diffusion within lipid bilayers. *Biomolecules*, 8(2). <https://doi.org/10.3390/biom8020030>
- Claridge, T. W. D. (1999). High-Resolution NMR Techniques in Organic Chemistry. *Tetrahedron Organic Chemistry Series*, 19, 384.
- Cocucci, E., Kim, J. Y., Bai, Y., & Pabla, N. (2017). Role of Passive Diffusion, Transporters, and Membrane Trafficking-Mediated Processes in Cellular Drug Transport. *Clinical Pharmacology and Therapeutics*, 101(1), 121–129. <https://doi.org/10.1002/cpt.545>
- Dumez, J. N. (2018). Spatial encoding and spatial selection methods in high-resolution NMR spectroscopy. *Progress in Nuclear Magnetic Resonance Spectroscopy*, 109, 101–134. <https://doi.org/10.1016/j.pnmrs.2018.08.001>
- Frérot, E., & Lichtenstein, A. H. (2012). Fats and Oils. *Springer Handbooks*, 2–4, 201–208. <https://doi.org/10.1016/B978-0-12-375083-9.00097-0>
- Gresley, A. le, Kenny, J., Cassar, C., Kelly, A., Sinclair, A., & Fielder, M. D. (2012). The application of high-resolution diffusion NMR to the analysis of manuka honey. *Food Chemistry*, 135(4), 2879–2886. <https://doi.org/10.1016/j.foodchem.2012.07.072>
- Hishikawa, D., Hashidate, T., Shimizu, T., & Shindou, H. (2014). Diversity and function of membrane glycerophospholipids generated by the remodeling pathway in mammalian cells. *Journal of Lipid Research*, 55(5), 799–807. <https://doi.org/10.1194/jlr.R046094>

Hyslop, W. B., & Lauterbur, P. C. (1991). Effects of restricted diffusion on microscopic NMR imaging. *Journal of Magnetic Resonance (1969)*, 94(3), 501–510. [https://doi.org/10.1016/0022-2364\(91\)90136-H](https://doi.org/10.1016/0022-2364(91)90136-H)

Kerssebaum, R. (2002). *DOSY and Diffusion by NMR A Tutorial for TopSpin 1.3*

Kuchel, P. W., Coy, A., & Stilbs, P. (1997). NMR “diffusion-diffraction” of water revealing alignment of erythrocytes in a magnetic field and their dimensions and membrane transport characteristics. *Magnetic Resonance in Medicine*, 37(5), 637–643. <https://doi.org/10.1002/mrm.1910370502>

Kuhnert, N., & Le-Gresley, A. (2005). The use of deep cavity tetraformyl calix [4] arenes in the synthesis of static and dynamic macrocyclic libraries. *Tetrahedron Letters*, 46(12), 2059–2062. <https://doi.org/10.1016/j.tetlet.2005.01.168>

Kuhnert, N., Le-Gresley, A., Rossignolo, G. M., Lopez-Periago, A., & Le-Gresley, A. (2005). Synthesis and capsule formation of upper rim substituted tetra-acrylamido calix [4] arenes. *Organic and Biomolecular Chemistry*, 46(7), 1157–1170. <https://doi.org/10.1039/b502378e>

Le Gresley, A., Simpson, E., Sinclair, A. J., Williams, N., Burnett, G. R., Bradshaw, D. J., & Lucas, R. A. (2015). The application of high-resolution diffusion NMR for the characterisation and quantification of small molecules in saliva/dentifrice slurries. *Analytical Methods*, 7(6), 2323–2332. <https://doi.org/10.1039/c4ay02681k>

Li, C., Zhan, H., Yan, J., Hao, M., Lin, E., Huang, Y., & Chen, Z. (2019). A pure shift and spin echo-based approach for high-resolution diffusion-ordered NMR spectroscopy. *Journal of Magnetic Resonance*, 305, 209–218. <https://doi.org/10.1016/j.jmr.2019.07.021>

Marguet, D., Lenne, P. F., Rigneault, H., & He, H. T. (2006). Dynamics in the plasma membrane: How to combine fluidity and order. *EMBO Journal*, 25(15), 3446–3457. <https://doi.org/10.1038/sj.emboj.7601204>

Maynard-Casely, H. E., Booth, N., Leung, A. E., Stuart, B. H., & Thomas, P. S. (2019). Potential of neutron powder diffraction for the study of solid triacylglycerols. *Food Structure*, 22. <https://doi.org/10.1016/j.foostr.2019.100124>

- Mika, J. T., Thompson, A. J., Dent, M. R., Brooks, N. J., Michiels, J., Hofkens, J., & Kuimova, M. K. (2016). Measuring the Viscosity of the Escherichia coli Plasma Membrane Using Molecular Rotors. *Biophysical Journal*, 111(7), 1528–1540. <https://doi.org/10.1016/j.bpj.2016.08.020>
- Morris, G. A. (2009). Diffusion-Ordered Spectroscopy. *Encyclopedia of Magnetic Resonance*, 1–13. <https://doi.org/10.1002/9780470034590.emrstm0119.pub2>
- Mozaffarian, D. (2016). Dietary and Policy Priorities for Cardiovascular Disease, Diabetes, and Obesity. *Circulation*, 133(2), 187–225. <https://doi.org/10.1161/CIRCULATIONAHA.115.018585>
- Neufeld, R., & Stalke, D. (2015). Accurate molecular weight determination of small molecules via DOSY-NMR by using external calibration curves with normalized diffusion coefficients. *Chemical Science*, 6(6), 3354–3364. <https://doi.org/10.1039/c5sc00670h>
- Nicolay, K., Braun, K. P. J., De Graaf, R. A., Dijkhuizen, R. M., & Kruiskamp, M. J. (2001). Diffusion NMR spectroscopy. *NMR in Biomedicine*, 14(2), 94–111. <https://doi.org/10.1002/nbm.686>
- Nilsson, M. (2009). The DOSY Toolbox: A new tool for processing PFG NMR diffusion data. *Journal of Magnetic Resonance*, 200(2), 296–302. <https://doi.org/10.1016/j.jmr.2009.07.022>
- Nilsson, M., Duarte, I. F., Almeida, C., Delgadillo, I., Goodfellow, B. J., Gil, A. M., & Morris, G. A. (2004). High-resolution NMR and diffusion-ordered spectroscopy of port wine. *Journal of Agricultural and Food Chemistry*, 52(12), 3736–3743. <https://doi.org/10.1021/jf049797u>
- Prades, J., Funari, S. S., Escribá, P. V., & Barceló, F. (2003). Effects of unsaturated fatty acids and triacylglycerols on phosphatidylethanolamine membrane structure. *Journal of Lipid Research*, 44(9), 1720–1727. <https://doi.org/10.1194/jlr.M300092-JLR200>
- Yeh, I. C., & Hummer, G. (2004). System-size dependence of diffusion coefficients and viscosities from molecular dynamics simulations with periodic boundary conditions. *Journal of Physical Chemistry B*, 108(40), 15873–15879. <https://doi.org/10.1021/jp0477147>

Chapter 5

Cocoa butter adulteration

5.1 Introduction

Cocoa (*Theobroma cacao* L.) is generally known to have originated from Central and South America. Cocoa is a native species of tropical humid forests on the lower eastern equatorial slopes of the Andes in South America. The word cacao is derived from the Olmec and the subsequent Mayan languages (Kakaw) and the chocolate-related term cacahuatl is Nahuatl (Aztec language) derived from Olmec/Mayan etymology. (Wood & Lass, 2001) Cocoa has been considered as the food of Gods. It is divine in origin. In 1737, the Swedish botanist Carolus Linnaeus named the cocoa tree *Theobroma cacao*. Now the official botanical name of cocoa is from the Greek word ambrosia. Purdy and Schmidt (1996) reported based on the archaeological information, that the Mayans cultivated cocoa 2,000–4,000 years before Spanish contact. It is recorded that cocoa was domesticated and consumed for the first time by the Maya and Aztecs as a source of energy and food. (Pätzold & Brückner, 2006)

The cocoa plant is usually a small tree with a height of 4 to 8 meters and it may reach up to 10 meters in height under the shadows by large forest trees. The fruit (pods) of cocoa reach up to 15–25 cm in length. The husk of the mature fruit or pod is thick and consists of between 30 to 50 seeds embedded in a thick mucilaginous pulp. *Theobroma cacao* (*T. cacao*) has large genetic diversity. There are four varieties of *T. cacao* tree, Forastero, Trinitario, Criollo and Nacional. Forastero from the Amazonas region and is grown mainly in West Africa as bulk cocoa. It is productive type cultivated wild variety. Its beans are small and flat and have violet cotyledons. Forastero is classified as a bulk, basic and ordinary cocoa with basic chocolate flavor. Criollo is highly aromatic and has nutty, earthy, flowery, and tea-like flavors. Venezuela is the largest producer of Criollo. Criollo is rarely grown because of disease susceptibility. Trinitario is a hybrid of Forastero and Criollo and is found only in the cultivated state in West India, South America, and Central America. Nacional is with fine flavor and is grown only in Ecuador. It has pale purple beans and produces Arriba flavor with aromatic, floral, spicy, and green notes. (Aprotosoiaie et al., 2016)

Cocoa forms the backbone of the economies of some countries in West Africa, such as Côte d'Ivoire and Ghana. It is the leading foreign exchange earner and a great source of income for many families in most of the world's developing countries. In Ghana, cocoa is the second foreign exchange earner and many farmers, and their families depend on it for their livelihood. Major changes have taken place in the world cocoa economy over the last 10 years up to the current 2012/2013 season. World cocoa production rose from nearly 3.2 million tons in the 2002/2003 cocoa season to an estimated 4 million tons forecast for the 2012 season. This represents an average annual growth rate of 3.3%, using a three-year moving average to smooth out the effect of weather-related aberrations. (Afoakwa, 2014) Over the past 50 years, much of the research into cocoa bean fermentation, drying and processing has been aimed at solving certain quality or flavor problems. The cocoa bean undergoes changes during processes from cocoa beans to the final chocolate. (Figure 5.1) Three basic processes are important for the treatment of fresh cocoa beans prior to fermentation i.e., pod storage, mechanical depulping and enzymatic depulping. Several chemical

changes occur during the fermentation process of cocoa beans. These chemical changes are useful to produce fine aroma of the cocoa. (Kuhnert et al., 2020)

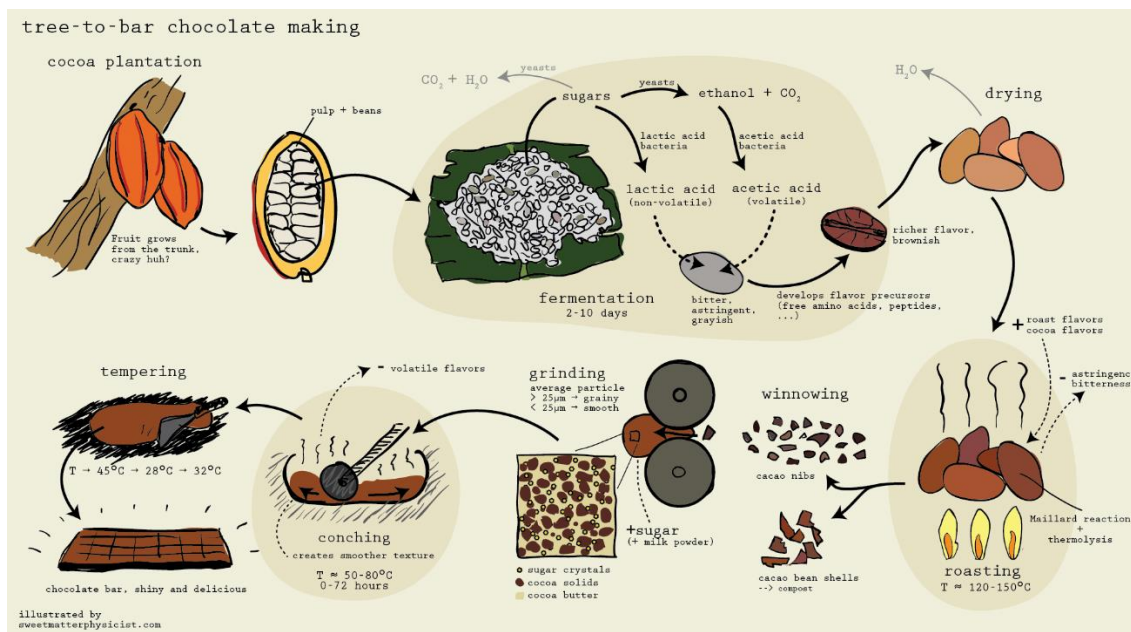


Figure 5.1 Stages in the processing of cocoa from tree to chocolate bar

(<http://sweetmatterphysicist.com/tree-to-bar-basics/>)

Fresh cocoa beans are depulped mechanically by the methods of presses, centrifuges or simply spreading beans onto a flat surface for several hours prior to fermentation. These methods cause a significant increase in the sweating produced in the first 24 hours of fermentation. (Rodriguez-Campos et al., 2011) The depulping is beneficial to shorten the fermentation time and efficiency of the pulp is improved to manufacture jams, marmalade, pulp juice, wine, or cocoa soft drinks. During fermentation of cocoa beans several chemical and enzymatic reactions take place which are important in the aroma and taste development of chocolate. The most important are Maillard reaction. Maillard reactions convert the flavor precursors into fine flavor active components. (Afoakwa et al., 2009) The cocoa flavor compounds are known to be produced upon roasting of the cocoa beans. During Maillard reaction, amino acids and short peptides are the main flavor compounds of the cocoa. These short peptide compounds are subject to several health benefits. (D'Souza et al., 2018) The quality of the cocoa bean is an important trademark for in the cocoa market. The quality of cocoa includes the aspects of flavor and purity and the physical characteristics depending upon the yield of cocoa nib. The chocolate quality depends upon the quality of cocoa beans used for its manufacture. Cocoa beans with good cocoa flavor potential produce a high-quality chocolate. (Rodriguez-Campos et al., 2011)

The chocolate is formed mainly from cocoa solids which include cocoa butter, sugar, and lecithin. The chocolate products available in the market consist of other ingredients such as nuts, fruits, and cereals. The main chocolate categories include white, dark and milk chocolates which differ in the content of cocoa fat, cocoa butter, and milk fat. Chocolate and chocolate products are high energy products.

Chocolate contains 30% fats and 45% carbohydrates. Chocolate also contains minerals such as potassium, magnesium, copper, and iron. (Torres-Moreno et al., 2015) The cocoa butter is rich in triacylglycerols (TAGs), alkaloids and carbohydrates. The high lipid content of cocoa butter consists of TAGs which are the source of energy and nutrition. (Sirbu et al., 2018) TAGs are the main constituent of cocoa butter. The TAGs profile can be used as a standard to check the quality of the cocoa butter and to produce different varieties of chocolate. Many cheap and easily available vegetable oils are used as replacers for the cocoa butter as they have TAGs composition identical to TAGs composition of cocoa butter. TAGs are important components of all-natural foods and can be used as fingerprints for the quality control. (Indelicato et al., 2017)

Several analytical methods have been developed to check the quality of chocolate and evidence frauds and adulterations provide that no vegetable fat must be used for the chocolate production. The exception to this regulation is the Member states who joined EU later. In those Member States an addition of 5% vegetable fats is allowed. The EU is in progress to decide that either the Member states must be allowed this limit or not. Until now the sensitive and precise quantification of the vegetable oils in cocoa butter has not been established. (Anklam et al., 1995) The addition of cheap oils and fats with similar TAGs composition in chocolate is a common practice in industry. The usual fats added to chocolate are cocoa butter equivalents (CBE), cocoa butter replacers (BRs) and cocoa butter substituents (CBSs). In some industries lard is also added as adulterant. (Che Man et al., 2005)

The cocoa butter equivalents (CBE) include non-lauric plant fats. These are similar in physical and chemical composition with the cocoa butter and can be mixed easily. Cocoa butter replacers (CBRs) are non-lauric fats with a distribution of fatty acid like cocoa butter but have a completely different structure of the triglycerides. These are compatible to cocoa butter only in small ratios. Cocoa butter substitutes (CBSs) are lauric acid containing plant fats but chemically totally different from cocoa butter. CBSs have some physical similarities that are suitable only to substitute cocoa butter to 100%. (Lipp & Anklam, 1998) The adulteration of food has been known since long time. Different cheap low-quality vegetable oils are similar in chemical composition with the expensive virgin oils and chocolate. Fraudulent and greedy investors use higher amounts of vegetable oils and fats than recommended in the chocolate production. It is important to detect and quantify the correct number of adulterants in cocoa butter to control the food frauds. (Sun et al., 2015) The adulteration in the cocoa butter is determined most by high resolution GLC, HPLC coupled with evaporative light scattering detector (ELSD) and mass spectrometry. (Simoneau et al., 2000) The adulteration in cocoa butter is also determined by infrared spectroscopy (IR), Raman spectroscopy and NMR spectroscopy. However, these methods were limited to the detection of the main marker compounds. For example, both cocoa butter and palm oil contain POS, but the relative amount is different in the two. (Teye et al., 2014) Gas chromatography (GC) allows the identification of straight-line relationship for the TAGs having carbon atoms between C₅₀ and C₅₄ in cocoa butter from different origins. This was further developed for the quantification of cocoa butter equivalents in cocoa butter even at smaller amounts. (Simoneau et al., 1999) GLC can be used for the quantification of CBE by the GLC data.

It is since there is a linear relationship between C_{50} and C_{54} TAGs of cocoa butter. (Yang et al., 2017) The quantification of cocoa butter equivalents by chromatographic methods such as GC and high-performance liquid chromatography together with statistical regression analysis is used to define the sample class based on its pattern of the measured features. Now-a-days analytical instruments i.e., GLC, MS and HPLC provides information about the variable and features of the samples and adulterants in food. This allows the multivariate analysis to detect and quantify the added adulterants and to point out biomarkers in food, cosmetics, and drugs. (Berrueta et al., 2007)

Vegetable oils and fats and animal fats are rich in triacylglycerol (TAGs). Δ ECN of TAGs from the theoretical and experimental equivalent carbon numbers helps to detect the adulterations of vegetable oils. Each vegetable oils have a distinguishing fatty acid content that acts as a biomarker to identify its adulteration. (Azadmard-Damirchi & Torbati, 2015) The most commonly palm, illipe, and shea butter oils have been used as adulterants in cocoa butter. Lard is also used to some extent due to its high fat content. These adulterants are bleached and blended for the purpose of mixing with the cocoa butter. These result in the formation of degradation products. The identification of these degradation products also helps to detect adulteration in the cocoa butter. (Crews et al., 1997) In multivariate analysis the detection of features and biomarkers is obtained by principal component analysis (PCA), partial least square analysis (PLS) and PLS discriminant analysis (PLS-DA). PCA detects the patterns in data based on chemical variations. PCA allows the visualization of the underlying patterns by reducing the data dimensionality and by retaining information present in the original data as much as possible. PLS is a supervised regression methods which extracts the latent (hidden) variables by the maximization of the covariance between observed variable x and response variables Y . (Megías-Pérez et al., 2018) The quantification of adulteration is also obtained by the analysis of degradation compounds such as sterols, cholesterol and steredienes in the cocoa. The analysis of these degradation products in chocolate helps to quantify adulterants with high precision. (Macarthur et al., 2000)

The various varieties of Theobroma are rich in fatty content. This has attained the attention of the drug and alimentary industries towards the use of Theobroma varieties as a low-cost renewable resource, rich in lipid contents. There is strict legislation for the use of the carcinogenic synthetic food additives such as butylated hydroxyanisole (BHA) and butylated hydroxytoluene (BHT). This has changed the priority of the manufacturers from synthetic to natural antioxidants. Theobroma cocoa and Theobroma subincanum seeds provide rich fatty acid content. In addition to this the seeds of Theobroma subincanum have high tocopherol, fatty acid and sterol content and can be used as a substitute for the synthetic antioxidant and as a low-cost renewable source of vitamin E for industrial processes in cosmetic, drugs and nutraceuticals. (Bruni et al., n.d.)

The adulteration studies and quantification of adulterants by various analytical techniques is very important to control food quality. Adulterants are important aspects in health risks. The use of low quality and cheap oils and fats in food can cause health hazards and result in several diseases. (Meenu et al., 2019) The food frauds are a threat to the World economy. It fails the traditional food safety and food

defense system. Food fraud prevention has emerged now an important food research area to control the economic growth and to prevent health hazards. (Spink et al., 2017)

The quantification of adulterants in cocoa by several analytical techniques is necessary to check the quality of cocoa and to produce new varieties with the desired level of nutrition and energy. Chemometric and multivariate analysis allow the determination of features and chemical composition. It provides information about the diversity of cocoa and other food products based on origin.

5.2 Experimental

5.2.1 Chemicals and reagents

The chemicals and reagents used for the adulteration study have been purchased from Sigma Aldrich, TCI-Germany, and Carl Roth Germany. The vegetable oils i.e., soybean oil, shea butter, palm oil, coconut oil, sunflower oil, rapeseed oil, apricot oil, almond oil, grapeseed oil, olive oil, argon oil, peanut oil, hazelnut oil, pumpkin seed oil, lard and CHOCOMATE 3100 used as adulterants have been purchased from the supermarket in Germany. The cocoa butter (CB) from Ghana and Ecuador have been supplied from the research laboratory of Prof. Dr. Nikolai Kuhnert.

5.2.2 Sample preparation

Mixtures of cocoa butters and adulterants i.e., soybean oil, shea butter, palm oil, coconut oil, sunflower oil, rapeseed oil, apricot oil, almond oil, grapeseed oil, olive oil, argon oil, peanut oil, hazelnut oil, pumpkin seed oil and lard have been prepared at the concentration of 10 % (90:10). All the mixtures were prepared on a weight basis by dissolving 10 mg of the adulterant in 90 mg of the cocoa butter. The mixtures of CBs with coconut oil and CHOCOMATE 3100 were prepared in 5%, 10 % and 20 % ratios by weight. The stock solutions of the mixture were prepared in a concentration of 1 mg/mL. Sample dilution was carried out by dissolving 10 mg of the adulterant sample and adding 1 mL of ethanol/chloroform solution. Then 1 mg of the sample solution was diluted up to 1:10 with ethanol/chloroform HPLC-grade (1:1 solution). Further dilution was carried out by adding tetra dodecyl ammonium bromide as an internal standard.

5.2.3 Sample analysis

Sample analysis was performed on high performance liquid chromatography coupled with microtof. Separation was achieved on a 3.0 x 150 mm i.d. Agilent Poroshell 120 column 4.0 μ m and 3.0 x 5 mm i.d. guard column of the same material (Agilent, Germany). Solvent A consisted of acetonitrile with 0.01 % formic acid and solvent B consisted of Ethanol (HPLC-grade) with 10 mmol/L ammonium format. Separation of the TAGs was achieved at a total flow rate of 800 μ L/min. The samples were run in triplicate in positive mode and principal component analysis (PCA) and partial least square- discriminant analysis (PLSDA) was performed to check the variance in the data.

5.2.4 Statistical analysis

Mass spectra of the adulterants and pure samples were analyzed by data analysis 4.0 (Bruker Daltonics). The spectra were recalibrated and mzxml files were created by using Mzmine 2.50 software giving peak area list and corresponding m/z ratio and retention times. (Myers et al., 2017) Heirarchical clustering was performed with orange software. Principal component analysis (PCA) and partial least square-

discriminant analysis (PLSDA), variable importance in projection (VIP), recursive SVM and Scree plot are performed by using Metaboanalyst software. (<http://www.metaboanalyst.ca>) (Tugizimana et al., 2016) PCA is used to detect patterns in data, based on chemical variations observed in large data sets. This was based on the detection of variation among different cocoa samples based on the TAGs composition from different origins i.e., Ghana and Ecuador.

5.3 Results & Discussion

In this work, the samples of cocoa butter from Ghana and Ecuador and vegetable oils and their mixtures in the concentration of 5%, 10% and 20% were analyzed by HPLC coupled with ESI-MS in positive ion mode. TAGs profiles have been obtained by HPLC—ESI-MS. The TAGs profiles in the pure samples i.e., cocoa butter from Ghana and Ecuador, vegetable oils and 5%, 10% and 20% adulterant mixtures are analyzed. The difference in the TAGs profiles of pure samples and adulterants allowed to identify the biomarkers (TAGs) to detect the adulteration of the vegetable oil in the cocoa butter. 5%, 10% and 20% mixtures of coconut oil and chocomate 3100 predicted that the adulterations can be detected at 5% level by comparing the TAGs profiles of the samples. (Figure 5.2) In almond oil the TAGs with molecular weight m/z 902, 874, 900 are identified as an indicator of adulterant with the cocoa butter from Ecuador. Similar is the case for the adulterant mixture of almond oil and cocoa butter Ghana. For the argon oil and apricot TAGs with molecular weight m/z 902 and 900 are the main TAGs to differentiate between the pure oils from the cocoa butter from Ecuador and Ghana. In Apricot and grapeseed oil only TAG with molecular weight m/z 902 has been identified. (Table 5.1)

In the coconut oil diacylglycerols (DAGs) are seen to be most abundant. The DAGs fragments in coconut oil are indefinable at 5% level. This is suggested that LC-MS is a reliable method for the authentication of adulterations of vegetable oils in cocoa butter. It is suggested that cheaper vegetable oils can be used for the quantification of adulteration in cocoa butter. These can also be used in the food authentication studies and in the production of new food varieties.

Table 5.1 Chemical structures of biomarkers (TAGs) identified in vegetable oils and fats from the LC-MS data

S. No.	Vegetable oils and fats	TAGs identified as biomarkers Molecular weight [M + NH ₄] ⁺	Chemical Formulae of TAGs	Chemical Structures of TAGs
1.	Coconut oil	876.824	C ₅₅ H ₁₀₆ NO ₆	POO
		954.866	C ₅₉ H ₁₁₈ NO ₇	SSA
2.	Grapeseed oil	986.939	C ₆₃ H ₁₁₈ NO ₆	LgSS (24:0, 18:0, 18:0)
		900.853	C ₅₇ H ₁₀₆ NO ₆	SLL
		954.866	C ₅₉ H ₁₁₈ NO ₇	SSA
3	Hazelnut oil	898.8081	C ₅₇ H ₁₀₄ NO ₆	OLL
		900.853	C ₅₇ H ₁₀₆ NO ₆	SLL
		954.866	C ₅₉ H ₁₁₈ NO ₇	SSA
4	Lard	898.8081	C ₅₇ H ₁₀₄ NO ₆	OLL
		900.853	C ₅₇ H ₁₀₆ NO ₆	SLL
		930.8783	C ₅₉ H ₁₁₀ NO ₆	ALO (20:0, 18:1, 18:2)
5	Olive oil	984.9165	C ₆₂ H ₁₁₄ NO ₇	LgOO (24:0, 18:1, 18:1)
		930.8783	C ₅₉ H ₁₁₀ NO ₆	ALO (20:0, 18:1, 18:2)
6	Palm oil	954.866	C ₅₉ H ₁₁₈ NO ₇	SSA
		984.9165	C ₆₂ H ₁₁₄ NO ₇	LgOO (24:0, 18:1, 18:1)
		930.8783	C ₅₉ H ₁₁₀ NO ₆	ALO (20:0, 18:1, 18:2)
		900.853	C ₅₇ H ₁₀₆ NO ₆	SLL
7	Peanut oil	989.966	C ₆₃ H ₁₂₄ NO ₆	SOLg (18:0, 18:1, 24:0)
8	Pumpkin seed oil	907.7017	C ₅₇ H ₁₁₂ NO ₆	SOS (18:0, 18:1, 18:0)
		908.7343	C ₅₇ H ₁₁₄ NO ₆	SSS (18:0, 18:0, 18:0)
		894.788	C ₅₅ H ₁₀₈ NO ₇	PL(-OH)S

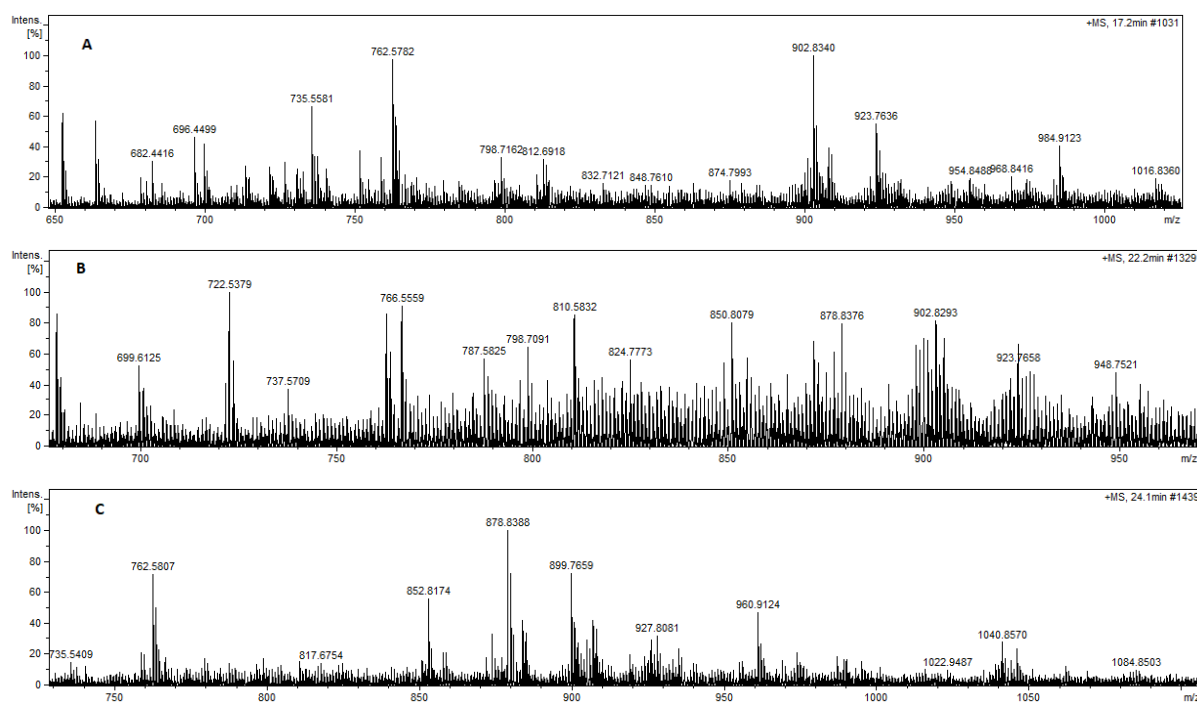


Figure 5.2 Mass spectrums in MS mode of A. Almond oil B. Cocoa butter Ghana and C. Cocoa butter

Ghana and 10% Almond oil showing the difference in TAGs profiles

The PCA plot of the LC-MS data of the cocoa butters from two origins i.e., Ghana and Ecuador, vegetable oils i.e., soybean oil, shea butter, palm oil, coconut oil, sunflower oil, rapeseed oil, apricot oil, almond oil, grapeseed oil, olive oil, argon oil, peanut oil, hazelnut oil, pumpkin seed oil, lard and CHOCOMATE 3100 and their mixtures in the 10% ratio are carried out. PCA plot shows that the adulterants of vegetable oils with the cocoa butter Ghana show high proportion of variance and are far separated by multivariate analysis based on chemical composition. (Figure 5.3) The variance explained for the principal components are 86.6% and 6.0% respectively. PCA was performed for the visualization and classification of diversity in TAGs profiles of the cocoa butter, vegetable oils and their adulterant mixtures. It is suggested that the geographical variation in the TAGs composition of cocoa butter and the differences of TAGs profiles observed in the cocoa butter and the vegetable oils are important parameters for the identification of adulterants in the cocoa butter and chocolate products. The pure samples and adulterants can be differentiated based on proportion of variance and principal components.

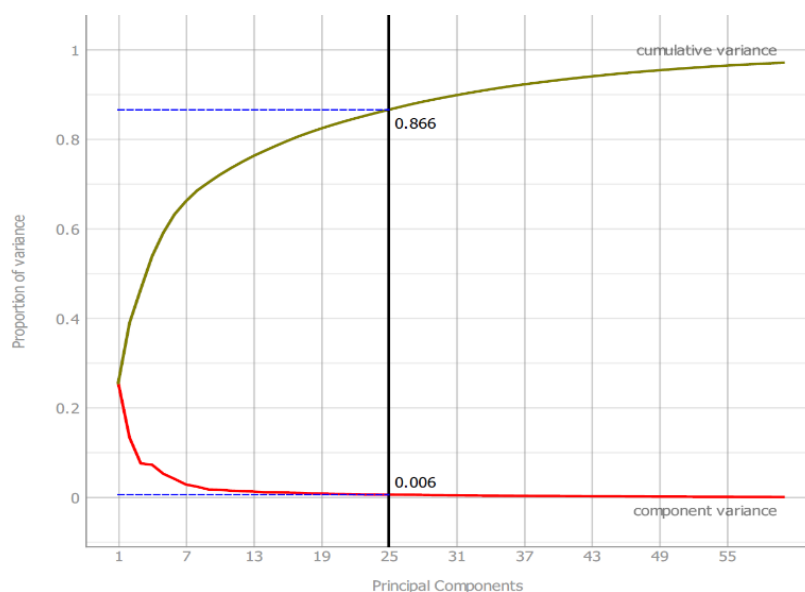


Figure 5.3 Principal component analysis (PCA) showing explained variance for the cocoa butter adulterant samples

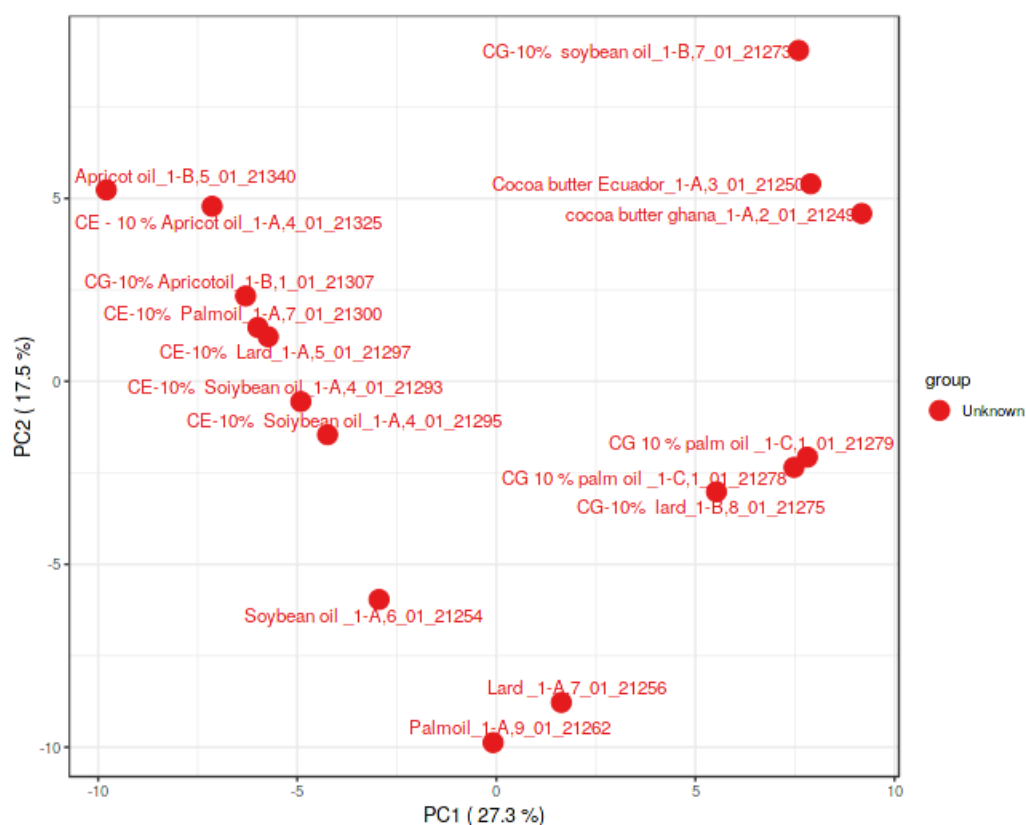


Figure 5.4 PCA plot obtained from the LC-MS data of the cocoa butter Ghana, cocoa butter Ecuador, soybean oil, palm oil, apricot oil, lard and their 10% adulterants mixtures

The principal component analysis of the LC-MS data of the cocoa butter Ghana, cocoa butter Ecuador, soybean oil, palm oil, apricot oil, lard and their 10% adulterants mixtures showed variance for the first and second components are 27.3% and 17.5% respectively. (Figure 5.4)

The geographical variation in cocoa butter composition of TAGs and regioisomeric differences of TAGs observed in the cocoa butter or the vegetable oils and CBEs are another parameter for the identification of adulterants in the cocoa butter and chocolate products.

The scree plot in figure 5.5 explains the variance up to 42.3 by the individual PCs. The PCA based upon the TAGs profiles of the adulterant samples shows that the pure samples and adulterant samples differ in their principal component distribution.

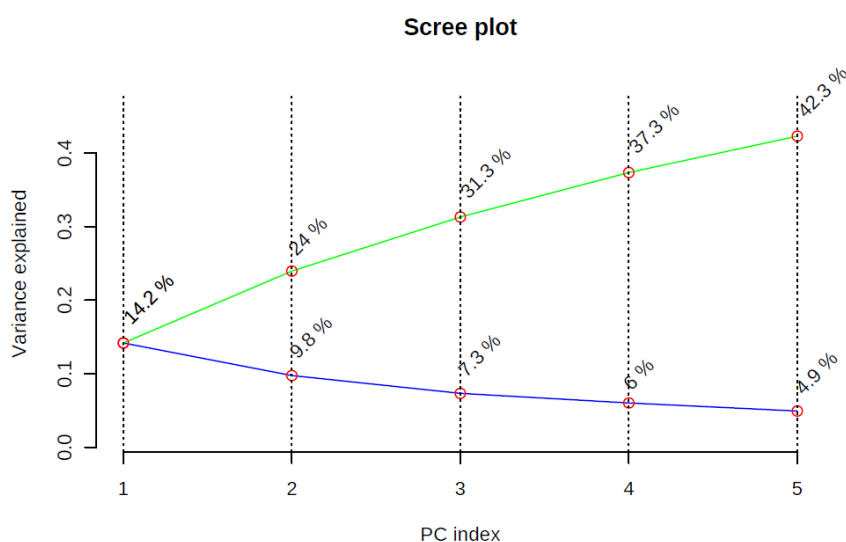


Figure 5.5 Scree plot showing the variance explained by PCs of the TAGs profiles. The green line shows the accumulative variance explained and blue line shows the variance explained by individual PCs of the TAGs profiles

The 2D score plots show that the variance explained by first and second PC1 are 14.2 % and PC2 9.8 % respectively. The Group 1 (red color) represents the cocoa butter Ghana (CG), cocoa butter Ecuador (EC) and the pure vegetable oils and group 2 (green color) the 5%, 10% and 20% mixtures of CE and CG with the vegetable oils. The adulterant samples and pure samples are clustered separately. There is a little variance observed for CG in group 1. This is suggested that the cocoa butters from different origins and their adulterants can be detected based on their variance from 2D loading plots. The variance explained in 3D score plots for PC1, PC2 and PC3 are 14.2 %, 9.8 % and 7.3 % respectively. (Figure 5.6) It suggests that the cocoa butters from Ghana and Ecuador show small variance.

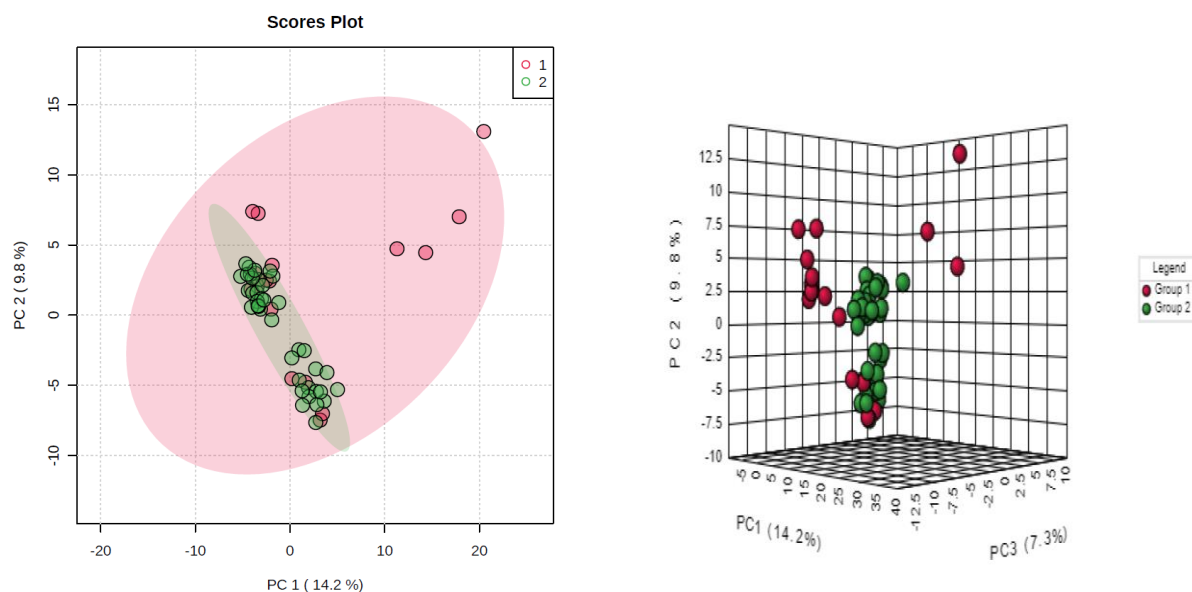


Figure 5.6 Score plots of the LC-MS data (2D) (left) and 3D score plots (right). The explained variances are shown in brackets. The Group 1 (red color) represents the cocoa butter Ghana (CG), cocoa butter Ecuador (EC) and the pure vegetable oils and group 2 (green color) the 5%, 10% and 20% mixtures of CE and CG with the vegetable oils.

The samples from the cocoa butter Ghana and Ecuador lie in the parallel to each other. The pure cocoa butters are separated from the mixtures. The multivariate analysis explains the variance between adulterants. It is suggested that the adulteration in cocoa butter and other food can be explained based on variance from multivariate statistical analysis.

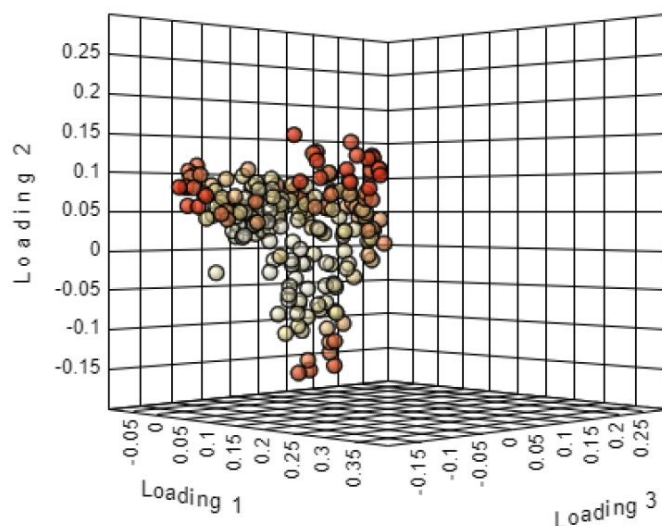


Figure 5.7 Loading plot of the LC-MS data for selected PCs of the TAGs profiles of the samples. The loading plot shows that the samples are clustered together and lie in the range of -0.15 to 0.15 in loading 2. (Figure 5.7) Partial least squares (PLS) analysis is a supervised regression method which attempts to extract latent (or hidden) variables by maximizing the covariance between observed variables X and response variables Y. PLS discriminant analysis (PLS-DA) is an extension of PLS for solving

classification problems. PLS-DAs and PCAs were performed using the R-package ropls. In both cases the data were mean-centered and scaled to unit variance. The score plots of PLS-DA in 2D show a variance of 10.4 % and 10.2 % for first and second components respectively. The 3D score plot shows a variance of 4.9 for the third component. This shows that the adulterations show variation up to considerable extent. (Figure 5.8)

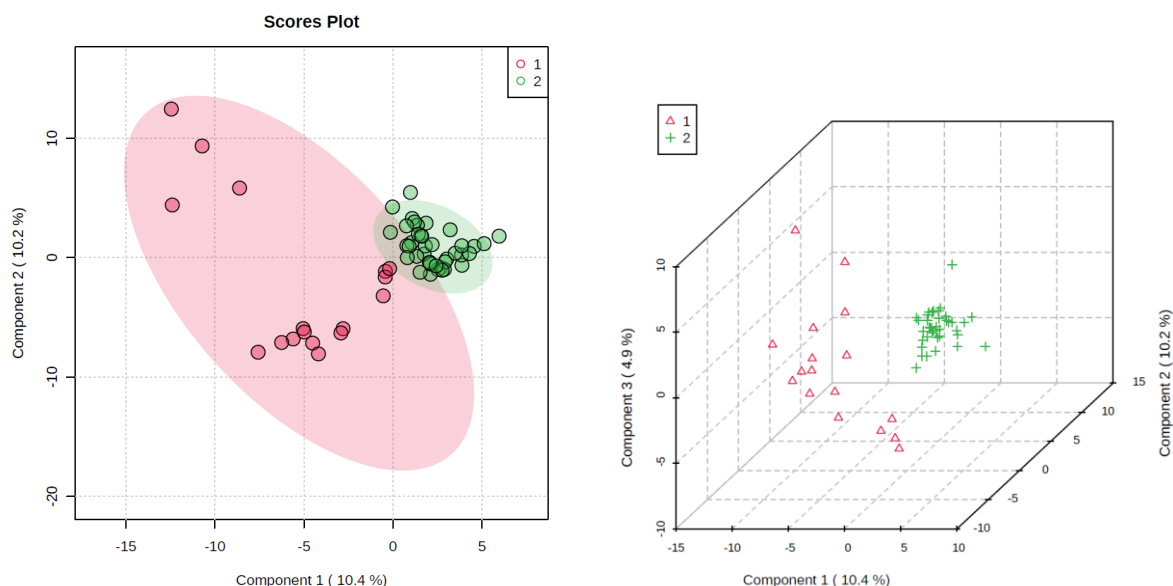


Figure 5.8 Score plots of PLS-DA based on the triacylglycerol profiles from the LC-MS data. The 2D score plots (left) and 3D score plot (right), the variance is shown in the brackets (The Group 1 (red color) represents the cocoa butter Ghana (CG), cocoa butter Ecuador (EC) and the pure vegetable oils and group 2 (green color) the 5, 10% and 20% mixtures of CE and CG with the vegetable oils)

The cross validation in PLS-DA with $Q^2 = 0.5$ showed to be the best classifier. In the VIP score of PLS-DA it comes clear that the triacylglycerols are present in highest score in the samples and are the indicative for the classification of the samples. (Figure 5.9) VIP score is a measure of a variable's importance in the PLSDA model. It summarizes the contribution of a variable to the model. The VIP score of PLSDA is calculated as a weighted sum of the squares correlations between the PLSDA components and the original variables. VIP score shows that the TAGs with high molecular weight are separated. There is less overlapping of the variables in the PLSDA. The x-variables are not positively related to each other. This suggests that the TAGs profiles of cocoa butter show variance from the mixtures.

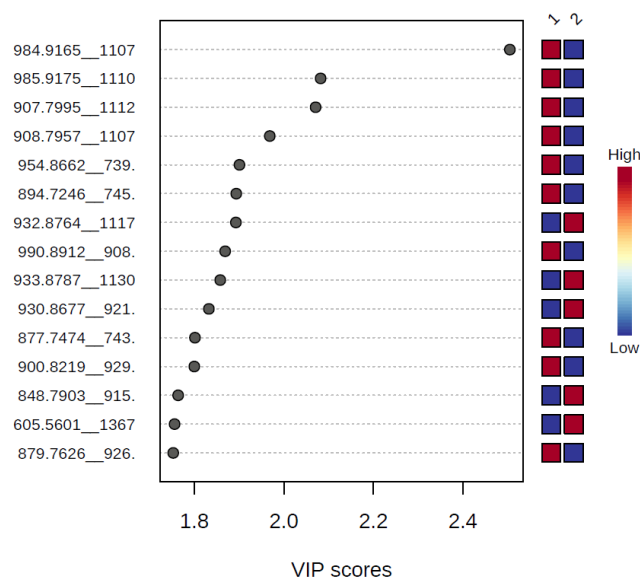


Figure 5.9 VIP score of the important features identified by PLS-DA. The colored boxes on the right side indicate the relative concentrations of the important component (TAGs) identified as biomarkers in the vegetable oils. Colors denote VIP scores of each variable (TAG), which indicate their discrimination power.

Table 5.2 Chemical structures of biomarkers (TAGS) of the vegetable oils identified in VIP scores

S. No.	Molecular weight	Chemical Formula	Chemical structure of TAG
1.	984.9165	$C_{62}H_{114}NO_7$	LgOO (24:0, 18:1, 18:1)
2.	985.9175	$C_{63}H_{118}NO_6$	LgSS (24:0, 18:0, 18:0)
3	907.7995	$C_{57}H_{112}NO_6$	SOS (18:0, 18:1, 18:0)
4	908.7957	$C_{57}H_{114}NO_6$	SSS (18:0, 18:0, 18:0)
5	954.8662	$C_{59}H_{118}NO_7$	SSA (18:0, 18:0, 20:0)
6	894.7256	$C_{55}H_{108}NO_7$	PL(-OH)S (16:0, 18:1 (-OH), 18:1)
7	894.7246	$C_{56}H_{112}NO_6$	MaSS (17:0, 18:0, 18:0)
8	932.8764	$C_{59}H_{114}NO_7$	AOO (20:0, 18:1, 18:1)
9	990.8912	$C_{63}H_{124}NO_6$	SOLg (18:0, 18:1, 24:0)
10	933.8787	$C_{59}H_{114}NO_6$	SOA (18:0, 18:1, 20:0)
11	930.8677	$C_{59}H_{110}NO_6$	ALO (20:0, 18:1, 18:2)
12	877.7474	$C_{55}H_{106}NO_6$	POO (16:0, 18:1, 18:1)
13	900.8219	$C_{57}H_{106}NO_6$	SLL (18:0, 18:2, 18:2)
14	840.7903	$C_{53}H_{104}NO_6$	PSP (16:0, 18:0, 16:0)
15	605.5601	$C_{36}H_{74}NO_6$	PPX (16:0, 16:0, 0:0)
16	879.7626	$C_{55}H_{110}NO_7$	PSS (16:0, 18:0, 18:0)

The VIP score shows the concentration of the TAGs biomarkers in the vegetable oils. The TAGs with m/z 900.8219, 877.7474, 930.8677, 932.8764 and 894.7246 are identified as the most common biomarkers in

the vegetable oils. It is observed from the LC-MS data of the cocoa butters and vegetable oils that these biomarkers are absent in the cocoa butter. So, it is suggested that adulterations in the cocoa butter can be detected with LC-MS and multivariate analysis.

Hierarchical clustering from the LC-MS data of all the samples was performed by distance measuring using Euclidean and clustering algorithm used ward. D. The clustering is performed with hclust function in package stat. The pure samples are clustered together, and adulterant mixtures of CG and CE are clustered separately. The size of the clusters in the hierarchical clustering shows the level of variance within the samples. (Figure 5.10)

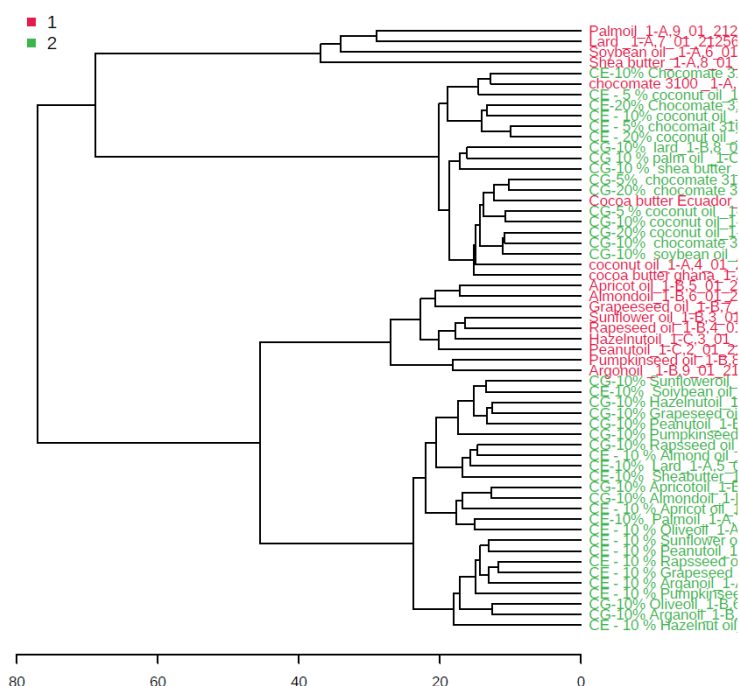


Figure 5.10 Hierarchical cluster from the LC-MS data of cocoa butter, vegetable oils, lard, CHOCOMATE-3100 and adulterant mixtures shown as dendrogram. brackets Group 1 (red color) = The cocoa butter Ghana (CG), cocoa butter Ecuador (EC) and the pure vegetable oils, Group 2 (green color) = 5, 10% and 20% mixtures of CE and CG with the vegetable oils

Palm oil, lard, soybean oil and shea butter fall in the highest rank of the clustering. It is suggested that there is a similarity in the TAGs composition of these samples. The 10 mixtures of cocoa butter Ghana and cocoa butter Ecuador fall far from each other in Hierarchical clustering. The CE is at the higher rank of the hierarchical clustering and adulterants of the CE with the vegetable oils are shifted towards lower ranks. CG is lower in hierarchical clustering than CE. The CG adulterants with vegetable oils are widely distributed above and below the ranking. This is suggested that there exists diversity among the percentage chemical composition of TAGs from different origins. It is suggested that it is related to the geographical and environmental conditions.

TAGs composition of the vegetable oils is suggested to be biomarkers for the detection of adulterations in food. The biomarkers are identified in the vegetable oils. The TAGs as biomarkers are present in the

vegetable oils and these are absent in the cocoa butter. So, these biomarkers can be used to identify adulterants in the cocoa butter.

5.4 Conclusion

The adulteration is an important phenomenon in food and pharmacokinetics. The TAGs profiles of the pure cocoa butters, vegetable oils and their adulterant mixtures are compared by the LC-MS analysis. TAGs profiles of the vegetable oils are different from the pure cocoa butters and considerable number of TAGs are identified as biomarkers in the vegetable oils. This is further identified in the multivariate analysis i.e., PCA and PLSDA. These TAGs biomarkers are further determined as important features in the VIP score by PLSDA. It is observed that the TAGs with m/z 900.8219, 877.7474, 930.8677, 932.8764 and 894.7246 are identified as the most common biomarkers in the vegetable oils and fats. The rest of the biomarkers occur to a lesser extent. This is suggested that the LC-MS analysis and multivariate analysis of the TAGs profiles of the cocoa butter and the adulterant samples can be a reliable method for the authentication of the food quality and to detect quantity of adulterants in chocolate, cocoa butter and fats and oils. This is also applicable in other food products. Due to the limitations of regioisomeric analysis and restrictions of the analytical measurements there were no clear biomarkers to identify adulterations in cocoa butter. It is suggested that following the discriminate analysis and profiling of the TAGs profiles of the pure samples and adulterants, we can quantify the level and variance of adulteration. This is also important to check the food quality and to prevent the health hazards to human life.

References

Afoakwa, E. O. (n.d.). *Cocoa Production and Processing Technology*

Afoakwa, E. O., Paterson, A., Fowler, M., & Ryan, A. (2009). Matrix effects on flavour volatiles release in dark chocolates varying in particle size distribution and fat content using GC-mass spectrometry and GC-olfactometry. *Food Chemistry*, 113(1), 208–215.

<https://doi.org/10.1016/j.foodchem.2008.07.088>

Anklam, E., Lipp, M., & Wagner, B. (1995). Forschungs beitrage/Research Papers HPLC with Light Scatter Detector and Chemometric Data Evaluation for the Analysis of Cocoa Butter and Vegetable Fats. In *Eur. J. Med. Res* (Vol. 1)

Aprotosoiaie, A. C., Luca, S. V., & Miron, A. (2016). Flavor Chemistry of Cocoa and Cocoa Products-An Overview. *Comprehensive Reviews in Food Science and Food Safety*, 15(1), 73–91.

<https://doi.org/10.1111/1541-4337.12180>

Azadmard-Damirchi, S., & Torbati, M. (2015). Adulterations in Some Edible Oils and Fats and Their Detection Methods. *Journal of Food Quality and Hazards Control*, 2(2), 38–44.

<https://jfqhc.ssu.ac.ir/article-1-143-en.html>

Berrueta, L. A., Alonso-Salces, R. M., & Héberger, K. (2007). Supervised pattern recognition in food analysis. In *Journal of Chromatography A* (Vol. 1158, Issues 1–2, pp. 196–214).

<https://doi.org/10.1016/j.chroma.2007.05.024>

Bruni, R., Medici, A., Guerrini, A., Scalia, S., Poli, F., Romagnoli, C., Muzzoli, M., & Sacchetti, G. (n.d.). *Tocopherol, fatty acids and sterol distributions in wild Ecuadorian Theobroma subincanum (Sterculiaceae) seeds*. www.elsevier.com/locate/foodchem

Che Man, Y. B., Syahariza, Z. A., Mirghani, M. E. S., Jinap, S., & Bakar, J. (2005). Analysis of potential lard adulteration in chocolate and chocolate products using Fourier transform infrared spectroscopy. *Food Chemistry*, 90(4), 815–819. <https://doi.org/10.1016/j.foodchem.2004.05.029>

Crews, C., Calvet-Sarrett, R., & Brereton, P. (1997). The Analysis of Sterol Degradation Products to Detect Vegetable Fats in Chocolate. *JAOCs*, 4, 1273–1280

- D'Souza, R. N., Grimbs, A., Grimbs, S., Behrends, B., Corno, M., Ullrich, M. S., & Kuhnert, N. (2018). Degradation of cocoa proteins into oligopeptides during spontaneous fermentation of cocoa beans. *Food Research International*, 109, 506–516. <https://doi.org/10.1016/j.foodres.2018.04.068>
- Indelicato, S., Bongiorno, D., Pitonzo, R., di Stefano, V., Calabrese, V., Indelicato, S., & Avellone, G. (2017). Triacylglycerols in edible oils: Determination, characterization, quantitation, chemometric approach and evaluation of adulterations. In *Journal of Chromatography A* (Vol. 1515, pp. 1–16). Elsevier B.V. <https://doi.org/10.1016/j.chroma.2017.08.002>
- Kuhnert, N., D'souza, R. N., Behrends, B., Ullrich, M. S., & Witt, M. (2020). Investigating time dependent cocoa bean fermentation by ESI-FT-ICR mass spectrometry. *Food Research International*, 133. <https://doi.org/10.1016/j.foodres.2020.109209>
- Lipp, M., & Anklam, E. (1998). Review of cocoa butter and alternative fats for use in chocolate-Part B. Analytical approaches for identification and determination INTRODUCTION SPECTROSCOPIC METHODS. In *Food Chemistry* (Vol. 62, Issue 1)
- Macarthur, R., Crews, C., & Brereton, P. (2000). An improved method for the measurement of added vegetable fats in chocolate. *Food Additives and Contaminants*, 17(8), 653–664. <https://doi.org/10.1080/02652030050083178>
- Meenu, M., Cai, Q., & Xu, B. (2019). A critical review on analytical techniques to detect adulteration of extra virgin olive oil. In *Trends in Food Science and Technology* (Vol. 91, pp. 391–408). Elsevier Ltd. <https://doi.org/10.1016/j.tifs.2019.07.045>
- Megías-Pérez, R., Grimbs, S., D'Souza, R. N., Bernaert, H., & Kuhnert, N. (2018). Profiling, quantification, and classification of cocoa beans based on chemometric analysis of carbohydrates using hydrophilic interaction liquid chromatography coupled to mass spectrometry. *Food Chemistry*, 258, 284–294. <https://doi.org/10.1016/j.foodchem.2018.03.026>
- Myers, O. D., Sumner, S. J., Li, S., Barnes, S., & Du, X. (2017). One Step Forward for Reducing False Positive and False Negative Compound Identifications from Mass Spectrometry Metabolomics Data: New Algorithms for Constructing Extracted Ion Chromatograms and Detecting Chromatographic Peaks. *Analytical Chemistry*, 89(17), 8696–8703. <https://doi.org/10.1021/acs.analchem.7b00947>

Pätzold, R., & Brückner, H. (2006). Gas chromatographic determination and mechanism of formation of D-amino acids occurring in fermented and roasted cocoa beans, cocoa powder, chocolate, and cocoa shell. *Amino Acids*, 31(1), 63–72. <https://doi.org/10.1007/s00726-006-0330-1>

Rodriguez-Campos, J., Escalona-Buendía, H. B., Orozco-Avila, I., Lugo-Cervantes, E., & Jaramillo-Flores, M. E. (2011). Dynamics of volatile and non-volatile compounds in cocoa (*Theobroma cacao* L.) during fermentation and drying processes using principal components analysis. *Food Research International*, 44(1), 250–258. <https://doi.org/10.1016/j.foodres.2010.10.028>

Simoneau, C., Hannaert, P., & Anklam, E. (n.d.). *Analytical, Nutritional and Clinical Methods Section Detection and quanti®cation of cocoa butter equivalents in chocolate model systems: analysis of triglyceride pro®les by high resolution GC*

Simoneau, C., Lipp´franz, M., Lipp´franz, L., & Anklam, U. E. (2000). Quantification of cocoa butter equivalents in mixtures with cocoa butter by chromatographic methods and multivariate data evaluation. In *Eur Food Res Technol* (Vol. 211). Springer-Verlag

Sirbu, D., Corno, M., Ullrich, M. S., & Kuhnert, N. (2018). Characterization of triacylglycerols in unfermented cocoa beans by HPLC-ESI mass spectrometry. *Food Chemistry*, 254, 232–240. <https://doi.org/10.1016/j.foodchem.2018.01.194>

Spink, J., Ortega, D. L., Chen, C., & Wu, F. (2017). Food fraud prevention shifts the food risk focus to vulnerability. In *Trends in Food Science and Technology* (Vol. 62, pp. 215–220). Elsevier Ltd. <https://doi.org/10.1016/j.tifs.2017.02.012>

Sun, X., Lin, W., Li, X., Shen, Q., & Luo, H. (2015). Detection and quantification of extra virgin olive oil adulteration with edible oils by FT-IR spectroscopy and chemometrics. *Analytical Methods*, 7(9), 3939–3945. <https://doi.org/10.1039/c5ay00472a>

Teye, E., Huang, X. yi, Lei, W., & Dai, H. (2014). Feasibility study on the use of Fourier transform near-infrared spectroscopy together with chemometrics to discriminate and quantify adulteration in cocoa beans. *Food Research International*, 55, 288–293. <https://doi.org/10.1016/j.foodres.2013.11.021>

Torres-Moreno, M., Torrescasana, E., Salas-Salvadó, J., & Blanch, C. (2015). Nutritional composition and fatty acids profile in cocoa beans and chocolates with different geographical origin and processing conditions. *Food Chemistry*, 166, 125–132.

<https://doi.org/10.1016/j.foodchem.2014.05.141>

Tugizimana, F., Steenkamp, P. A., Piater, L. A., & Dubery, I. A. (2016). A conversation on data mining strategies in LC-MS untargeted metabolomics: Pre-processing and pre-treatment steps. *Metabolites*, 6(4). <https://doi.org/10.3390/metabo6040040>

Wood, G. A. R., & Lass, R. A. (2001). *Cocoa-fourth edition (Tropical agricultural series)* (4th ed.). Wiley-Blackwell

Yang, M., Fan, Y., Wu, P. C., Chu, Y. D., Shen, P. L., Xue, S., & Chi, Z. Y. (2017). An extended approach to quantify triacylglycerol in microalgae by characteristic fatty acids. *Frontiers in Plant Science*, 8. <https://doi.org/10.3389/fpls.2017.01949>

Young, C. C., Pic, R. M., & Yo11xy, Y. (n.d.), *The Interpretation of GLC Triglyceride Data for the Determination of Cocoa Butter Equivalents in Chocolate: A New Approach*

Conclusion

Triacylglycerols are important components of vegetable oils and fats and animal fats. These are composed of glycerol back bone with three fatty acids esterified at three stereochemical positions of the glycerol. The central position i.e. sn-2 differs in the chirality from the sn-1 and sn-3 positions. The triacylglycerols are present in plasma membrane and in biological systems. They are constituents of metabolites. In the vegetable oils and fats and animal fats, the triacylglycerols possess specific arrangement of palmitic and linoleic acids in nature. In the plasma membrane and other biological membranes, they are involved in passive diffusion of the substances and drugs across the membrane. They are the source of lipid trafficking and lipolysis. The movement of substances is usually characterized by the diffusion coefficients of the triacylglycerols. The chemical structure of triacylglycerols such as size of the fatty acyl chain and degree of unsaturation are important in the fluidity and viscosity of the plasma membrane. Triacylglycerols with small sized fatty acyl chains and unsaturated fatty acids decrease the viscosity of the membrane and increase its fluidity.

The research work of this thesis is based on the purpose to synthesize triacylglycerols as synthetic standards to measure the diffusion NMR of the triacylglycerols and determine their diffusion coefficients with their average errors of measurements. For this purpose, a number of symmetrical and unsymmetrical triacylglycerols with saturated and unsaturated fatty acids have been synthesized. For symmetrical triacylglycerols synthesis, a reported Hassner esterification methods has been used. The synthesis of unsymmetrical triacylglycerols was achieved in a multistep method from a reported procedure. The fatty acids chosen for this synthesis are palmitic acid, stearic acid, oleic acid, linoleic acid and linolenic acid. The two-small sized triacylglycerols were also used i.e. trioctanoic acid and trilaureic acid. The palmitic and linoleic acids are the most common fatty acids present in most of the natural foods. Linoleic acids and linolenic acids are the main components of the biological membranes. The fish and meat contain some smaller sized triacylglycerols which are thought to be beneficial to reduce the harmful effects of trans fatty acids in them. The synthesis of triacylglycerols with these fatty acids can be useful in the study of passive movements across the biological membranes, the food quality and drug transport inside the cells.

The diffusion coefficients show a variation from saturated to unsaturated fatty acyl chains and from high molecular weight to smaller molecular weight. It has been observed that the monounsaturated triacylglycerols have higher diffusion coefficients than the diunsaturated and saturated triacylglycerols. This explores the mystery about the folded structure of monounsaturated triacylglycerols. this shows that the unsaturated triacylglycerols have a bent structure. This is suggested that the di unsaturated triacylglycerols have restricted or rigid structure due to the presence of a greater number of double bonds. The saturated triacylglycerols with high molecular weight diffuse faster and show higher diffusion coefficients than the smaller molecular weight triacylglycerols. This

suggests that the large sized saturated triacylglycerols have less Vander Waals interactions in their structure than the small sized. The smaller sized triacylglycerols i.e. trioctanein and trilaurein show a much higher diffusion coefficient. This gives an idea that the smaller sized triacylglycerols are folded inside their structure to produce more diffusibility. These studies of diffusion coefficients are very important as these can further explore the kinetics and stereochemical aspects involved in natural phenomenon in living organisms such as change in phase behavior of the plasma membrane and balance of lipolysis and lipid signaling. The parameters can be determined to cure the genetic diseases, diabetics and cardiovascular diseases associated with the incorrect triacylglycerols composition in the living organisms.

Furthermore, the absolute quantification of triacylglycerols have been performed with 8-point calibration curves. The calibration curves were plotted from the peak area of the chromatogram and the concentration of the analyte sample. The statistical regression analysis with ANOVA was done to check the linearity of the regression, residual standard deviation (RSD) and trends of variation from the residual plots. The intercept is negative in the calibration curves. In the calibration curve, the intercept was not forced set to zero. The negative intercept shows that the low concentration of the triacylglycerols can produce response with UV-detector. In the regression analysis, the intercept is negative mathematically when the sub x is not equal to zero. The slope and intercept have reverse relation to each other. the negative intercept also predicts that the triacylglycerols show a matrix effect in the HPLC analysis.

These studies of triacylglycerols can be useful in drug chemistry. The chemical structure of drugs is designed as such that its diffusion coefficient is suitable to cross the plasma membrane of the cell. The regioisomeric arrangement of fatty acids in triacylglycerol can be specified by 2D NOESY and 2D ROESY. This is useful to identify the triacylglycerols composition of complex mixtures from natural foods. The statistaical analysis of synthetic triacylglycerols can be further extended to develop new analytical methods.

Supplementary information

Chapter 2

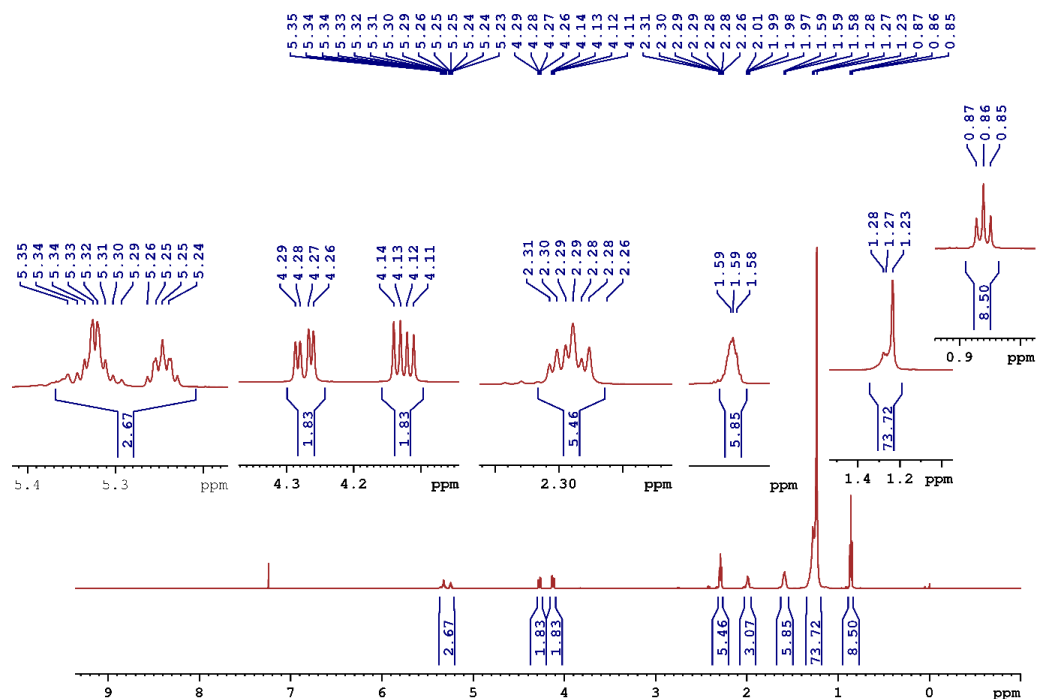
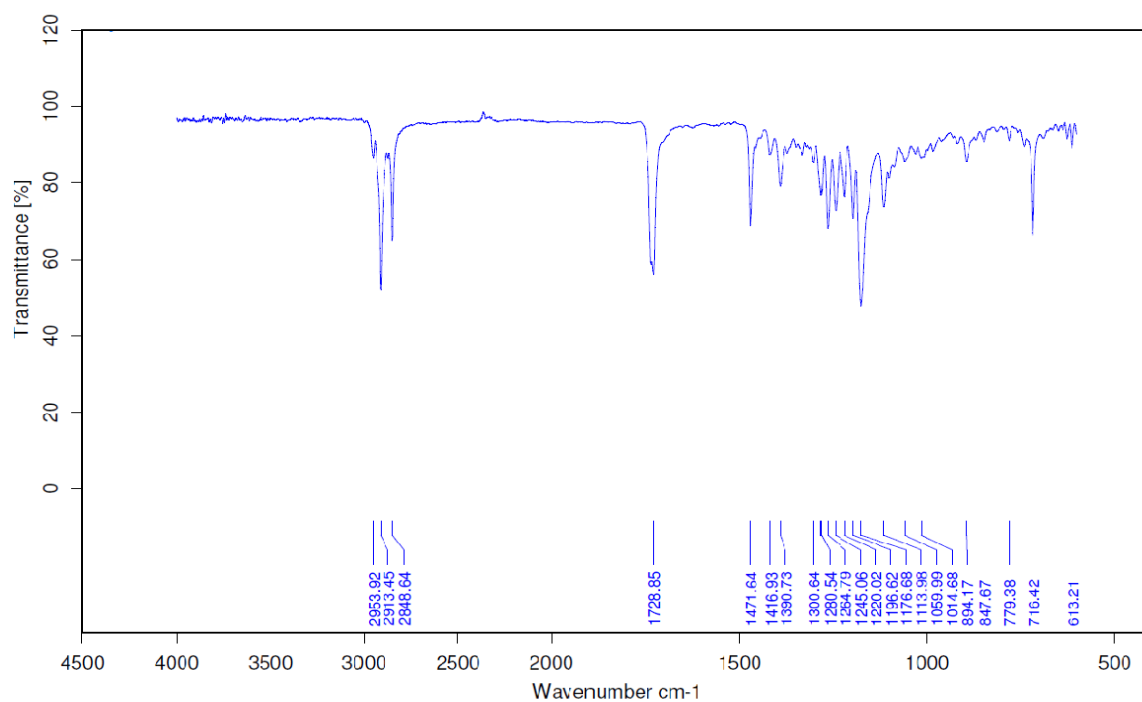
Figure 1. ¹H-NMR (600 MHz, CDCl₃) spectrum of 1,2,3-tripalmitoyl glycerol [Tripalmitin (PPP-Isomer)]

Figure 2. IR spectrum of 1,2,3-tripalmitoyl glycerol [Tripalmitin PPP] (1)

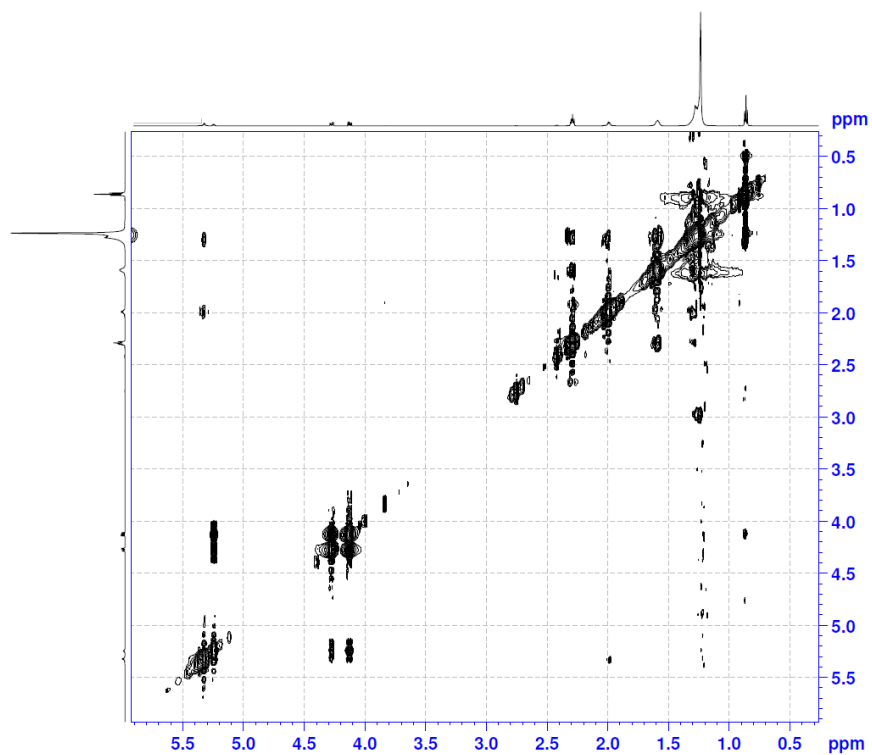


Figure 3. 2D NOESY of Isomer of 1,2,3-tripalmitoyl glycerol [Tripalmitin PPP-Isomer] (1)

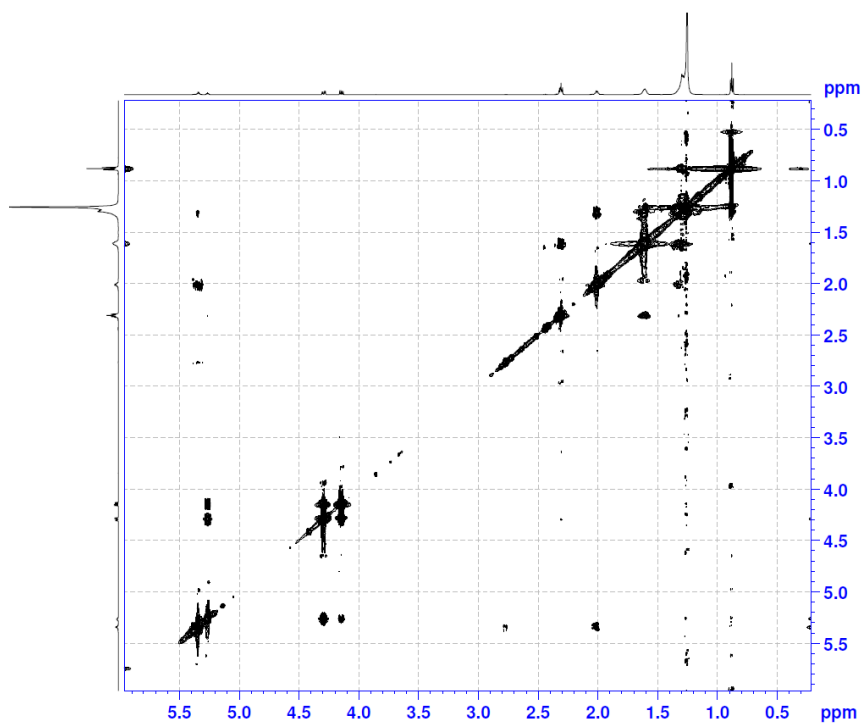


Figure 4. 2D ROESY of Isomer of 1,2,3-tripalmitoyl glycerol [Tripalmitin PPP-Isomer] (1)

Chemical structure: 1,2,3-Tristearoyl glycerol [Tristearin (SSS)]

¹³C NMR spectrum (CDCl₃) showing chemical shifts (ppm):

- Carbonyl region (172-174 ppm): 172.29, 171.87
- Alkyl chain region (28-34 ppm): 28.70, 28.66, 28.62, 28.50, 28.48, 28.36, 28.29, 28.27, 28.11, 28.07, 33.21, 33.04
- Methyl region (-24 to -22 ppm): 23.90, 23.85

Full spectrum (0-220 ppm) and zoomed-in regions are shown.

135

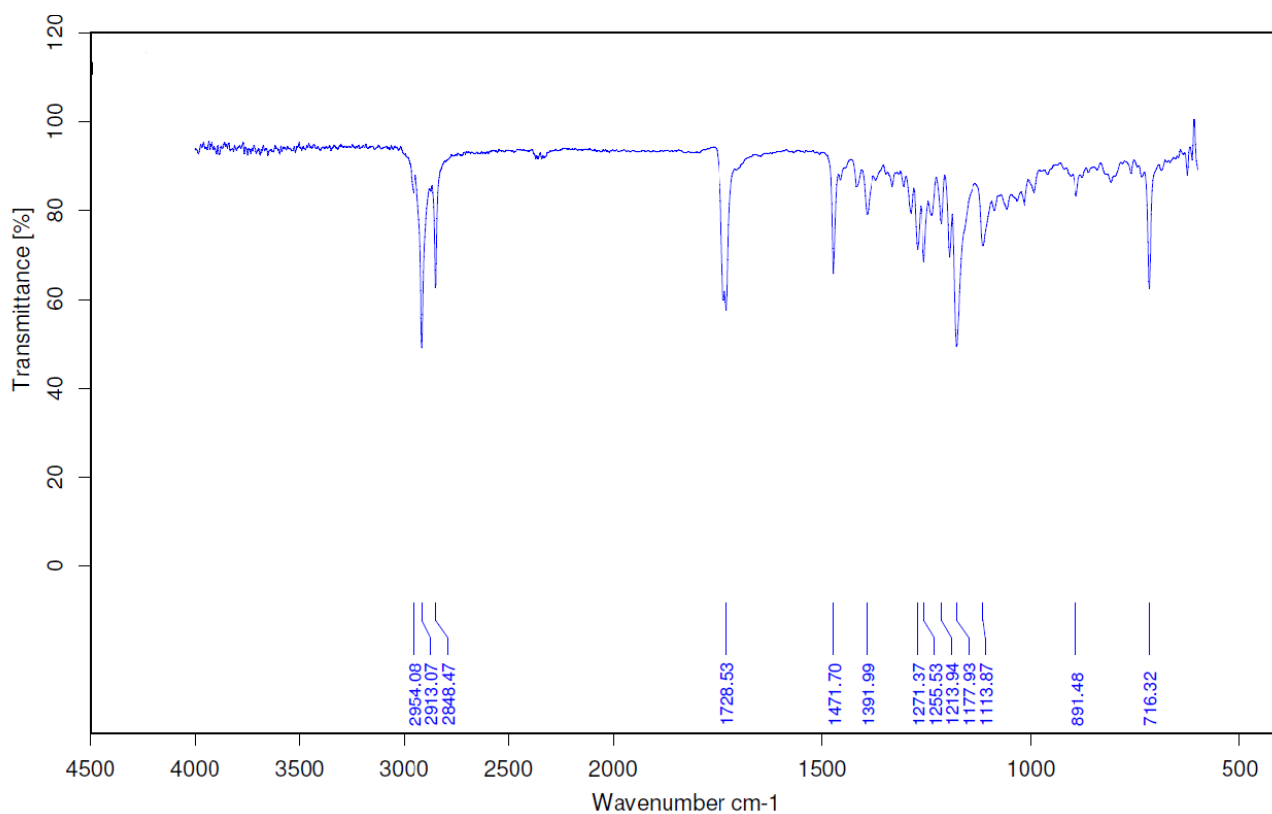


Figure 7. IR spectrum of 1,2,3-tristearoyl glycerol [Tristearin SSS] (2)

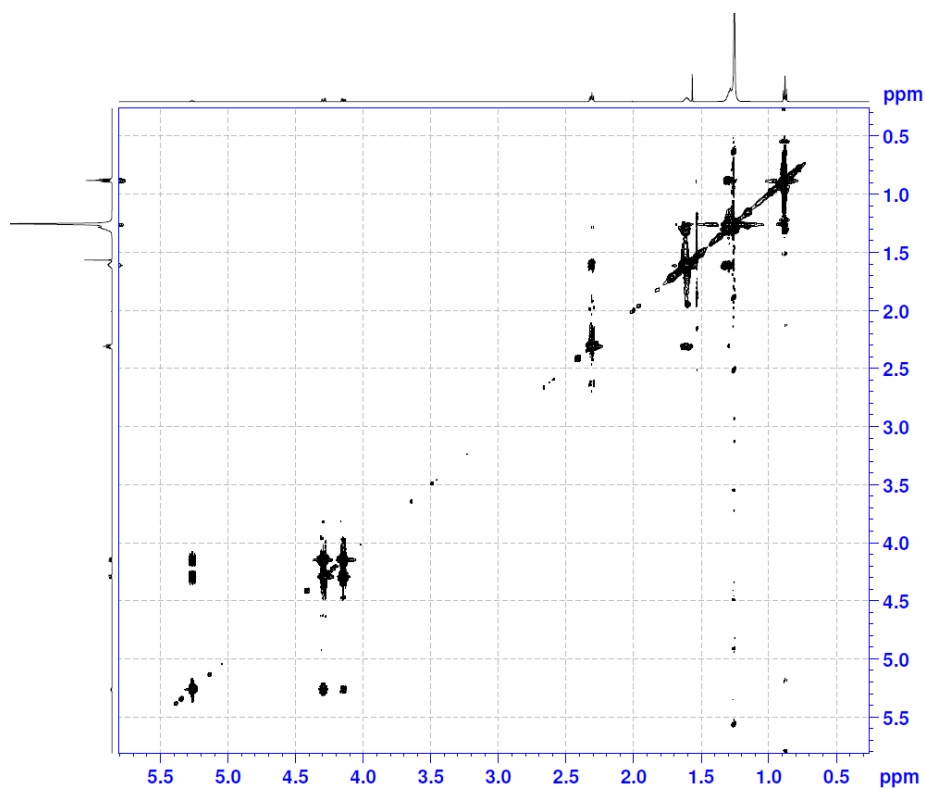


Figure 8. 2D ROESY of 1,2,3-tristearoyl glycerol [Tristearin SSS] (2)

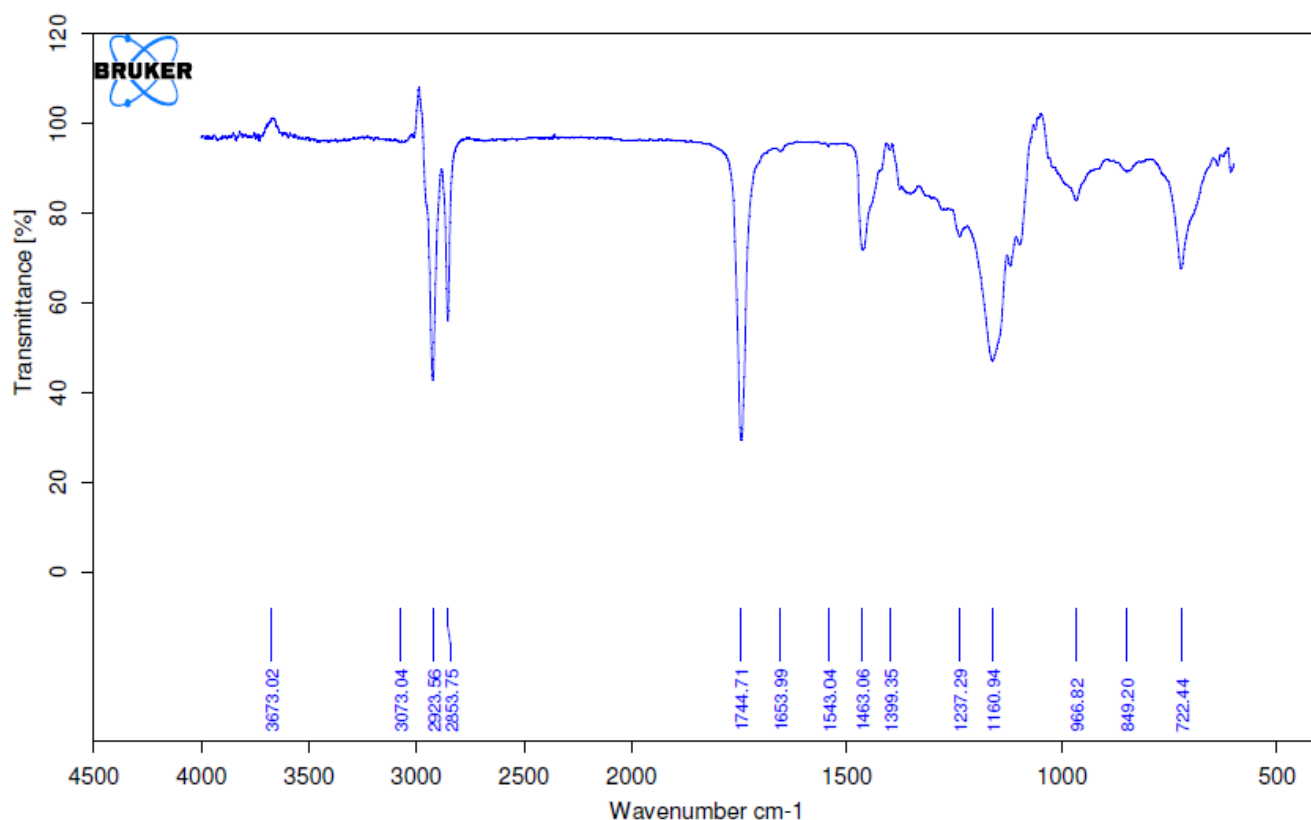
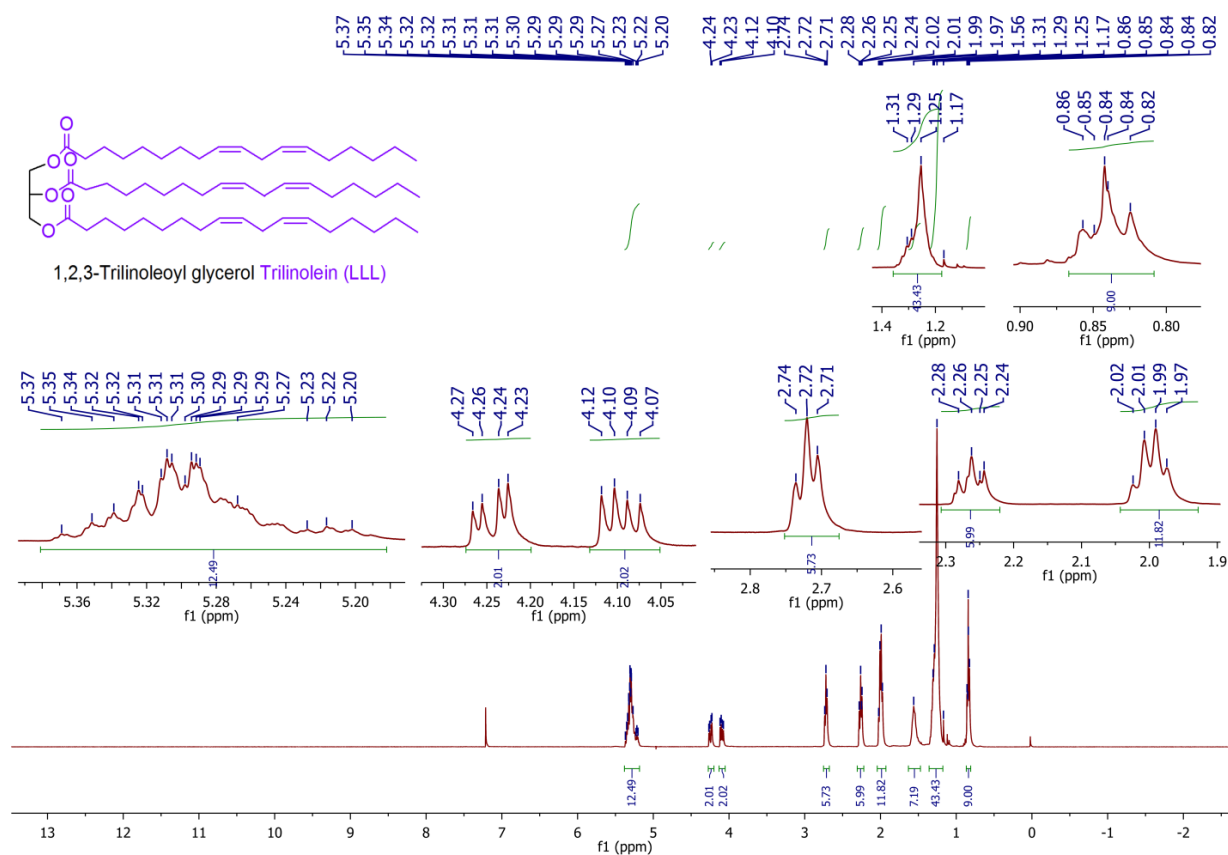


Figure 9. IR spectrum of 1,2,3-Trioleoyl glycerol [Triolein OOO] (3)

Figure 10. ^1H -NMR (600 MHz, CDCl_3) spectrum of 1,2,3-Trilinoleoyl glycerol [Trilinolein LLL] (4)

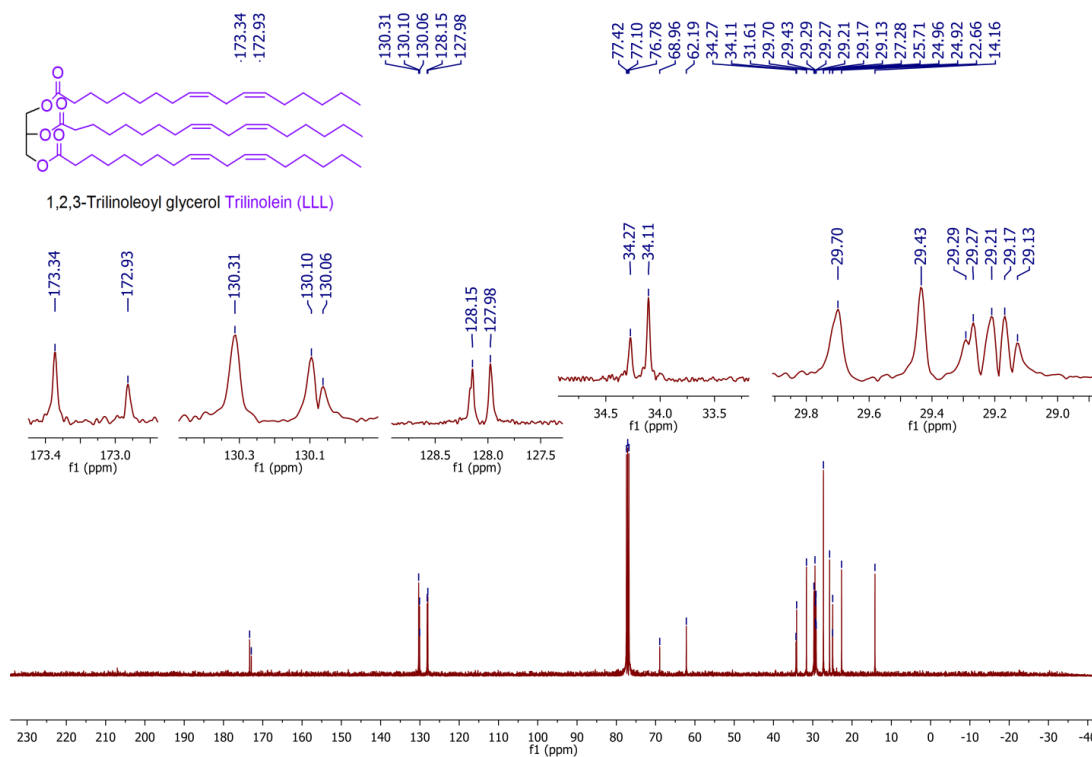


Figure 11. ^{13}C -NMR (100 MHz, CDCl_3) spectrum of 1,2,3-Trilinoeoyl glycerol [Trilinolein LLL] (4)

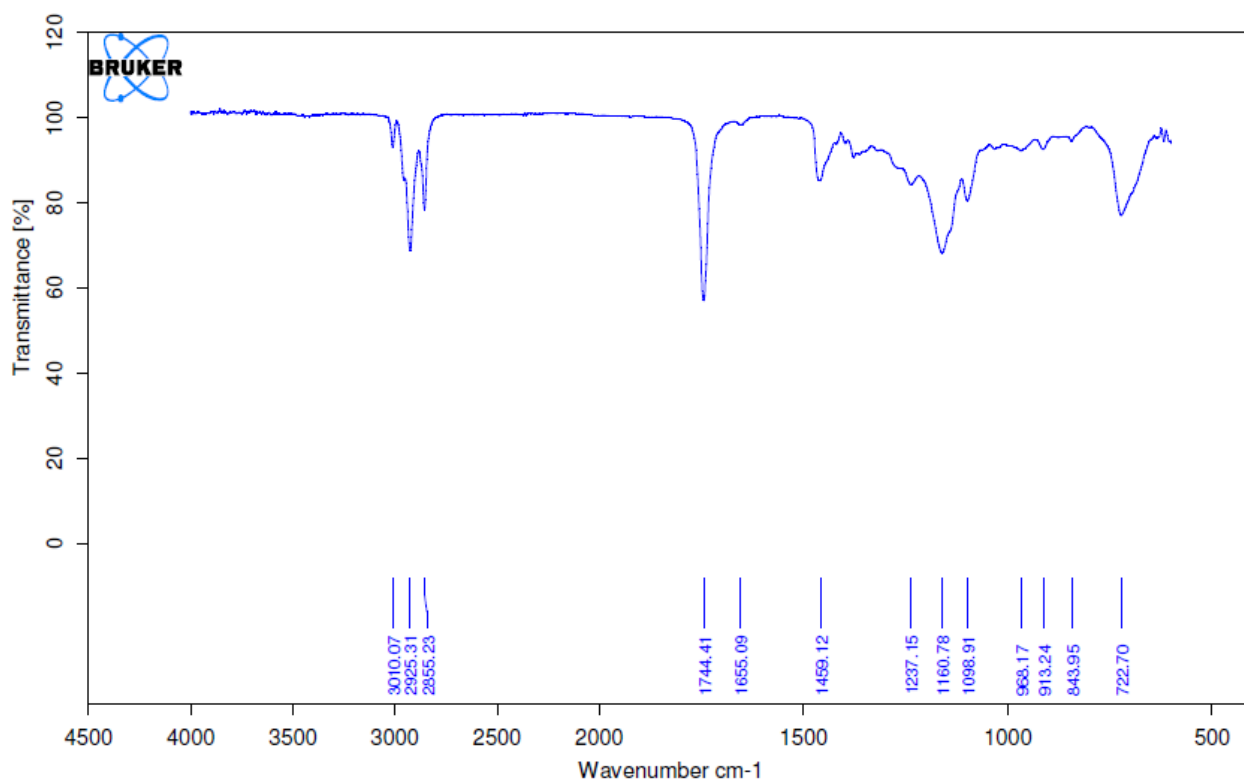


Figure 12. IR spectrum of 1,2,3-Trilinoeoyl glycerol [Trilinolein LLL] (4)

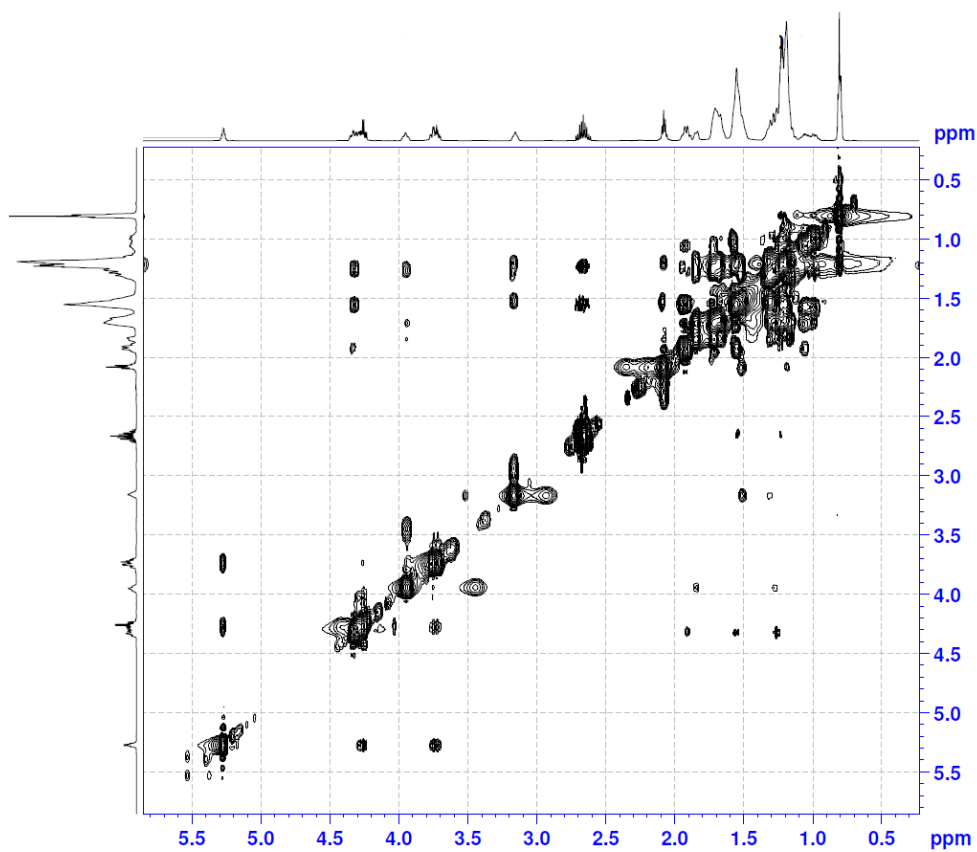


Figure 13. 2D NEOSY of 1,2,3-Trioctanoyl glycerol [Trioctanein OcOcOc] (5)

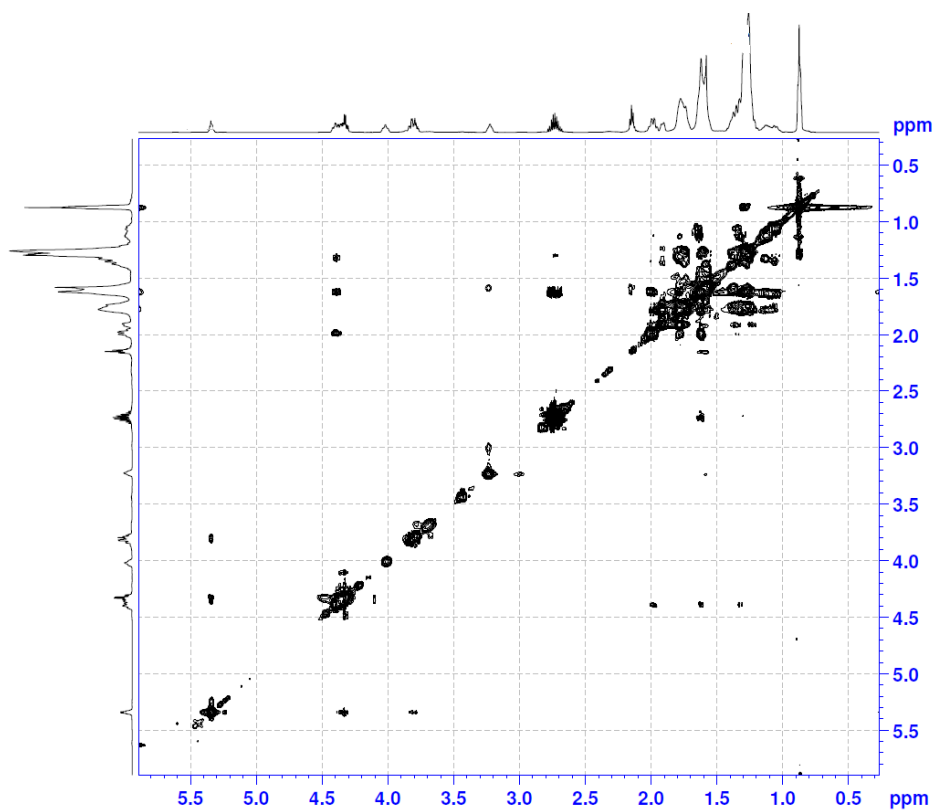
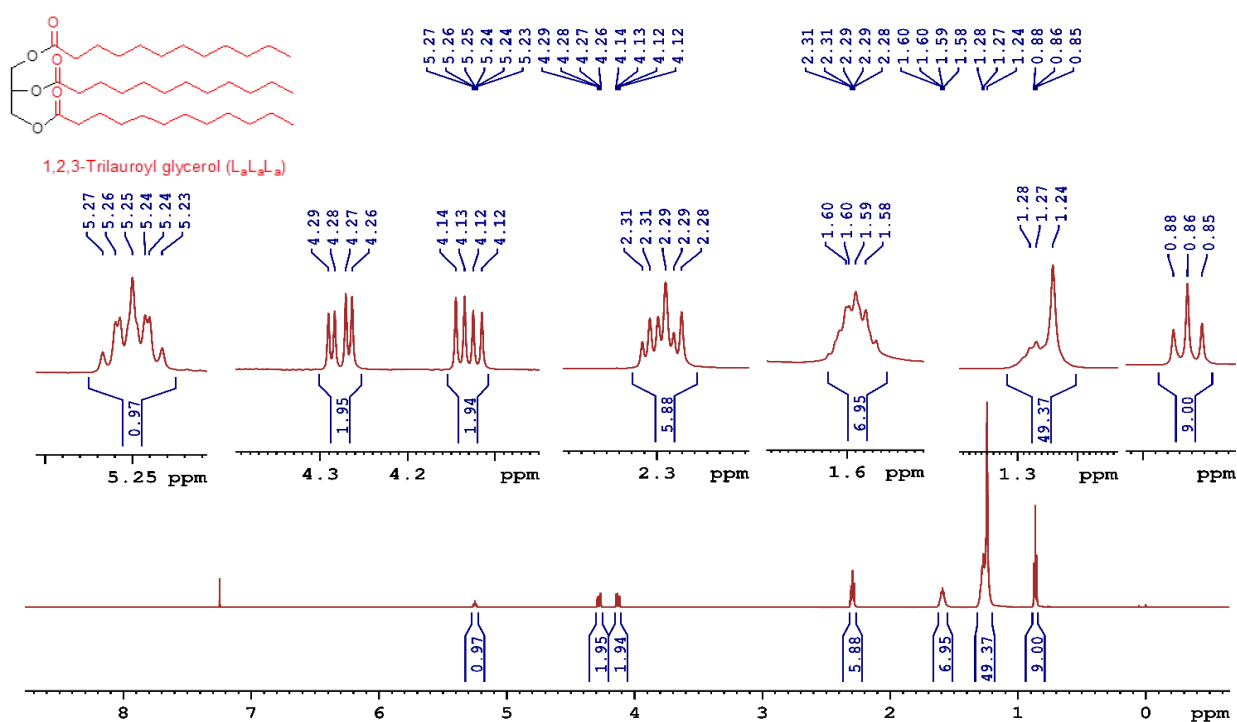
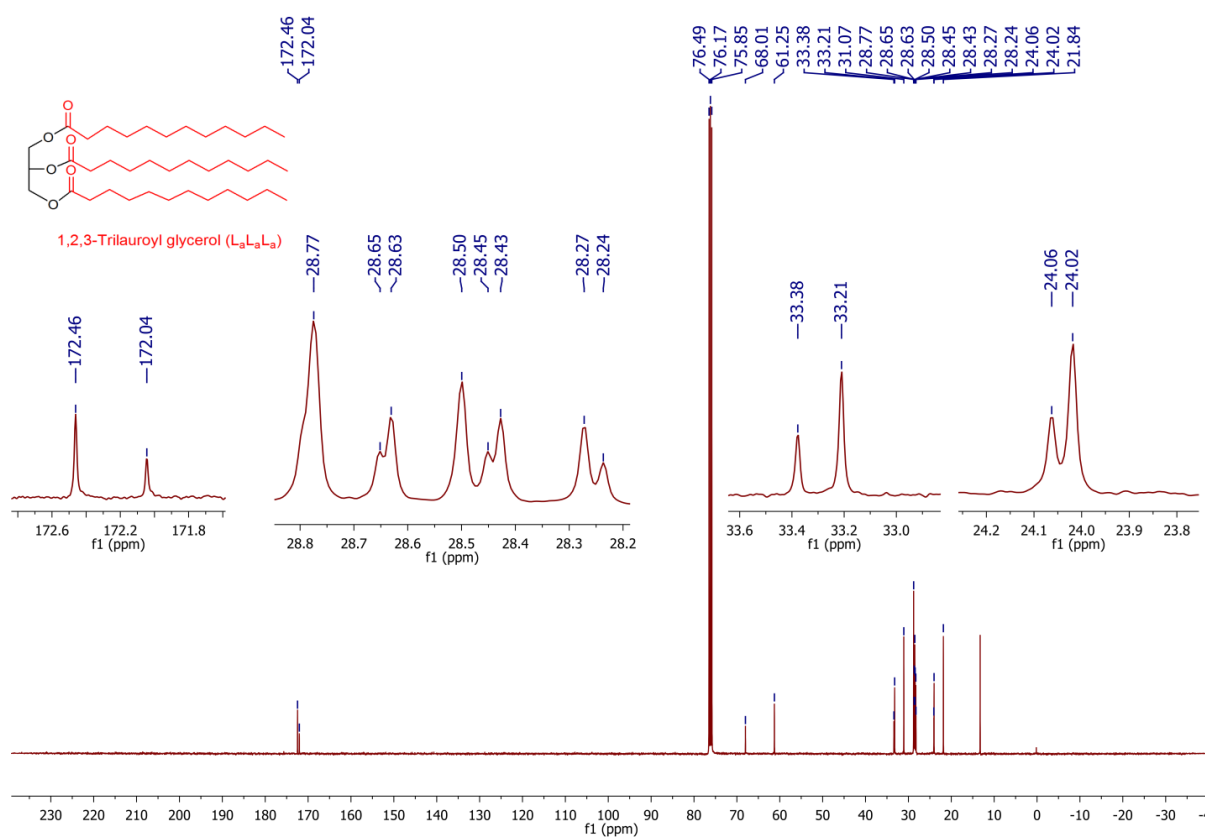


Figure 14. 2D ROESY of 1,2,3-Trioctanoyl glycerol [Trioctanein OcOcOc] (5)

Figure 15. ^1H -NMR (600 MHz, CDCl_3) spectrum of 1,2,3- Trilauroyl glycerol [Trilaurein $L_\alpha L_\alpha L_\alpha$] (6)Figure 16. ^{13}C -NMR (100 MHz, CDCl_3) spectrum of 1,2,3-Trilauroyl glycerol [Trilaurein $L_\alpha L_\alpha L_\alpha$] (6)

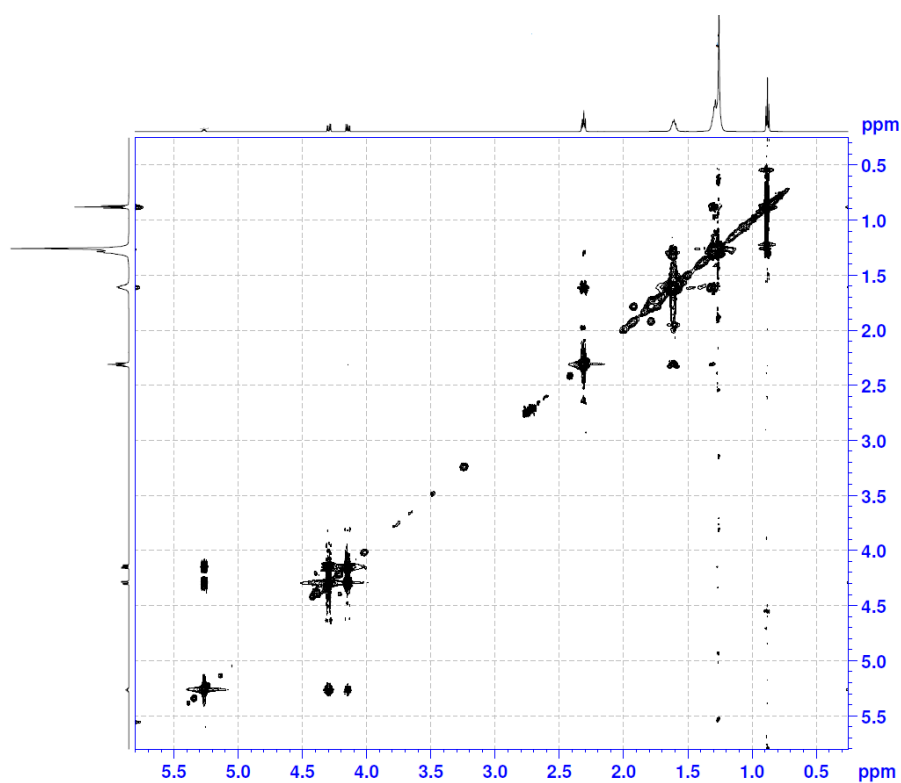
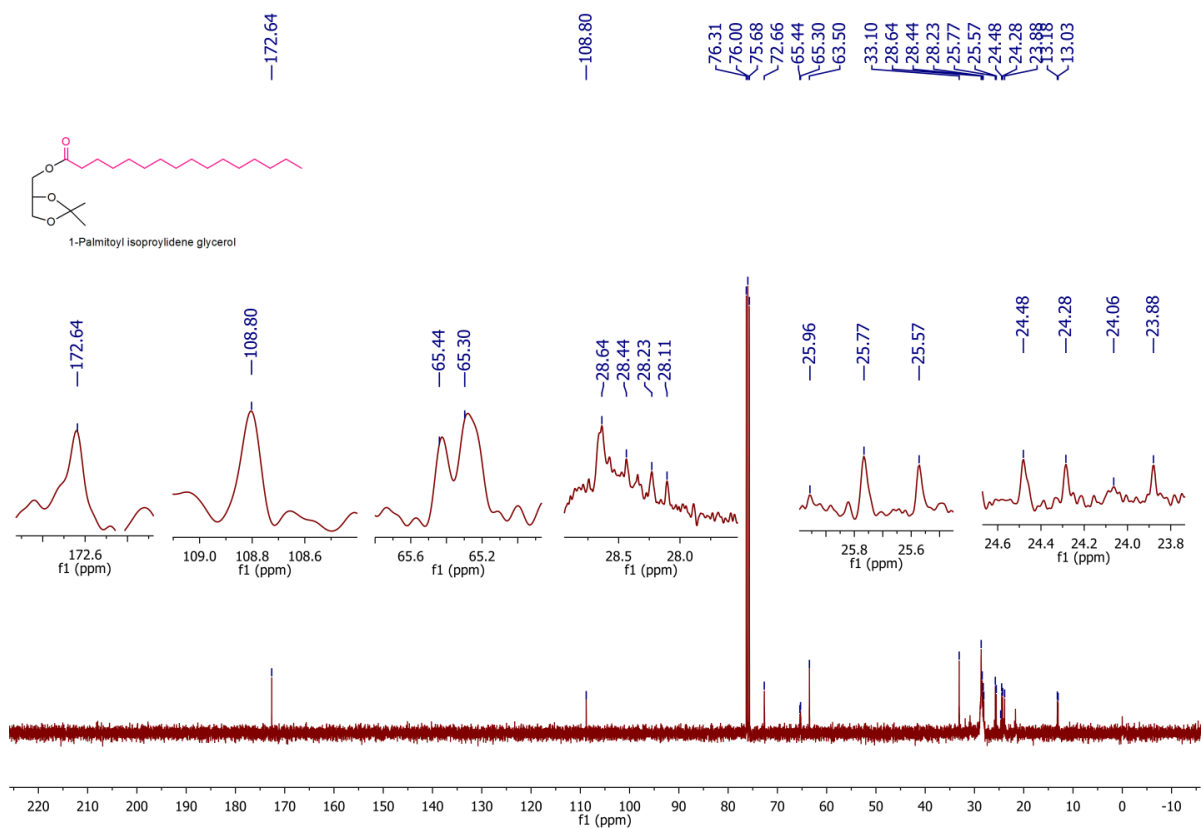


Figure 17. 2D ROESY of 1,2,3-Trilauroyl glycerol [Trilaurein LaLaLa] (6)

Figure 18. ^{13}C -NMR (100 MHz, CDCl_3) spectrum of 1-Palmitoyl isopropylidene glycerol (7)

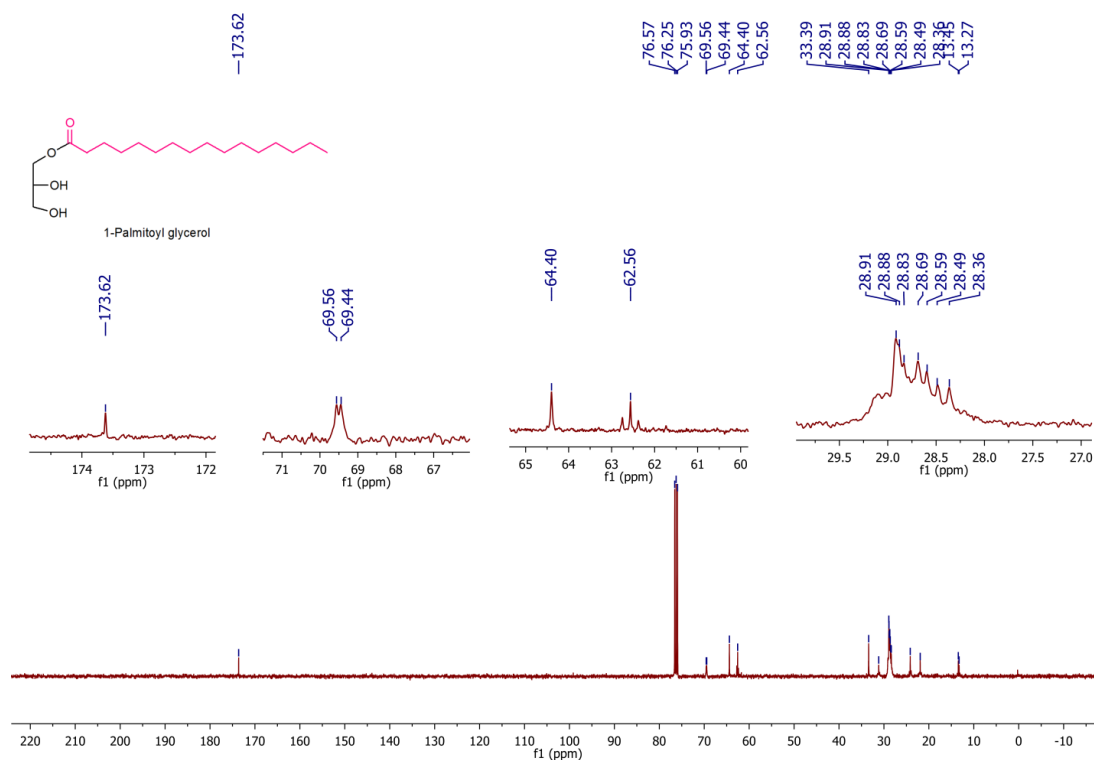


Figure 19. ^{13}C -NMR (100 MHz, CDCl_3) spectrum of 1-Palmitoyl glycerol (8)

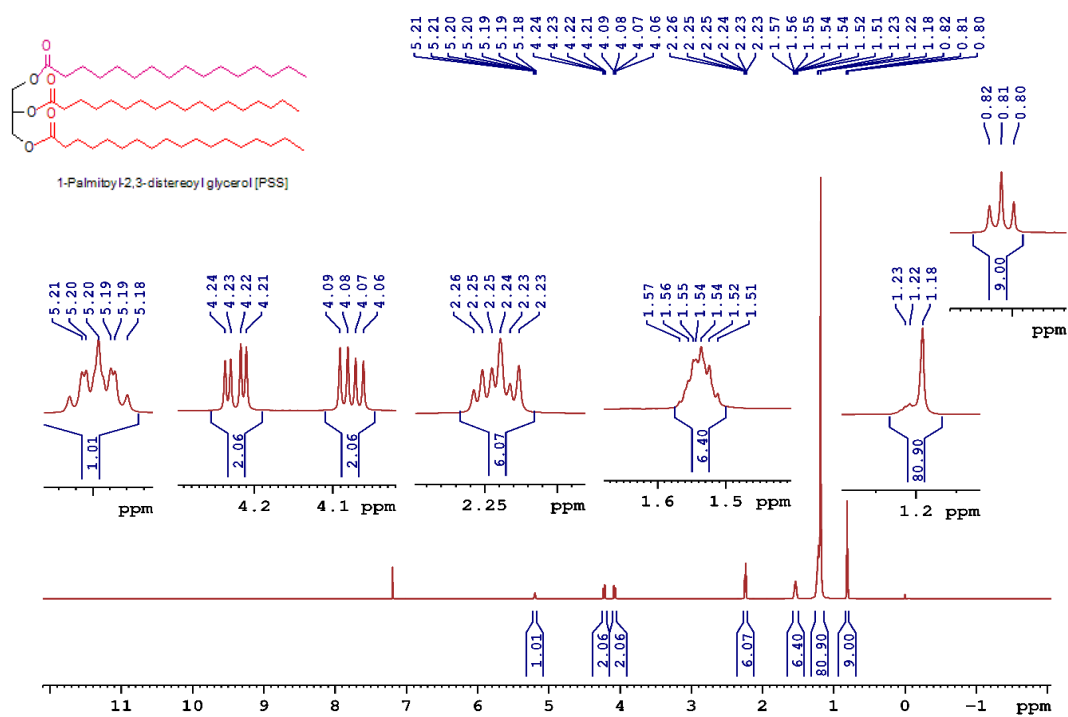
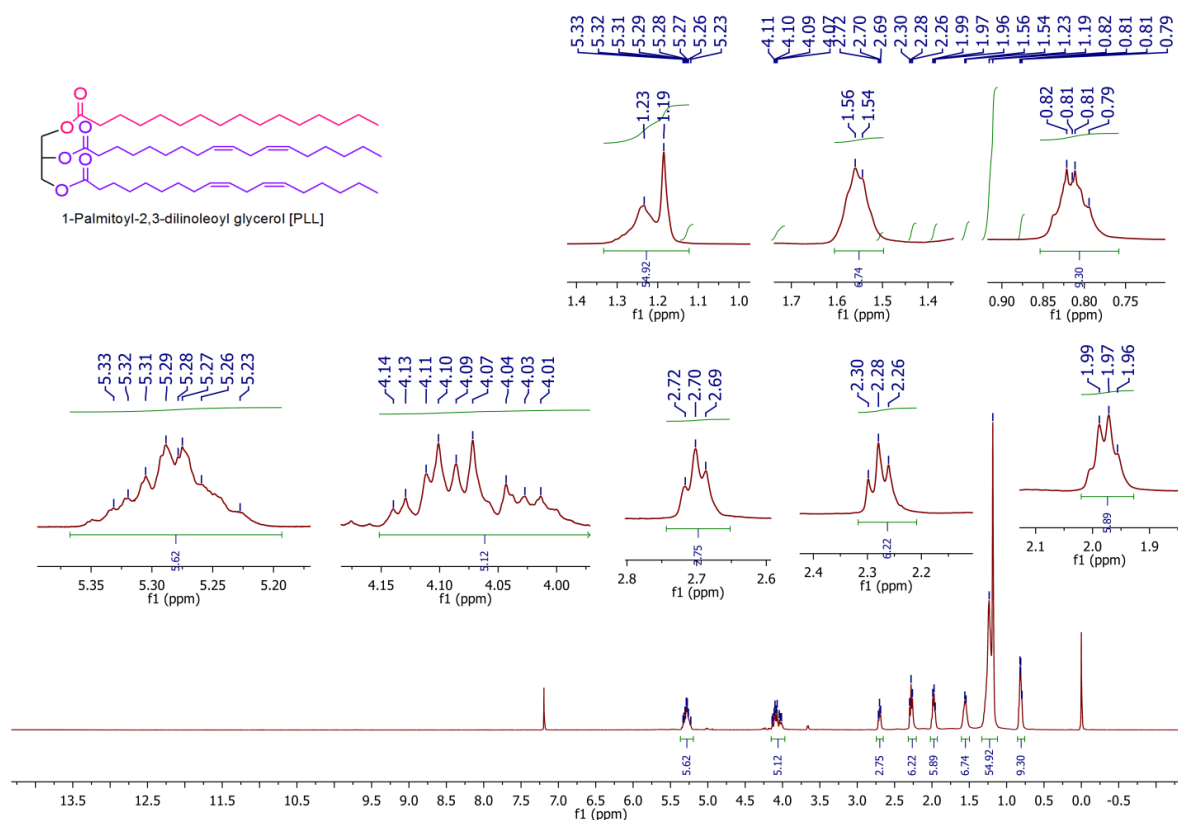
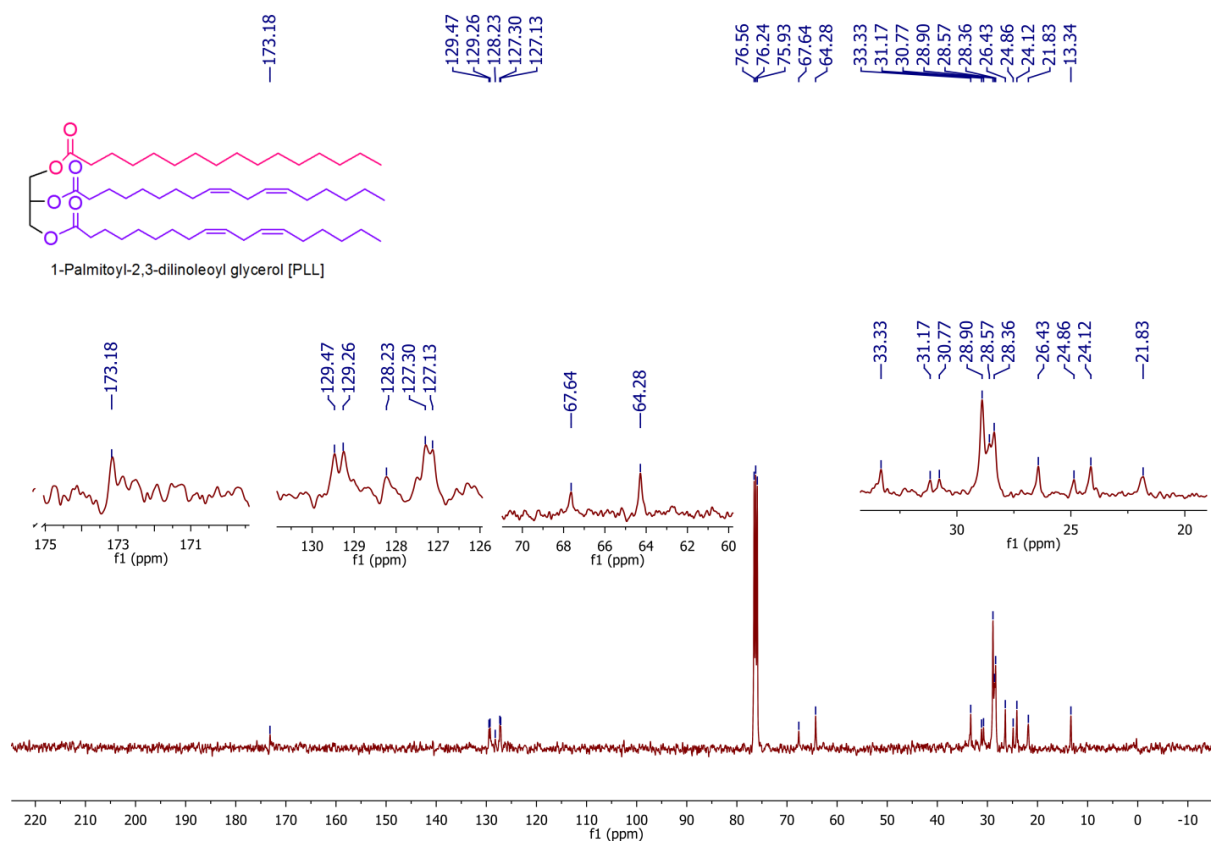
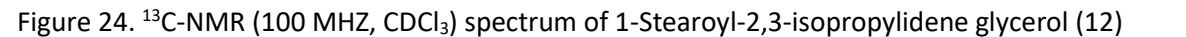
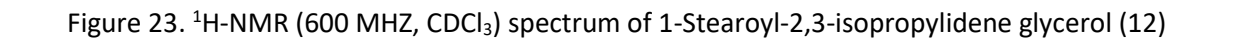
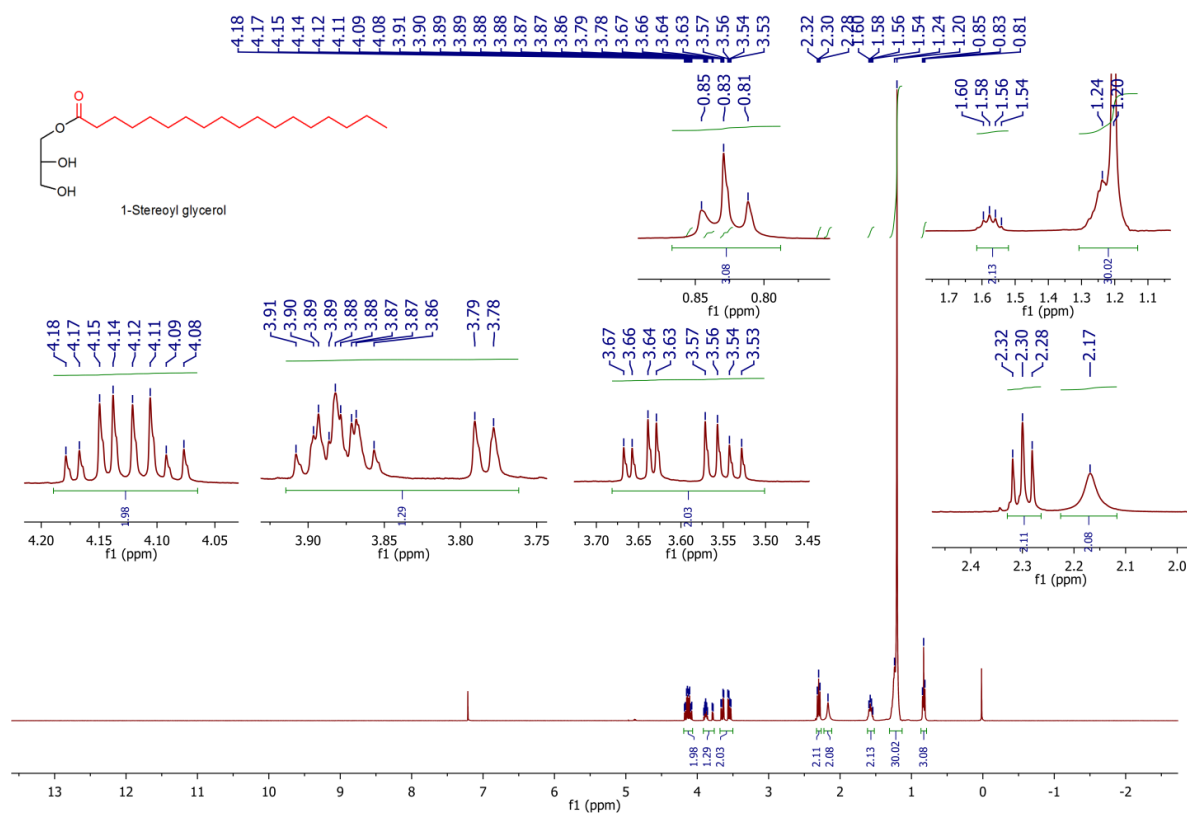
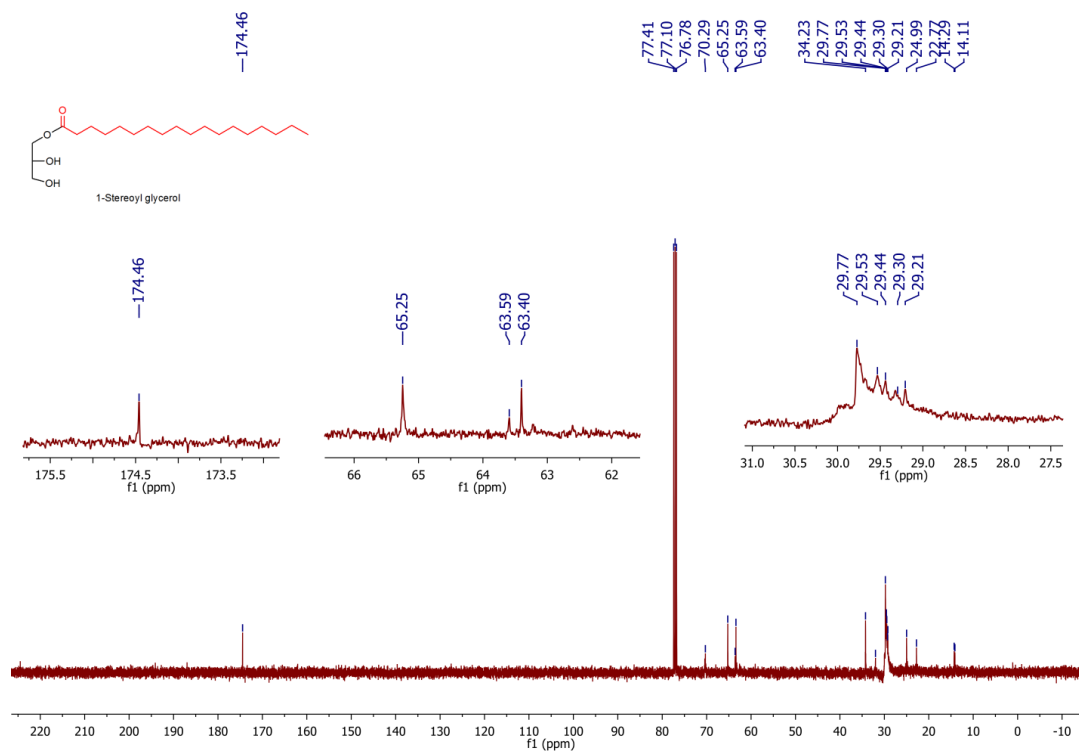
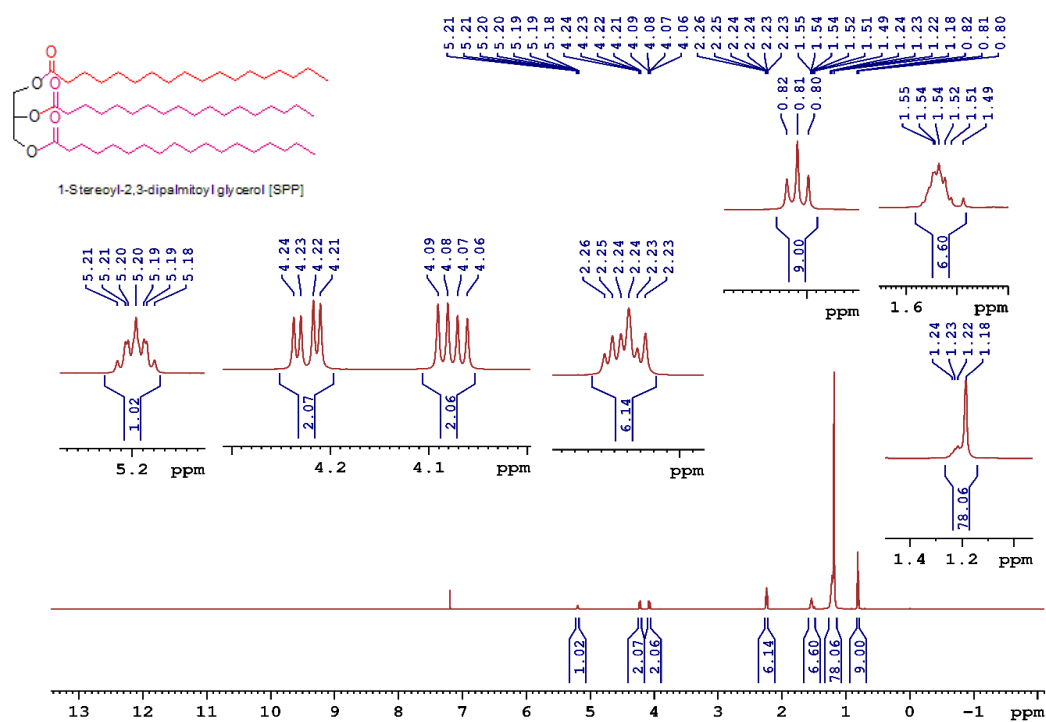
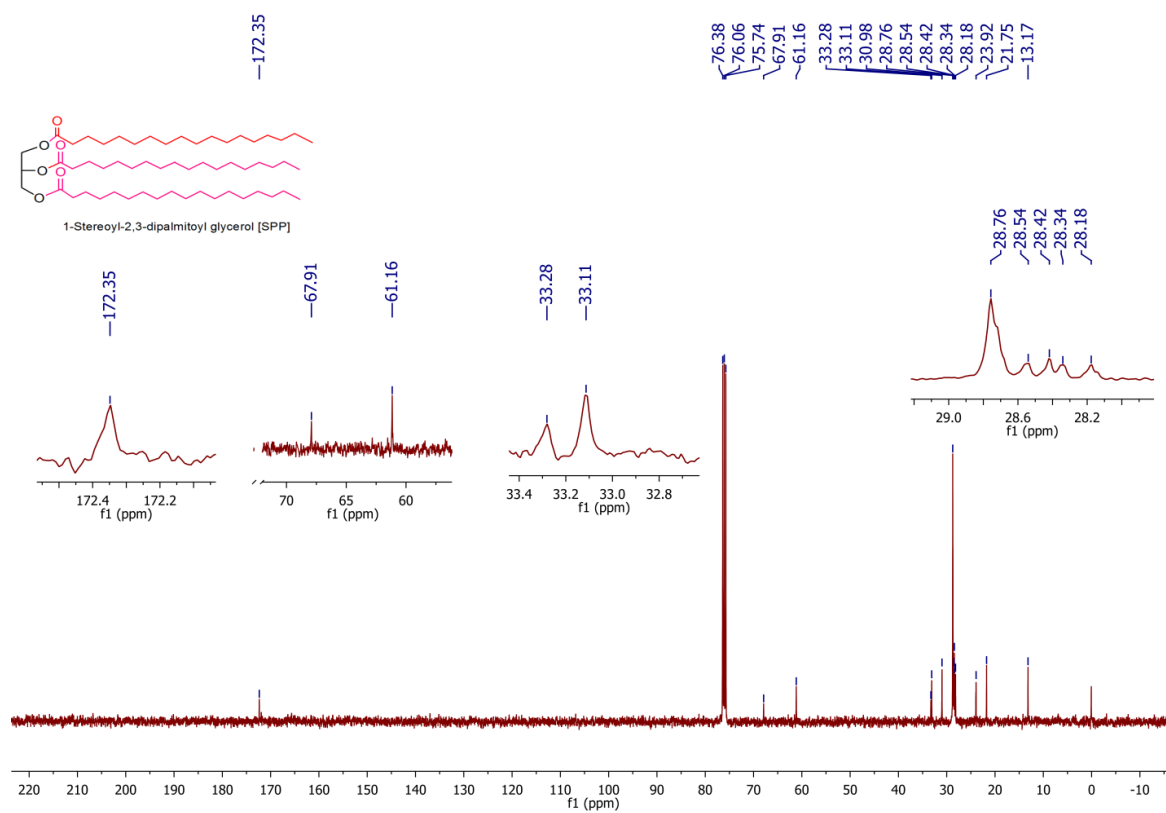


Figure 20. ^1H -NMR (600 MHz, CDCl_3) spectrum of 1-Palmitoyl-2, 3-distereoyl glycerol [PSS] (10)

Figure 21. ^1H -NMR (600 MHz, CDCl_3) spectrum of 1-Palmitoyl-2, 3-dilinoleoyl glycerol [PLL] (11)Figure 22. ^{13}C -NMR (100 MHz, CDCl_3) spectrum of 1-Palmitoyl-2, 3-dilinoleoyl glycerol [PLL] (11)



Figure 25. ¹H-NMR (600 MHz, CDCl₃) spectrum of 1-Stearoyl glycerol (13)Figure 26. ¹³C-NMR (100 MHz, CDCl₃) spectrum of 1-Stearoyl glycerol (13)

Figure 27. ^1H -NMR (600 MHz, CDCl_3) spectrum of 1-Stereoyl-2, 3-palmitoyl glycerol [SPP] (14 a)Figure 28. ^{13}C -NMR (100 MHz, CDCl_3) spectrum of 1-Stereoyl-2, 3-palmitoyl glycerol [SPP] (14 a)

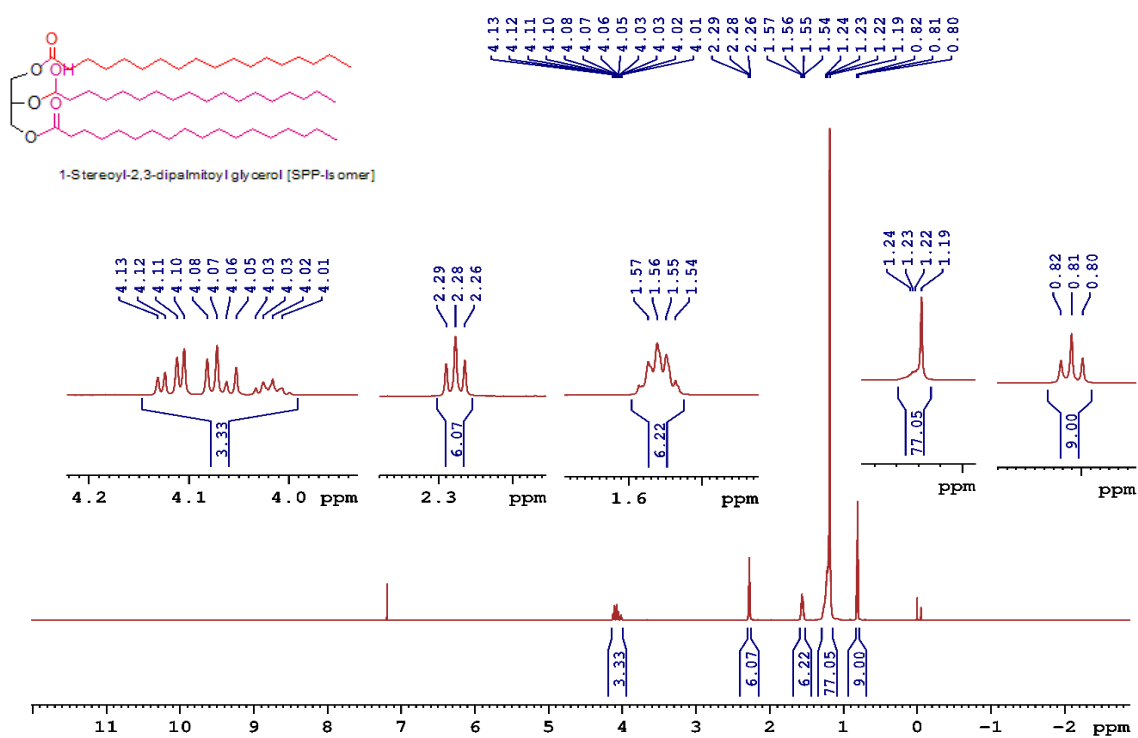


Figure 29. ^1H -NMR (600 MHz, CDCl_3) spectrum of 1-Stereoyl-2, 3-palmitoyl glycerol [SPP-ISOMER] (14 b)

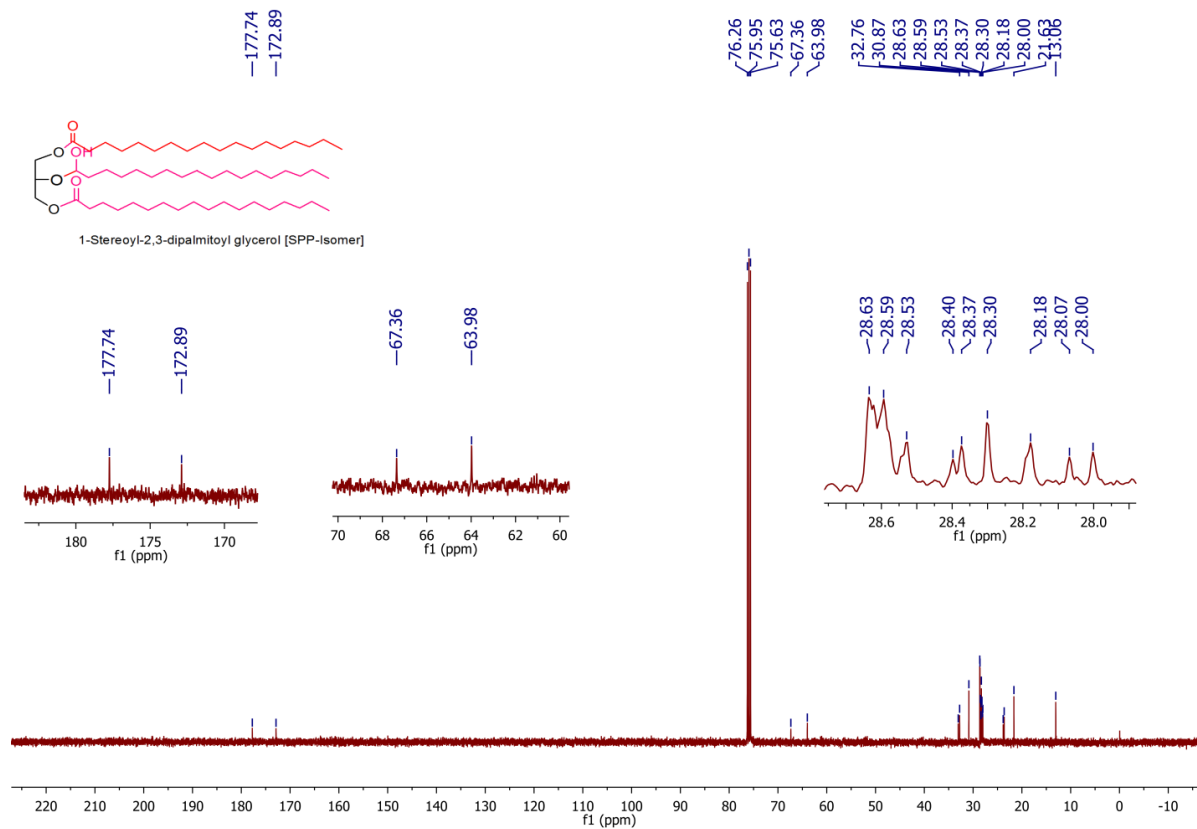


Figure 30. ^{13}C -NMR (100 MHz, CDCl_3) spectrum of 1-Stereoyl-2, 3-palmitoyl glycerol [SPP-ISOMER] (14 b)

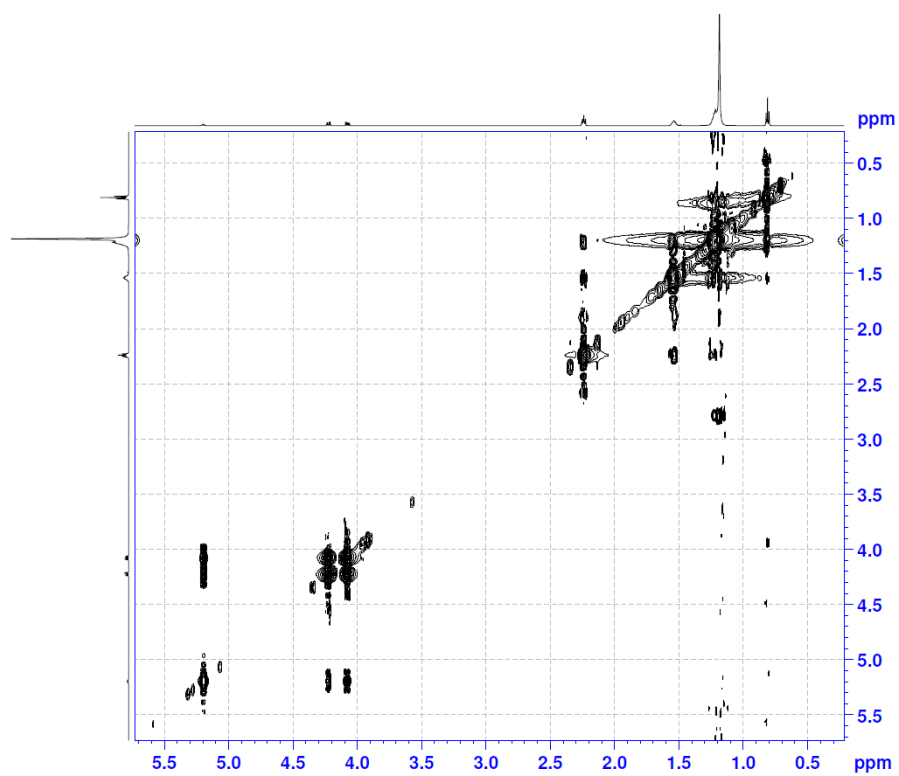


Figure 31. 2D NOESY of 1-Stereoyl-2, 3-palmitoyl glycerol [SPP] (14 a)

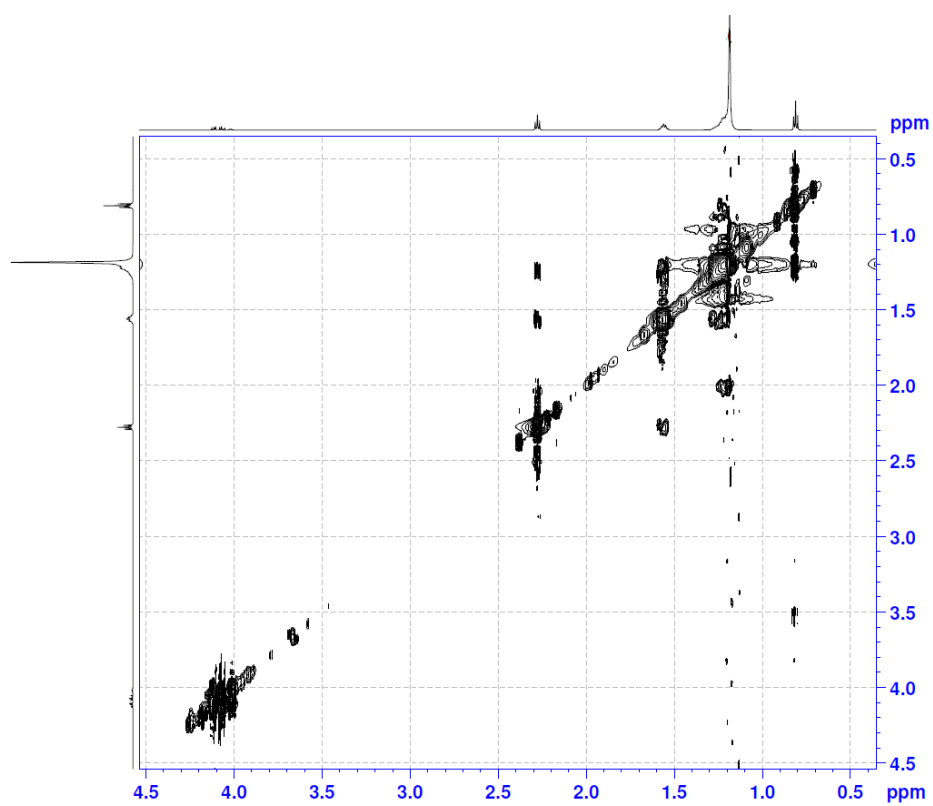


Figure 32. 2D NOESY of Isomer of 1-Stereoyl-2, 3-palmitoyl glycerol [SPP-ISOMER] (14 b)

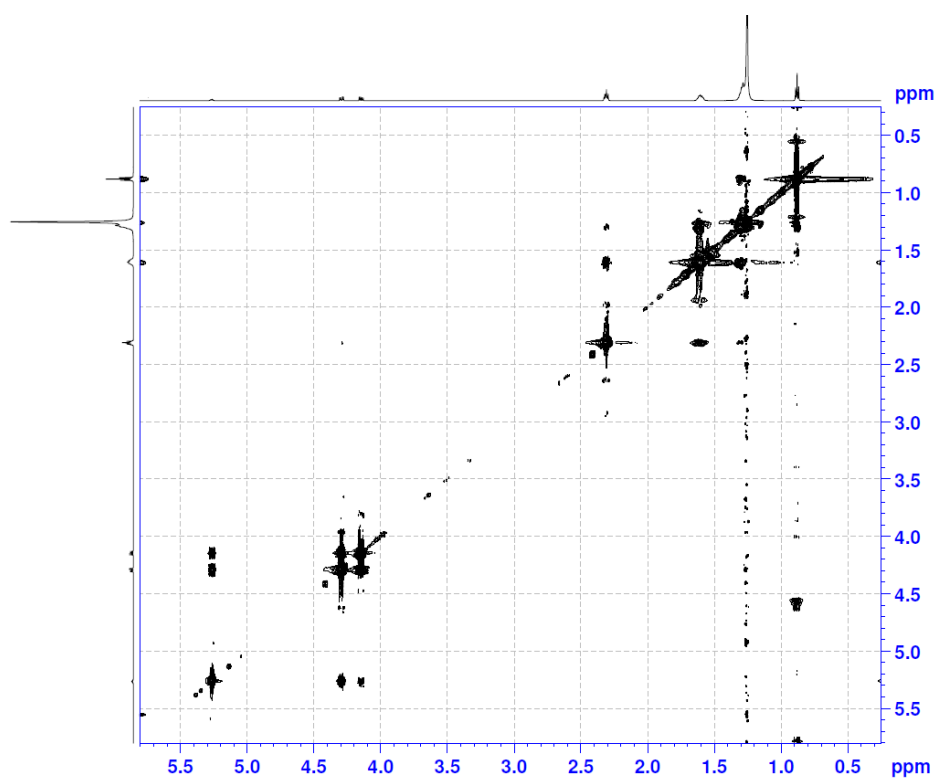


Figure 33. 2D ROESY of 1-Stereoyl-2, 3-palmitoyl glycerol [SPP] (14 a)

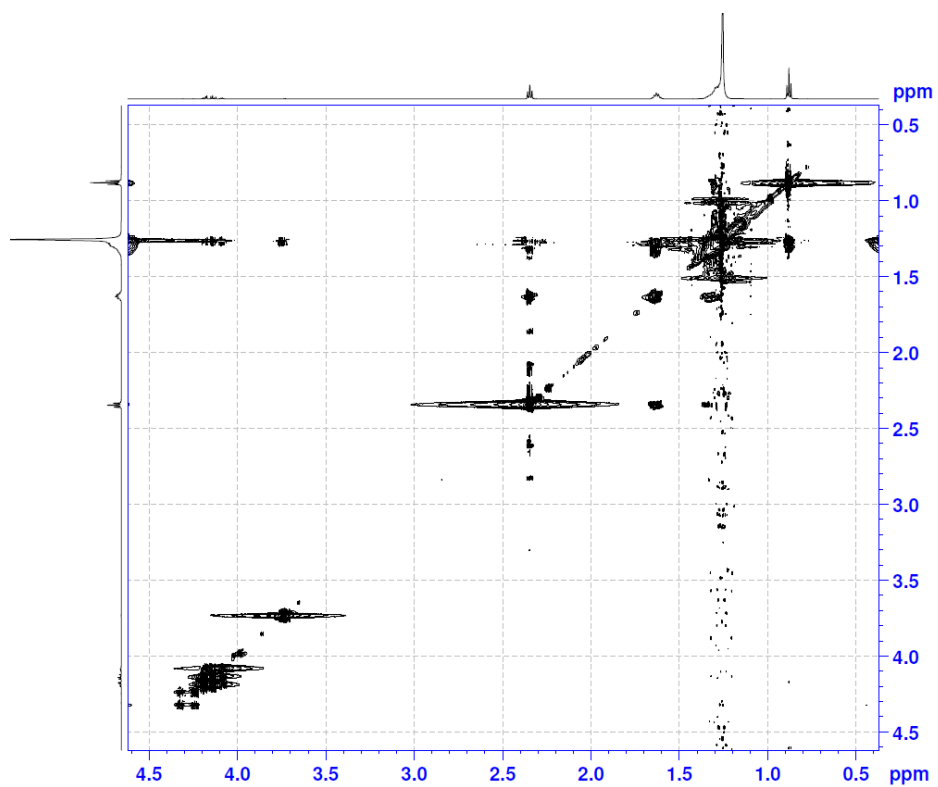


Figure 34. 2D ROESY of Isomer of 1-Stereoyl-2, 3-palmitoyl glycerol [SPP-ISOMER] (14 b)

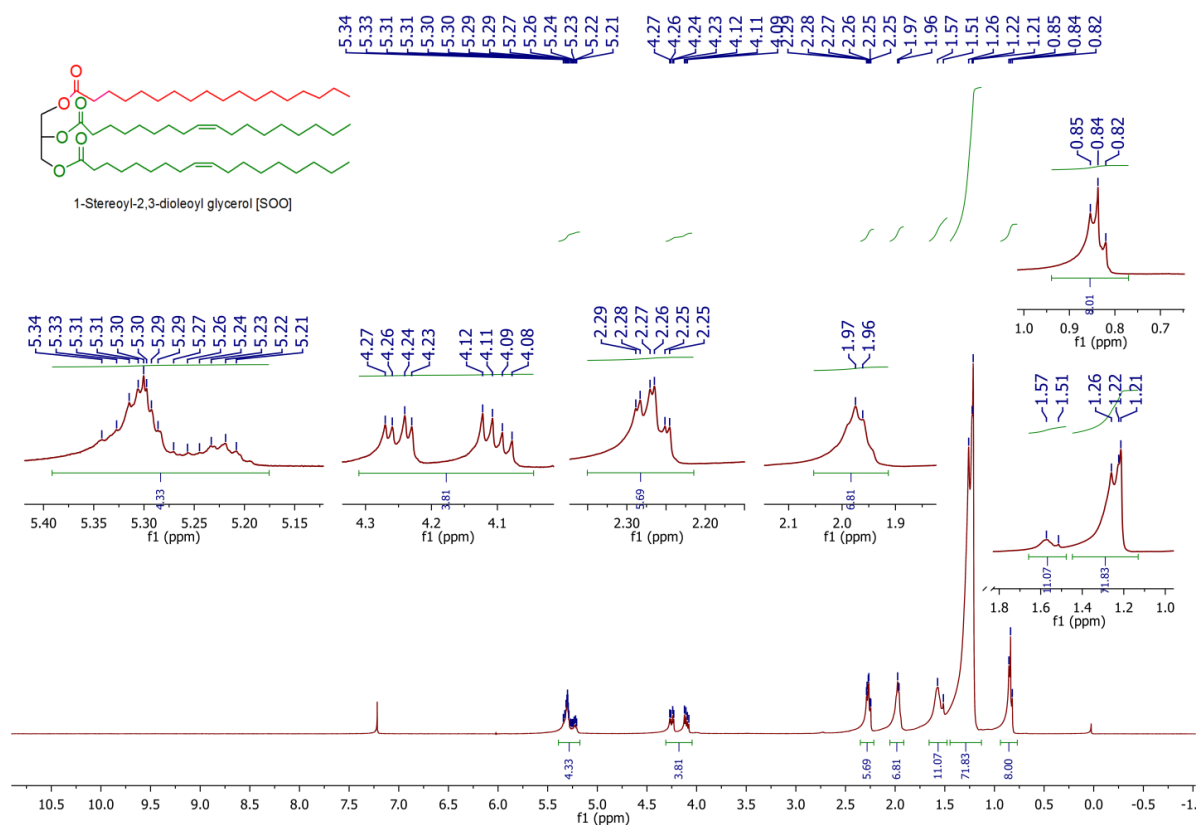


Figure 35. ¹H-NMR (600 MHz, CDCl₃) spectrum of 1-Stereoyl-2,3-oleoyl glycerol [SOO] (15)

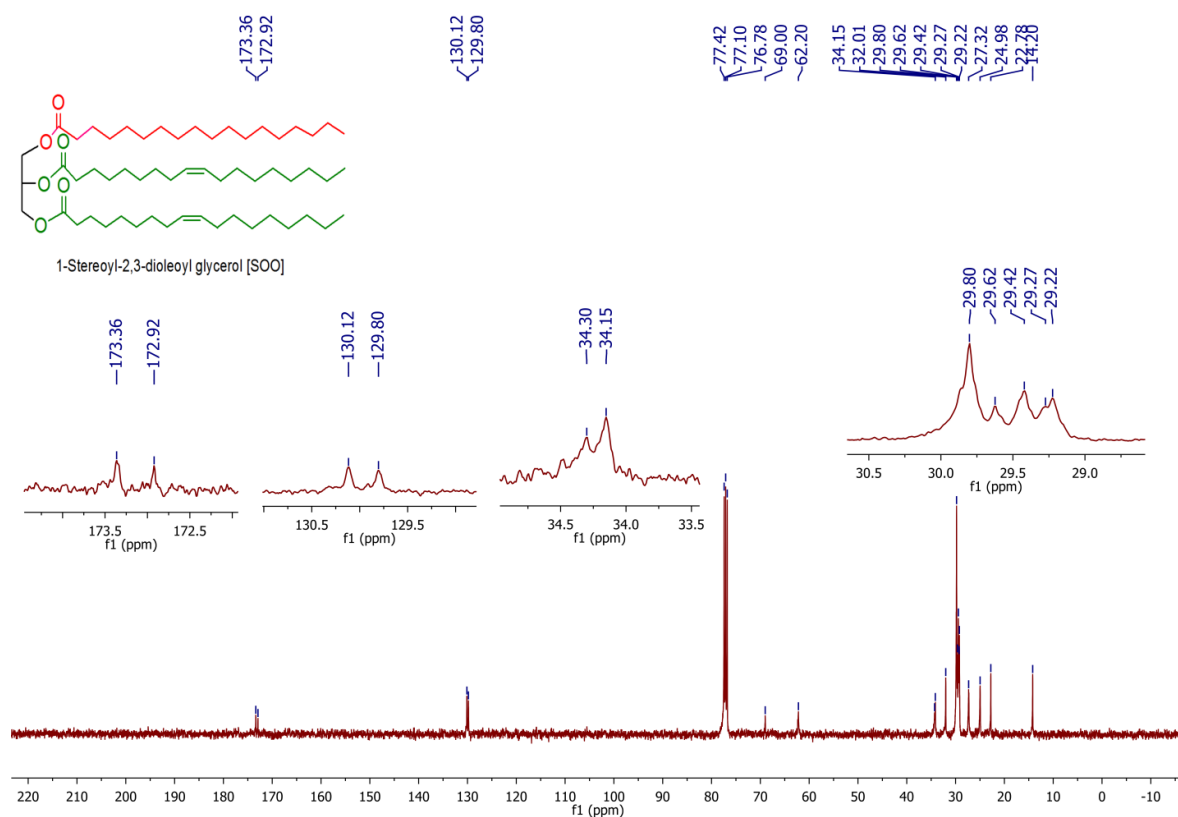
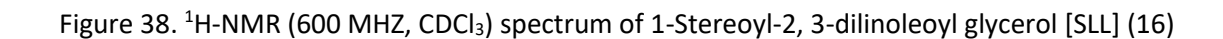
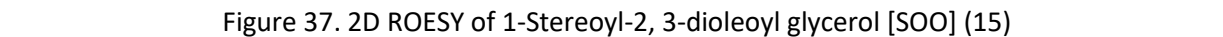
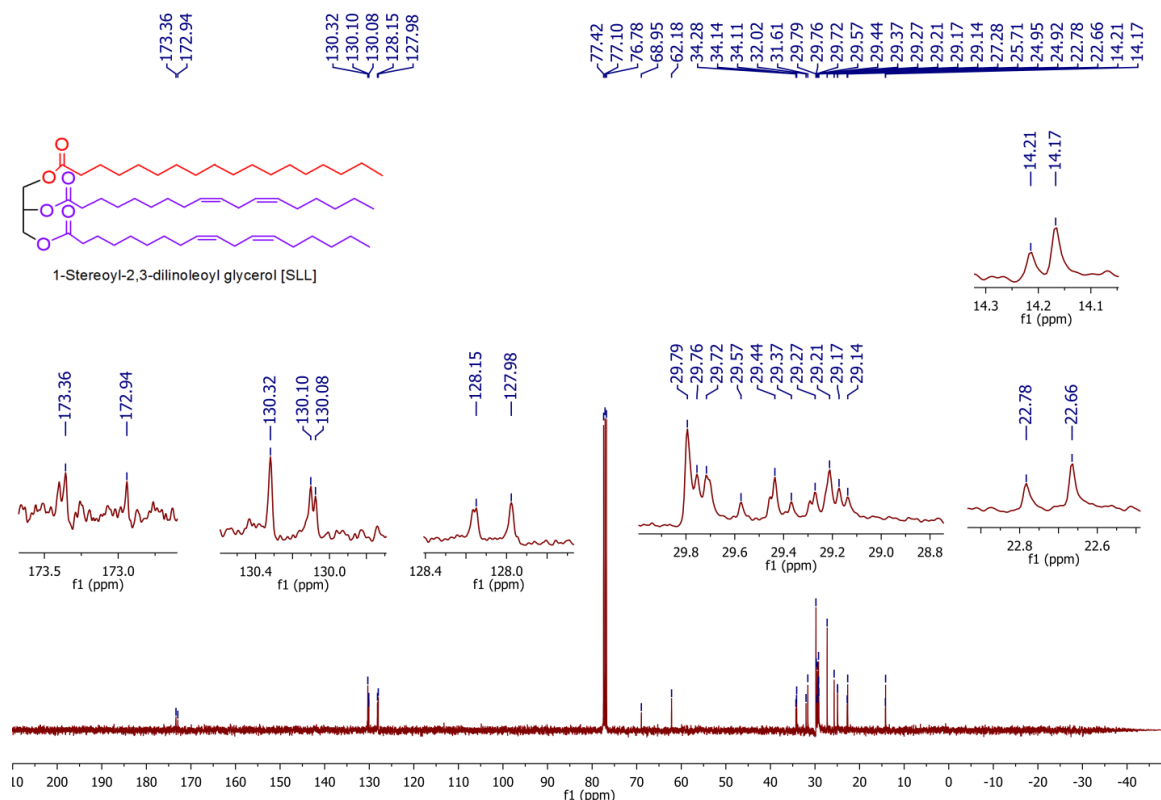
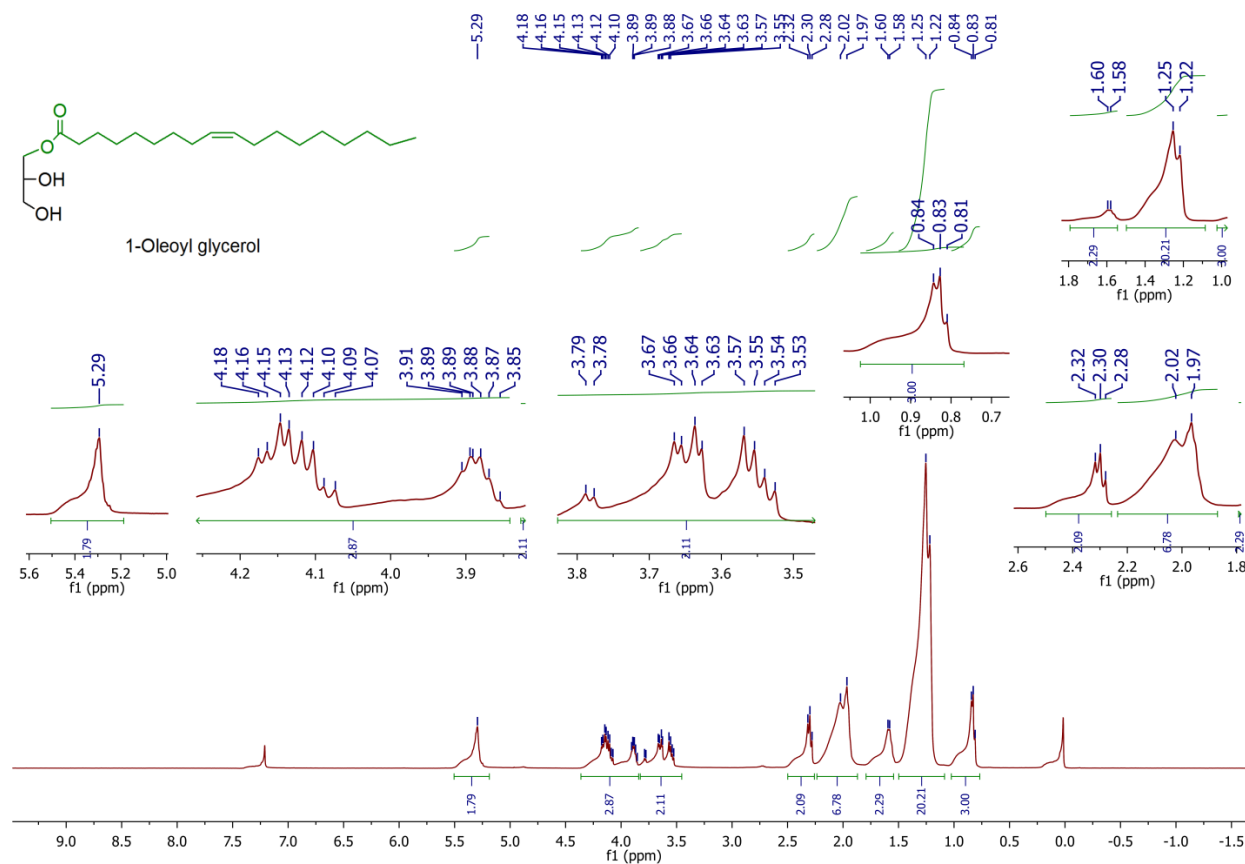
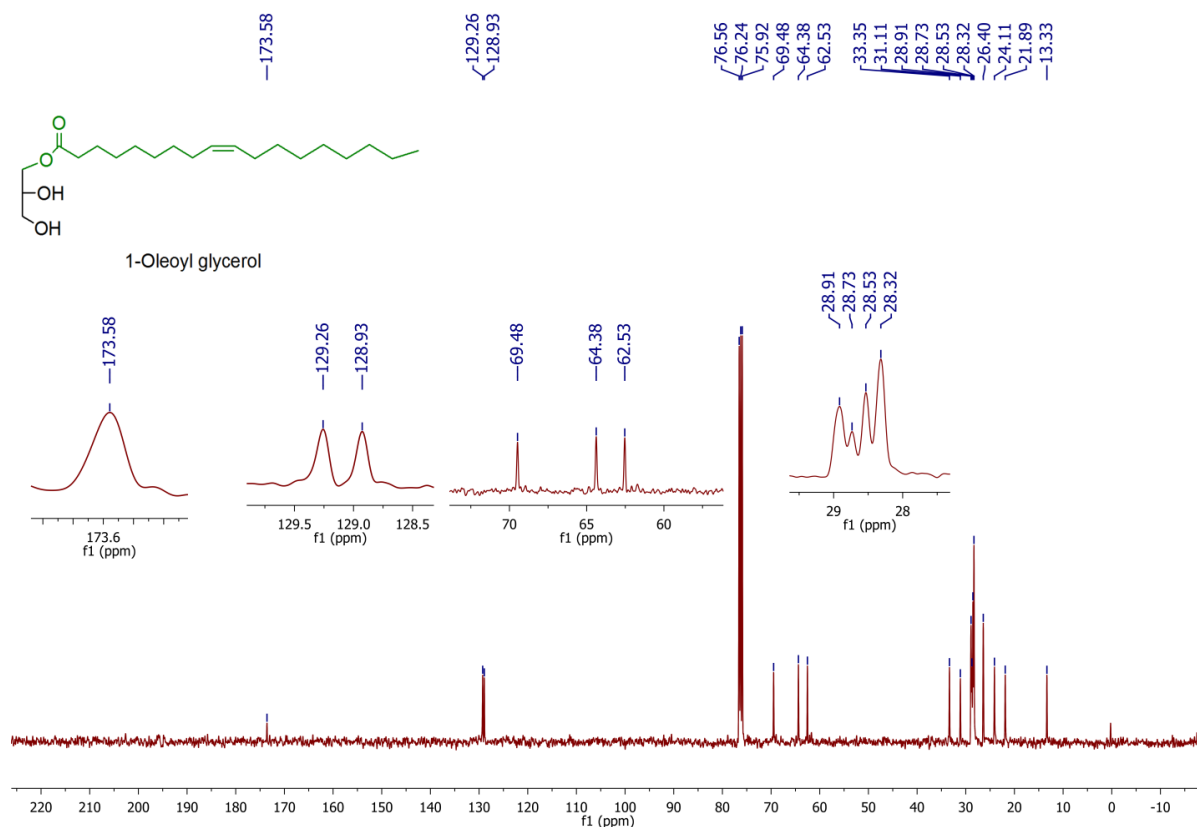
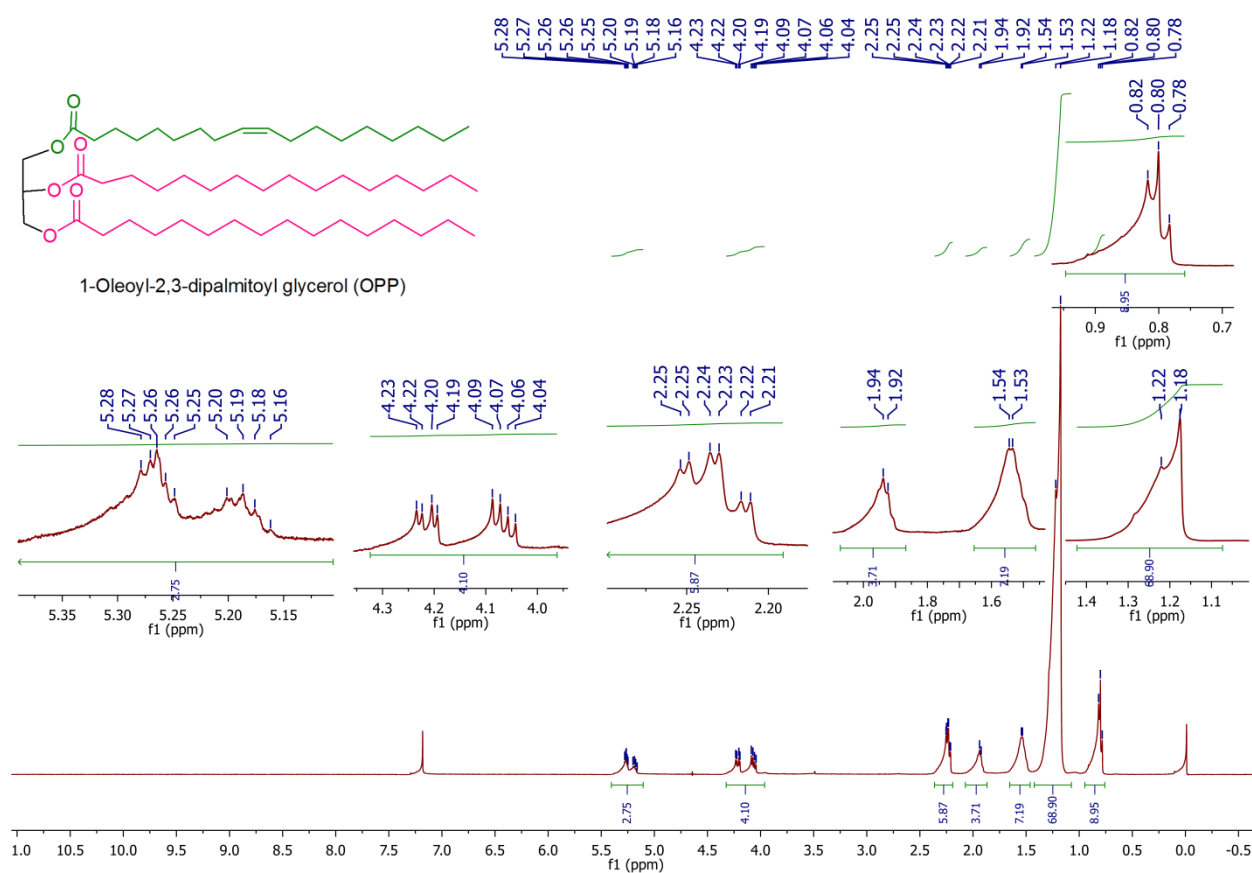
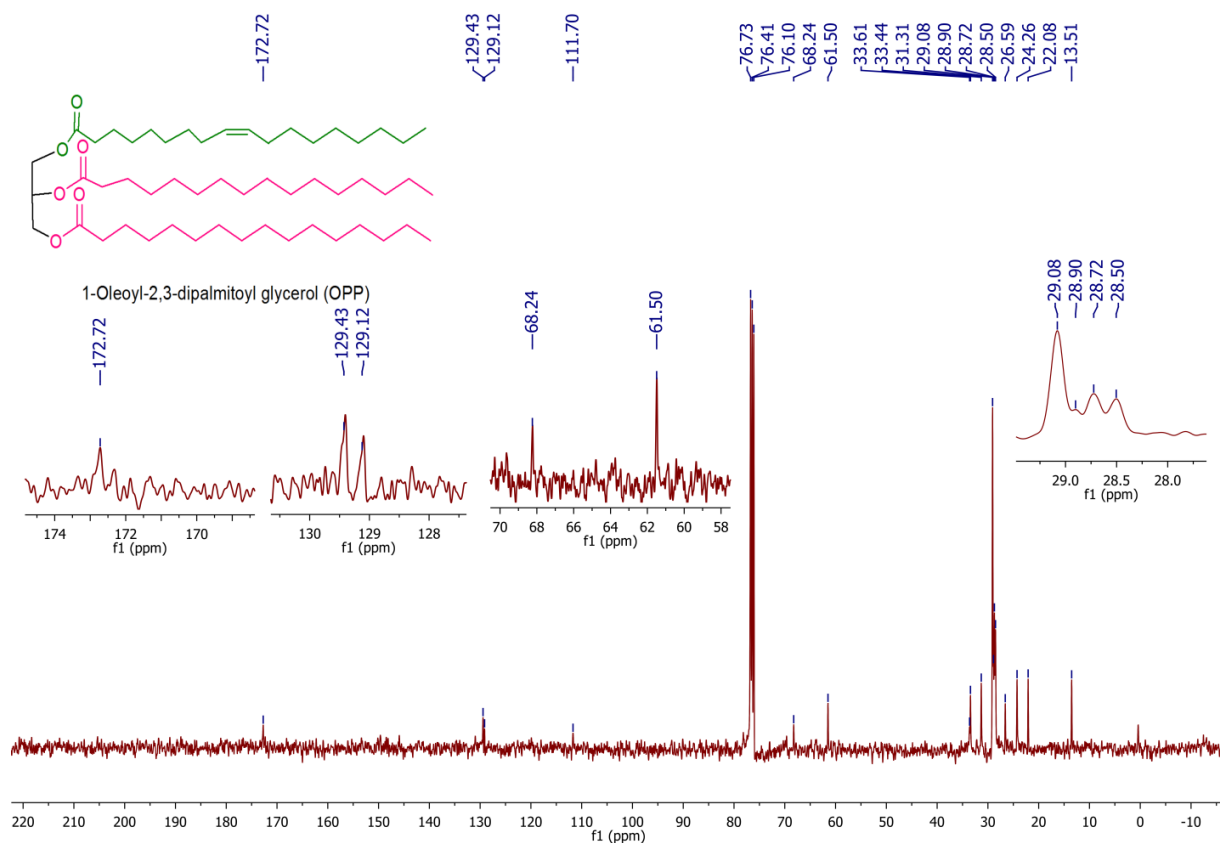
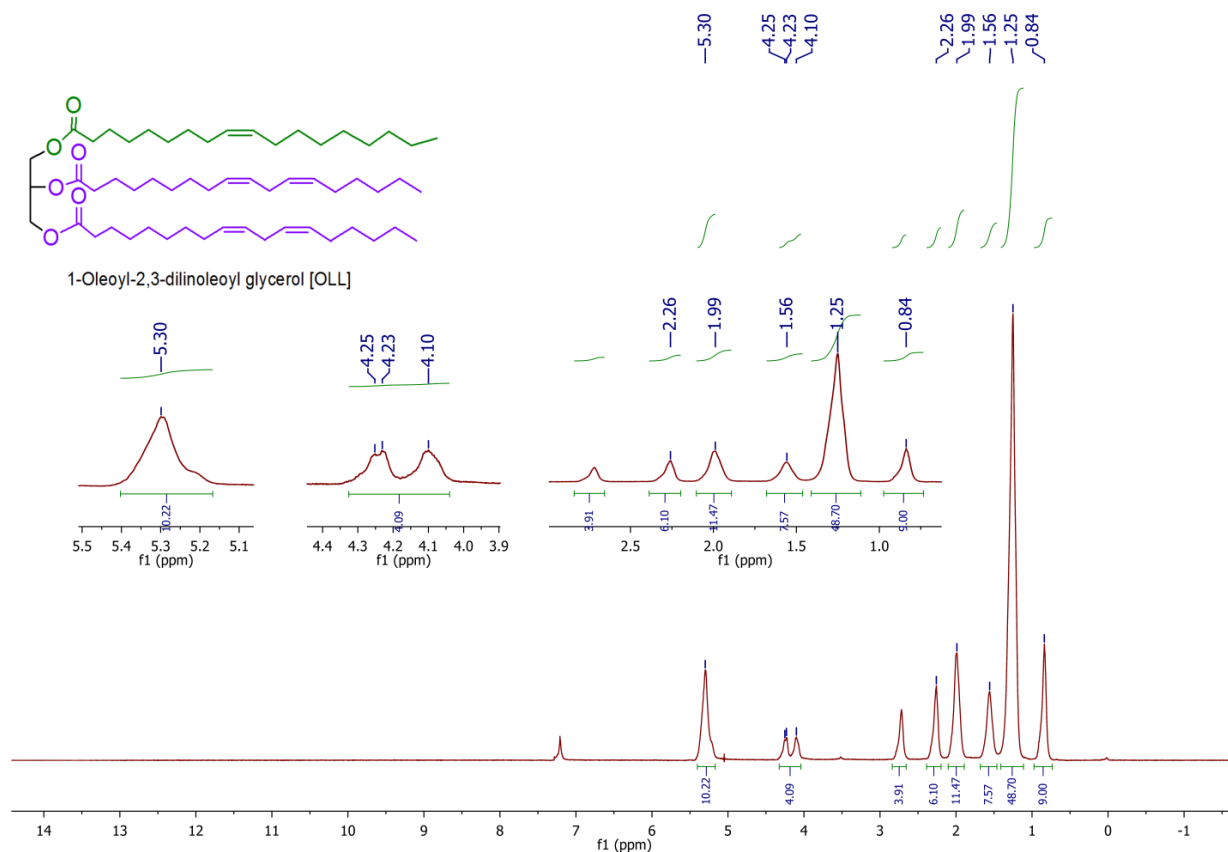


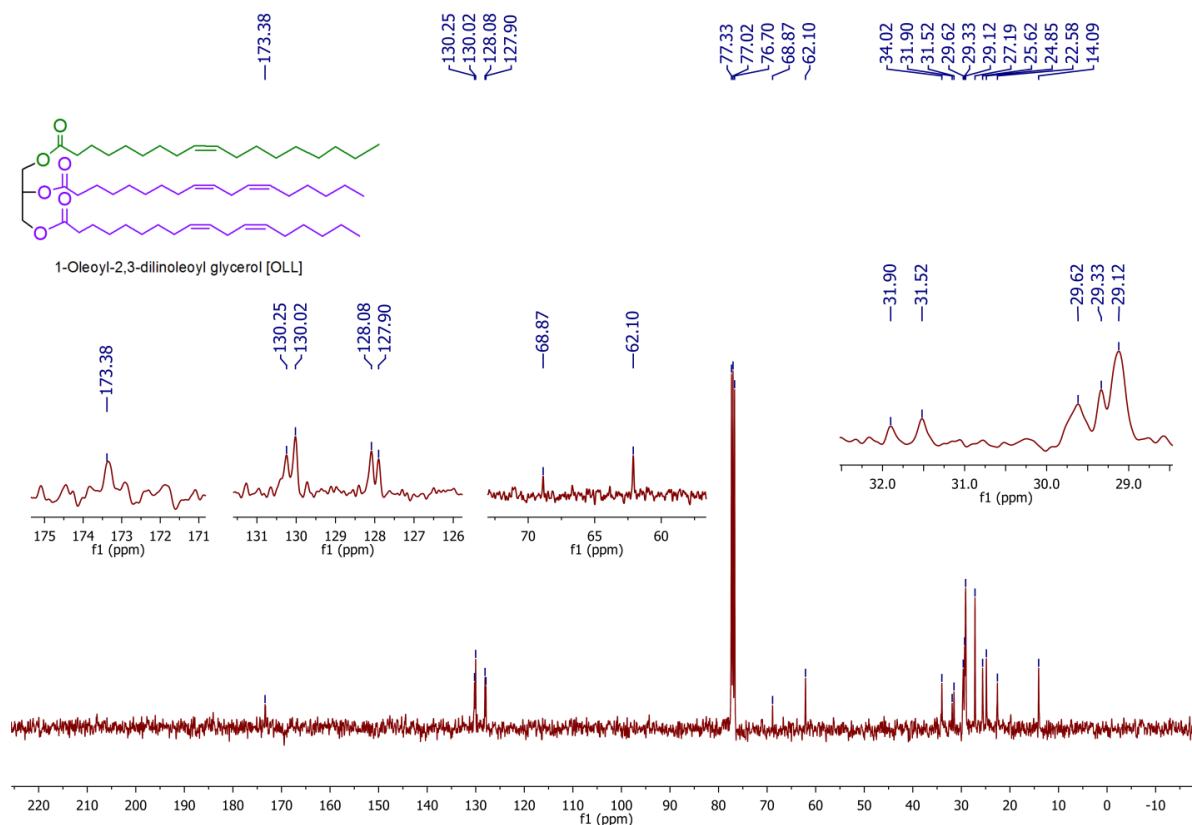
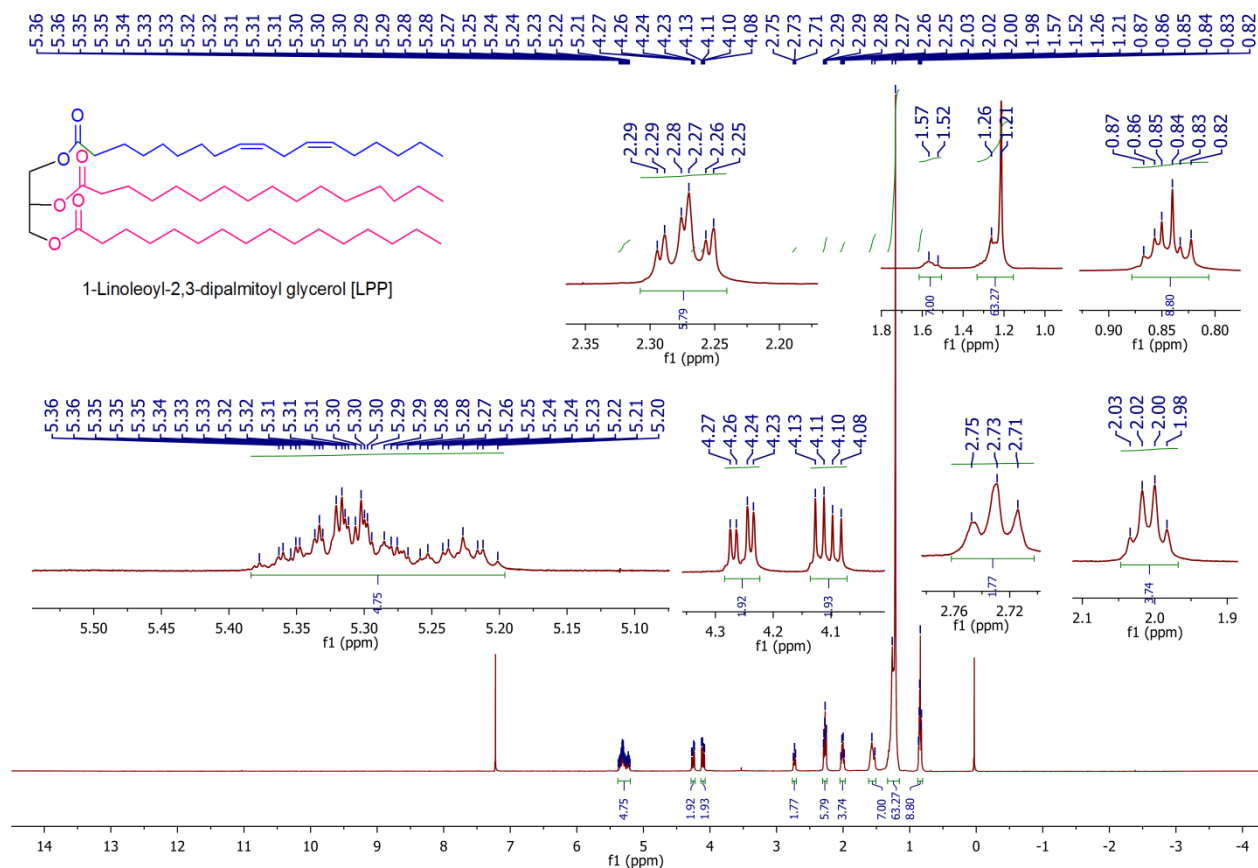
Figure 36. ¹³C-NMR (100 MHz, CDCl₃) spectrum of 1-Stereoyl-2,3-oleoyl glycerol [SOO] (15)



Figure 39. ^{13}C -NMR (100 MHz, CDCl_3) spectrum of 1-Stereoyl-2, 3- dilinoleoyl glycerol [SLL] (16)Figure 40. ^1H -NMR (600 MHz, CDCl_3) spectrum of 1-Oleoyl glycerol (17)

Figure 41. ¹³C-NMR (100 MHz, CDCl₃) spectrum of 1-Oleoyl glycerol (17)Figure 42. ¹H-NMR (600 MHz, CDCl₃) spectrum of 1-Oleoyl-2,3-dipalmitoyl glycerol [OPP] (18)

Figure 43. ¹³C-NMR (100 MHz, CDCl₃) spectrum of 1-Oleoyl-2, 3-dipalmitoyl glycerol [OPP] (18)Figure 44. ¹H-NMR (600 MHz, CDCl₃) spectrum of 1-Oleoyl-2, 3-dilinoleoyl glycerol [OLL] (19)

Figure 45. ¹³C-NMR (100 MHz, CDCl₃) spectrum of 1-Oleoyl-2, 3-dilinoleoyl glycerol [OLL] (19)Figure 46. ¹H-NMR (600 MHz, CDCl₃) spectrum of 1-Linoleoyl-2, 3-dipalmitoyl glycerol [LPP] (22)

1-Linoleoyl-2,3-dioleoyl glycerol [LOO]

Chemical structure of 1-Linoleoyl-2,3-dioleoyl glycerol (LOO) is shown. The molecule consists of a glycerol backbone esterified with one linoleic acid chain (18:2 n-7) and two oleic acid chains (18:1 n-7).

The ^1H NMR spectrum (CDCl₃) shows the following peaks and integrations:

- 5.27 ppm (m, 1H, integration 8.83)
- 4.23 ppm (m, 2H, integration 4.13)
- 4.21 ppm (m, 2H, integration 2.05)
- 4.09 ppm (m, 2H, integration 6.13)
- 4.08 ppm (m, 2H, integration 11.66)
- 4.07 ppm (m, 2H, integration 6.75)
- 2.70 ppm (m, 2H, integration 55.77)
- 2.24 ppm (m, 2H, integration 9.00)
- 1.95 ppm (m, 2H, integration 2.05)
- 1.54 ppm (m, 2H, integration 6.13)
- 1.23 ppm (m, 2H, integration 11.66)
- 0.81 ppm (m, 2H, integration 6.75)
- 0.00 ppm (TMS, integration 9.00)

156

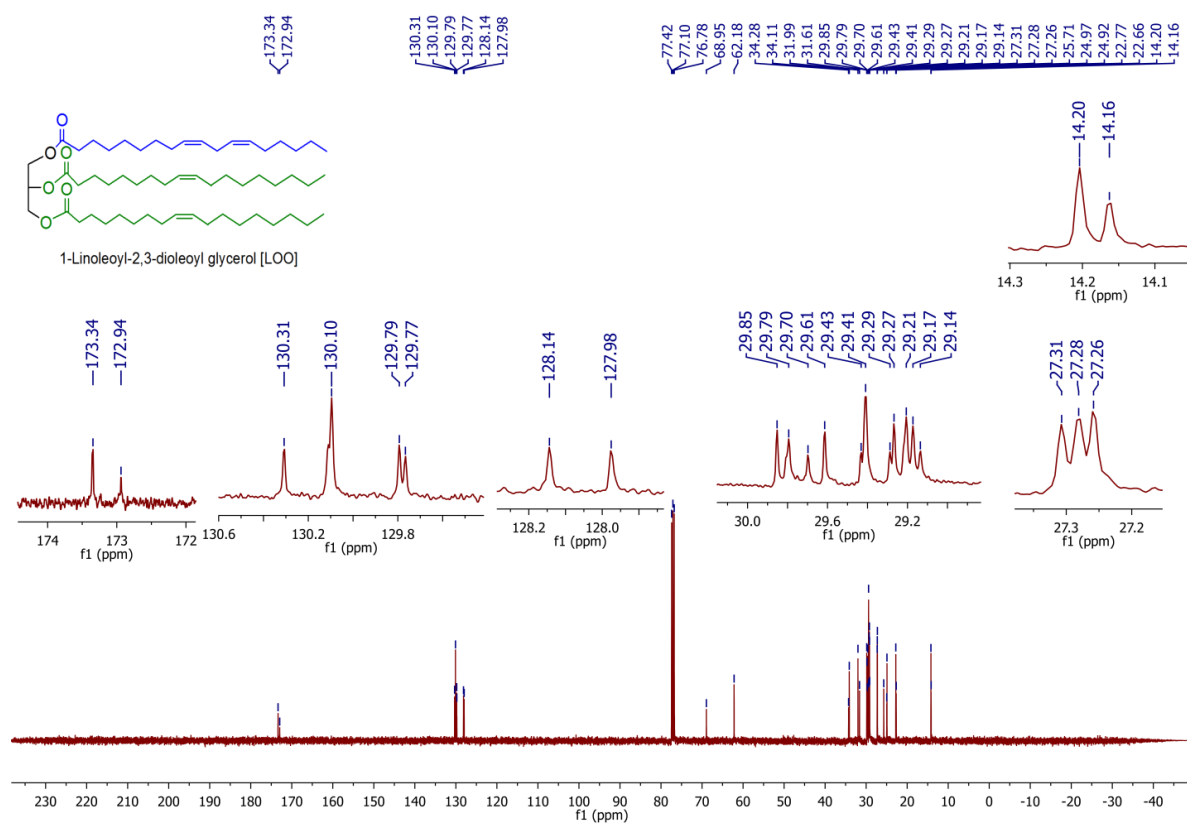


Figure 49. ^{13}C -NMR (100 MHz, CDCl_3) spectrum of 1-Linoleoyl-2, 3-dioleoyl glycerol [LOO] (23)

Chapter 4 Absolute Quantification of Triacylglycerols (TAGs)

Table 1 The regression data for residual standard deviation of PSS

S. No.	Concentration $\mu\text{g/L}$ x_i	Peak area y_i	$(x_i - \bar{x})^2$	Predicted $\hat{y}_i = mx_i + c$	Residuals $y_i - \hat{y}_i$	Residuals ² $(y_i - \hat{y}_i)^2$	RSD $\sqrt{\frac{1}{n-2} \sum_{i=1}^n (y_i - \hat{y}_i)^2}$
1	100	157745852	3600	157745852	0	0	S(r)= 6.66E+06
2	75	124026336	1225	122434191.2	1592144.757	2.53492E+12	
3	50	77573927	100	77756951.11	-183024.1081	33497824149	
4	25	29015956	225	33079710.97	-4063754.973	1.65141E+13	
5	15	12962664	625	15208814.92	-2246150.919	5.04519E+12	
6	10	6377879	900	6273366.892	104512.1081	10922780741	
7	5	2134192	1225	- 2662081.135	26624215327	7.08849E+20	
8	\bar{x}	\bar{y}	$\sum (x_i - \bar{x})^2$			$\sum (y_i - \hat{y}_i)^2$	
9	40	409836806	7900			7.08849E+20	

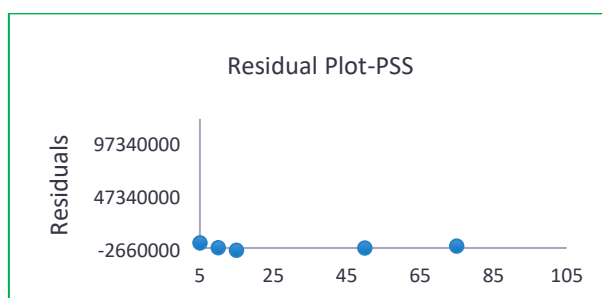


Table 2 The regression data for residual standard deviation of SPP

S. No.	Concentration $\mu\text{g/L}$ x_i	Peak area y_i	$(x_i - \bar{x})^2$	Predicted $\hat{y}_i = mx_i + c$	Residuals $y_i - \hat{y}_i$	Residuals ² $(y_i - \hat{y}_i)^2$	RSD $\sqrt{(y_i - \hat{y}_i)^2/n-2}$
1	100	137962524	3600	137240683.7	721840.2911	5.21053E+11	S(r)= 2.19E+05
2	75	100452568	1225	101136641.7	-684073.7468	4.67957E+11	
3	50	65191863	100	65032599.78	159263.2152	25364771713	
4	25	28314158	225	28928557.82	-614399.8228	3.77487E+11	
5	15	13200144	625	14486941.04	-1286797.038	1.65585E+12	
6	10	6726024	900	7266132.646	-540108.6456	2.91717E+11	
7	5	2289600	1225	45324.25316	-4530135716	2.05221E+19	
8	\bar{x}	\bar{y}	$\sum (x_i - \bar{x})^2$			$\sum (y_i - \hat{y}_i)^2$	
9	40	50590983	7900			2.05221E+19	

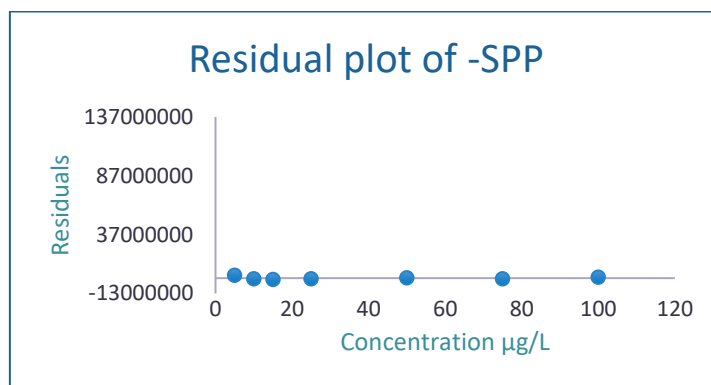


Table 3 The regression data for residual standard deviation of SOO

S. No.	Concentration $\mu\text{g/L}$ x_i	Peak area y_i	$(x_i - \bar{x})^2$	Predicted $\hat{y}_i = mx_i + c$	Residuals $y_i - \hat{y}_i$	Residuals ² $(y_i - \hat{y}_i)^2$	RSD $\sqrt{(y_i - \hat{y}_i)^2/n-2}$
1	100	140562320	3600	142647282.9	-2084963	4.35E+12	S(r)= 1.19E+06
2	75	107865534	1225	104857328.8	3008205	9.05E+12	
3	50	68480373	100	67067374.65	1412998	2.00E+12	
4	25	26631180	225	29277420.53	-2646241	7.00E+12	
5	15	12159573	625	14161438.89	-2001866	4.01E+12	
6	10	5974578	900	6603448.063	-628870	3.95E+11	
7	5	1986193	1225	954542.7595	2940736	8.65E+12	
8	\bar{x}	\bar{y}	$\sum (x_i - \bar{x})^2$			$\sum (y_i - \hat{y}_i)^2$	
9	40	363659751	7900		3.54E+13	3.54E+13	

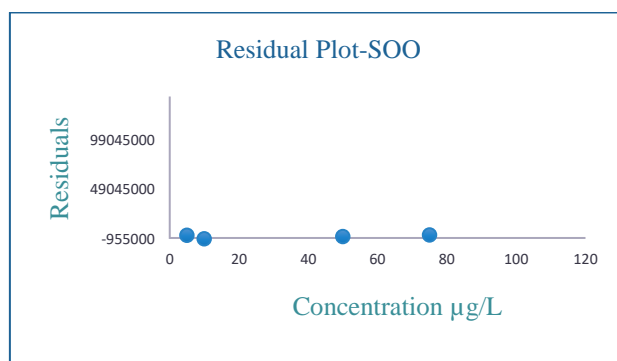


Table 4 The regression data for residual standard deviation of PPP

S. No.	Concentration $\mu\text{g/L}$ x_i	Peak area y_i	$(x_i - \bar{x})^2$	Predicted $\hat{y}_i = mx_i + c$	Residuals $y_i - \hat{y}_i$	Residuals ² $(y_i - \hat{y}_i)^2$	RSD $\sqrt{(y_i - \hat{y}_i)^2/n-2}$
1	100	2415552	3600	2182668.018	232883.9819	54234949033	S(r)= 8.01E+04
2	75	1420628	1225	1580989.767	-160361.7665	25715896155	
3	50	758532	100	979311.5149	-220779.5149	48743594208	
4	25	305076	225	377633.2633	-72557.26334	5264556463	
5	15	168953	625	136961.9627	31991.0373	1023426467	
6	10	50158	900	16626.31239	33531.68761	1124374074	
7	5	51582.5	1225	-103709.3379	155291.8379	24115554928	
8	\bar{x}	\bar{y}	$\sum (x_i - \bar{x})^2$			$\sum (y_i - \hat{y}_i)^2$	
9	40	5170481.5	7900			1.60222E+11	

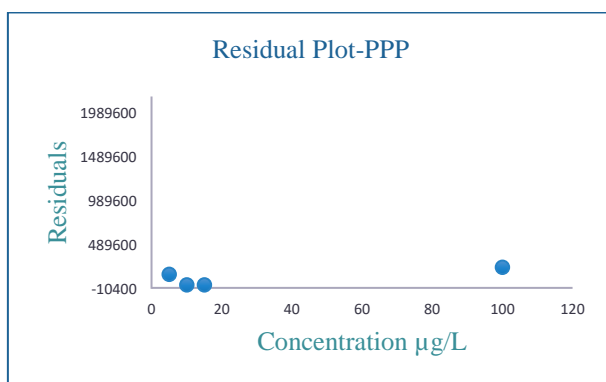


Table 5 The regression data for residual standard deviation of POO

S. No.	Concentration $\mu\text{g/L}$ x_i	Peak area y_i	$(x_i - \bar{x})^2$	Predicted $\hat{y}_i = mx_i + c$	Residuals $y_i - \hat{y}_i$	Residuals ² $(y_i - \hat{y}_i)^2$	RSD $\sqrt{(y_i - \hat{y}_i)^2/n-2}$
1	100	115484573	3600	117067098.9	-1582525.904	2.50439E+12	S(r)= 1.08E+08
2	75	88901674	1225	86000405.08	2901268.925	8.41736E+12	
3	50	55361858	100	54933711.25	428146.7541	1.8331E+11	
4	25	21096484	225	23867017.42	-2770533.417	7.67586E+12	
5	15	9877967	625	11440339.89	-1562372.885	2.44101E+12	
6	10	5030787	900	5227001.119	-196214.1193	38499980632	
7	5	1795893	1225	-986337.6465	2782230.646	7.74081E+12	
8	\bar{x}	\bar{y}	$\sum (x_i - \bar{x})^2$			$\sum (y_i - \hat{y}_i)^2$	
9	40	2.98E+08	7900			2.90012E+13	

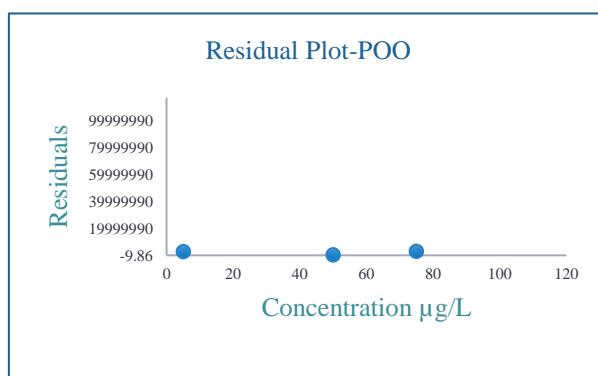


Table 6 The regression data for residual standard deviation of OOO

S. No.	Concentration $\mu\text{g/L}$ x_i	Peak area y_i	$(x_i - \bar{x})^2$	Predicted $\hat{y}_i = mx_i + c$	Residuals $y_i - \hat{y}_i$	Residuals ² $(y_i - \hat{y}_i)^2$	RSD $\sqrt{(y_i - \hat{y}_i)^2/n-2}$
1	100	61814396	3600	55999235.23	5815160.774	3.38161E+13	S(r)= 2.04E+04
2	75	36498660	1225	40359906.14	-3861246.144	1.49092E+13	
3	50	19362583	100	24720577.06	-5357994.061	2.87081E+13	
4	25	6516402	225	9081247.979	-2564845.979	6.57843E+12	
5	15	2952217	625	2825516.346	126700.6537	16053055650	
6	10	1494971	900	-302349.4702	1797320.47	3.23036E+12	
7	5	614689	1225	-3430215.287	4044904.287	1.63613E+13	
8	\bar{x}	\bar{y}	$\sum (x_i - \bar{x})^2$			$\sum (y_i - \hat{y}_i)^2$	
9	40	129253918	7900			1.0362E+14	

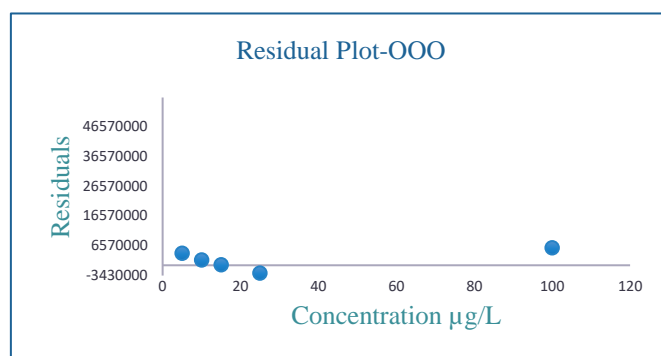


Table 7 The regression data for residual standard deviation of LPP

S. No.	Concentration $\mu\text{g/L}$ x_i	Peak area y_i	$(x_i - \bar{x})^2$	Predicted $\hat{y}_i = mx_i + c$	Residuals $y_i - \hat{y}_i$	Residuals ² $(y_i - \hat{y}_i)^2$	RSD $\sqrt{(y_i - \hat{y}_i)^2/n-2}$
1	100	146835439	3600	152499827.8	-5664388.785	3.20853E+13	S(r)= 1.97E+06
2	75	118976164	1225	112831449.5	6144714.459	3.77575E+13	
3	50	77034217	100	73163071.3	3871145.703	1.49858E+13	
4	25	31652746	225	33494693.05	-1841947.054	3.39277E+12	
5	15	15452872	625	17627341.76	-2174469.756	4.72832E+12	
6	10	8167467	900	9693666.108	-1526199.108	2.32928E+12	
7	5	2951135	1225	1759990.459	1191144.541	1.41883E+12	
8	\bar{x}	\bar{y}	$\sum (x_i - \bar{x})^2$			$\sum (y_i - \hat{y}_i)^2$	
9	40	4.01E+08	7900			9.66978E+13	

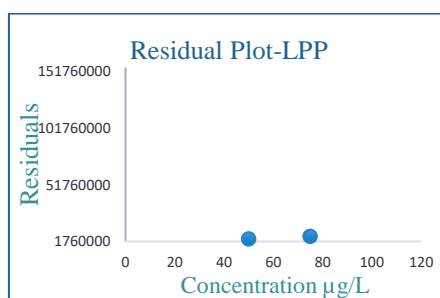


Table 8 The regression data for residual standard deviation of SLL

S. No.	Concentration $\mu\text{g/L}$ x_i	Peak area y_i	$(x_i - \bar{x})^2$	Predicted $\hat{y}_i = mx_i + c$	Residuals $y_i - \hat{y}_i$	Residuals ² $(y_i - \hat{y}_i)^2$	RSD $\sqrt{(y_i - \hat{y}_i)^2/n-2}$
1	100	145532838	3600	151402535.8	-5869697.767	3.44534E+13	S(r)= 2.03E+06
2	75	117196199	1225	112266806.4	4929392.6	2.42989E+13	
3	50	79001432	100	73131077.03	5870354.967	3.44611E+13	
4	25	33042976	225	33995347.67	-952371.6655	9.07012E+11	
5	15	16117914	625	18341055.92	-2223141.919	4.94236E+12	
6	10	8449247	900	10513910.05	-2064663.045	4.26283E+12	
7	5	2996891	1225	26867664.172	310126.8282	96178649575	
8	\bar{x}	\bar{y}	$\sum (x_i - \bar{x})^2$			$\sum (y_i - \hat{y}_i)^2$	
9	40	4.02E+08	7900			1.03422E+14	

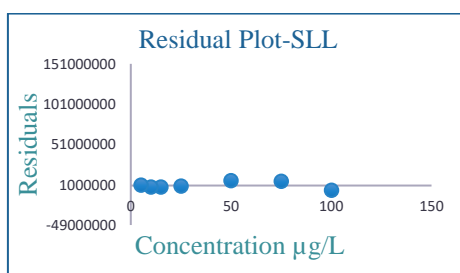


Table 9 The regression data for residual standard deviation of OLL

S. No.	Concentration $\mu\text{g/L}$ x_i	Peak area y_i	$(x_i - \bar{x})^2$	Predicted $\hat{y}_i = mx_i + c$	Residuals $y_i - \hat{y}_i$	Residuals ² $(y_i - \hat{y}_i)^2$	RSD $\sqrt{\sum (y_i - \hat{y}_i)^2 / n - 2}$
1	100	121948483	3600	128534152.1	-6585669.148	4.3371E+13	S(r)= 2.13E+06
2	75	101367708	1225	95754671.61	5613036.39	3.15062E+13	
3	50	68675871	100	62975191.07	5700679.928	3.24978E+13	
4	25	30538635	225	30195710.53	342924.4656	1.17597E+11	
5	15	15118731	625	17083918.32	-1965187.319	3.86196E+12	
6	10	8325784	900	10528022.21	-2202238.212	4.84985E+12	
7	5	3068580	1225	3972126.104		8.16396E+11	
8	\bar{x}	\bar{y}	$\sum (x_i - \bar{x})^2$			$\sum (y_i - \hat{y}_i)^2$	
9	40	349043792	7900			1.17021E+14	

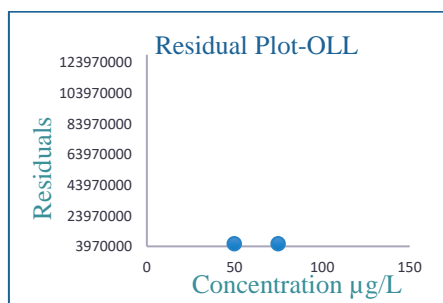


Table 10 The regression data for residual standard deviation of LLL

S. No.	Concentration $\mu\text{g/L}$ x_i	Peak area y_i	$(x_i - \bar{x})^2$	Predicted $\hat{y}_i = mx_i + c$	Residuals $y_i - \hat{y}_i$	Residuals ² $(y_i - \hat{y}_i)^2$	RSD $\sqrt{\sum (y_i - \hat{y}_i)^2 / n - 2}$
1	100	3124852	3600	2878931.081	245920.9186	60477098218	S(r)= 8.55 E+06
2	75	1946012	1225	2103976.762	-157964.7618	24952865956	
3	50	1079737	100	1329022.442	-249285.4421	62143231660	
4	25	468575	225	554068.1225	-85493.12251	7309073997	
5	15	265501	625	244086.3947	21414.60533	458585321.6	
6	10	170817	900	89095.53074	81721.46926	6678398538	
7	5	77791	1225	-65895.33318	143686.3332	20645762343	
8	\bar{x}	\bar{y}	$\sum (x_i - \bar{x})^2$			$\sum (y_i - \hat{y}_i)^2$	
9	40	7.13E+06	7900			1.82665E+11	

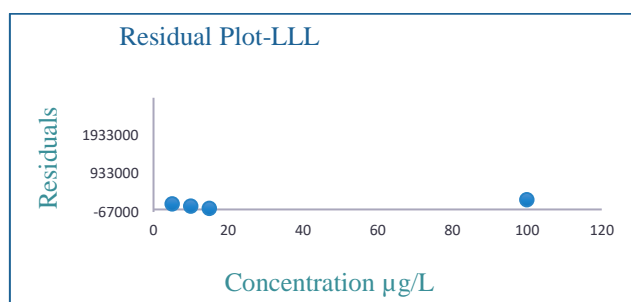


Table 11 The regression data for residual standard deviation of SSS

S. No.	Concentration $\mu\text{g/L}$ x_i	Peak area y_i	$(x_i - \bar{x})^2$	Predicted $\hat{y}_i = mx_i + c$	Residuals $y_i - \hat{y}_i$	Residuals ² $(y_i - \hat{y}_i)^2$	RSD $\sqrt{\sum (y_i - \hat{y}_i)^2 / n - 2}$
1	100	126511128	3600	124954553.9	1556574.051	2.42292E+12	S(r)= 2.06 E+06
2	75	92982520	1225	90675623.55	2306896.446	5.32177E+12	
3	50	52426544	100	56396693.16	-3970149.158	1.57621E+13	
4	25	16140968	225	22117762.76	-5976794.763	3.57221E+13	
5	15	6541398	625	8406190.604	-1864792.604	3.47745E+12	
6	10	3047054	900	1550404.525	1496649.475	2.23996E+12	
7	5	1146235	1225	-5305381.554	6451616.554	4.16234E+13	
8	\bar{x}	\bar{y}	$\sum (x_i - \bar{x})^2$			$\sum (y_i - \hat{y}_i)^2$	
9	40	2.99E+08	7900			1.0657E+14	

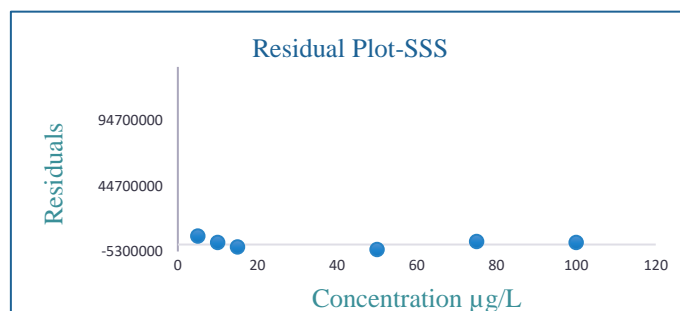


Table 12 The regression data for residual standard deviation of PPP cocoa butter

S. No.	Cocoa butter origin	Concentration $\mu\text{g/L}$ x_i	Peak area y_i	$(x_i - \bar{x})^2$	Predicted $\hat{y}_i = mx_i + c$	Residuals $y_i - \hat{y}_i$	Residuals ² $(y_i - \hat{y}_i)^2$	RSD $\sqrt{\sum (y_i - \hat{y}_i)^2 / n - 2}$
1	Ecuador	13.411	76336	3861.628	76336	0	0	S(r)= 5.911 E-12
2	Ghana	13.270	72813	3879.172	72813	0	0	
3	Cameron dry	11.408	26434.6	4114.581	26434.6	0	0	
4	Cameron wet	10.710	9055.4	4204.614	9055.4	-2.36469E-11	5.59174E-22	
5	Ghana dry	13.246	72223	3882.162	72223	0	0	
6	Ghana wet	13.508	78742	3849.582	78742	0	0	
7		\bar{x}	\bar{y}	$\sum (x_i - \bar{x})^2$			$\sum (y_i - \hat{y}_i)^2$	
8		75.553		23791.740			5.59174E-22	

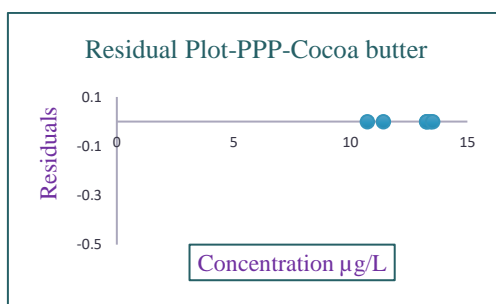


Table 13 The regression data for residual standard deviation of POO cocoa butter

S. No.	Cocoa butter origin	Concentration $\mu\text{g/L}$ x_i	Peak area y_i	$(x_i - \bar{x})^2$	Predicted $\hat{y}_i = mx_i + c$	Residuals $y_i - \hat{y}_i$	Residuals ² $(y_i - \hat{y}_i)^2$	RSD $\sqrt{\sum (y_i - \hat{y}_i)^2/n-2}$
1	Ecuador	7.371	1864674	1293.553	1864674	0	0	S(r)= 2.328E-10
2	Ghana	7.183	1630555	1307.111	1630555	0	0	
3	Cameron dry	7.538	2072186	1281.568	2072186	0	0	
4	Cameron wet	7.659	2223513	1272.919	2223513	0	0	
5	Ghana dry	6.888	1262926	1328.529	1262926	0	0	
6	Ghana wet		1026237	1342.416	1026237	-9.313E-10	8.67362E-19	
7		\bar{x}	\bar{y}	$\sum (x_i - \bar{x})^2$			$\sum (y_i - \hat{y}_i)^2$	
8		43.337	10080091	7826.098			8.67362E-19	

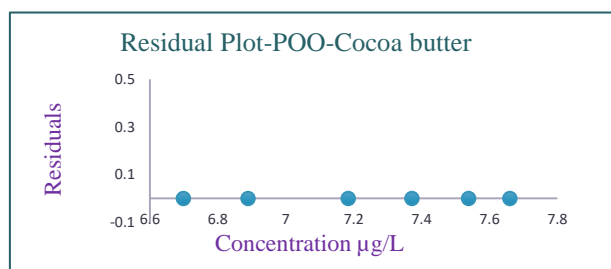


Table 14 The regression data for residual standard deviation of OOO cocoa butter

S. No.	Cocoa butter origin	Concentration $\mu\text{g/L}$ x_i	Peak area y_i	$(x_i - \bar{x})^2$	Predicted $\hat{y}_i = mx_i + c$	Residuals $y_i - \hat{y}_i$	Residuals ² $(y_i - \hat{y}_i)^2$	RSD $\sqrt{\sum (y_i - \hat{y}_i)^2 / n - 2}$
1	Ecuador	11.616	113671	3397.257	113671	0	0	S(r)= 2.513E-13
2	Ghana	11.608	108826	3398.190	108826	0	0	
3	Cameron dry	11.760	207070.4	3380.492	207070.4	-3.7835E-10	1.43149E-19	
4	Cameron wet	11.750	200120	3381.655	200120	0	0	
5	Ghana dry	11.633	124886	3395.276	124886	0	0	
6	Ghana wet	11.535	61655	3406.706	61655	-9.3132E-10	8.67362E-19	
7		\bar{x}	\bar{y}	$\sum (x_i - \bar{x})^2$			$\sum (y_i - \hat{y}_i)^2$	
8		69.902	816228.4	20359.578			1.01051E-18	

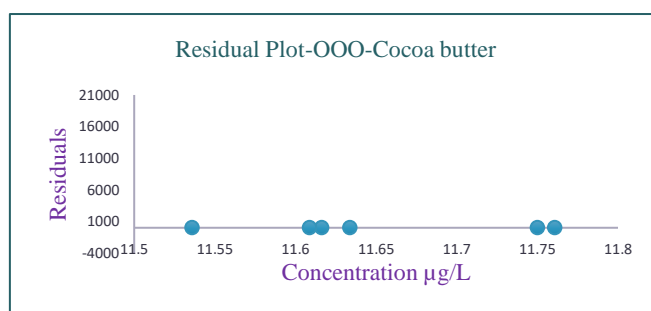


Table 15 The regression data for residual standard deviation of LPP cocoa butter

S. N o.	Cocoa butter origin	Concentration $\mu\text{g/L}$ x_i	Peak area y_i	$(x_i - \bar{x})^2$	Predicted $\hat{y}_i = mx_i + c$	Residuals $y_i - \hat{y}_i$	Residuals ² $(y_i - \hat{y}_i)^2$	RSD $\sqrt{\sum (y_i - \hat{y}_i)^2 / n - 2}$
1	Ecuador	5.184	1783621	535.737	1783621	1.86265E-09	3.46945E-18	S(r)= 6.160E-10
2	Ghana	4.875	1290897	550.137	1290897	0	0	
3	Cameron dry	4.683	985696	559.180	985696	9.31323E-10	8.67362E-19	
4	Cameron wet	4.677	975734	559.464	975734	0	0	
5	Ghana dry	4.509	708022	567.440	708022	9.31323E-10	8.67362E-19	
6	Ghana wet	4.402	536572	572.549	536572	9.31323E-10	8.67362E-19	
7		\bar{x}	\bar{y}	$\sum (x_i - \bar{x})^2$			$\sum (y_i - \hat{y}_i)^2$	
8		28.330	6280542	3344.508			6.07153E-18	

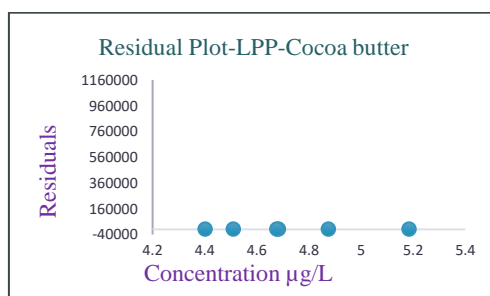


Table 16 The regression data for residual standard deviation of SOO cocoa butter

S. No.	Cocoa butter origin	Concentration $\mu\text{g/L}$ x_i	Peak area y_i	$(x_i - \bar{x})^2$	Predicted $\hat{y}_i = mx_i + c$	Residuals $y_i - \hat{y}_i$	Residuals ² $(y_i - \hat{y}_i)^2$	RSD $\sqrt{\sum (y_i - \hat{y}_i)^2 / n - 2}$
1	Ecuador	7.148	2195328	1408.425	2195328	0	0	S(r)= 4.656E-10
2	Ghana	7.753	3111285	1363.381	3111285	0	0	
3	Cameron dry	7.787	3164036.8	1360.872	3164036.8	0	0	
4	Cameron wet	8.256	3873183.7	1326.489	3873183.7	0	0	
5	Ghana dry	7.027	2012842.7	1417.796	2012842.7	0	0	
6	Ghana wet	6.706	1525751	1441.796	1525751	1.86265E-09	3.46945E-18	
8		\bar{x}	\bar{y}	$\sum (x_i - \bar{x})^2$			$\sum (y_i - \hat{y}_i)^2$	
9		44.677	15882427.2	8318.488			3.46945E-18	

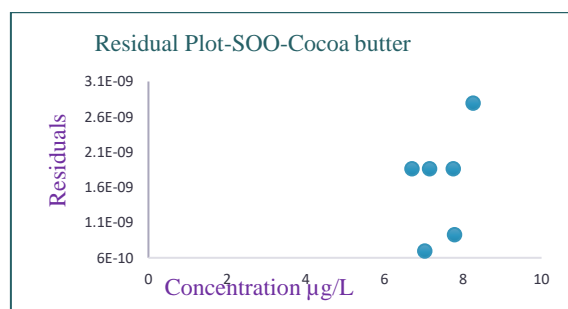


Table 17 The regression data for residual standard deviation of OPP cocoa butter

S. No.	Cocoa butter origin	Concentration $\mu\text{g/L}$ x_i	Peak area y_i	$(x_i - \bar{x})^2$	Predicted $\hat{y}_i = mx_i + c$	Residuals $y_i - \hat{y}_i$	Residuals ² $(y_i - \hat{y}_i)^2$	RSD $\sqrt{\sum (y_i - \hat{y}_i)^2 / n - 2}$
1	Ecuador	70.387	110876595	48385.041	110876632.1	-37.11670	1377.6501	S(r)= 1.33E+2
2	Ghana	61.356	95324952	52439.626	95324975.28	-23.2771	541.8247	
3	Cameron dry	38.885	56629167.4	63236.155	56629229.42	-62.0192	3846.3916	
4	Cameron wet	42.348	62593088.1	61506.480	62592620.81	467.2915	218361.40	
5	Ghana dry	38.835	56542977	63261.304	56543127.9	-150.8976	22770.097	
6	Ghana wet	38.542	56038379	63408.779	56038572.98	-193.9807	37628.549	
8		\bar{x}	\bar{y}	$\sum (x_i - \bar{x})^2$			$\sum (y_i - \hat{y}_i)^2$	
9		290.353	4.38E+08	352237.385			284525.915	

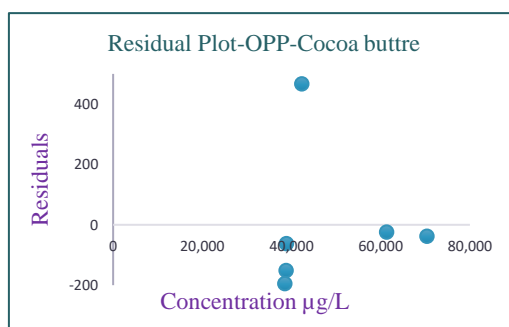


Table 18 The regression data for residual standard deviation of SOS cocoa butter

S. N o.	Cocoa butter origin	Concentration $\mu\text{g/L}$ x_i	Peak area y_i	$(x_i - \bar{x})^2$	Predicted $\hat{y}_i = mx_i + c$	Residuals $y_i - \hat{y}_i$	Residuals ² $(y_i - \hat{y}_i)^2$	RSD $\sqrt{\sum (y_i - \hat{y}_i)^2 / n - 2}$
1	Ecuador	84.481	135146197	202707.052	135146670.5	473.4804	224183.7701	S(r)= 226.103
2	Ghana	133.451	219474602	161009.587	219474539	62.9918	3967.9754	
3	Cameron dry	69.633	109577983.8	216297.546	109577951	32.7783	1074.4193	
4	Cameron wet	79.435	126457434.6	207276.236	126457301	133.6230	17855.1324	
5	Ghana dry	85.558	137000900	201738.417	137001298.1	-398.0974	158481.6044	
6	Ghana wet	82.153	131138424	204808.743	131137781.8	642.1846	412401.1425	
8		\bar{x}	\bar{y}	$\sum (x_i - \bar{x})^2$			$\sum (y_i - \hat{y}_i)^2$	
9		534.711	8.59E+8	1193837.583			817964.0442	

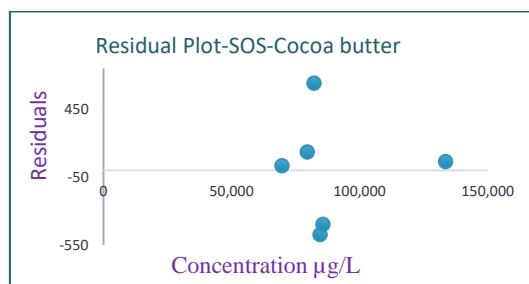


Table 19 The regression data for residual standard deviation of SOA cocoa butter

S. No.	Cocoa butter origin	Concentration $\mu\text{g/L}$ x_i	Peak area y_i	$(x_i - \bar{x})^2$	Predicted $\hat{y}_i = mx_i + c$	Residuals $y_i - \hat{y}_i$	Residuals ² $(y_i - \hat{y}_i)^2$	RSD $\sqrt{\sum (y_i - \hat{y}_i)^2 / n - 2}$
1	Ecuador	6.294	505581	1094.021	505960.41	-379.410	143952.22	S(r)= 346.82
2	Ghana	6.995	1712633	1048.140	1713137.11	-504.118	254135.79	
3	Cameron dry	6.454	782030.7	1083.463	781492.89	537.802	289231.72	
4	Cameron wet	6.517	889365.2	1079.319	889983.81	-618.614	382683.35	
5	Ghana dry	6.729	1255987.9	1065.434	1255064.35	923.540	852927.47	
6	Ghana wet	6.381	655822	1088.274	65781.20	40.799	1664.627	
8		\bar{x}	\bar{y}	$\sum (x_i - \bar{x})^2$			$\sum (y_i - \hat{y}_i)^2$	
9		39.370	5801419.8	6458.654			1924595.20	

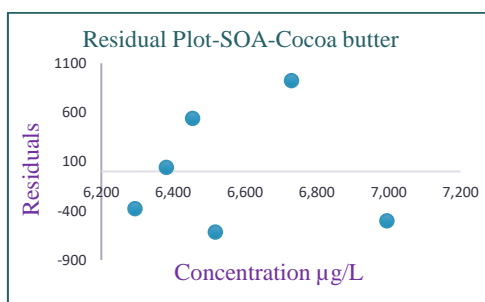


Table 20 The regression data for residual standard deviation of PLO cocoa butter

S. No.	Cocoa butter origin	Concentration $\mu\text{g/L}$ x_i	Peak area y_i	$(x_i - \bar{x})^2$	Predicted $\hat{y}_i = mx_i + c$	Residuals $y_i - \hat{y}_i$	Residuals ² $(y_i - \hat{y}_i)^2$	RSD $\sqrt{\sum (y_i - \hat{y}_i)^2 / n - 2}$
1	Ecuador	6.183	314893	928.664	315206.37	-313.379	98206.51	S(r)= 274.27
2	Ghana	6.072	124481	935.442	123859.17	621.826	386667.71	
3	Cameron dry	6.128	220827	932.019	220394.70	432.299	186882.52	
4	Cameron wet	6.124	213729	932.264	213499.30	229.693	52759.28	
5	Ghana dry	6.087	149296	934.524	149716.90	-420.904	177160.45	
6	Ghana wet	6.063	107795	935.992	108344.53	-549.535	301989.39	
8		\bar{x}	\bar{y}	$\sum (x_i - \bar{x})^2$			$\sum (y_i - \hat{y}_i)^2$	
9		36.657	1131021	5598.908			1203665.89	

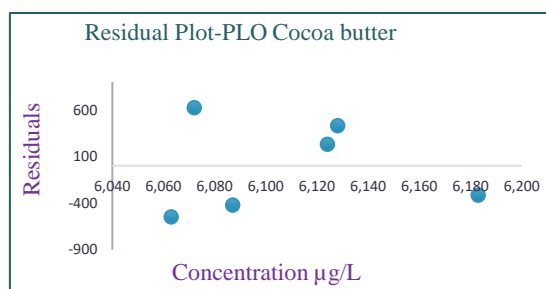


Table 21 The regression data for residual standard deviation of SOMa cocoa butter

S. No.	Cocoa butter origin	Concentration $\mu\text{g/L}$ x_i	Peak area y_i	$(x_i - \bar{x})^2$	Predicted $\hat{y}_i = mx_i + c$	Residuals $y_i - \hat{y}_i$	Residuals ² $(y_i - \hat{y}_i)^2$	RSD $\sqrt{\sum (y_i - \hat{y}_i)^2 / n - 2}$
1	Ecuador	6.129	222141	940.710	221937.70	203.290	41326.84	S(r)= 146.38
2	Ghana	6.168	289134	938.319	288944.42	189.579	35940.41	
3	Cameron dry	6.116	199862	941.507	199602.13	259.860	67527.33	
4	Cameron wet	6.137	235579.7	940.219	235682.67	-102.976	10604.09	
5	Ghana dry	6.105	180562.7	942.183	180702.81	-140.111	19631.14	
6	Ghana wet	6.145	249018	939.729	249427.64	-409.642	167806.93	
8		\bar{x}	\bar{y}	$\sum (x_i - \bar{x})^2$			$\sum (y_i - \hat{y}_i)^2$	
9		36.80	1376297.4	5642.669			342836.77	

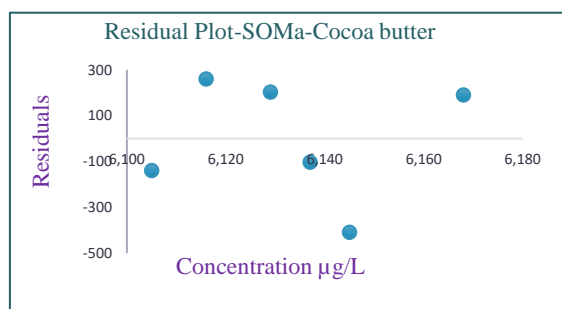
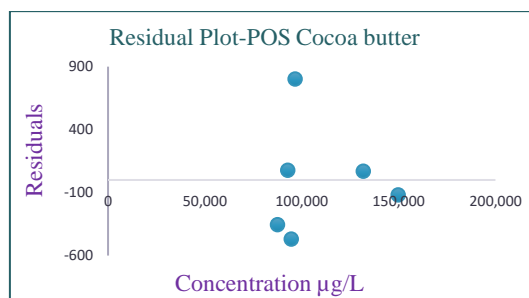


Table 22 The regression data for residual standard deviation of POS cocoa butter

S. No.	Cocoa butter origin	Concentration $\mu\text{g/L}$ x_i	Peak area y_i	$(x_i - \bar{x})^2$	Predicted $\hat{y}_i = mx_i + c$	Residuals $y_i - \hat{y}_i$	Residuals ² $(y_i - \hat{y}_i)^2$	RSD $\sqrt{\sum (y_i - \hat{y}_i)^2 / n - 2}$
1	Ecuador	131.624	216328839	271271.180	216328770.8	68.207	4652.232	S(r)= 251.48
2	Ghana	149.720	247490797	252748.513	247490915.4	-118.358	14008.799	
3	Cameron dry	87.444	140248422.7	319244.210	140248778.1	-355.446	126342.133	
4	Cameron wet	96.522	155882311.5	309068.171	155881511.8	799.690	639504.639	
5	Ghana dry	94.463	152335348.4	311361.768	152335819.1	-470.678	221538.332	
6	Ghana wet	92.688	149279264	313345.811	149279187.4	76.586	5865.435	
8		\bar{x}	\bar{y}	$\sum (x_i - \bar{x})^2$			$\sum (y_i - \hat{y}_i)^2$	
9		652.461	1061564983	1777039.655			1011911.57	



Chapter 5 Diffusion NMR of dietary triacylglycerols

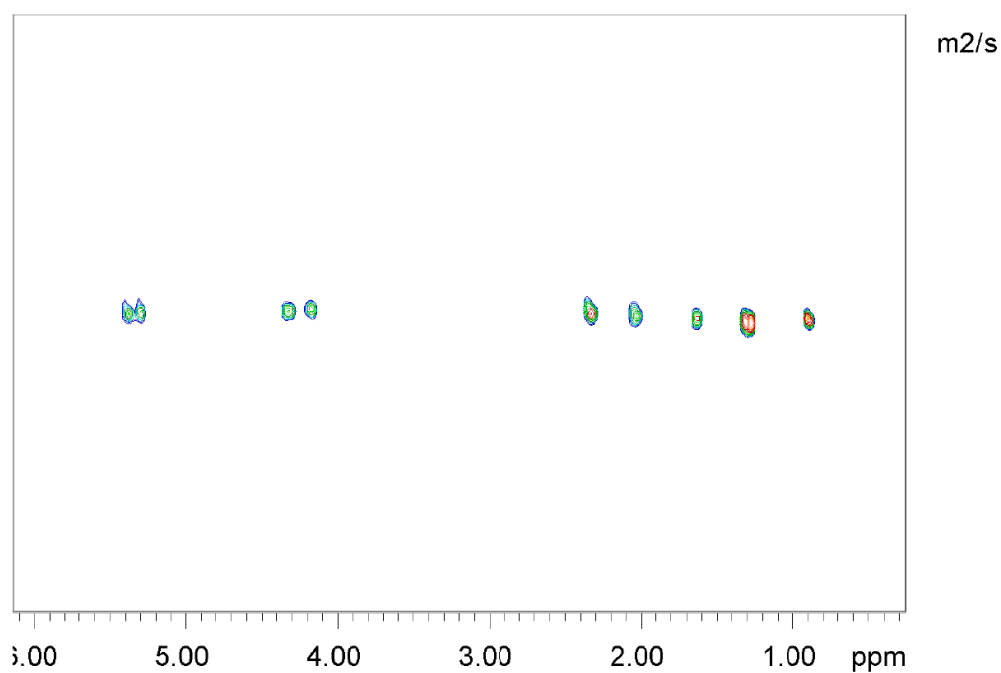


Figure 1. 2D DOSY of Isomer of 1,2,3-tripalmitoyl glycerol [Tripalmitin PPP-Isomer] (1)

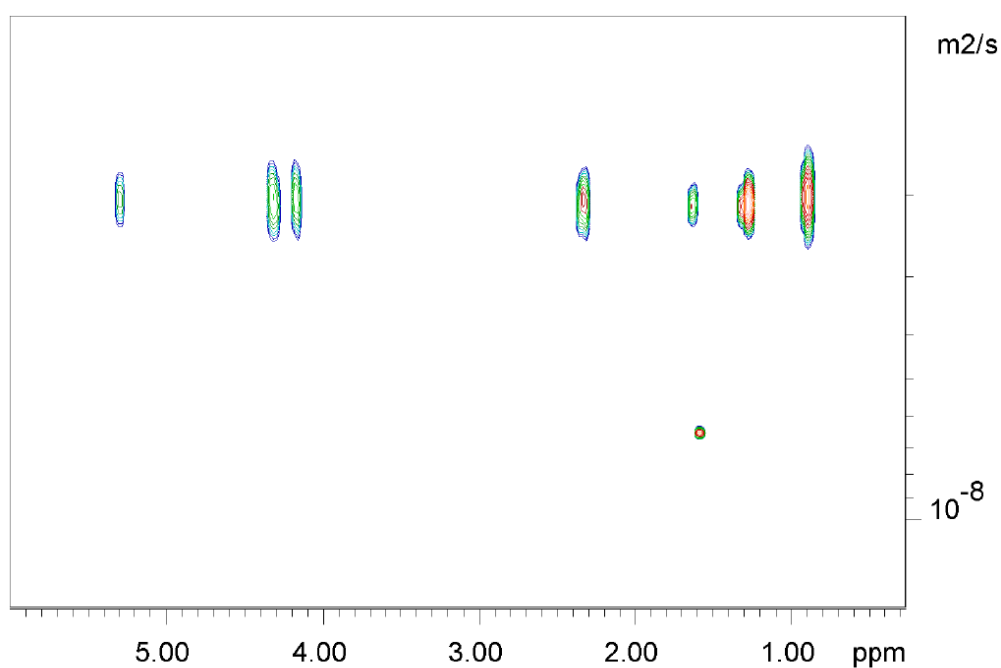


Figure 2. 2D DOSY of 1,2,3-tristearoyl glycerol [Tristearin SSS] (2)

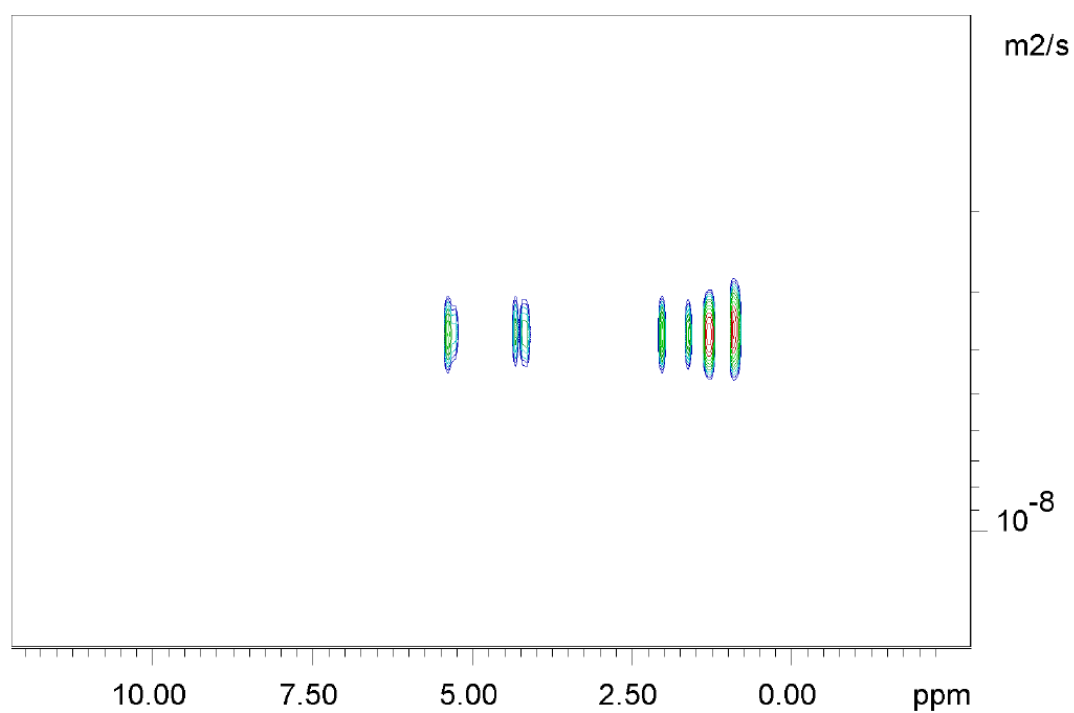


Figure 3. 2D DOSY of 1,2,3-Trioleoyl glycerol [Triolein OOO] (3)

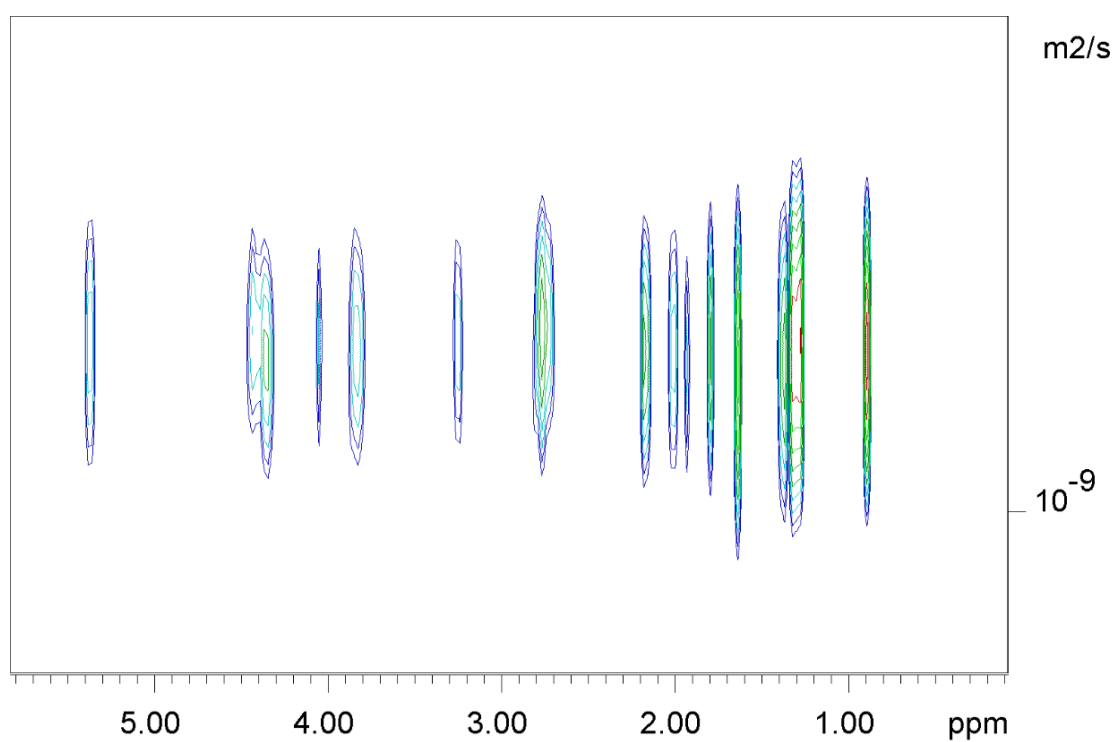


Figure 4. 2D DOSY of 1,2,3-Trioctanoyl glycerol [Trioctanein OcOcOc] (5)

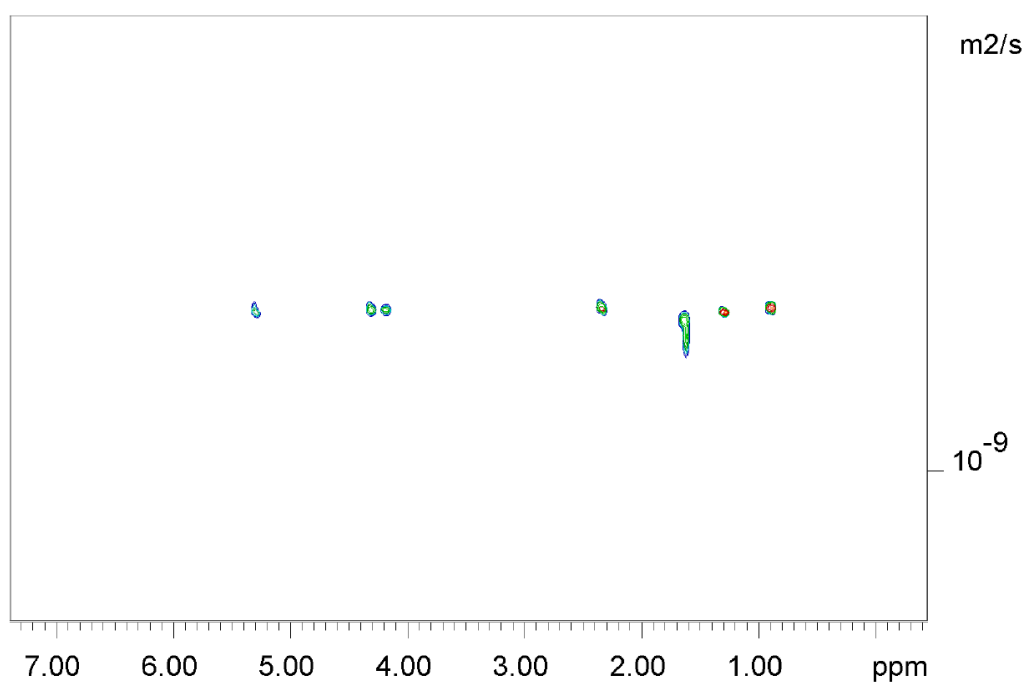


Figure 5. 2D DOSY of 1,2,3-Trilauroyl glycerol [Trilaurein LaLaLa] (6)

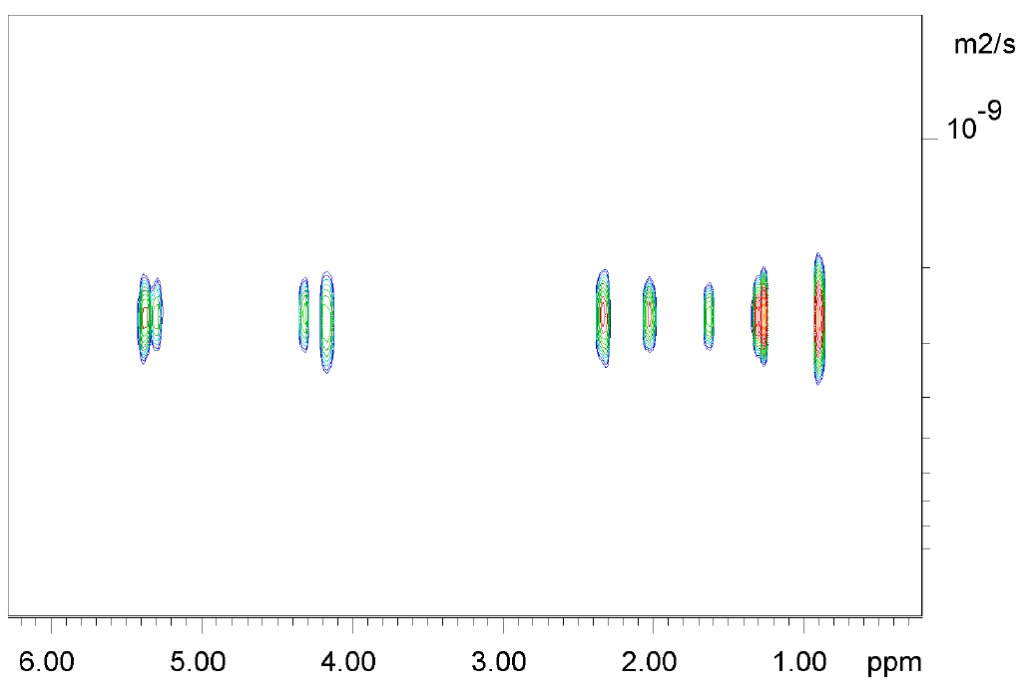


Figure 6. 2D DOSY of 1-Palmitoyl-2,3-dioleoyl glycerol [POO] (9)

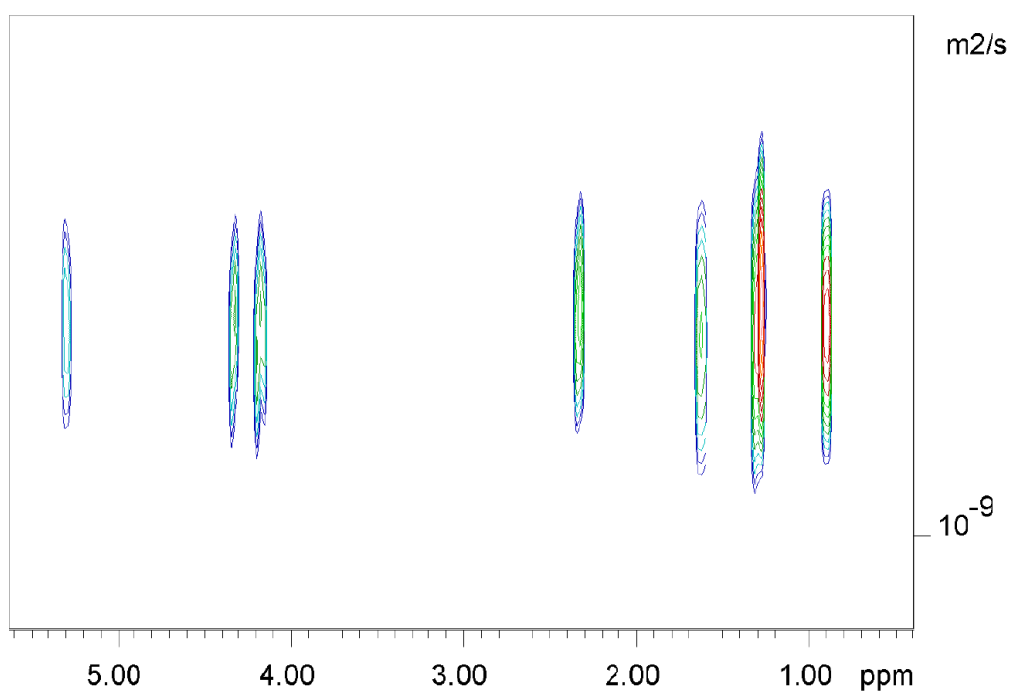


Figure 7. 2D DOSY of 1-Palmitoyl-2, 3-distereoyl glycerol [PSS] (10)

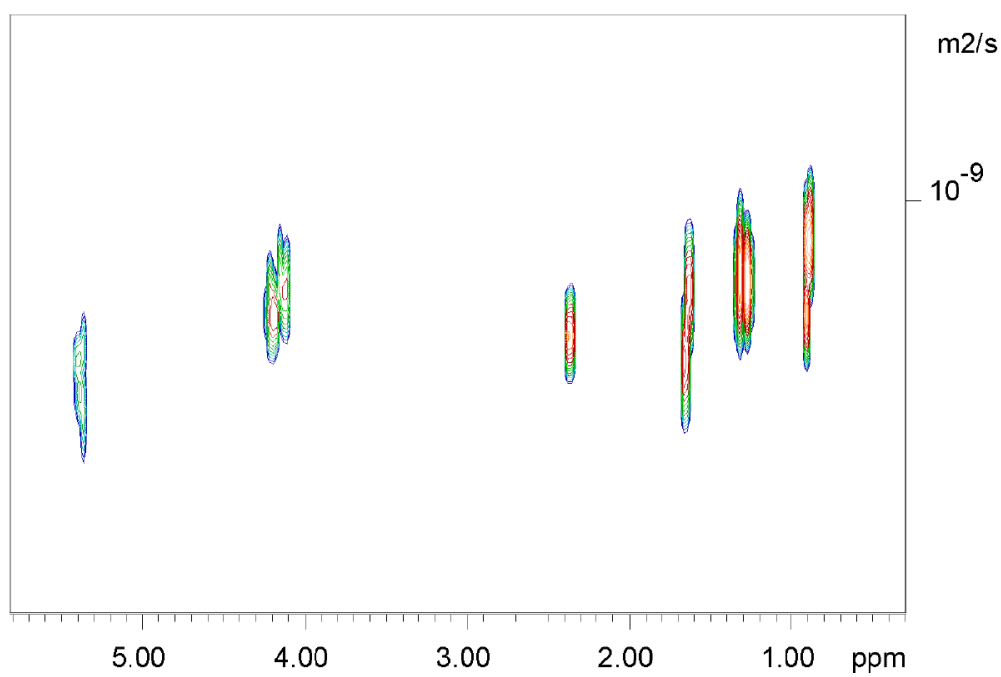


Figure 8. 2D DOSY of 1-Palmitoyl-2, 3-dilinoleoyl glycerol [PLL] (11)

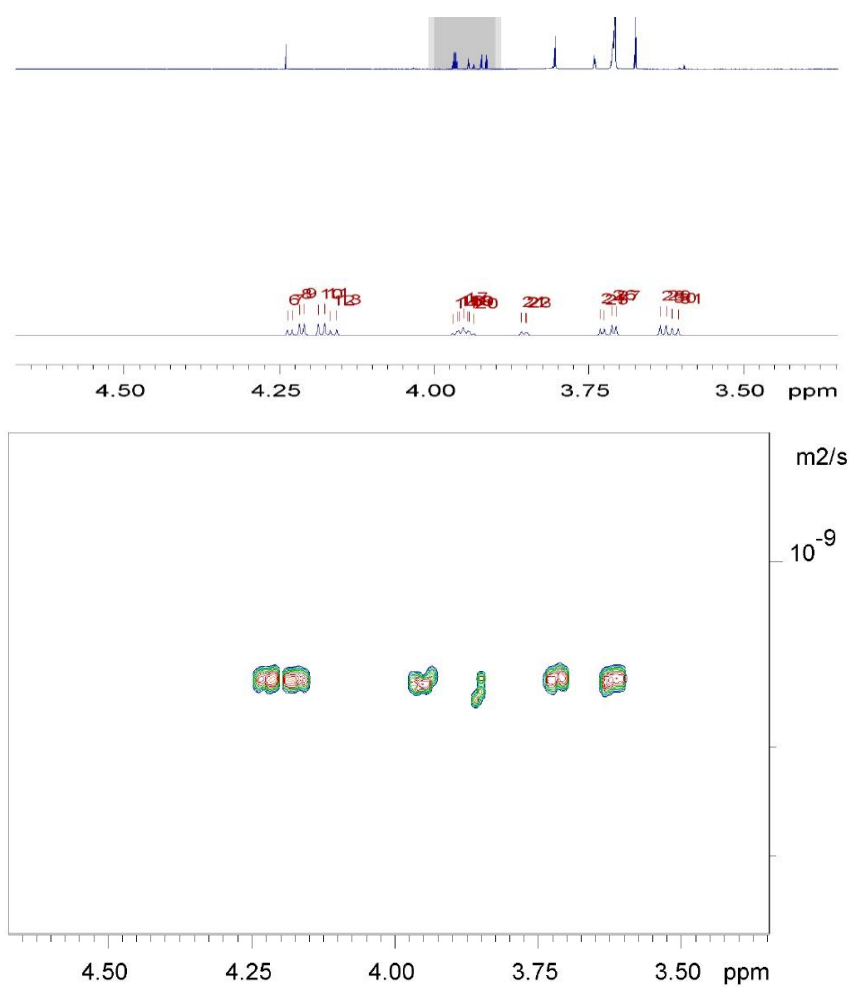


Figure 9. 2D DOSY of 1-Stearoyl glycerol (13)

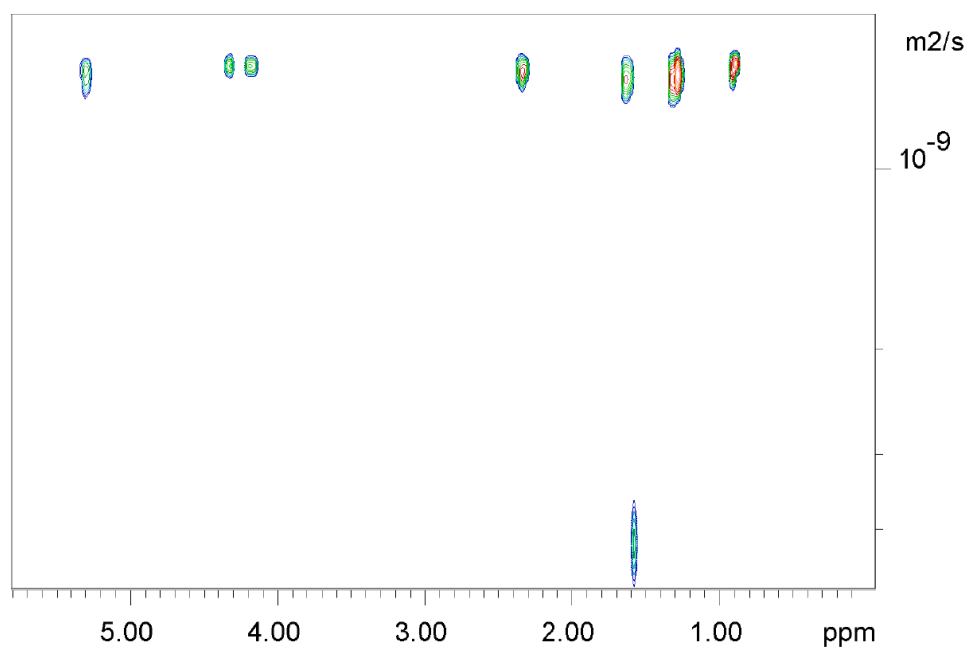


Figure 10. 2D DOSY of 1-Stearoyl-2, 3-palmitoyl glycerol [SPP] (14 a)

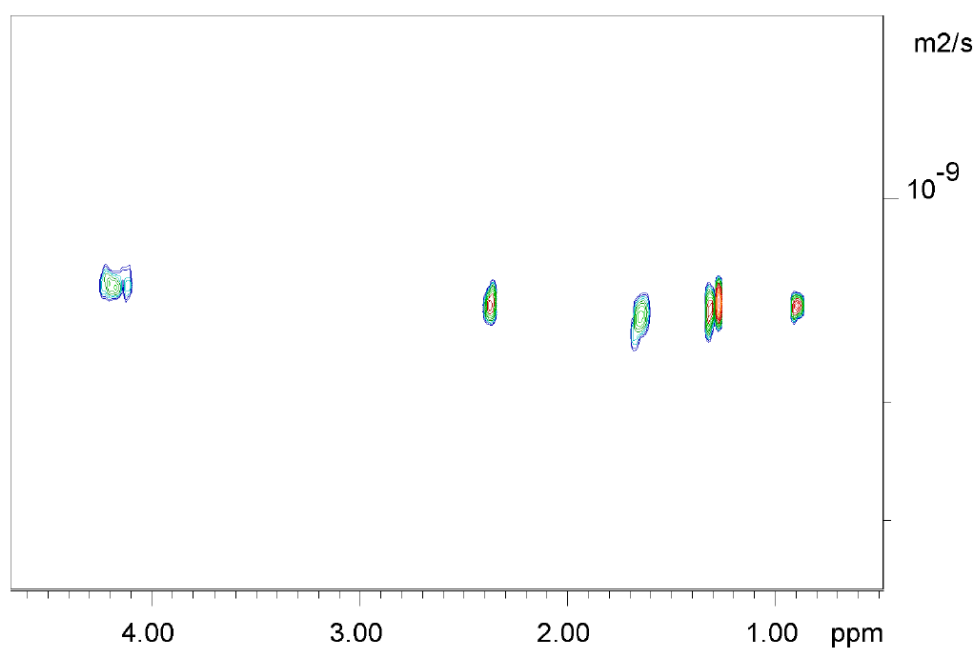


Figure 11. 2D DOSY of Isomer of 1-Stereoyl-2, 3-palmitoyl glycerol [SPP-ISOMER] (14 b)

Chapter 6 Cocoa butter adulteration studies by discriminative analysis



Figure 1. PCA loading of cocoa butter, vegetable oils, lard and cocoa butter adulterant samples

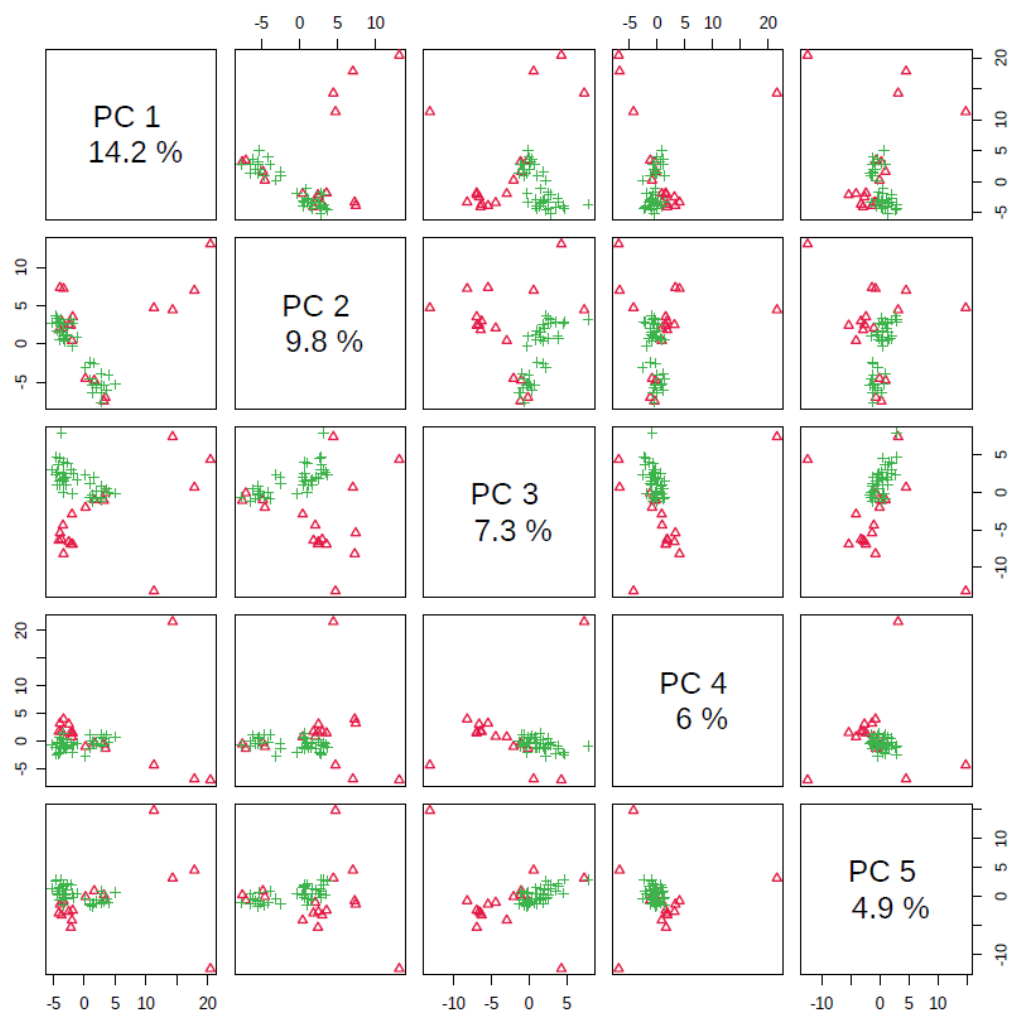


Figure 2 Pair wise score plots from PCA showing the various separation patterns among the most significant PCs